Environmental Regulation of the End-of-Flowering in Angiosperms

Pablo González-Suárez

Submitted in accordance with the requirements for the degree of

Doctor of Philosophy

The University of Leeds

Faculty of Biological Sciences

School of Biology

September 2023

The candidate confirms that the work submitted is his own, except where work which has formed part of jointly authored publications has been included. The contribution of the candidate and the other authors to this work has been explicitly indicated below. The candidate confirms that appropriate credit has been given within the thesis where reference has been made to the work of others.

Todo lo que escribo se lo dedico a mi abuela

Acknowledgements

Having worked on this thesis for the past years, I have spent a fair amount of time thinking about time. Mainly, what it means to plants and, by extension, also what it means to me. I have learnt to value it a bit more and, here, I would like to thank all the people that have gifted me with their time along the way. Mostly, Tom, for always being there during this journey, for the infinite trust in me and the stories that I wanted to tell and for teaching me a lot of what I now know about science, plants and others. A Ph.D. was definitely not the easiest thing to do, but I am incredibly happy that I did it and it would have not been possible without you. I am also extremely grateful to others that have mentored me along the way. Specially to Laura, for introducing me to the insanities of cereal development and giving me fantastic support and scientific advise over the past four years. But also to Rea and Krzysztof, for inspiring me to think harder about how plants do things and for teaching me things that I did not know computers could do. And to Candela, for pushing me to do this and for being an incredible scientific role model.

Fortunately, I have had the most amazing bunch of people around me during these years, in and out of work. I am immensely thankful to my colleagues from the department, for their incredible support and for keeping me sane during the craziest times. To all members of the Bennett lab and specially to Catriona, for teaching me a lot about flowering and the end of it, and to Cara, for being an amazing friend. During this time, I have been lucky enough to supervise 5 wonderful students: Megan, Arran, Tom, Faye and Lateefat. To them, I thank for pushing me to be a better mentor and for blessing me with their time and enthusiasm. To my other two musketeers, Roza and Kate, thank you for all the laughs, the tears, the shenanigans, and for all the love. Having you in my life has been an absolute wonder.

My parents have never really understood what it is that I do for a living, but they have given me endless and unconditional support during my whole academic ride (and life, for that matter). First, from the room next door and, then, from 1,200 km away. To them I owe being here today, doing this. And to Johan, my home away from home, I must thank for putting up with me for the past 4 years, for this adventure that we have just lived together, and for the many that I am sure are to come. Thank you for being the best possible start and end to this journey.

Abstract

Flowering is a key phase in plant development, whose timing is crucial to synchronise a plant's life cycle with the changing seasons. Environmental signals are fundamental in determining when flowering starts in angiosperms, but their effects during the end-of-flowering are only beginning to be understood. The work presented here provides a detailed characterization of the environmental control of end-of-flowering in the model plant *Arabidopsis thaliana* and other angiosperms, and suggests a key role for temperature, day length and nutrient availability as regulators of inflorescence arrest. Furthermore, the genetic regulation of end-of-flowering has been examined both in standard laboratory accessions and in naturally-occurring populations. This has led to the identification of a novel role for the floral integrator *FLOWERING LOCUS T* (*FT*) in the control of inflorescence meristem arrest and its response to environmental signals. Additionally, systems biology and bioinformatic approaches have been utilized to identify potential genes underlying arrest, both FT-dependent and independent. Taken together, the data gathered here demonstrate that the environment has a clear impact on both the duration of flowering and the reproductive output of plants, and shed light into the genetic signals underlying this processes. Better understanding the environmental control of end-of-flowering is a necessary first step towards improving the productivity of crops and here, its relevance has been demonstrated for hexaploid wheat (*Triticum aestivum*), a species of world-wide commercial importance.

Table of Contents

List of Tables

List of Figures

Abbreviations

1001G	1001 Genomes Project
ABA	Abscisic acid
ABI5	ABA INSENSITIVE 5
AG	AGAMOUS
AHK2/3/4	ARABIDOPSIS HISTIDINE KINASE 2/3/4
ANOVA	Analysis of variance
AP1/2	APETALA 1
ARR	Arabidopsis response regulator
ATS	*Arabidopsis thaliana* salts
BAP	N6-benzylaminopurine
BOP1	BLADE ON PETIOLE 1
cv.	Cultivated variety
CAL	CAULIFLOWER
CaMV	Cauliflower mosaic virus
CCA1	CIRCADIAN CLOCK ASSOCIATED 1
CDF	CYCLING DOF FACTOR
cDNA	Copy deoxyribonucleic acid
CDS	Coding sequence
CIB	CRYPTOCHROME-INTERACTING BASIC-HELIX-LOOP-HELIX
CK	Cytokinin
CLV1/2/3	CLAVATA 1/2/3
CO	CONSTANS
COP1	CONSTITUTIVE PHOTOMORPHOGENIC 1
CRY1/2	CRYPTOCHROME 1/2
CV	Coefficient of variation
D.p.b.	Days post-bolting
D14	DWARF 14
DEG	Differentially expressed gene
DEX	Dexamethasone
DMSO	Dimethyl sulfoxide

DNA	Deoxyribonucleic acid
DNF	DAY NEUTRAL FLOWERING
ELF3/4/9	EARLY FLOWERING 3/4/9
FAF2/4	FANTASTIC FOUR 2/4
FBH1-4	FLOWERING BHLH 1-4
FCA	FLOWERING CONTROL LOCUS A
FDR	False discovery rate
FKF1	FLAVIN-BINDING, KELCH REPEAT, F BOX 1
FLC	FLOWERING LOCUS C
FLM	FLOWERING LOCUS M
FM	Floral meristem
FUL	FRUITFUL
FR	Far red
FRI	FRIGIDA
FT	FLOWERING LOCUS T
GI	GIGANTEA
GLM	Generalized linear model
GO	Gene ontology
GR	Glucocorticoid receptor
GWAS	Genome-wide association study
HB-3	HOMEOBOX 3
HB53	HOMEOBOX 53
HOS1	HIGH EXPRESSION OF OSMOTICALLY RESPONSIVE GENES 1
HSD	Honestly Significant Difference
ID	Identifier
IM	Inflorescence meristem
JA	Jasmonic acid
JMJ14	JUMONJI 14
KMD2/4	KISS ME DEADLY 2/4
KNU	KNUCKLES
LB	Luria-Bertani
LHY	LATE ELONGATED HYPOCOTYL
LKP	LOV KELCH PROTEIN
LRT	Likelihood ratio test

MAF1-5	MADS AFFECTING FLOWERING 1-5
MAX1	MORE AXILLARY GROWTH 1
mRNA	Messenger ribonucleic acid
N	Nitrogen
NAA	1-naphtaleneacetic acid
NASC	Nottingham Arabidopsis Stock Centre
NPA	N-1-naphthylphthalamic acid
P	Phosphorus
PATS	Polar auxin transport stream
PCA	Principal Component Analysis
PCR	Polymerase chain reaction
PEBP	Phosphatidylethanolamine-binding protein
PEP1	PERPETUAL FLOWERING 1
PHYA/B	PHYTOCHROME A/B
PIF4/5	PHYTOCHROME INTERACTING FACTOR 4/5
PRR	PSEUDO-RESPONSE REGULATOR
PTM	PHD TYPE TRANSCRIPTION FACTOR WITH TRANSMEMBRANE DOMAINS
QTL	Quantitative trait locus
RIL	Recombinant inbred line
RNA	Ribonucleic acid
RNA-Seq	Ribonucleic acid sequencing
ROS	Reactive oxygen species
RT-qPCR	Reverse transcription quantitative polymerase chain reaction
SAM	Shoot apical meristem
sFTP	Secure file transfer protocol
SL	Strigolactone
SM	Spikelet meristem
SMXL	SUPRESSOR OF MAX2-LIKE
SNP	Single nucleotide polymorphism
SOC1	SUPRESSOR OF OVEREXPRESSION OF CONSTANS 1
SPA	SUPRESSOR OF PHYA-105 1
SPL	SQUAMOSA PROMOTER BINDING PROTEIN-LIKE
STM	SHOOT MERISTEMLESS

STUbL	SUMO-targeted ubiquitin ligase
SVP	SHORT VEGETATIVE PHASE
T6P	Trehalose 6-phosphate
TAIR	The Arabidopsis Information Resource
TAR2	TRYPTOPHAN AMINOTRANSFERASE RELATED 2
TEM1/2	TEMPRANILLO 1/2
TFL1	TERMINAL FLOWER 1
TPP	TREHALOSE PHOSPHATASE
TPS	TREHALOSE SYNTHASE
TPS1/11	TREHALOSE PHOSPHATE SYNTHASE 1/11
TSF	TWIN SISTER OF FT
UV-A	Ultraviolet A
v/v	Volume/volume
VCF	Variant call format
VST	Variance stabilizing transformation
w/v	Weight/volume
WUS	WUSCHEL
ZTL	ZEITLUPE

List of Publications

González-Suárez, P., Walker, C.H., Bennett, T., 2020. Bloom and bust: understanding the nature and regulation of the end of flowering. Current Opinion in Plant Biology 57, 24-30. https://doi.org/10.1016/j.pbi.2020.05.009

O'Connor, K., **González-Suárez, P.**, Dixon, L.E., 2020. Temperature Control of Plant Development. Annual Plant Reviews Online 3 (4), 563-606. https://doi.org/10.1002/9781119312994.apr0745

Ware, A., Walker, C.H., Šimura, J., **González-Suárez, P.,** Ljung, K., Bishopp, A., Wilson, Z.A., Bennett, T., 2020. Auxin export from proximal fruits drives arrest in temporally competent inflorescences. Nature Plants 6, 699-707. https://doi.org/10.1038/s41477-020-0661-z

González-Suárez, P., Walker, C.H., Bennett, T., 2023. FLOWERING LOCUS T mediates photo-thermal timing of inflorescence meristem arrest in Arabidopsis thaliana. Plant Physiology 192 (3), 2276-2289. https://doi.org/10.1093/plphys/kiad163

List of Contributions

Most of the work within this thesis has either been carried out by me or by others under my supervision. Below is a detailed list of all the instances in which work carried out by others is used, either directly or indirectly.

In Chapter 3, experiments shown in **Figure 3.3** and **Figure 3.9** were designed and performed by me based on preliminary results collected by Tom Lock and Megan Pierce, respectively. The experiments presented in **Figure 3.11C-F** were designed and performed jointly by Roza Bilas and me.

In Chapter 4, the experiment shown in **Figure 4.1A-B** was designed and carried out by Catriona Walker. Roza Bilas assisted in the data collection for **Figure 4.4A-B**.

In Chapter 6, the experiments presented in **Figure 6.3** and **Figure 6.5** were designed jointly by Tom Lock and me, and performed by Tom Lock. The experiment presented in **Figure 6.7** was designed and performed jointly by Tom Lock and me. Catriona Walker assisted in the experimental treatments corresponding to the experiment shown in **Figure 6.8**.

In Chapter 7, Roza Bilas assisted in the data collection for **Figure 7.3**. Laura Dixon assisted in the experimental treatments corresponding to the experiment shown in **Figure 7.4**. For **Figure 7.8** and **Figure 7.9**, plant growth and harvesting of samples was performed jointly by Mary McKay, Catriona Walker, Josie Driver and me. All of the data presented in both figures was collected by me.

In all cases, the data was analysed and interpreted by me.

Chapter 1: Introduction

Flowering plants (i.e., angiosperms) possess an enormous variety of reproductive strategies, and different species have acquired specialized structures through their evolutionary history. Regardless of this remarkable diversity, one thing is common to all angiosperms: flowering must occur at the right time. This allows plants to synchronize their reproduction with optimal environmental conditions, maximizing their chances of reproductive success and offspring production (Bratzel and Turck, 2015). After decades of research, we now know that the timing of flowering is controlled by a complex regulatory network involving not only external cues but also endogenous signals. Currently, up to seven different genetic pathways have been described to control the timing of flowering in angiosperms (Quiroz et al., 2021; Song et al., 2015; Srikanth and Schmid, 2011).

While flowering time has been extensively studied over the years, the vast majority of work has aimed to decipher why and how flowering begins. In contrast, the end-of-flowering has often been neglected and, as a result, very little is known about this biological process as well as the molecular mechanisms involved in it (Balanzà et al., 2023). In particular, the environmental control of end-of-flowering is largely under-described, despite the undeniable relevance of environmental signals in triggering the onset of flowering (González-Suárez et al., 2020; Miryeganeh et al., 2018). In this context, the main goal of this thesis is to understand how environmental signals affect the duration of the reproductive phase and, ultimately, how they drive the plant’s decision to stop flowering.

1.1. Flowering Comes to an End

Research on the end-of-flowering has been fragmentary, and there does not seem to be a universal consensus of what it really consists of (Bawa et al., 2003). Different interpretations of when flowering ends can be found in the literature. Some authors define the end-of-flowering as the moment at which all flowers have opened and the fruit set is already formed and visible (Gentilucci and Burt, 2018; Matsoukis et al., 2018). Others define the duration of flowering as the period during which pollination occurs (Jones et al., 2017; Royo et al., 2016). In ecological studies, the end-of-flowering has been often recorded at the population (Francis and Gladstones, 1974) or even community (Bawa et al., 2003; Cortés-Flores et al., 2017) levels. Regardless of the definition, however, most authors agree that the end-of-flowering is key for the plant's reproductive success (Dorji et al., 2020; Nagahama et al., 2018) and that it can even be more sensitive to environmental inputs than the onset of flowering (Nagahama et al., 2018).

From a developmental point of view, the life cycle of most angiosperms is governed by transitions between phases, which ultimately determine what structures, if any, are being produced and where resources are being allocated. The germination of the seed can be regarded as one of the first developmental transitions in an angiosperm's life. Shortly after it, the plant goes through a vegetative phase in which leaves and branches are produced (Liu et al., 2009). After the plant reaches sexual maturity, and when the external conditions are suitable, a different type of developmental transition marks the end of the vegetative phase and the start of reproduction. This is named floral transition and represents the onset of flowering (Pidkowich et al., 1999). After floral transition takes place, the plant starts to produce inflorescences, specialized structures that harbour the flowers and, later, the fruits.

Taking all of this into account, and considering the whole plant as a system, the end-of-flowering could be regarded as another type of developmental transition,

one that marks the end of the reproductive period and triggers either the return to a vegetative phase (in polycarpic species that flower multiple times) or the end of the plant's lifespan (in monocarpic species that only flower once). The latter is the case of the model plant *Arabidopsis thaliana*, which undergoes monocarpic senescence (Thomas, 2013). The association between end-of-flowering and senescence in monocarpic species is not fully resolved, but it has been proposed that whole-plant senescence only begins after flowering comes to an end (Balanzà et al., 2023; Miryeganeh, 2021; Wang et al., 2020), and that these processes are genetically linked (Miryeganeh, 2020; Wingler et al., 2010).

1.1.1. Inflorescence Meristem Arrest

Due to their plastic development, adult plant structures are not preformed embryonically as it would be the case in animal species. Instead, they are produced by meristems, i.e., niches of undifferentiated stem cells which hold the potential to form different types of plant tissues (Liu et al., 2009; Melzer et al., 2008). During the vegetative phase, the shoot apical meristem (SAM) controls plant growth and the production of aerial non-reproductive structures such as leaves. Later on, and following floral transition, the plant begins producing reproductive structures. These are typically generated by an inflorescence meristem (IM), which forms after the conversion of a pre-existing vegetative SAM. While active, the IM gives rise to an inflorescence and produces floral meristems (FMs), each of which generates a single flower (Liu et al., 2009; Pidkowich et al., 1999).

For end-of-flowering to take place, the proliferative activity of the IM must cease first through a phenomenon often termed IM arrest or proliferative arrest. Evidence supporting this idea comes from early work with *A. thaliana*, whose inflorescences stop producing new flowers after approximately 15-20 days under

standard conditions, forming a terminal cluster of undeveloped FMs in the apex (Hensel et al., 1994) (**Figure 1.1**). While proliferative arrest was originally proposed to occur globally within the plant (Hensel et al., 1994), later research has demonstrated that it is regulated locally at each inflorescence (Ware et al., 2020).

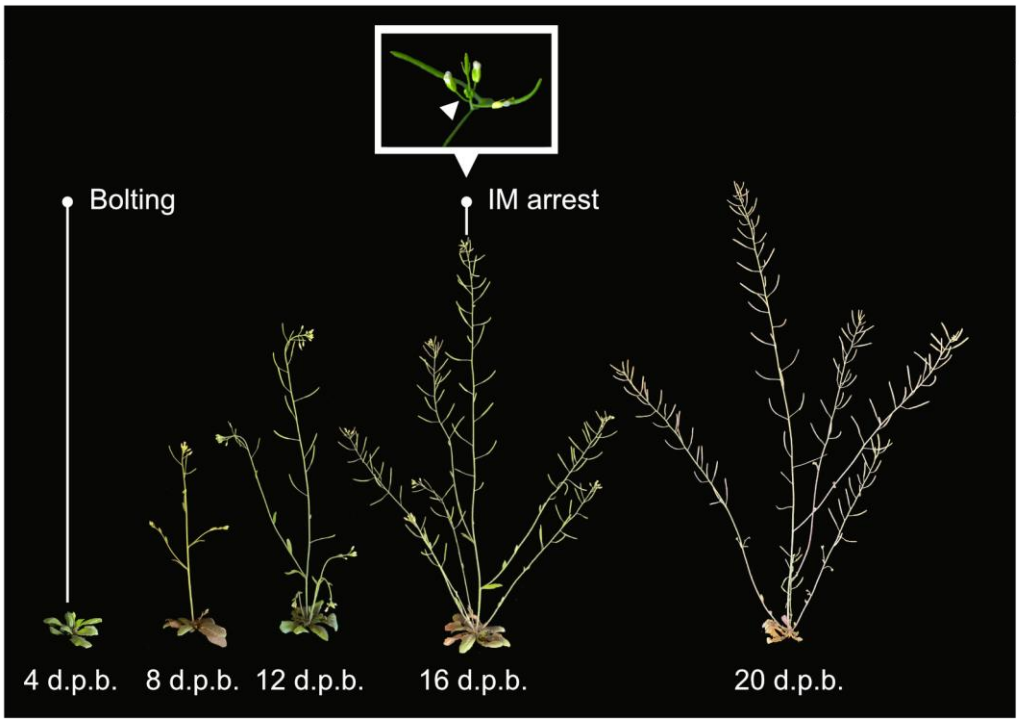

Figure 1.1. End-of-flowering in *Arabidopsis thaliana*

Time-lapse of *Arabidopsis thaliana* during flowering, i.e., from bolting to arrest of all inflorescences. IM: Inflorescence meristem. D.p.b.: Days post-bolting.

IM arrest encompasses an active, controlled process which is not just a consequence of senescence or the exhaustion of resources. Further, it has been demonstrated that its timing is tightly controlled by endogenous signals, particularly by the presence of fertile fruits within the plant (Goetz et al., 2021; Hensel et al., 1994; Ware et al., 2020; Wuest et al., 2016). Seed production is known to promote IM arrest in *A. thaliana*. Accordingly, male-sterile *ms1-1* mutants and plants subjected to a continuous removal of developing fruits show a delayed inflorescence arrest (Hensel et al., 1994; Ware et al., 2020). In both cases, plants do not show standard arrest

phenotypes but instead exhibit a variety of developmental abnormalities, with their IM typically differentiating into a terminal flower rather than undergoing arrest (Hensel et al., 1994). In addition to fertile fruits, ageing also controls IM arrest through a characterized molecular pathway that adds another layer to the autonomous regulation of inflorescence arrest (Balanzà et al., 2018).

Research carried out in the past few years has shed light on the physiological basis of IM arrest. Soon after floral transition, the IM starts to gradually decrease in size, a process that begins as early as one week after flowering (Walker et al., 2023; Wang et al., 2020). This continues throughout the reproductive phase and, interestingly, even after IM arrest has taken place (Wang et al., 2020). At the cellular level, this correlates with a decrease in cell size and number (Merelo et al., 2022) as well as a vacuolation of meristematic cells (Wang et al., 2020), which is a sign of cellular differentiation and senescence (Rhinn et al., 2019). The former two are likely caused by an interruption of the mitotic programme, which in turn represses cell division and growth (Merelo et al., 2022). Ultimately, the current understanding is that this cessation in cell division triggers arrest at the IM and, in agreement with this, arrested IMs show transcriptomic signatures associated with low mitotic activity (Wuest et al., 2016). Interestingly, arrest is reversible and the proliferative activity of IMs can be restored by surgically removing fruits (Wuest et al., 2016), suggesting that IM arrest triggers the dormancy and not the death of stem cells (Balanzà et al., 2023). The transcriptome profile of arrested IMs supports this idea, and highly resembles that of dormant axillary meristems (Wuest et al., 2016).

1.1.2. Floral Arrest

Even after IM arrest, the preformed floral primordia continue to develop and open into flowers (Walker et al., 2023). Thus, arrest at the flower level, i.e., floral arrest, constitutes a second necessary milestone for end-of-flowering in *A. thaliana*. Indeed, shortly after IM arrest has taken place, floral arrest interrupts the development of the youngest floral primordia, i.e., those at a developmental stage of 9 or below (Walker et al., 2023); which ultimately leads to the formation of the cluster of undeveloped buds typical of arrested inflorescences (Hensel et al., 1994) (**Figure 1.1**). Unlike IM arrest, floral arrest is only partially reversible. Upon reactivation of the IM, only the developmentally youngest among the arrested floral primordia, i.e., those at a developmental stage of 5 or below; resume their development (Walker et al., 2023). This suggests that floral arrest triggers both senescence in the oldest primordia and dormancy in the youngest, although the molecular mechanisms surrounding either of these processes still remain unknown.

1.1.3. End-of-Flowering in Other Species

Numerous studies demonstrate that the genetic network controlling the timing of flowering is largely conserved in the plant kingdom. However, the comparative study of end-of-flowering among different species becomes difficult considering the enormous variety of growth habits and inflorescence types present in the plant kingdom (Benlloch et al., 2007; Prusinkiewicz et al., 2007). Furthermore, most of the processes surrounding reproductive arrest have been described in *A. thaliana*, with very little information available for other non-model plant organisms.

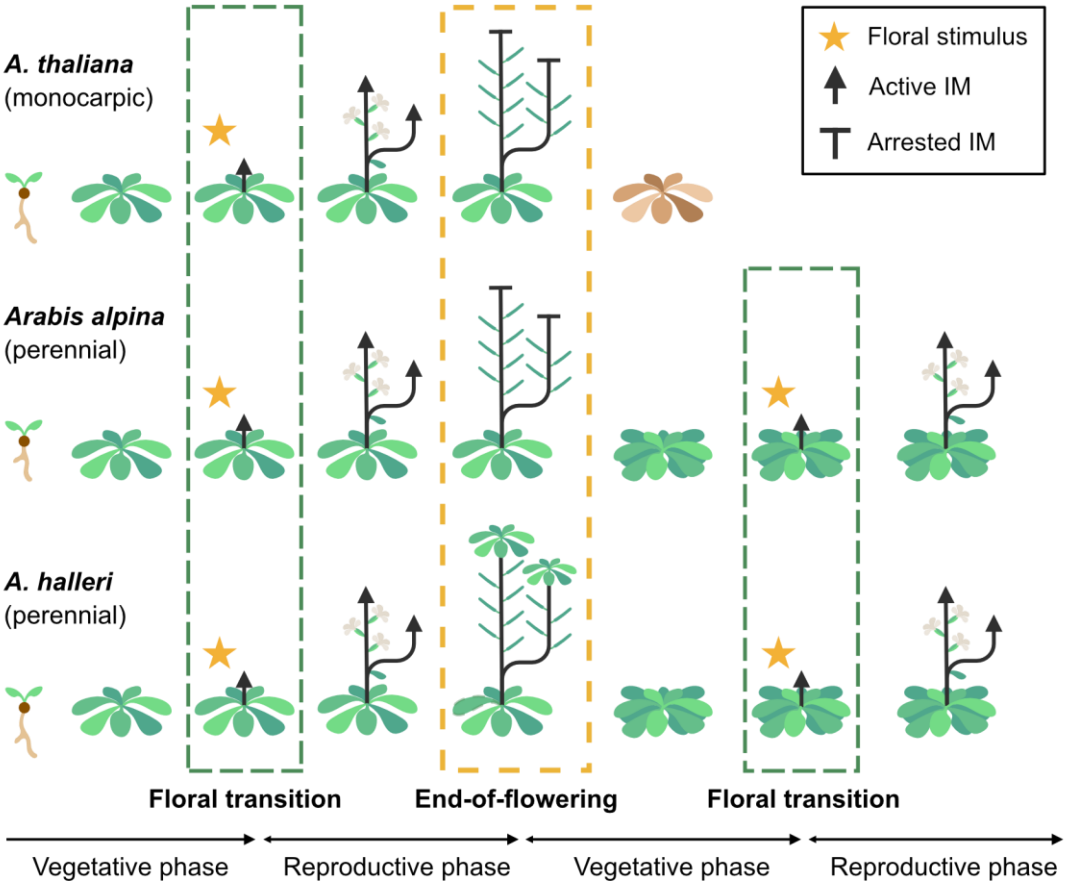

Figure 1.2. End-of-flowering in the Brassicaceae family

Cartoon of the main developmental phases in the monocarpic *Arabidopsis thaliana* (top) and the perennials *Arabis alpina* (middle) and *Arabidopsis halleri* (bottom). In monocarpic species that flower only once, like *A. thaliana*, inflorescence arrest is followed by whole-plant senescence. In perennials, on the other hand, end-of-flowering can be regarded as a developmental transition that allows the plant to terminate flowering and resume vegetative growth. Although the way to achieve this may differ between species, a new floral stimulus can reactivate flowering from new meristem in both cases, allowing for a second reproductive episode.

Most species from the Brassicaceae family, to which *A. thaliana* belongs, have an indeterminate inflorescence in which the IM is kept undifferentiated throughout the plant's lifetime (Ratcliffe et al., 1998; Weberling, 1992). In this context, inflorescence arrest is likely achieved through arrest of the IM and, subsequently, of the developing primordia in a manner similar to *A. thaliana*, although the evidence

supporting this idea is scarce for other species. Additionally, while IM arrest provides a good framework for explaining end-of-flowering in individual inflorescences, it can prove insufficient when trying to understand reproductive termination at the whole-plant level. This is particularly true for polycarpic species such as the perennial *Arabis alpina*. Recent work suggests that, once the reproductive phase is over, individual inflorescences of *A. alpina* arrest while vegetative growth is resumed in by a 'bud-bank' of vegetative meristems (Vayssières et al., 2020). In *Arabidopsis halleri*, another close relative of *A. thaliana*, inflorescences undergo a vegetative reversion after the reproductive season (Aikawa et al., 2010; Shimizu et al., 2011). As a result, aerial rosettes are formed which contribute to the clonal reproduction of the species. Presumably, vegetative growth is resumed in the main rosette and new inflorescences will be formed in the next reproductive season. In any case, these observations suggest that, regardless of the fate of the IM in individual inflorescences, there must be a mechanism that regulates a vegetative transition at the whole-plant level in polycarpic plants (**Figure 1.2**). Several authors have suggested that this vegetative transition is genetically regulated, although the underlying mechanisms are still largely unknown (Carrasco et al., 2013; Francis and Gladstones, 1974; Kays and Kultur, 2005).

Even less is known about the end-of-flowering in species with determinate inflorescences, where the IM eventually differentiates, turning into a terminal flower (Ratcliffe et al., 1998). This is the case of many crops, including temperate annual grasses from the Poaceae family such as hexaploid wheat, *Triticum aestivum* (Caselli et al., 2020). In wheat, inflorescences are organized in specialized structures named spikes (Caselli et al., 2020; Kirby and Appleyard, 1984) (**Figure 1.3**). Upon floral transition, the SAM turns into a spike meristem, which forms a number of subordinate spikelet meristems (SM). These SMs generate the wheat inflorescences, also known as spikelets. In each spikelet, the SM initiates several floret meristems, which may give rise to grain-bearing florets. Eventually, the spike meristem acquires

determinacy forming a terminal spikelet itself (Benlloch et al., 2007; Bradley et al., 1997). However, the SMs are indeterminate, similar to IMs from *A. thaliana*, suggesting that they may arrest in a similar manner (**Figure 1.3**). Within this complex spike architecture, it is unclear how end-of-flowering is mediated, as several developmental transitions need to take place, including the differentiation of the spike meristem and the arrest of the SMs. Interestingly, SMs initiate up to 12 floret meristems per spikelet, of which only 1-4 tend to become fertile (Bonnett, 1936; Fischer, 1984). The remaining florets undergo cellular autophagy (Glick et al., 2010), degenerating similarly to FMs from *A. thaliana*, which suggests that abortion of florets may be a form of floral arrest and adds a third layer to the complicated nature of end-of-flowering in wheat. Remarkable research efforts have been directed to better understand the regulation of terminal spikelet formation in wheat, whereas SM arrest and floret degeneration are less well-studied.

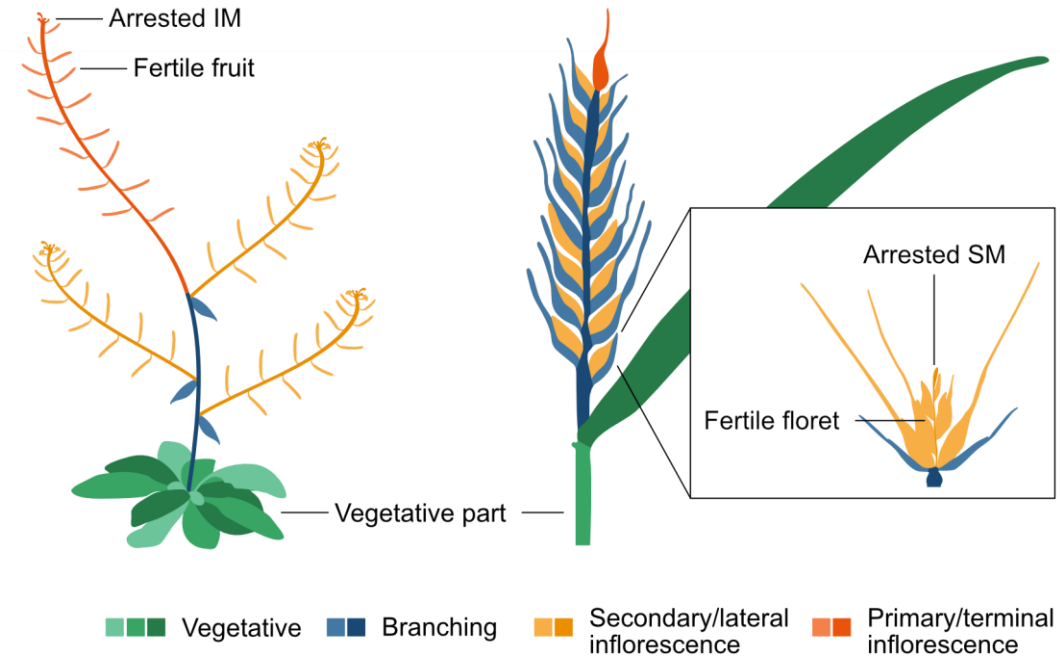

Figure 1.3. Inflorescence architecture in *Triticum aestivum*

Comparative view of inflorescence architecture in *Arabidopsis thaliana* (left) and *Triticum aestivum* (right). Colours indicate functionally and developmentally similar structures. IM: Inflorescence meristem. SM: Spikelet meristem.

1.2. Molecular Control of the End-of-Flowering

Having been largely overlooked over the years, relatively little is known about the molecular background of the end-of-flowering. However, research on the field has recently gained traction, leading to several pieces of work that have shed light on the regulation of this process at genetic and hormonal levels (Balanzà et al., 2023).

1.2.1. Genetic Regulation of End-of-Flowering

During end-of-flowering, IMs from *A. thaliana* experience a process similar to bud dormancy, whereby their cell cycle is interrupted and their proliferative activity, shut down (Merelo et al., 2022; Wang et al., 2020; Wuest et al., 2016). It is likely that this process is at least partially mediated by the homeodomain transcription factor *WUSCHEL* (*WUS*). Before and during flowering, *WUS* acts as a meristem identity marker, maintaining the population of stem cells in the SAM and IM, respectively, undifferentiated (Schoof et al., 2000). This is achieved through a negative feed-back loop in which the *CLAVATA* (*CLV*) genes *CLV1*, *CLV2* and *CLV3* are involved. Briefly, *WUS* promotes the transcription of *CLV3*, whose protein product undergoes post-transcriptional modifications becoming a peptide capable of binding to the receptors *CLV1* and *CLV2*, ultimately triggering a process that leads to the transcriptional repression of *WUS* (Brand et al., 2000; Schoof et al., 2000). This interplay between *WUS* and the *CLV* module is key to maintain the niche of stem cells and, thus, both are necessary for IM activity.

Though the formation and maintenance of IMs is well described, less is known about the processes that underlie their ageing and eventual fate. Interestingly, IM arrest is characterized by a decline in *WUS* expression, which is no longer detected in arrested IMs, suggesting that down-regulation of *WUS* may be necessary for meristematic arrest (Balanzà et al., 2018; Goetz et al., 2021; Merelo et al., 2022;

Wang et al., 2020; Wuest et al., 2016). In contrast, *CLV3* is still expressed in arrested IMs until senescence is initiated, likely to avoid the reactivation of *WUS* (Wang et al., 2020). As arrested IMs are able to re-activate, it is possible that processes that induce the reactivation of inflorescences, such as fruit removal, may induce the transcriptional repression of *CLV3*, favouring the up-regulation of *WUS* and, thus, the resumption of IM activity (Merelo et al., 2022; Wang et al., 2020). Another gene important for meristem maintenance, *SHOOT MERISTEMLESS* (*STM*) (Long et al., 1996), shows a transcriptional profile similar to *CLV3* during end-of-flowering (Balanzà et al., 2018), but its role, if any, during IM arrest still remains undescribed.

The decline in *WUS* expression during IM arrest seems to be controlled, at least partially, by plant age through a relatively well described genetic pathway that leads to the transcriptional repression of *APETALA2* (*AP2*), an activator of *WUS* (Balanzà et al., 2018) (**Figure 1.4**). This process is mediated by the MADS box transcription factor FRUITFUL (FUL) and two miRNAs which have a key role in ageing, i.e., *miR156* and *miR172*. During the early stages of development, *miR156* levels are high and *miR172* levels are low, but with the increase of plant age, *miR156* starts to gradually decrease as *miR172* builds up (Wang, 2014). The accumulation of *miR172* during late development has been demonstrated to control IM arrest, as *miR172* represses the transcription of *AP2* and *AP2*-like genes by directly binding to their promoter (Balanzà et al., 2018). Similar to *miR172*, *FUL* levels increase in an age-dependent manner and FUL is also capable of physically binding the region upstream of *AP2* and *AP2*-like genes, repressing their expression (Balanzà et al., 2018). As AP2 is known to promote the expression of *WUS* (Würschum et al., 2006), the *miR172*- and FUL-dependent down-regulation of *AP2* is believed to be key for IM arrest. In accordance with this, inducing an ectopic expression of *AP2* is sufficient to reactivate arrested IMs (Martínez-Fernández et al., 2020). It has been proposed that *FUL* may also lie upstream in the regulation of *CLV3* and *STM* (Balanzà et al., 2018), although this possibility remains to be appropriately tested.

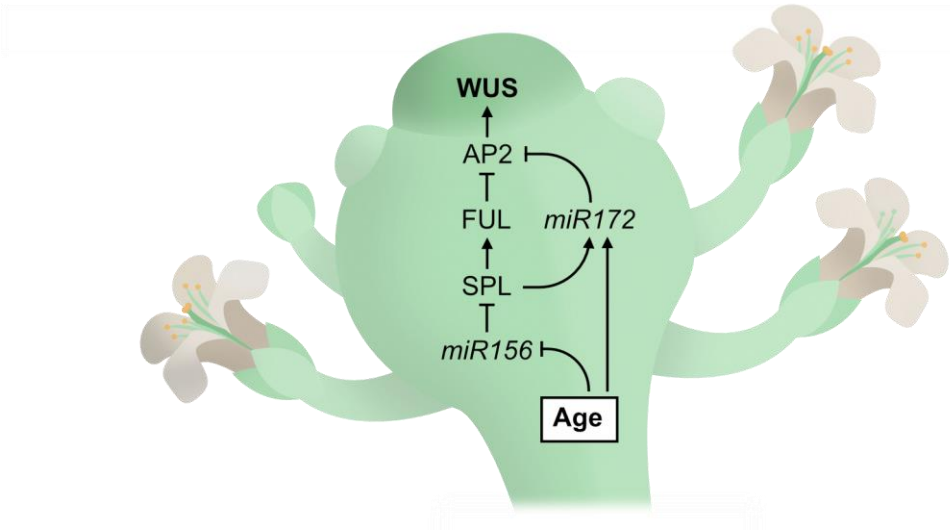

Figure 1.4. Model for the genetic regulation of IM arrest by the age pathway

Diagram depicting the main interactions between components of the age pathway during IM arrest in *Arabidopsis thaliana*. Arrows indicate transcriptional activation and blunted-end arrows represent transcriptional repression.

1.2.2. Regulation by Hormones and Other Signaling Molecules

In recent years, several independent studies have highlighted the relevance of hormonal signaling during end-of-flowering, both for the regulation of arrest and the maintenance of a dormant status in arrested IMs (Balanzà et al., 2023). Cytokinin (CK) is probably one of the hormones with the best characterized role in arrest at the meristematic level. During end-of-flowering, CK levels decrease, leading to an extreme reduction in CK signaling at the IM, which is almost undetectable in arrested IMs (Merelo et al., 2022; Walker et al., 2023). This suggests that CK represses arrest and maintains the activity of the IM, which is in agreement with its established role in stimulating the proliferative activity of the SAM (Yang et al., 2021). In accordance with this, CK signaling is rapidly restored after the reactivation of IMs induced by fruit removal, and exogenous application of N6-benzylaminopurine (BAP), a synthetic CK, can delay arrest and even reactivate arrested IMs (Merelo et al., 2022; Walker et al., 2023).

It has been proposed that CK may control IM activity by regulating the mitotic division of meristematic cells in a WUS-dependent manner (Merelo et al., 2022). Indeed, CK is known to regulate the expression of *WUS* through type-B *Arabidopsis* response regulators (ARRs) (Meng et al., 2017), which mediate the primary responses to CK at the transcriptional level (Zubo and Schaller, 2020). However, the implication of this pathway during end-of-flowering, as well as the potential role of type-B ARRs in arrest is still not well characterized. Interestingly, CK signaling seems to crosstalk with the age-dependent pathway, as FUL represses CK-dependent pathways (Merelo et al., 2022). Specifically, it has been suggested that AP2 may also promote arrest through the transcriptional repression of *KISS ME DEADLY* (K*MD*) genes *KMD2* and *KMD4*, negative regulators of CK signaling (Balanzà et al., 2023), however this has not been demonstrated experimentally. In addition, gain-of-function mutants of *ARABIDOPSIS HISTIDINE KINASE 2* (*AHK2*) and *AHK3*, both CK receptors, are impaired in the timing of both IM and floral arrest (Bartrina et al., 2017; Walker et al., 2023), suggesting that CK signaling may participate in both processes.

Auxin is another hormone with a central role during end-of-flowering, particularly in coordinating the development of the mother plant with that of the newly produced fruits. Recently, auxin exported from the fruits has been proposed to promote inflorescence arrest. Accordingly, a single application of the auxin analog 1-naphthaleneacetic acid (NAA) is sufficient to trigger arrest in a sterile mutant and mutants with disrupted auxin transport show delayed inflorescence arrest (Ware et al., 2020). Auxin synthesized in the aerial part of the plant is known to be loaded into a rootward-moving stream named the polar auxin transport stream (PATS) (van Berkel et al., 2013). Thus, the current model is that developing fruits, as strong auxin producers, may outcompete newer organs, such as younger floral primordia, in a competition to export auxin. Various pieces of evidence support this model. Prior to arrest, auxin transport decreases at the apical part of the inflorescence (Goetz et al., 2021). Furthermore, an exogenous application of the auxin transport inhibitor N-1-

naphthylphthalamic acid (NPA) in the apical area of the inflorescence can trigger premature arrest (Ware et al., 2020). Altogether, these observations suggest that auxin transport from fruits inhibits the auxin export from the latest-produced floral primordia, which could ultimately lead to an arrest in their development, although the molecular basis of this process is still largely uncharacterized.

In addition to CK and auxin, other hormones have been implicated in the control of end-of-flowering during the last years. One of them is abscisic acid (ABA), which has been proposed to participate in IM arrest. The transcriptomic profile of arrested IMs shows a strong up-regulation of ABA-related genes (Wuest et al., 2016). Moreover, this activation of ABA signaling seems to be, at least partially, mediated by AP2, which targets genes associated with ABA synthesis, signaling and response (Martínez-Fernández et al., 2020). Jasmonic acid (JA) is another hormone recently proposed to have a role in the regulation of arrest (J. Kim et al., 2013). However, it is not currently clear whether the effect of JA on arrest is direct or not and further research is still necessary for better understanding its functions during end-of-flowering. Lastly, there are two types of non-hormonal signaling molecules that are beginning to gain attention in the context of end-of-flowering: sugars and reactive oxygen species (ROS). At the IM level, arrest coincides with a clear reduction in sugar signaling, suggesting that sugar metabolism may play a role during this process (Goetz et al., 2021). Specifically, it has been proposed that this could be mediated by the trehalose-6-phosphate (T6P) pathway, although more work is necessary to fully characterize the function of sugars, including T6P, as signaling molecules during inflorescence arrest (Balanzà et al., 2023). On the other hand, ROS accumulate in IMs during arrest (Wang et al., 2020) and ROS-related genes are over-represented in the transcriptomic profile of arrested IMs (Wang et al., 2022; Wuest et al., 2016). In the SAM, the ROS $O2^{\cdot-}$ and H_2O_2 participate in the maintenance of the stem cell pool in a WUS-dependent manner (Zeng et al., 2017), raising the possibility that they also control *WUS* during IM arrest, although this still remains to be properly tested.

1.3. Environmental Control of End-of-Flowering

As sessile organisms, plants face a variety of adversities during their lifetime without the ability to escape danger or stressful circumstances (Domagalska and Leyser, 2011). It is therefore crucial for them to properly synchronize such an energy-demanding process as flowering with the appropriate environmental conditions (Bratzel and Turck, 2015; Li et al., 2016). To achieve this, plants are capable of sensing environmental signals and altering their reproductive development accordingly (Kudoh, 2019). Indeed, the central role of the environment in timing the beginning of flowering has been widely described in numerous species (Lifschitz et al., 2014; Song, 2016; Srikanth and Schmid, 2011). It has been proposed that environmental inputs also impact the timing of end-of flowering (Miryeganeh, 2020; Miryeganeh et al., 2018; Nagahama et al., 2018), although the evidence supporting this idea is scarce.

1.3.1. Temperature Control of End-of-Flowering

Along with light, temperature is one of the most well-described environmental cues that affect flowering time (Song, 2016; Srikanth and Schmid, 2011). In the model species *A. thaliana*, warmer temperatures tend to promote the transition into flowering through a genetically controlled mechanism, the ambient temperature pathway (Capovilla et al., 2015). Though evidence supporting a role for temperature during end-of-flowering is limited, a number of reports point towards the idea that warm temperatures could also accelerate end-of-flowering in a range of species, including the annual *Cardamine hirsuta* (Cao et al., 2016), the perennial *Arabidopsis halleri* (Nagahama et al., 2018; Satake et al., 2013) and even *Citrus* trees (Lomas and Burd, 1983). However, contradictory results have also been found. Such is the case of alpine species from the genus *Potentilla*, in which the duration of flowering

does not respond to warming (Dorji et al., 2020). These disagreements could be due to the use of different methods to measure floral duration or to different species showing differential responses to environmental factors. Accordingly, various species from the tropical dry forest showed differential responses to environmental factors in regards to the duration of flowering (Cortés-Flores et al., 2017).

Recent research supports a key role for ambient temperature in controlling end-of-flowering in *A. thaliana*, with plants exposed to higher temperatures showing a reduced duration of flowering (Miryeganeh, 2020). This is somewhat consistent with a previous work which demonstrated that warmer temperatures accelerate the timing of seed dispersal (Springthorpe and Penfield, 2015). However, the genetic basis of this process remains largely uncharacterized and it is still unclear at which point in development temperature regulates end-of-flowering. In any case, the response to temperature seems pivotal for the synchronization of life history transitions with the environment under natural conditions, particularly in plants adapted to seasonal climates. Indeed, a shortening the duration of flowering in plants that germinate later in spring ensures that reproductive development is completed before the arrival of the hotter and drier season of summer (Miryeganeh, 2020; Miryeganeh et al., 2018).

Vernalization is a different process mediated by temperature. Upon exposure to a prolonged period of cold, certain species, including winter accessions of *A. thaliana*, acquire the competence to flower (Lempe et al., 2005). In plants with a vernalization requirement, exposure to long spans of cold accelerates the transition into flowering through a process genetically controlled by the vernalization pathway (Kim and Sung, 2014). This phenomenon is particularly important in temperate areas, where it ensures that plants flower in favourable seasons (Luo and He, 2020). However, despite the great impact of vernalization on the onset of flowering, its role during end-of-flowering still remains uncharacterized.

1.3.3. Light Control of End-of-Flowering

Light is another well-described environmental input known to regulate reproductive development. However, it is also a complex signal with different characteristics, most of which affect the timing of flowering, including light quality, light intensity and day length (Ausin et al., 2004). The latter is perhaps the best understood in the context of flowering. As a facultative long-day plant, *A. thaliana* transitions into flowering earlier when grown under longer day lengths (Melzer et al., 2008), a process largely controlled at the molecular level by the photoperiod pathway (Song et al., 2015; Srikanth and Schmid, 2011). Even though the effect of light on the onset of flowering has long been established, its impact on end-of-flowering is still unclear. In wheat and other cereals, photoperiod-insensitive genotypes exhibit a shorter duration of flowering under non-inductive short days (Royo et al., 2016), suggesting that day length may play a role in end-of-flowering. Early works on end-of-flowering in *A. thaliana* indicate that day length could also affect the timing of inflorescence arrest in this species (Hensel et al., 1994), although a more detailed examination would allow to confirm this as well as to assess the effect of other light components.

1.3.4. Control of End-of-Flowering by Other Environmental Factors

Another environmental factor that has been suggested to control the end-of-flowering is nutrient availability. A study on pea reported that nitrogen starvation reduced the duration of flowering, and that this effect was exclusively due to an acceleration of the end of flowering (Jeuffroy and Sebillotte, 1997). Aside from abiotic cues, certain biotic factors may play a role in the end of flowering, such as herbivory or competition for resources. For instance, a study reported differences in the duration of flowering between plants that are pollinated by different types of insects,

highlighting the importance of interactions with the surrounding organisms (Cortés-Flores et al., 2017). A different example is plant-plant interactions. Crowding, i.e., the presence of a high density of plants in a given space, is known to affect plant growth and alter flowering phenology. In the herbaceous *Cardamine hirsuta*, a high density of plants shortens the duration of flowering, suggesting that the limitation of resources caused by competition was able to accelerate the end of flowering (Cao et al., 2016). Nevertheless, neither the effect of nutrient availability nor that of biotic factors has been explored before during end-of-flowering in *A. thaliana*.

1.4. Molecular Basis of the Environmental Control

Although fragmentary, research on the end-of-flowering supports the idea that the environment plays a key role in the regulation of this process. But how this environmental regulation works at the molecular level still remains a mystery and the current genetic models for inflorescence arrest do not include such external cues. Taking this into account, the key to unravel how the environment drives the end of flowering may lie in a good understanding of how it drives its initiation. Since floral transition and arrest constitute tightly related developmental transitions, it is possible that similar molecular signals participate in both processes.

To date, up to seven molecular pathways have been described to control flowering time in *A. thaliana*: photoperiod, ambient temperature, vernalization, age, autonomous, gibberellin and trehalose-6-phosphate (Quiroz et al., 2021; Song et al., 2015; Srikanth and Schmid, 2011). Each one depends on distinct signaling components, but they all tend to converge on just a few genes that act as central regulators, collectively known as floral integrators, which ultimately allow to coordinate endogenous and environmental signals to shape reproductive development (Song et al., 2015).

1.4.1. *FLOWERING LOCUS T:* A Central Regulator of Flowering

In many plant species, the timing of floral transition is determined by the balance between signaling molecules that promote flowering and those that inhibit it (Higuchi, 2018). The main flowering-promotive gene characterized so far is *FLOWERING LOCUS T* (*FT*), which encodes a phosphatidylethanolamine-binding protein (PEBP). *FT* is considered a central regulator of flowering time, as it integrates much of the external information perceived by the plant through well-described molecular pathways (Bratzel and Turck, 2015; Turck et al., 2008; Wickland and

Hanzawa, 2015). Generally speaking, once environmental conditions are optimal for the plant to flower, a series of upstream mechanisms lead to the expression of *FT* in the companion cells of the leaf phloem (Corbesier et al., 2007). FT protein is then loaded into the phloem and transported to the SAM, where it complexes with the bZIP-type transcription factor FLOWERING LOCUS D (FD) (Wigge et al., 2005). The FT-FD complex can then activate the expression of downstream meristem identity genes, triggering the conversion of the SAM into an IM and, thus, the transition into flowering (Corbesier et al., 2007; Notaguchi et al., 2008).

While FT has a pivotal role in controlling flowering time, it is not the only signal that promotes the transition into flowering. *TWIN SISTER OF FT* (*TSF*), a close paralog of *FT*, also induces flowering by interacting with FD and activating downstream meristem identity genes (Wickland and Hanzawa, 2015). Moreover, gibberellin is a flowering-promotive hormone with a particularly important function in the induction of flowering in non-inductive short days (Wilson et al., 1992) through a mechanism that is, at least partially, FT-independent (Hisamatsu and King, 2008).

1.4.2. The Role of Light in Flowering Time

At the molecular level, the photoperiod pathway, which mediates the regulation of flowering time by day length, is perhaps the most well-described floral pathway (Song et al., 2015; Srikanth and Schmid, 2011). In *A. thaliana*, a facultative long-day plant (Kobayashi and Weigel, 2007), floral transition is accelerated by longer day lengths. This is achieved through the induction of *FT* as a result of an intricate signaling cascade that controls the expression and protein stability of both FT and its main transcriptional activator, *CONSTANS* (*CO*) (Song et al., 2015) (**Figure 1.5**). In short, *CO* mRNA and protein levels are highly controlled by the circadian clock and light signaling components and, therefore, show a circadian

rhythm (**Figure 1.5A**). Under long days, *CO* expression and protein stability peak towards the end of the day, which promotes the transcription of *FT* at dusk. In contrast, under short days, *CO* transcriptional down-regulation and CO protein destabilization decrease CO to barely detectable levels, inactivating the induction of *FT* and, thus, delaying flowering. A handful of regulators of both *CO* and *FT* have been characterized so far, among which GIGANTEA (GI) and the CYCLING DOF FACTOR (CDF) family play a central role (Song et al., 2015; Srikanth and Schmid, 2011; Turck et al., 2008) (**Figure 1.5B**).

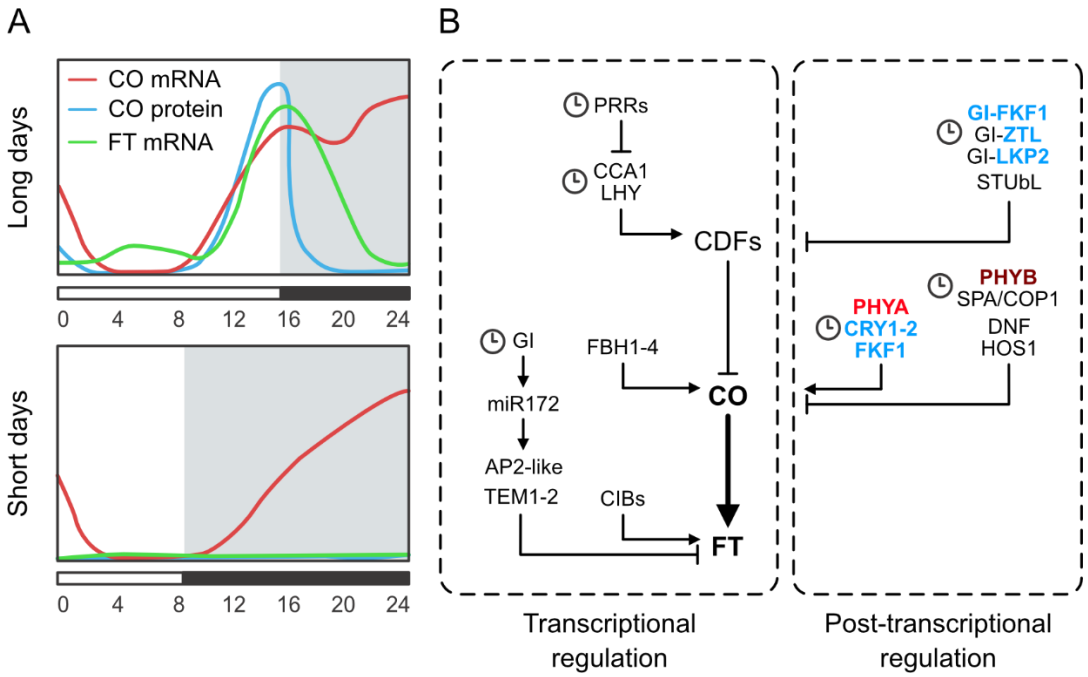

Figure 1.5. Molecular mechanisms involved in the photoperiod pathway

A. Diurnal fluctuations in the levels of *CO* mRNA, CO protein and *FT* mRNA during long days (top) and short days (bottom). **B.** Genes from the photoperiod pathway and the circadian clock that exert a regulation on FT and/or CO. Colours indicate ability to perceive light at certain wavelength (blue, red or far red). Clock symbols are assigned to components of the circadian clock. Adapted from Turck et al., 2008. Arrows indicate transcriptional or post-transcriptional activation and blunt-ended arrows indicate repression.

Although less characterized at the genetic level, light quality also impacts flowering time in *A. thaliana*. Specifically, blue and far-red (FR) light tend to accelerate flowering while red light tends to repress it (Song et al., 2015). This is mediated by a range of photoreceptors, mainly phytochromes and cryptochromes. Phytochromes are red and FR light absorbing photoreceptors (Rockwell et al., 2006). There are 5 homologues in *A. thaliana*, among which PHYTOCHROME A (PHYA) has been suggested as the one responsible for the acceleration of flowering by FR light whereas PHYTOCHROME B (PHYB) seems to control the repressing effect of red light (Valverde et al., 2004). The remaining three, i.e., PHYTOCHROME C, D and E; are thought to have redundant roles, at least in the control of flowering. Contrary to phytochromes, cryptochromes are blue and UV-A light absorbing photoreceptors (Rockwell et al., 2006). In *A. thaliana*, both existing homologues, CRYPTOCHROME 1 (CRY1) and CRY2 participate in the promotion of flowering by blue light, with CRY2 having the main role (Zuo et al., 2011). The exact mechanism through which photoreceptors regulate flowering time is not fully resolved, although it requires, at least partially, crosstalk with the photoperiod pathway (Valverde et al., 2004).

It is worth noting that light intensity also affects flowering time in *A. thaliana*, with higher light intensities accelerating the transition into flowering (Susila et al., 2016). The genetic pathway underlying this response is very poorly understood, but it seems to involve retrograde signaling form the chloroplast and the two transcription factors FLOWERING LOCUS C (FLC) and PHD TYPE TRANSCRIPTION FACTOR WITH TRANSMEMBRANE DOMAINS (PTM) (Feng et al., 2016).

1.4.3. The Role of Temperature in Flowering Time

Aside from light, temperature also has a great impact on the timing of flowering. In *A. thaliana*, warm temperatures accelerate flowering (Balasubramanian

et al., 2006) while cold ones delay it (Lee et al., 2013). This is regulated by the ambient temperature pathway (also named the thermosensory pathway), which, similarly to the photoperiod pathway, operates in an *FT*-dependent manner but which is much less understood (O'Connor et al., 2020). However, a few of its components have been identified, including floral repressors like SHORT VEGETATIVE PHASE (SVP) and members of the FLOWERING LOCUS C (FLC) clade, which includes FLC, FLOWERING LOCUS M (FLM, also called MAF1) and four other related genes, MAF2-5. FLC and its homolog FLM interact with SVP forming a complex that represses the transcription of *FT* and other floral promoters (Capovilla et al., 2015). In the case of FLM, only one of its splicing variants, FLM-β, which is predominant at low temperatures, seems to exert this repression. Under higher temperatures, alternative splicing of FLM shifts and favours the dominant-negative form, FLM-δ, which replaces FLM-β in the SVP-FLM complex, rendering it inactive (Capovilla et al., 2017; Lee et al., 2013). This, added to the inhibition of SVP-FLM complexes which also takes place at high temperatures, releases the inhibition of *FT*, ultimately promoting flowering (Capovilla et al., 2017) (**Figure 1.6**).

Other than through SVP and the FLC family, temperature leads to the regulation of *FT* via several less well-known mechanisms. Two genes from the autonomous pathway, FLOWERING CONTROL LOCUS A (FCA) and FVE are also involved in the ambient temperature pathway as strong floral activators. Not only do they induce *FT* directly but they also repress *SVP* under higher temperatures, triggering an acceleration of flowering (Ausin et al., 2004). Another mechanism involved in the thermal control of flowering, specially under high temperatures, acts through PHYB and the bHLH transcription factors PHYTOCHROME INTERACTING FACTOR 4 (PIF4) and PIF5. Both PIF4 and its close homolog PIF5 promote flowering through activation of *FT*, a process that is favoured in warmer temperatures and which strongly depends on the photoperiod pathway (Fernández et al., 2016) (**Figure 1.6**). It has been suggested that the PIF4-dependent activation of *FT* is mainly

relevant in short days, where heat up-regulates PIF4 through both FCA and EARLY FLOWERING 3 (ELF3) (Press et al., 2016).

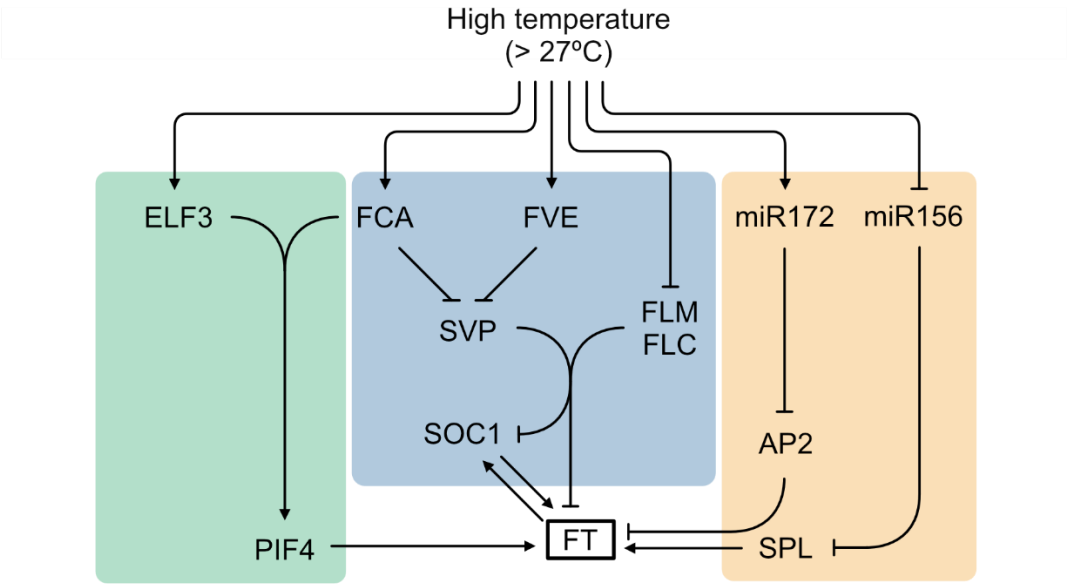

Figure 1.6. Molecular mechanisms involved in the thermosensory pathway

Diagram highlighting the genes from the thermosensory pathway that exert a regulation on FT in *Arabidopsis thaliana*. The PIF4 module (left) is tightly related to day length. The SVP-FLC module (centre) relies on the joint activity of SVP and members of the FLC clade, which decreases with increasing temperature. The miRNA module (right) is influenced by temperature through the relative abundances of *miR172* and *miR156*. Arrows indicate transcriptional or post-transcriptional activation and blunt-ended arrows indicate repression.

Interestingly, *miR156* and *miR172* have also been proposed as part of the ambient temperature pathway, since their abundance is sensitive to temperature. While *miR156* levels increase at lower temperatures, those of *miR172* do so at higher ones (Lee et al., 2013). Both are involved in the transcriptional regulation of *FT* indirectly via the *miR172*-dependent down-regulation of AP2, a repressor of *FT*, and the *miR156*-dependent repression of SQUAMOSA PROMOTER BINDING PROTEIN-LIKE 3 (SPL3), an activator of FT (Capovilla et al., 2015) (**Figure 1.6**).

In addition to the ambient temperature pathway, the vernalization pathway mediates responses to temperature by repressing the transition into flowering unless the vernalization requirement is met, i.e., until the plant has experienced a sufficiently long span of cold (Luo and He, 2020). The transcriptional regulator FRIGIDA (FRI) plays a central role in this process and is a major determinant of natural variation in the flowering time of *A. thaliana* (Lempe et al., 2005). Prior to vernalization, FRI represses flowering by maintaining a high expression of the floral repressor FLC (Michaels and Amasino, 1999). However, the long exposure to cold temperatures leads to the inactivation of *FLC*, releasing the inhibition of *FT* and triggering the transition into flowering. This only holds true for winter accessions of *A. thaliana*, e.g., Kondara, which carry functional *FRI* alleles. In contrast, rapidly cycling accessions, including the widely used laboratory genotypes Col-0 and Ler, contain one or two deletions in the *FRI* locus, which render FRI inactive and eliminates the vernalization requirement (Johanson et al., 2000).

1.4.4. The Regulation of Flowering Time in Other Species

Numerous studies suggest that the genetic network controlling the timing of flowering is largely conserved in plants (Benlloch et al., 2007). Moreover, the role of *FT* orthologs as promoters of flowering has been well described in a wide range of species (Turck et al., 2008; Wickland and Hanzawa, 2015). However, most of the processes mentioned before have been identified in *A. thaliana* or in related perennial eudicots and, while genes may be functionally conserved across evolutionary distant species, their placement within molecular pathways and responses to the environment tend to differ (Cockram et al., 2007). This is particularly true for monocots including wheat, which is a facultative long-day plant adapted to temperate climates and capable to respond to day length, vernalization and ambient temperature (Greenup et al., 2009). Generally speaking, the genes and proteins that

control flowering time in *A. thaliana* operate through similar molecular mechanisms in wheat (Hill and Li, 2016). However, due to multiple hybridization events taking place throughout its domestication, hexaploid wheat shows a remarkable level of genetic redundancy (Wang et al., 2013) which, in some cases, has given rise to gene neo- and/or sub-functionalization (Bennett and Dixon, 2021).

In wheat, the control of flowering time is classically attributed to three groups of loci: photoperiod (*PPD*), vernalization (*VRN*) and earliness *per se* (*EPS*) (Hill and Li, 2016). The first encompasses three homologs from the pseudo-response regulator family that regulate the regulation of flowering time by photoperiod, i.e., *PPD-A1*, *PPD-B1* and *PPD-D1* (Bentley et al., 2013; Li et al., 2016). These lie upstream of *VRN3*, also named *FT1*, one of the homologous of *FT* in wheat, which offers a regulatory checkpoint where both the photoperiod and vernalization pathways converge (Yan et al., 2006). Similar to *A. thaliana*, *FT1* expression in wheat takes place in the leaves, from which FT1 protein is transported to the SAM (Li et al., 2015). In the SAM, FT1 forms protein complexes with FD-like and 14-3-3 proteins which are able to transcriptionally activate downstream genes, including *VRN1*, a MADS-box transcription factor associated with floral identity and homologous to *AP1* from *A. thaliana* (Yan et al., 2003; Li et al., 2015). In addition, FT1 also promotes the expression of *VRN1* in the leaves, and the resulting VRN1 protein is able to repress the transcription of *VRN2*, a third *VRN* gene which encodes a protein with a protein-protein interaction domain (Yan et al., 2004). Conversely, VRN2 represses the expression of *FT1*, acting as a floral repressor that creates a complex feed-back loop which allows to fine-tune the response to day length and temperature signals in wheat. In contrast to *PPD* and *VRN* loci, *EPS* genes are associated with autonomous pathways that are photoperiod- and vernalization-independent (Hill and Li, 2016), suggesting a lesser role in the control of flowering time by the environment, although they can respond to certain environmental cues (Appendino and Slafer, 2003).

1.4.5. Flowering Time Genes in the End-of-Flowering

In contrast to the vast amount of information that is currently available on the molecular regulation of floral transition in response to the environment, virtually nothing is known about how the environment may regulate end-of-flowering. To an extent, flowering is initiated in response to a floral stimulus which informs the plant that the environmental conditions are suitable for flowering (**Figure 1.7A**). Generally speaking, this floral stimulus typically corresponds to either an increase in flowering-promotive signals like FT or a decrease in flowering-repressive molecules such as FLC. It is thus possible that a withdrawal of the same floral stimulus causes end-of-flowering, e.g., a down-regulation of *FT* and/or an up-regulation of *FLC* (González-Suárez et al., 2020) (**Figure 1.7B**). This idea is in fact not novel, and has been previously proposed by several authors. A mathematical model created by Satake et al. predicted that end-of-flowering would coincide with a decrease in *FT* and an increase in FLC (Satake et al., 2013). This appears to be the case in *A. thaliana*, where *FT* levels decline as *FLC* levels peak at the end of the reproductive period (Miryeganeh et al., 2018; Wuest et al., 2016), suggesting a role for both signals in arrest. However, different trends are found in other organisms, suggesting that the relative importance of FT and FLC may vary between species. In *A. halleri*, *FT* levels also decline at the end of flowering (Nagahama et al., 2018). While this does not seem to correlate with an increase in FLC levels in this study, other works report an up-regulation of FLC towards end-of-flowering which would be consistent with the patterns observed in *A. thaliana* (Shimizu et al., 2011). In the perennial *A. alpina*, FLC probably plays a greater role, as mutants lacking the *FLC* ortholog *PERPETUAL FLOWERING 1* (*PEP1*) are unable to resume vegetative growth after flowering (Bergonzi et al., 2013; Wang et al., 2009). As a result, individual inflorescences arrest, but the plant remains in a perpetual reproductive episode.

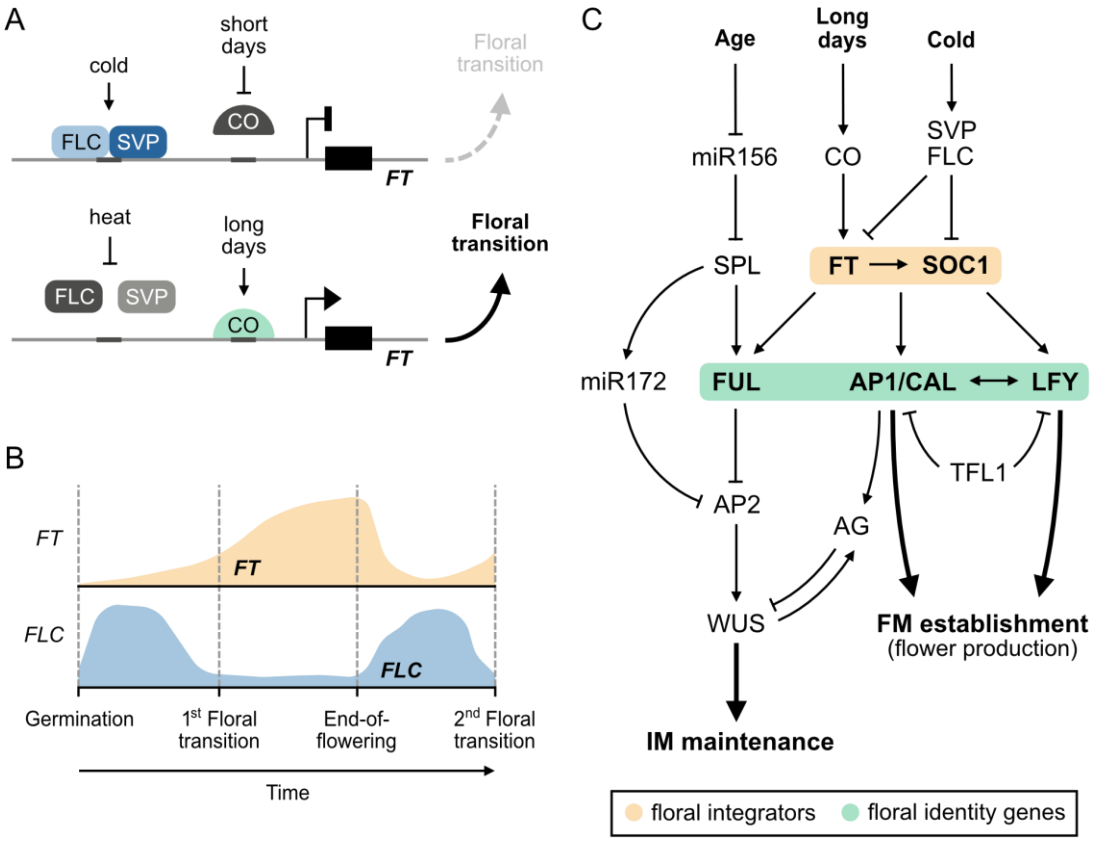

Figure 1.7. Environmental regulation of end-of-flowering at the molecular level

A. Upstream regulation of *FT* in response to environmental signals in *Arabidopsis thaliana*. Cold promotes the formation of FLC-SVP, a complex that represses *FT* expression, while moderate increases in temperature inhibit the formation of the complex. Day length also affects *FT* expression through CO, which peaks at the end of long days. **B.** Predicted expression of *FT* and *FLC* throughout the life cycle of a generic perennial species from the Brassicaceae family. The relevant developmental transitions are indicated below. **C.** Proposed model for the environmental control of inflorescence arrest in *Arabidopsis thaliana* at the molecular level. Photo-thermal information is processed by the floral integrators *FT* and *SOC1*, which are up-regulated in response to favourable conditions, leading to an induction of meristem identity genes that are crucial for IM maintenance and flower production. Downstream targets of *FT* and *SOC1* include *FUL*, *AG* and, ultimately, *WUS.* Arrows indicate transcriptional or post-transcriptional activation and blunt-ended arrows represent repression.

The downstream targets of FT and FLC during arrest are still unknown. FT is known to induce the expression of *FUL* (Collani et al., 2019), suggesting that the age pathway of IM arrest may be under control by the environment in an FT-dependent manner (**Figure 1.7C**). An alternative explanation may lie in a different target of both FT and FLC, *SUPRESSOR OF CONSTANS 1* (*SOC1*). SOC1, also considered a floral integrator (Bratzel and Turck, 2015), is a MADS-box transcription factor whose functions partially overlap with those of FUL (Melzer et al., 2008). Simultaneously to the induction of *FUL*, FT also triggers the expression of *SOC1*. The SOC1 protein is then able to interact with FUL and other proteins to up-regulate the floral identity gene *APETALA 1* (*AP1*) (Balanzà et al., 2014; Lee and Lee, 2010). This process is fundamental to ensure FM identity, since *AP1* also shuts down the activity of *WUS* through the activation of another MADS-box transcription factor, AGAMOUS (AG), which is a repressor of *WUS* (Lenhard et al., 2001). The activation of AG has classically been associated with FMs but, recently, it has been demonstrated that the same could apply to the IM (Balanzà et al., 2019). Therefore, regulation of WUS in the IM could also be mediated by FT, which raises a new potential pathway for the control of inflorescence arrest in *A. thaliana* (**Figure 1.7C**). Nevertheless, the mechanisms surrounding the regulation of IM arrest by the environment and, specifically, by FT, are still hugely understudied, and further investigation is necessary to better understand them.

1.5. Aims

Considering how little is currently known about the impact of the environment on the end-of-flowering, the main aim of this thesis is to characterize the environmental control of this developmental transition at both the physiological and genetic levels. To achieve this, the following specific goals are proposed:

1) To characterize the effect of different environmental signals on inflorescence arrest in *A. thaliana.*
2) To identify genes underlying the environmental control of arrest in *A. thaliana* and, particularly, to characterize the potential role of the floral integrator *FT*.
3) To explore the natural variation of end-of-flowering responses among natural accessions of *A. thaliana*.
4) To assess the effects of the environmental control of end-of-flowering and ageing on offspring production in *A. thaliana*.
5) To characterize the environmental control of end-of-flowering in other plant species and, particularly, in hexaploid wheat (*T. aestivum*).

.

Chapter 2: Material and Methods

2.1. Biological Material

2.1.1. *Arabidopsis thaliana*

Arabidopsis thaliana Col-0 was used as the reference genotype for all plant experiments, unless otherwise specified. Other natural accessions of *A. thaliana* that were used are indicated in **Table 2.1**, and a summary of all mutants used throughout this thesis can be found in **Table 2.2**. All of the mutants were in the Col-0 background except for *co-2*, *ft-1*, *gi-4*, *phyA-201* and *phyB-1*, which were in the Ler background, and all had been characterized before.

Table 2.1. Natural accessions of *Arabidopsis thaliana* used in this work

The first and second columns indicate the abbreviated and full names of each accession. Identifiers for the Nottingham Arabidopsis Stock Centre (NASC) and the 1001 Genomes Project (1001G) are included in the third to and fourth columns. Country of origin is indicated in the last column.

Identifier	Name	NASC	1001G	Country
Aa-0	Aua	N76428	7000	Germany
Altenb-2	Altenburg	N76353	9970	Italy
Ang-0	Angleur	N76436	6992	Belgium
Angel-1	Sant Angelo	N76362	9980	Italy
Angit-1	Ponte Angitola	N76366	9981	Italy
Bå1-2	Ba	N76676	8256	Sweden
Bå4-1	Ba	N76677	8258	Sweden
Bla-2	Blanes	N28080	N/A	Spain
Blh-1	Bulhary	N28089	7034	Czech Republic
Bolin-1	Bolintin Vale	N76373	10004	Romania
Boot-1	Boot, Eskdale	N76452	7026	United Kingdom

Identifier	Name	NASC	1001G	Country
Borsk-2	Borskoje	N76421	9957	Russia
Bra-1	Braithwaite	N77832	5717	United Kingdom
Col-0	Columbia	N76778	6909	United States
Col-2	Columbia	N28170	N/A	United States
Copac-1	Copac	N76420	10005	Serbia
Edi-5	Edinburgh	N28962	N/A	United Kingdom
Ei-2	Eifel	N76478	6915	Germany
Ema-1	East Malling	N76480	7109	United Kingdom
En-1	Enkheim	N76841	8290	Germany
Ey15-2	Eyach	N76399	N/A	Germany
Fei-0	St. Maria d. Feiria	N76412	9941	Portugal
Gd-1	Gudow	N76491	7161	Germany
Gel-1	Geleen	N76492	7143	Netherlands
Hi-0	Hilversum	N76921	N/A	Netherlands
HKT2.4	Heiligkreuztal 2	N76404	9995	Germany
Hs-0	Hannover, Stroehen	N76515	7162	Germany
HSm	Horni Smrcne	N76941	8236	Czech Republic
Is-1	Isenburg	N28362	N/A	Germany
Jl-3	Jl	N76519	7424	Czech Republic
Jm-0	Jamolice	N76520	7177	Czech Republic
Kidr-1	Kidrjasovo	N76376	9960	Russia
Kondara	Kondara	N76532	6929	Tajikistan
Koz-2	Kolyvanskoe ozero	N76383	9953	Russia
Krot-0	Krottensee	N76534	7203	Germany
Kyoto	Kyoto	N76535	7207	Japan
Lag2-2	Lagodechi	N76390	9990	Georgia
Lago-1	Rocigliano-Lago	N76367	9963	Georgia
Lecho-1	Lechovo	N76371	9987	Romania
Ler	Landsberg	N1642	6932	Germany
Lo-2	Lorrach	N78269	7242	Germany
Li-3	Limburg	N28454	N/A	Germany
MOG-11	MOG-11	N77503	N/A	France

Identifier	Name	NASC	1001G	Country
Moran-1	Morane	N76363	N/A	Italy
Mrk-0	Märkt	N76554	N/A	Germany
Nie1-2	Niederreutin	N76402	9996	Germany
No-0	Nossen	N77128	7273	Germany
Nw-4	Neuweilnau	N28577	N/A	Germany
Ove-0	Ovelgoenne	N76569	7287	Germany
PAR-8	PAR-8	N77513	N/A	France
Petro-1	Petrovac	N76370	10017	Serbia
Ra-0	Randan	N76582	6958	France
RAN	RAN	N77516	N/A	France
Rue3-1-31	Rubgarten - 3	N76406	9997	Germany
Rd-0	Rodenbach	N76584	8366	Germany
Shigu-2	Shiguljovsk	N76374	9959	Russia
Sij-1	Sidzhak	N76379	10008	Uzbekistan
Sij-2	Sidzhak	N76380	10009	Uzbekistan
Slavi-1	Slavianka	N76419	9985	Bulgaria
Star-8	Starzach	N76400	9998	Germany
Stepn-1	Stepnoje	N76378	9956	Russia
Stepn-2	Stepnoje	N76377	9955	Russia
Timpo-1	Timpo Ulivi	N76424	9968	Italy
Tottarp-2	Tottarp	N77381	6243	Sweden
Tu-0	Turin	N76617	7375	Italy
TueSB30-3	Tubingen – Schonblick 30	N76403	9999	Germany
Ullapool-3	Ullapool	N75649	N/A	United Kingdom
UKID96	UKID96	N78791	5800	United Kingdom
Uod-7	Uod	N22613	6976	Austria
Van-0	Vancouver	N1584	7383	Canada
Wal-HasB-4	Walddorf-Haslach	N76408	N/A	Germany
WAR	WAR	N8143	7477	United States
Ws-0	Wassilewskija	N1602	7396	Russia
Ws-2	Wassilewskija	N1601	6981	Russia
Yeg-1	Yeghegis	N76394	10011	Armenia

Table 2.2. Mutants of *Arabidopsis thaliana* used in this work

The first, second and third columns indicate the name of the mutant, the background and the allele, respectively. The fourth column includes the identifier of the mutated gene. The last column indicates the source of the germplasm.

Mutant	Backg.	Alleles	Gene ID	Source
arr1	Col-0	*arr1-4*	AT3G16857	NASC (N6972)
arr3,4,5, 6,7,15	Col-0	*arr3* *arr4* *arr5* *arr6* *arr7* *arr15-2*	AT1G59940 AT1G10470 AT3G48100 AT5G62920 AT1G19050 AT1G74890	Donated (Zhang et al., 2011)
co	Ler	*co-2*	AT5G15840	NASC (N55)
d14	Col-0	*d14-1*	AT3G03990	NASC (N913109)
elf3	Col-0	*elf3-7*	AT2G25930	NASC (N3793)
elf4	Col-0	*elf4-1*	AT2G40080	NASC (N9879)
flc	Col-0	*flc-6*	AT5G10140	NASC (N541126)
flm	Col-0	*flm-3*	AT1G77080	NASC (N667504)
ft	Col-0	*ft-10*	AT1G65480	NASC (N9869)
ft	Ler	*ft-1*	AT1G65480	NASC (N56)
gi	Ler	*gi-4*	AT1G22770	NASC (N181)
max4	Col-0	*max4-5*	AT4G32810	Donated (Bennett et al., 2006)
phyA	Ler	*phyA-201*	AT1G09570	NASC (N6219)
phyB	Ler	*phyB-1*	AT2G18790	NASC (N69)
pif4 pif5	Col-0	*pif4-2* *pif5-3*	AT2G43010 AT3G59060	NASC (N68096)
smxl6,7,8	Col-0	*smxl6-4* *smxl7-3* *smxl8-1*	AT1G07200 AT2G29970 AT2G40130	Donated (Soundappan et al., 2015)
svp	Col-0	*svp-32*	AT2G22540	NASC (N666411)
tsf	Col-0	*tsf-1*	AT4G20370	Donated (Yamaguchi et al., 2005)

2.1.2. *Triticum aestivum*

Spring hexaploid wheat (*Triticum aestivum*) *cv.* Cadenza was used as the reference genotype for plant experiments, unless otherwise specified. Additionally, a collection of 37 landraces was used, all of which were obtained from the International Maize and Wheat Improvement Center (CIMMYT) (**Table 2.3**).

Table 2.3. Landraces of *Triticum aestivum* used in this work

The first column indicates the accession code used throughout the text. The second and third columns contain the identifiers as catalogued by the CIMMYT. The last column indicates the country of origin.

Code	Identifier	Name	Origin
003	BW 7227	Artemovka	Former Soviet Union
004	BW 9798	K6867	Kenya
005	BW 11386	Australiano	Bolivia
007	BW 19498	Lohari Y91-92 NO. 123	Nepal
008	BW 19506	Lohari Y91-92 NO.70	China
009	CWI 2164	K7176.29	Kenya
010	CWI 2165	K7155.22	Kenya
011	CWI 2166	K7155.41	Kenya
012	CWI 2167	K7155.66	Kenya
014	CWI 3574	Improved Fife	United States
015	CWI 3909	Oubaard	South Africa
016	CWI 3923	Rooi Egipties	South Africa
017	CWI 3924	Rooi Indies	South Africa
018	CWI 3926	Rooi Spitskop	South Africa
019	CWI 3927	Rooi Stormberg	South Africa
020	CWI 3961	UNIE 31	South Africa
021	CWI 6075	KOELZ W 9375:AE	India
023	CWI 6095	KOELZ W 9469:AE	India
024	CWI 6106	KOELZ W 9555:AE	India
025	CWI 6109	KOELZ W 9558:AE	India

Code	Identifier	Name	Origin
029	CWI 7394	Hindi 62	Egypt
030	CWI 8095	Hindi	Egypt
031	CWI 8293	Noe	Bolivia
032	CWI 8320	Plan Alto	Brazil
033	CWI 9391	PI 250413	Pakistan
035	CWI 11053	Najah-Leb	Lebanon
036	CWI 11149	Generoso	Argentina
037	CWI 11729	Red Fife	Australia
039	CWI 12972	Surhak 5688	Former Soviet Union
040	CWI 13229	Darkan	Australia
042	CWI 13339	Chul Bidai	Uzbekistan
043	CWI 13369	Ontario Wonder	United States
046	CWI 13371	Humpback	United States
048	CWI 13434	Indian	United States
049	CWI 13473	Federation	Australia
050	CWI 13561	White-Russian	China

2.1.3. Other Plant Species

Four additional species were used, all from the Brassicaceae, i.e., *Capsella bursa-pastoris*, *Capsella rubella*, *Cardamine hirsuta* and *Olimarabidopsis pumila*.

2.1.4. Bacterial Strains

New England Biolabs 10-β competent *Escherichia coli* (New England Biolabs, C3019H) was used for cloning. Electro-competent *Agrobacterium tumefaciens* GV3101 was used for genetic transformation of *A. thaliana*.

2.2. Growth Media

2.2.1. Plant Growth Media

Arabidopsis thaliana salts (ATS) media (Wilson et al., 1990) was used for the growth of *A. thaliana*. Standard ATS contained KNO_3 (5 mM), KH_2PO_4 (2.5 mM), $MgSO_4$ (2 mM), $Ca(NO_3)_2$ (2 mM), Fe-EDTA (50 µM) and the following micronutrients: H_3BO_3 (70 µM), $MnCl_2$ (14 µM), $CuSO_4$ (0.5 µM), $ZnSO_4$ (1 µM), $NaMoO_4$ (0.2 µM), NaCl (10 µM) and $CoCl_2$ (0.01 µM).

A nitrate (NO_3^-)-limiting growth media was used to test the effect of nitrate on inflorescence arrest (see Chapter 3: **Figure 3.10**). This was based on a modified version of the ATS media which contained 0.5 mM of KNO_3, 0.5 mM of $Ca(NO_3)_2$, supplemented with KCl (4.5 mM) and $CaCl_2$ (1.5 mM) and with the rest of the components unaltered.

2.2.2. Bacteria Growth Media

Escherichia coli was grown on Luria-Bertani (LB) media (Bertani, 1951) prepared using LB broth (Fisher BioReagents, BP1426-2) following the manufacturer's guidelines. *Agrobacterium tumefaciens* was grown on 2x YT media (Sigma Aldrich, Y2377) with rifampicin (100 µg/ml) and gentamicin (10 µg/ml).

When appropriate, growth media was supplemented with antibiotics for the selection of genetically transformed bacteria. Either kanamycin or streptomycin, depending on the antibiotic resistance of the bacteria, were added to the growth media to a final concentration of 50 µg/ml.

2.3. Primers

2.3.1. Cloning Primers

Table 2.4. Primers used for cloning

Name	Sequence 5'-3'
35Spro F	TGAGACTTTTCAACAAAGGGTAATAT
35Spro R	TGTCCTCTCCAAATGAAATGAACT
35Spro attB1 F	GGGGACAAGTTTGTACAAAAAAGCAGGCTTGAGAC TTTTCAACAAAGGGTAATAT
35Spro attB5r R	GGGGACAACTTTTGTATACAAAGTTGTTGTCCTCTC CAAATGAAATGAACT
FT CDS F	ATGTCTATAAATATAAGAGACCCTCT
FT CDS R	AAGTCTTCTTCCTCCGCAG
FT CDS attB5 F	GGGGACAACTTTGTATACAAAAGTTGGTATGTCTAT AAATATAAGAGACCCTCT
FT CDS attB2 R	GGGGACCACTTTGTACAAGAAAGCTGGGTAAAGTC TTCTTCCTCCGCAG

2.3.2. RT-qPCR Primers

Table 2.5. Primers used for RT-qPCR

Name	Sequence 5'-3'
FT QPCR F	CAACCCTCACCTCCGAGAATAT
FT QPCR R	TGCCAAAGGTTGTTCCAGTTGT
UBC9 QPCR F	AGCAATGGAAGCATCTGCCT
UBC9 QPCR R	CTTTTGGGTCCAGGTCCGAG

2.4. Plasmids

Table 2.6. Plasmids used for cloning

Plasmid	Antibiotic resistance	Source
pDONR221 P5-P2	Kanamycin	Thermo Fisher Scientific
pDONR221 P1-P5r	Kanamycin	Thermo Fisher Scientific
GR pFP101	Spectinomycin, streptomycin	Darren Machin

2.5. Enzymes and Kits

Table 2.7. List of enzymes and kits used

Name	Manufacturer	Reference	Purpose
Phusion High-Fidelity DNA Polymerase	New England Biolabs	M0530S	Polymerase chain reaction (PCR), high-fidelity
Taq DNA Pol, ThermoPol Buffer	New England Biolabs	M0267S	Polymerase chain reaction (PCR), low-fidelity
Gateway BP Clonase II Enzyme Mix	Invitrogen	11789100	Cloning
Gateway LR Clonase Enzyme Mix	Invitrogen	11791019	Cloning
RNeasy Plant Mini Kit	Qiagen	74904	RNA extraction
TURBO DNA-free Kit	Invitrogen	AM1907	DNA digestion
Transcriptor First Strand cDNA Synthesis Kit	Roche	4896866001	Synthesis of cDNA
PowerUp SYBR Green Master Mix	Applied Biosystems	A25742	Real-time quantitative PCR (RT-qPCR)

2.6. Plant Growth Conditions

2.6.1. Growth of *A. thaliana* in Soil

In most cases, *A. thaliana* was grown in plant growth chambers (Grobotic Systems), controlled environment rooms (Sanyo) or controlled temperature glasshouses where the temperature was set at 22ºC, the day length, at 16 h of light; and the light intensity, at 100 µmol s^{-1} m^{-2}. Light was supplied by cool-white fluorescent tubes except in the glasshouses, where it was provided by LED lighting (Attis 7, Phytolux). Unstratified seeds were directly sown on 100 ml pots containing a 2:1 (v/v) mixture of compost (Petersfield 2 Supreme, Petersfield) and perlite (Sinclair Perlite, LS Systems Limited). Pots were covered with lids for one week, after which plants were watered three times per week until senescence. Unless otherwise specified, a single plant was grown per pot. Where vernalization was necessary, this was performed by transferring one-week-old seedlings to a growth chamber (Sanyo) set at 10ºC and 8 h light for three weeks, unless otherwise stated. Three different biological control products were used for prevention and control of pests. Predatory mites (Hypoline M, Bioline Agrosciences) and nematodes (Exhibitline Sf, Bioline Agrosciences) were used for the control of scarid fly. Predatory mites (Amblyline CU, Bioline AgroSciences) were used for the control of thrips. Deviations from these standard growth conditions are explained throughout the text.

2.6.2. Growth of *A. thaliana in vitro*

A. thaliana was grown *in vitro* in a single occasion (see Chapter 3, **Figure 4.7**). Before *in vitro* culture, *A. thaliana* seeds were surface-sterilised as follows. First, they were incubated in 70% ethanol for 5 min, followed by a second incubation in 7% bleach for 15 min. Finally, they were washed five times with sterile water. After

sterilization, seeds were sown onto glass jars containing 200 ml of 0.8% agar-solidified Arabidopsis thaliana Salts (ATS) media (Wilson et al., 1990) adjusted at pH 5.6 and supplemented with 1% (w/v) sucrose. Jars were placed in the dark at 4ºC during two days for stratification. Next, they were transferred to a constant temperature room set at 20ºC and a 16/8 h light/dark cycle, where light was provided by fluorescent tubes (36W, Osram) at 120 µmol m^{-2} s^{-1}.

2.6.3. Growth of Other Plant Species

For experiments involving other species from the Brassicaceae family other than *A. thaliana*, seeds were directly sown onto 100 ml pots containing compost (Petersfield 2 Supreme, Petersfield) and stratified for two days in the dark at 4ºC, after which they were transferred to controlled environment rooms (Sanyo) or controlled temperature glasshouses. Unless otherwise specified, temperature was 20ºC, day length, 16 h light; and light intensity, 100 µmol s^{-1} m^{-2}.

For experiments involving *T. aestivum*, unstratified seeds were sown on pots containing compost (Petersfield 2 Supreme, Petersfield). Pot volume was 100 ml with the exception of two experiments (see Chapter 8: **Figure 8.4**, **Figure 8.9**), in which it was 500 ml. Plants were grown in controlled environment rooms (Sanyo) or controlled temperature glasshouses set at 22ºC, 16 h light and 100 µmol s^{-1} m^{-2}.

2.6.4. Growth of Bacteria

Cultures of *E. coli* for cloning and genetic transformation were sown in Luria-Bertani (LB) media (Bertani, 1951) and grown for one day at 37ºC in the dark, with no shaking. Cultures of *A. tumefaciens* for genetic transformation were sown in 2x YT media and grown for two days at 29ºC in the dark with shaking.

2.7 Experimental Treatments

2.7.1. Water Treatments

For experiments controlling the water supply (see Chapter 3: **Figure 3.9**), seeds were directly sown onto 100 ml pots filled with a 1:1 (v/v) mixture of compost and perlite, as normal. Water was supplied from the bottom and trays were covered with lids to maintain humidity and promote germination. After one week, lids and any remaining water were removed. From this point onwards, water was supplied to pots from the top with a serological pipette every two days. The volume of water used was either 15 ml, for the low water treatment; or 35 ml, for the high water treatment.

2.7.2. Nitrate Treatments

For experiments controlling the supply of nitrate (see Chapter 3: **Figure 3.10**), 100 ml pots were filled with a 1:1 (v/v) mixture of vermiculite and sand. A small quantity of compost, i.e., approximately 1 cm^3, was placed on top of the substrate, and seeds were sown onto it. Water was provided from the bottom and trays were covered with lids to maintain humidity and promote germination. After one week, lids and the remaining water were removed and 30 ml of water started to be supplied to pots from the top every two days. Once a week, water was replaced with growth media, either ATS, for control plants; or a N-limiting version of ATS, for the low N treatment.

2.7.3. Application of DEX to Inflorescences

One experiment involved treating individual inflorescences of *A. thaliana* with dexamethasone (DEX) (see Chapter 6: **Figure 6.8**). To do this, plants were grown at

standard conditions until flowering. Approximately 10 days after bolting, and once secondary inflorescences were clearly visible, three inflorescences per plant were separately tagged and subjected to different treatments. One was left untreated, one was treated with DEX and the last was treated with a control solution. A 10 mM DEX stock solution was prepared by dissolving DEX in 70% ethanol, 2% DMSO solution. For the DEX treatment, this was further dissolved into lanolin to a final concentration of 1 mM, and the DEX-lanolin mixture was applied to the base of the inflorescence. For the control treatment, a 70% ethanol, 2% DMSO solution was mixed with lanolin.

2.7.4. Spikelet Removal

One experiment involved surgically removing individual spikelets from a developing wheat spike (see Chapter 7: **Figure 7.4**). To do this, *T. aestivum cv.* Mulika plants were grown in standard conditions for three months, as previously described. The spikelet removal treatment was applied when plants had ~6 emerged leaves and before heading by cutting an opening of ~1x5 cm in the main stem at the height of the developing spike using a surgical blade. Next, 3-6 of the bottom-most spikelets were removed with forceps, after which the opening was gently sealed with parafilm. A different set of plants was subjected to a control treatment by performing the surgical cut without removing any spikelets, and a last group was left untreated.

2.8. Crossing of *A. thaliana*

Crossing of *A. thaliana* plants (see Chapter 5) was performed approximately 10 days after flowering of both parentals, once opened flowers were visible in secondary inflorescences. For each inflorescence of the mother plant, tweezers were used to gently remove all reproductive nodes (i.e., siliques, flowers and floral

primordia) and the inflorescence meristem (IM), leaving only the oldest unopened bud. Next, sepals, petals and anthers of the remaining bud were carefully removed. On the following day, anthers from the father plant were collected with forceps and tapped on the stigma of the mother plant, transferring the donor pollen. Pollinated plants were grown for 1-2 more weeks, until siliques were fully mature, after which the hybrid seed was collected from them.

2.9. Phenotypic Measurements in the Brassicaceae

2.9.1. Bolting

Twice a week, plants were checked for signs of bolting. Bolting was defined as the first day on which floral buds were visible in the centre of the rosette. The number of leaves at bolting was also recorded.

2.9.2. Inflorescence Duration and Fruit Set

After bolting, the number of siliques and flowers in the primary inflorescence were counted three times per week. Inflorescence arrest was defined as the last day on which a new flower was opened in the primary inflorescence and inflorescence duration, as the difference in days between bolting and inflorescence arrest. The number of fruits per inflorescence was also recorded after arrest.

2.9.3. Lifespan

Lifespan was calculated as the difference in days between sowing of a plant and arrest of its primary inflorescence.

2.9.4. Inflorescence Meristem Measurements

For experiments focusing on the inflorescence meristem (IM), primary inflorescences were sampled at the time points indicated throughout the text. Siliques and flowers were counted. Next, floral primordia were dissected out of the apex of the inflorescence using tweezers under a digital microscope (Keyence VHX-7000), recording the number of primordia in the process. The total number of reproductive nodes per inflorescence was calculated as the sum of siliques, flowers and primordia. After removing all floral primordia, the exposed IM was imaged and the meristem diameter was measured using the software ImageJ (Schneider et al., 2012).

2.9.5. Inflorescence Length, Internode Length and Plant Height

Inflorescence length was measured from the base to the apex of the inflorescence with a measuring tape. For secondary and tertiary inflorescences, the base was the join with the sustaining inflorescence. For the primary, it was the join with the upper-most secondary inflorescence. The spacing between each consecutive secondary inflorescence was measured with a calliper, and internode length was calculated as the average of these. Plant height was defined as the distance between the base of the main stem and the apex of the primary inflorescence.

2.9.6. Number of Fruits per Inflorescence and Total Fruits

Inflorescences were classified in three types, i.e., primaries, which are at the top of the main stem; secondaries, which branch out from the main stem; and tertiaries, which branch out from secondaries. The number of inflorescences of each type was recorded. Next, the number of siliques was counted for each inflorescence,

and averaged for each inflorescence type. The total number of fruits per plant was calculated as the sum of fruits from all inflorescences within a plant.

2.9.7. Fruit Length, Number of Seeds per Fruit and Seed Area

Siliques from the primary inflorescence were collected separately once they were ripened. For each, fruit length was defined as the distance between the pedicel and the apex of the valves of the silique, measured with a calliper. After recording fruit length, the valves and replum were gently removed with forceps, and the seeds were then placed on a piece of qualitative filter paper (Whatman). Seeds were placed under a digital microscope (Keyence VHX-7000) and imaged. Finally, the software ImageJ (Schneider et al., 2012) was used to count the number of seeds and measure the seed area, which was averaged for all seeds within a single fruit.

2.9.8. Dry Shoot Weight

To record dry shoot weight, plants were grown until arrest of the primary inflorescence. At this point, shoots including all inflorescences were bagged for each plant separately, and plants were left to grow for 1-2 additional weeks. After visible whole-plant death, bags were collected and weighted in a scale.

2.10. Phenotypic Measurements in Brassicaceae

For other species from the Brassicaceae family, inflorescence duration was defined as the time between the first day when an opened flower was observed in the primary inflorescence and the last day in which a new flower was opened.

Measurements of fruit length, the number of seeds per fruit and seed area were performed as previously described for *A. thaliana*.

2.10. Phenotypic Measurements in *T. aestivum*

For experiments with *T. aestivum*, all measurements were taken from the spike located in the main stem.

2.10.1. Spike Length

The length of the spike was defined as the distance between the base of the bottom-most spikelet and the top of the outer glume in the terminal spikelet, measured with a calliper.

2.10.2. Number of Spikelets per Spike

For each spike, the total number of spikelets were counted. Bottom-most spikelets which did not contain any fertile florets were classified as vestigial spikelets, and the number of vestigial spikelets per spike was also recorded.

2.10.3. Number of Florets per Spikelet

Each spikelet was collected separately making note of its relative position within the spike. Next, individual florets were dissected out of the spikelet using forceps, and the number of florets per spikelet was recorded in the process. Unless otherwise stated (e.g., in experiments in which the number of florets was quantified

for all spikelet positions), the number of florets was defined as the average for the three spikelets located in the middle of the spike.

2.10.4. Number of Seeds per Spike and Seed Weight

Seeds were removed from all florets within a spike, and the number of seeds was counted. Next, seeds were collected and weighted in a scale.

2.10.5. Floret Production Measurements

One experiment involved tracking floret production over time (see Chapter 7: **Figure 7.10**). To do this, developing spikes were dissected out of the main stem under a digital microscope (Keyence VHX-7000) at the time points indicated in the text. The number of floret primordia was then counted for three spikelets from different positions within the spike, i.e., the bottom-most, the middle and the terminal spikelet.

2.11. Analysis of Gene Expression

2.11.1. Sample Collection

Samples for the analysis of gene expression, either through RT-qPCR or RNA-Sequencing, were harvested at various points and from different tissues, as specified throughout the text (see Chapters 4, 5 and 6). In all cases, plant tissue was collected into a 2-ml microcentrifuge tube containing two metallic beads and immediately frozen in liquid nitrogen. Frozen samples were stored at -80ºC until RNA extraction. For RT-qPCR experiments, each sample contained either one mature

rosette leaf, 2 mature cauline leaves, a pool of 10-15 inflorescence meristems (IMs) or a pool of 10 siliques. For RNA-Sequencing experiments, the content of each sample was a pool of 12 IMs.

2.11.2. Real-time Quantitative PCR (RT-qPCR)

Frozen samples were lysed using a TissueLyser LT (Qiagen). Next, lysed samples were used for RNA extraction, DNA digestion and cDNA synthesis (see **Table 2.7** for kits used). The quality of the extracted RNA was checked using a NanoDrop Lite Spectrophotometer (Thermo Scientific). Finally, RT-qPCR was performed in a CFX Real-time System (Bio-Rad). All primer sequences are indicated in **Table 2.5**. *UBIQUITIN CONJUGATING ENZYME 9* (*UBC9*) was used as the reference gene based on its known stable expression across different tissues and developmental stages (Czechowski et al., 2005; Cheng et al., 2021; Ferreira et al., 2023).

2.11.3. RNA Sequencing

2.11.3.1. Experimental Design

The two RNA-sequencing datasets analysed in this project (see Chapters 3 and 4) were produced from samples obtained in the same experiment. *A. thaliana* plants from three different genotypes, i.e., Col-0, *ft-10* and Kondara; were sown at the same time and grown in standard conditions. IM samples were harvested at four and 12 days after bolting for each genotype as previously described and used for RNA extraction and sequencing.

2.11.3.2. Library Construction and Sequencing

Total RNA was extracted using a RNeasy Plant Mini Kit (Qiagen, 74904), and subject to DNA digestion with a TURBO DNA-free™ Kit (Invitrogen, AM1907). Samples containing 1 µg of total RNA were submitted to Genewiz (Azenta Life Sciences) for library preparation and sequencing. The mRNA was selected using poly(A) enrichment, and the quality of the constructed libraries was checked. Finally, the libraries were sequenced using Illumina NovaSeq, from which 150 bp paired-end reads were produced. Raw RNA-Sequencing data, in FASTQ format, was delivered through sFTP (Secure File Transfer Protocol).

2.12. Generation of *35S:FT-GR* transgenic lines

2.12.1. Cloning

A strategy based on the Gateway Cloning technology (Thermo Fisher Scientific) was followed for generating the *35S:FT-GR* transgenic vector (see **Table 2.7** for kits used). The cauliflower mosaic virus promoter (*CaMV 35S*) and the full coding sequence (CDS) of *FLOWERING LOCUS T* (*FT*) were amplified and cloned separately. The 660 bp CDS of *FT* was obtained from The Arabidopsis Information Resource (TAIR) (Berardini et al., 2015) and a pair of primers were designed to amplify it from cDNA. The template cDNA used was from leaf tissue of *A. thaliana* Col-0 plants. A different set of primers was designed to amplify the *35S* promoter from a different plasmid. Once both *FT* and *35S* were amplified, a second set of PCRs was performed with primers containing the Gateway attB sites. Finally, attB-tagged *FT* and *35S* were introduced into separate Gateway donor vectors, i.e., pDONR221 P1-P5r and pDONR221 P5-P2, respectively. Entry clones containing *35S* and *FT*

were assembled into a modified pFP101 destination vector containing a glucocorticoid receptor (GR) tag (**Figure 2.1A**).

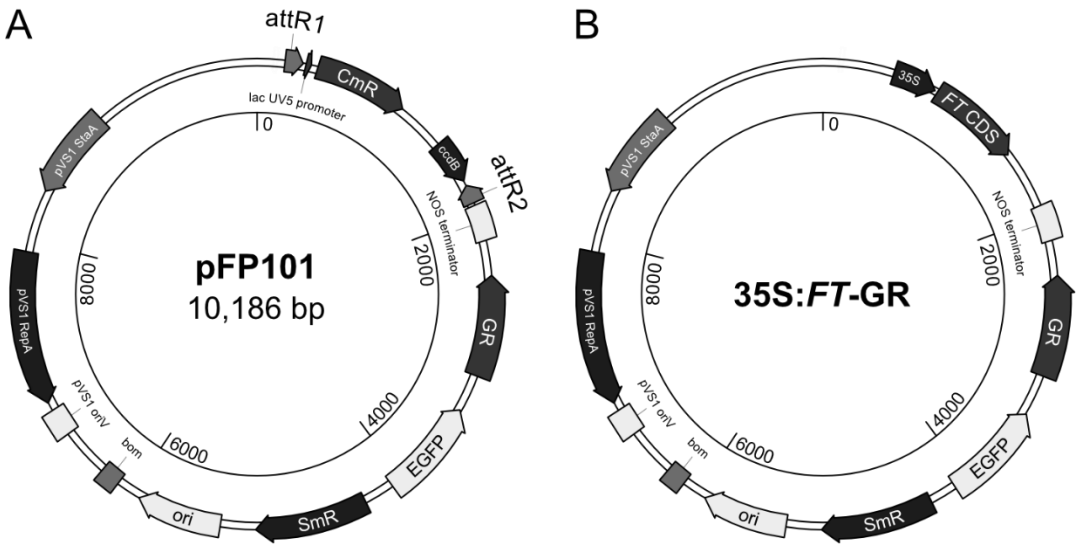

Figure 2.1. Diagram of the plasmids used for the generation of *35S:FT-GR*

A. Modified pFP101 vector containing the glucocorticoid receptor (GR) tag used as destination vector. **B.** Final *35S:FT-GR* expression vector used for the transformation of *A. thaliana*.

2.12.2. Genetic Transformation of Bacteria

E. coli was used throughout the cloning of *35S:FT-GR*. Heat shock genetic transformation of *E. coli* was performed as follows. First, 2 µl of the BP/LR reaction product were added to a microcentrifuge tube containing 10 µl of thermo-competent *E. coli*, followed by an incubation on ice for 30 minutes. Next, the bacteria was subjected to a heat shock at 42ºC for 45 seconds using a bench Thermomixer (Eppendorf). Immediately after the heat shock, the bacteria were placed on ice for 2 minutes, after which 1 ml of growth media was added to the tube and the bacteria were incubated for 1 hour at 37ºC with shaking. Antibiotic selection was used to recover successfully transformed *E. coli*. Kanamycin and streptomycin were used for

the selection of colonies transformed with pDONR221 and pFP101 vectors, respectively.

A. tumefaciens was used to mediate the transformation of *A. thaliana*. To introduce the final *35S:FT-GR* expression vector (**Figure 2.1B**) into *A. tumefaciens*, bacteria were genetically transformed by electroporation as follows. First, 200 ng of the plasmid were added to a microcentrifuge tube containing 20 µl of electro-competent *A. tumefaciens*. The bacteria-plasmid mixture was transferred to a cuvette and pulsed with 1.8 kV in an *E. coli* pulser (Bio Rad). This was followed by a short incubation on ice for 5 minutes and, after the addition of 1 ml of growth media, a longer incubation at 28ºC for 2 hours, with no shaking. Antibiotic selection with streptomycin, rifampicin and gentamycin was used to recover transformed *A. tumefaciens*.

2.12.3. Genetic Transformation of *A. thaliana*

The *35S:FT-GR* expression vector (**Figure 2.1B**) was transformed into *A. thaliana* using the floral dip method (Clough and Bent, 1998) and *A. tumefaciens* previously transformed with the expression vector. Expression of the EGFP gene, which is present within the *35S:FT-GR* vector under a seed-specific promoter, was used as a selection marker for successful transformation in T1 seeds (Bensmihen et al., 2004). These were grown and left to self for one generation, after which fluorescent seeds from 12 independent plants. Only fluorescent T2 seeds were used for further experiments.

2.12.4. Sequencing

Colony PCR and Sanger sequencing were performed after each bacterial transformation to confirm successful transformation and guarantee the lack of polymerase errors in the final vector.

2.12. Bioinformatic Analyses

2.12.1. RNA-Sequencing Data Analysis

2.12.1.1. Quantification, Filtering, Normalization and Transformation

The program kallisto (Bray et al., 2016) was used to quantify transcript abundances from RNA-Sequencing data in FASTQ format. Next, the R package DESeq2 (Love et al., 2014) was used for filtering, normalization and transformation of raw read counts. Before data exploratory analysis, a minimal filtering step was applied by removing any genes which had no counts or a single count across all samples. Normalization and transformation were also applied prior to exploratory data analysis. For normalization, the median ratio method was used (Anders and Huber, 2010). Normalized counts were used for visualizations of read counts at the gene level. For transformation, the Variance Stabilizing Transformation (VST) method was applied (Anders and Huber, 2010). Transformed read counts were used for exploratory data analysis.

2.12.1.2. Exploratory Data Analysis

Principal Component Analysis (PCA) was used for dimensionality reduction on the VST-transformed read counts using the R package DESeq2 to explore global differences among samples at the whole-transcriptome level. Sample-to-sample Euclidean distances were also calculated with base R using the VST-transformed

read counts. The R package pheatmap was used for hierarchical clustering based on these Euclidean distances and for data visualization.

2.12.1.3. Differential Expression Analysis

Differential expression analysis was carried out using the R package DESeq2 through a pipeline including the following steps. First, the raw count data was normalized to account for potential differences in sequencing depth. Next, dispersion values were estimated for each gene. Finally, Generalized Linear Models (GLMs) were fitted for each gene. GLMs are based on the negative binomial distribution, which is suitable for various forms of counts data (Love et al., 2014).

The selected statistical test was the Likelihood Ratio Test (LRT), which is well-suited for the analysis of time-course data. In LRT, two nested models are fitted per gene, i.e., a full model containing the variable of interest and a reduced model without it. Thus, LRT reports differences in deviance between these two models, allowing to draw conclusions on the importance of the variable of interest in explaining the expression levels for each gene. Specifically, the LRT used for the analysis of RNA-Sequencing data (see Chapters 4 and 5) aimed to assess the effect of genotype over time, i.e., the interaction term between time and genotype, on gene expression. Thus, the LRT tested the following two models.

$$\begin{cases} H_0 & \text{expression} \sim \text{time} + \text{genotype} \\ H_1 & \text{expression} \sim \text{time} + \text{genotype} + \text{time:genotype} \end{cases}$$

Where H_0 is the model corresponding to the null hypothesis and H_1 is the one corresponding to the alternative hypothesis. The p-values were adjusted using the Benjamini and Hochberg approach (Benjamini and Hochberg, 1995), which controls the False Discovery Rate (FDR) associated with performing multiple statistical tests on the same dataset. For all tests, genes were considered statistically significant when the FDR-adjusted p-value was less than 0.05.

2.12.1.4. Clustering

For differentially expressed genes, an unsupervised classification approach was used to identify groups with similar expression. The R package Mfuzz, which is based on the soft clustering of data (Kumar and E. Futschik, 2007), was used for this. Log-transformed, normalized and standardized read counts were used as an input. The number of clusters was selected by choosing the smallest cluster number that minimized the distance between the cluster centroids, as suggested by the package developers. The results were visualized using the R packages Mfuzz and pheatmap.

2.12.1.5. Gene Ontology Enrichment

The R package clusterProfiler (Wu et al., 2021) was used to perform Gene Ontology (GO) enrichment on sets of differentially expressed genes. The chosen approach for this was an over-representation analysis, and an adjusted p-value of 0.05 was selected as the significance threshold.

2.12.2. Genomic Variant Analysis

A Variant Call Format (VCF) file containing genomic variants between the Col-0 and Kondara *A. thaliana* accessions was downloaded from the 1,001 Genomes webpage (https://1001genomes.org/index.html) (Alonso-Blanco et al., 2016). This VCF file contains information about genomic variants between genotypes, e.g., insertions, deletions or single nucleotide polymorphisms (SNPs); for different genomic locations. The software snpEff (Cingolani et al., 2012) was used to predict the functional effect of genomic variants using the VCF file as an input and with the default settings. Variants with a predicted high functional impact, e.g., the loss or gain of a start codon, were filtered and used for further analysis, as specified in the text.

2.12.3. Genome-Wide Association Study (GWAS)

The genome-wide association study (GWAS) was conducted using GWA-Portal (https://gwas.gmi.oeaw.ac.at/) (Seren, 2018). Phenotypic measurements of interest were averaged for each accession, log-transformed and used as an input. A dataset containing 250,000 SNPs from 62 of the 69 phenotyped accessions was selected (Horton et al., 2012), and the GWAS was performed using a linear model with the default parameters. The p-values were adjusted were adjusted using the Bonferroni and Benjamini and Hochberg approaches to account for multiple statistical comparisons.

2.13. Experimental Design and Statistical Analyses

2.13.1. Sample Size and Replication

Sample sizes for all experiments are stated in the figure legends. For RT-qPCR and RNA-Sequencing experiments, 3 biological replicates are used, which correspond to samples obtained from different plants or sets of plants. The latter case applies to cauline leaves and IMs (see Sample Collection, 2.11.1). For physiological measurements, each biological replicate represents a distinct plant. All physiological assays started with a minimum of 8 biological replicates per treatment, condition and/or time point. Some of these were lost throughout the experiment due to watering issues or pests. For time-series experiments, observations at different time points are independent from one another and not repeated measurements.

2.13.2. Statistical Analysis

With the exception of bioinformatic analyses, the pipeline followed to perform statistical analysis on the experimental data was as follows. First, the Shapiro-Wilk test (Shapiro and Wilk, 1965) was applied to check whether the data was normally distributed or not. For normal data, statistical differences between different groups were assessed through a Student's t test (Student, 1908) (for 2 groups) or an ANOVA test (Girden, 1992) (for more than 2 groups). If the data was not normal, statistical differences between different groups were assessed through an unpaired Wilcoxon test (Wilcoxon, 1945) (for 2 groups) or a Kruskal-Wallis test (Kruskal and Wallis, 1952) (for more than 2 groups). Post hoc multiple comparisons were performed after an ANOVA or Kruskal-Wallis test through a Tukey's Honest Significant Difference test (HSD) (Tukey, 1949) (for normal data) or a pairwise Wilcoxon test (for non-normal data). Where appropriate, a linear model was fitted to the data using the least squares regression. All analyses were performed in R (R Core Team, 2022).

Chapter 3: Characterization of the Environmental Control of Inflorescence Arrest in *A. thaliana*

3.1. Introduction

Because of their sessile nature, it is crucial for plants to synchronize their life cycle with their environment and, thus, they have evolved sophisticated mechanisms to identify the perfect time to flower (Li et al., 2016). Flowers are very sensitive to harsh climate and seed maturation is an energetically demanding process, so coordinating the reproductive period with the right conditions allows plants to increase the chances of reproductive success (Bratzel and Turck, 2015). Due to this, environmental cues play a central role in controlling when flowering starts in numerous species (Higuchi, 2018; Song, 2016; Srikanth and Schmid, 2011).

Temperature and light are by far the most well-described environmental signals that affect flowering time (Srikanth and Schmid, 2011), with three characterized molecular pathways: the vernalization pathway (Kim, 2020), the photoperiodic pathway (Song et al., 2015) and the ambient temperature pathway (Capovilla et al., 2015). However, other environmental inputs such as nutrient availability or certain abiotic stresses can control flowering time, although the underlying genetic regulation is poorly understood (Ausin et al., 2004). Given the key importance of the environment in shaping the transition into flower, it has been suggested that environmental stimuli may also control the end-of-flowering, albeit evidence supporting this idea is scarce and fragmentary (Miryeganeh, 2020; Miryeganeh et al., 2018; Nagahama et al., 2018).

While the effect of temperature on the end-of-flowering has not been examined in the model plant *A. thaliana*, moderate increases in ambient temperature are known to accelerate end-of-flowering in other species (Cao et al., 2016; Lomas and Burd, 1983; Nagahama et al., 2018; Satake et al., 2013). In *A. thaliana*, increases in ambient temperature tend to accelerate floral transition while decreases tend to delay it (Balasubramanian et al., 2006; Lee et al., 2013). An additional temperature-regulated process is vernalization, which affects winter accessions of *A. thaliana*. Upon exposure to a prolonged cold period, the vernalization pathway confers these accessions competence to flower, which ensures that flowering occurs during favourable seasons, particularly in temperate areas (Luo and He, 2020). Although much is known about the effect of both ambient temperature and vernalization on the beginning of flowering, literature on their impact on the end-of-flowering is currently lacking.

In addition to temperature, light is a key environmental factor that regulates flowering time. Different light components are known to affect the timing of flowering, such as light quality, intensity and day length (Ausin et al., 2004). The latter is particularly well studied in many species, including *A. thaliana*. As a facultative long-day plant, an increase in day length accelerates flowering in *A. thaliana* (Melzer et al., 2008), a process that is regulated at the molecular level by the photoperiodic pathway. Preliminary work suggest that day length could also impact the timing of end-of-flowering (Hensel et al., 1994), although this has never been formally investigated. However, in other species such as wheat, photoperiod-insensitive mutant lines show significantly shorter durations of flowering (Royo et al., 2016). While inconclusive, these results could suggest that day length may play a role in the control of end-of-flowering in the plant kingdom, a hypothesis that would require appropriate examination.

Another environmental factor that has been suggested to control end-of-flowering is nutrient availability. In pea, nitrogen starvation accelerates end-of-flowering (Jeuffroy and Sebillotte, 1997). The effect of nutrient supply on the end-of-flowering has never been studied in *A. thaliana*. However, nutrient availability has clear impacts on reproductive plant development (Poorter et al., 2012; Vidal et al., 2014) and limiting concentrations of key nutrients, such as nitrogen or phosphate, affect the timing of flowering (Kant et al., 2011; Lin and Tsay, 2017).

Aside from abiotic cues, certain biotic factors could play a role in controlling the end of flowering, such as herbivory or competition for resources. An example of this is plant density, which can decrease the availability of resources per individual. Crowding, i.e., the presence of a high density of plants in a given space, affects plant growth and flowering phenology. Again, effects of crowding or other biotic signals in the end-of-flowering in *A. thaliana* have never been investigated. Nevertheless, research on the close relative *Cardamine hirsuta* shows that crowding can shorten the duration of flowering (Cao et al., 2016), suggesting that these signals could also affect end-of-flowering in *A. thaliana*.

3.2. Aims

In light of the lack of information regarding the effect of environmental signals on the end-of-flowering, the main aim of this chapter is to explore the environmental control of inflorescence arrest in *A. thaliana*, specifically:

1) To characterise the effect of temperature on inflorescence arrest.
2) To characterise the effect of light on inflorescence arrest.
3) To characterise the effect of nutrient availability on inflorescence arrest.
4) To characterise the effect of biotic factors on inflorescence arrest.

3.3. Results and Discussion

3.3.1. Temperature During Flowering Controls Inflorescence Arrest

To determine the impact of ambient temperature on inflorescence arrest, inflorescence duration and fruit number was recorded for *A. thaliana* Col-0 plants grown at four different temperatures: 17ºC, 20ºC, 22ºC and 27ºC (16 h day length). For this temperature range, inflorescence duration was clearly affected by temperature, with plants undergoing an earlier arrest at warmer temperatures (**Figure 3.1A**). The longest inflorescence duration was recorded at 17ºC (32 days on average) and the shortest, at 27ºC (19 days). In addition to inflorescence duration, temperature showed an effect on the number of fruits produced in the inflorescence. Generally, fewer fruits per inflorescence were observed for plants grown at warmer temperatures (**Figure 3.1B**). Interestingly, longer durations did not necessarily lead to greater fruit numbers per inflorescence. For instance, while inflorescences from plants grown at 17ºC lasted ~5 days longer than those of plants grown at 20ºC, both produced a similar number of fruits.

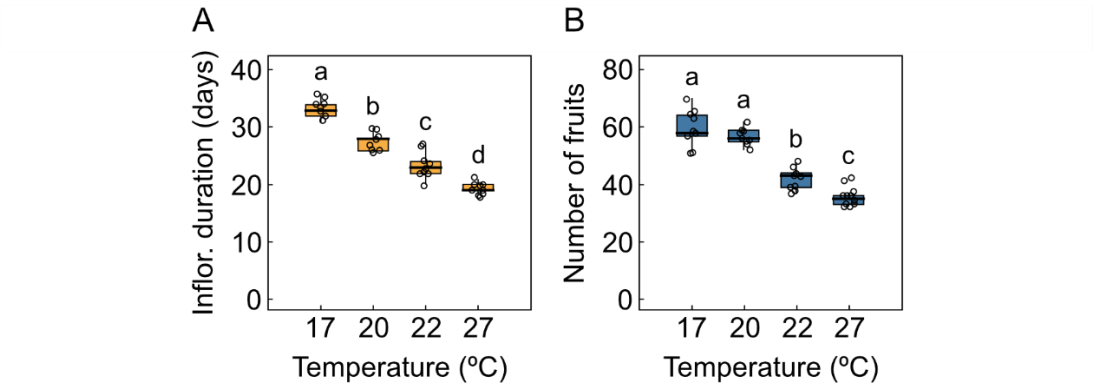

Figure 3.1. Inflorescence arrest is affected by growth temperature

Inflorescence duration (**A**) and number of fruits per inflorescence (**B**) in plants grown at 17ºC, 20ºC, 22ºC or 27ºC (16 h-day length, 100 µmol m^{-2} s^{-1}) (N=9-13). Different letters indicate statistical differences between conditions (ANOVA, Tukey HSD test, $P<0.05$).

These results unequivocally showed that temperature impacts the timing of inflorescence arrest as well as fruit number. The optimal temperature described for the growth of *A. thaliana* is 22-23ºC (Rivero et al., 2014), with a moderate decrease or increase in temperature leading to delayed or accelerated transition into flowering, respectively (Blázquez et al., 2003). Interestingly, the same trend was observed here for the timing of arrest, suggesting that temperature operates similarly at the onset and end of flowering and that moderate increases in ambient temperature accelerate developmental transitions of the shoot apical meristem (SAM) in a general sense.

An interesting question raised by these data was whether inflorescence duration is affected by the temperature experienced by the plants during their whole life cycle or the flowering phase exclusively. To test this, plants were grown under either 20ºC or 27ºC until bolting. Immediately after bolting was recorded, a subset of plants were transferred from 20ºC to 27ºC and vice versa, and inflorescence arrest and fruit number were recorded. In accordance with previous results, plants grown at 27ºC during their whole lifespan showed a shorter inflorescence duration (**Figure 3.2A**) and a lower fruit number (**Figure 3.2B**). A similar effect of temperature on inflorescence duration was observed regardless of the temperature experienced by the plants before bolting. In contrast, the number of fruits was significantly impacted by the temperature at which plants were exposed prior to flowering. The same pattern was observed for a different experiment where plants were either grown at 17ºC, 22ºC, or transferred from 17ºC to 22ºC upon bolting. Once again, inflorescence duration was largely determined by the temperature during flowering alone (**Figure 3.2C**), while fruit number was also affected by the temperature experienced during the vegetative phase (**Figure 3.2D**).

These observations suggest that temperature during the reproductive phase is the main driver of inflorescence duration, with prior temperature experienced during the vegetative phase having little to no effect. The transfer between

temperatures was carried out when bolting was visible as a cluster of developing floral primordia at the centre of the rosette. Thus, it is expected that the SAM would already have transitioned into an inflorescence meristem (IM) some time prior to the transfer, which could explain the effect of past temperature on fruit set (**Figure 3.2B**, **Figure 3.2D**) but not inflorescence duration (**Figure 3.2A**, **Figure 3.2C**).

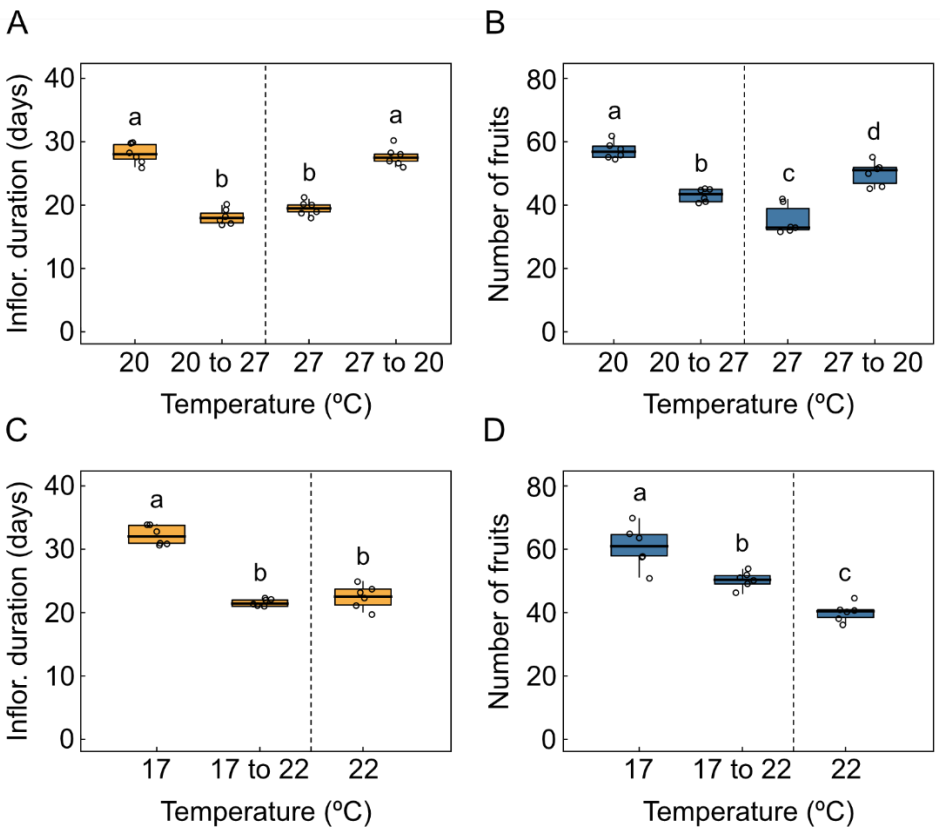

Figure 3.2. Temperature during flowering alone regulates inflorescence arrest

A-B. Inflorescence duration (**A**) and number of fruits per inflorescence (**B**) in plants grown at 20º or 27ºC (16 h-day length, 100 µmol m^{-2} s^{-1}), or reciprocally transferred between the two temperatures at bolting (N=6). **C-D.** Inflorescence duration (**C**) and number of fruits per inflorescence (**D**) in plants grown at 17ºC or 22ºC (16-h day length, 100 µmol m^{-2} s^{-1}), or transferred from 17ºC to 22ºC at bolting (N=6). Different letters indicate statistical differences between conditions (for A and D: ANOVA, Tukey HSD test, $P<0.05$; for B and C: Kruskal-Wallis rank sum test, pairwise Wilcoxon test with Benjamini and Hochberg correction, $P<0.05$).

3.3.2. Vernalization Accelerates Inflorescence Arrest

To assess the effect of vernalization on inflorescence arrest, four different accessions of *A. thaliana* were used: two rapid-cycling genotypes, Col-0 and Ws-0, which do not accelerate flowering in response to vernalization, and two winter annuals, Bla-2 and Kondara, which are vernalization-responsive. These were vernalized for different durations (0, 1, 3, or 5 weeks) at 10ºC and 8 h day length before being transferred to flowering-promotive conditions (20ºC, 16-h day length). Flowering time (in number of rosette leaves), inflorescence duration and fruit number were recorded for each combination of genotype and vernalization treatment. As expected, prolonged exposure to vernalizing conditions accelerated flowering time in the winter accessions, Bla-2 and Kondara, but not in the rapid-cycling genotypes, Col-0 and Ws-0 (**Figure 3.3A**). Interestingly, vernalization also accelerated inflorescence arrest, leading to shorter inflorescence durations in plants that had been vernalized for longer (**Figure 3.3B**). Little to no difference was found in Col-0 and Ws-0 except for the longest vernalization treatment, but the effect of vernalization on inflorescence duration was obvious in winter accessions. The effect of vernalization was also apparent in the number of fruits produced per inflorescence. While Col-0 and Ws-0 produced similar fruit numbers regardless of the vernalization treatment, both of the winter accessions produced more fruits after longer exposures to vernalizing conditions (**Figure 3.3C**).

To some extent, the effect of vernalization on the timing of arrest was similar to that observed for ambient temperature (**Figure 3.1A**). Environmental conditions that are known to accelerate the transition into flowering, such as prolonged exposure to winter, also brought about an earlier inflorescence arrest. At the molecular level, the ambient temperature and vernalization pathways are controlled by different sets of molecules. However, they tend to converge on the same floral integrators, such as *FLOWERING LOCUS T* (*FT*) and *SUPPRESSOR OF OVEREXPRESSION OF*

CONSTANS 1 (*SOC1*). Given the dual effect of ambient temperature and vernalization as promoters of both floral transition and arrest, it is therefore possible that the same genetic signals that underlie the beginning of flowering also operate during end-of-flowering.

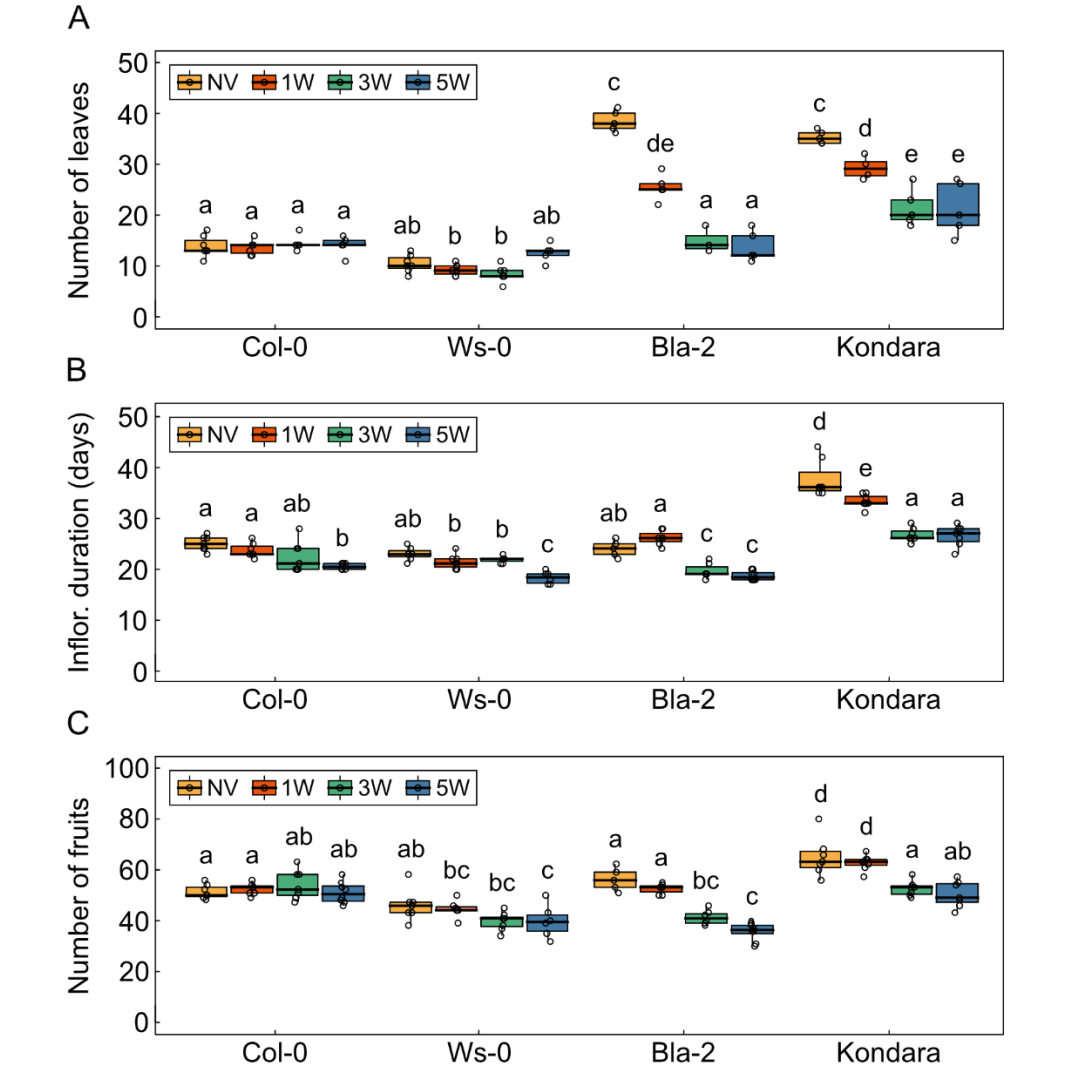

Figure 3.3. Vernalization accelerates flowering time and inflorescence arrest

Number of rosette leaves (**A**), inflorescence duration (**B**) and number of fruits per inflorescence (**C**) in non-vernalized plants (NV) and plants vernalized for one (1W), three (3W) or five (5W) weeks (16-h day length, 120 µmol m^{-2} s^{-1}) (N=5-8). The genotype is indicated in the x-axis. Different letters indicate statistical differences (ANOVA, Tukey HSD test, P<0.05).

3.3.3. Light Intensity Does Not Affect Inflorescence Arrest

Along with temperature, light is the main environmental cue that affects the timing of flowering. Due to the complex nature of light, its different characteristics, i.e., intensity, quality and day length; must be considered separately. Firstly, to assess the impact of light intensity on inflorescence arrest, plants were grown at three different light intensities (i.e., 50, 100 and 150 µmol m^{-2} s^{-1}) and inflorescence duration and fruit number were recorded for each treatment. The results showed that changes in light intensity had no effect on inflorescence duration (**Figure 3.4A**). In contrast, increasingly greater intensities led to greater inflorescence fruit number (**Figure 3.4B**).

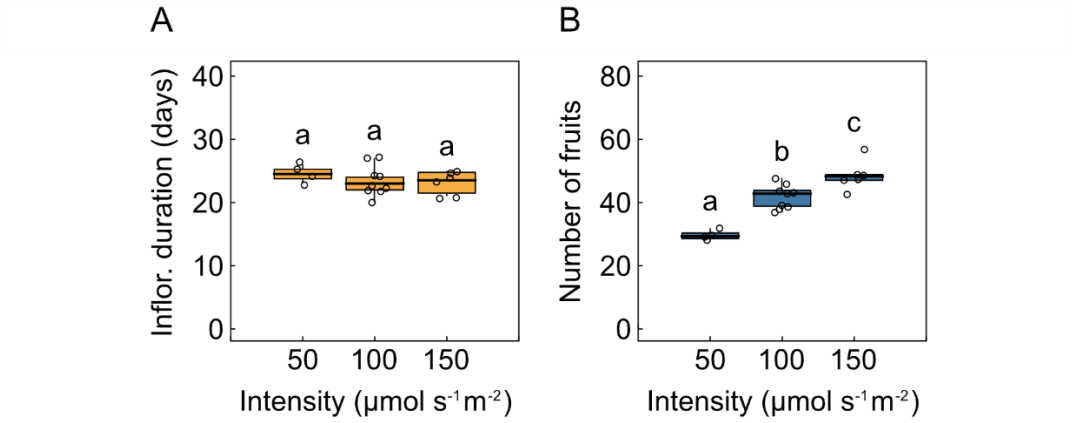

Figure 3.4. Light intensity does not affect inflorescence arrest

Inflorescence duration (**A**) and number of fruits per inflorescence (**B**) in plants grown at 50, 100 or 150 µmol m^{-2} s^{-1} (20ºC, 16-h day length) (N=4-9). Different letters indicate statistical differences (ANOVA, Tukey HSD test, P<0.05).

While the effect of light intensity on flowering is not as well understood as that of temperature, light intensity does impact floral transition in *A. thaliana* (Susila et al., 2016). However, the data presented here suggests that it does not affect the timing of arrest, at least for the range of intensities that were assessed. It is interesting to note that there is an effect in the number of fruits. Generally speaking, photosynthetic

rate increases proportionally to light intensity (Wimalasekera, 2019), which offers a possible explanation for these data. As greater availabilities of photosynthate can facilitate an increase in growth rate, plants grown under different light intensities might show different rates of flower opening, i.e., florochron, while arresting at the same time.

3.3.4. Day Length Controls Inflorescence Arrest

In addition to light intensity, day length is an important component of light, which is known to affect the timing of flowering. To assess its potential effect on inflorescence arrest, inflorescence duration and fruit number were recorded for plants grown in two different day lengths: 8 hours of light or 16 hours of light. In addition, some plants were reciprocally transferred between the two conditions after bolting to specifically test the effect of the day length during flowering. In sharp contrast to light intensity, day length had a significant effect on inflorescence duration, which was greater for plants grown in longer days (**Figure 3.5A**). However, this did not lead to changes in inflorescence fruit number, which was similar regardless of the day length (**Figure 3.5B**). It should also be noted that day length during flowering was the main factor affecting inflorescence duration, with little to no effect of prior day length experienced during the vegetative phase (**Figure 3.5A**).

The lack of effect on fruit set could be attributed to day length affecting florochron in a manner similar to light intensity and, indeed, day length is known to affect growth rate in *A. thaliana* (Baerenfaller et al., 2015). This would imply that, despite plants flowering for longer in shorter day lengths (**Figure 3.5A**), they open flowers more slowly, ultimately leading to the same number of fruits per inflorescence (**Figure 3.5B**). Altogether, these data suggest that day length controls inflorescence

duration in *A. thaliana*, and that the day length experienced during the reproductive phase is the main driver of inflorescence arrest.

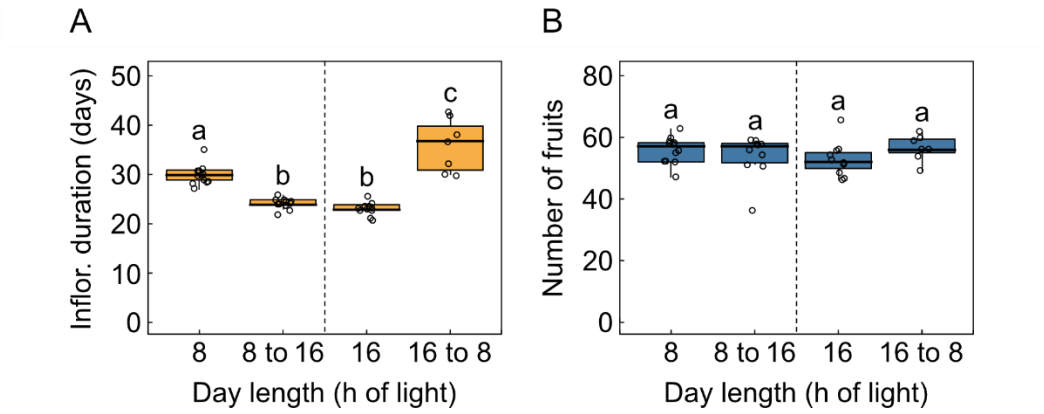

Figure 3.5. Inflorescence arrest is affected by day length

Inflorescence duration (**A**) and number of fruits per inflorescence (**B**) in plants grow under 8 or 16 hours of light per day (22ºC, 120 µmol m^{-2} s^{-1}), or reciprocally transferred between the two upon bolting (N=12). Different letters indicate statistical differences (ANOVA, Tukey HSD test, P<0.05).

3.3.5. Photo-thermal Cues Regulate Inflorescence Meristem Arrest

After characterising the effect of temperature and day length on inflorescence duration, a new set of experiments was designed to understand photo-thermal regulation at the IM level. Longer day lengths and warmer temperatures accelerated inflorescence arrest (**Figure 3.1A**, **Figure 3.5A**). Thus, it was hypothesized that the shortening of inflorescence duration would be due to an earlier arrest of the IM. To test this, the number of reproductive nodes (i.e., fruits, flowers and unopened floral primordia) produced by the IM and the IM diameter were tracked throughout flowering. Two separate experiments were performed, one with plants flowering in either 8- or 16-hour-long days (22ºC) and another with plants flowering at either 15ºC or 20ºC (16-h day length). In both cases, plants were originally grown under

flowering-inducing conditions (16-h day length and 20ºC, respectively) and the treatments were applied after visible bolting.

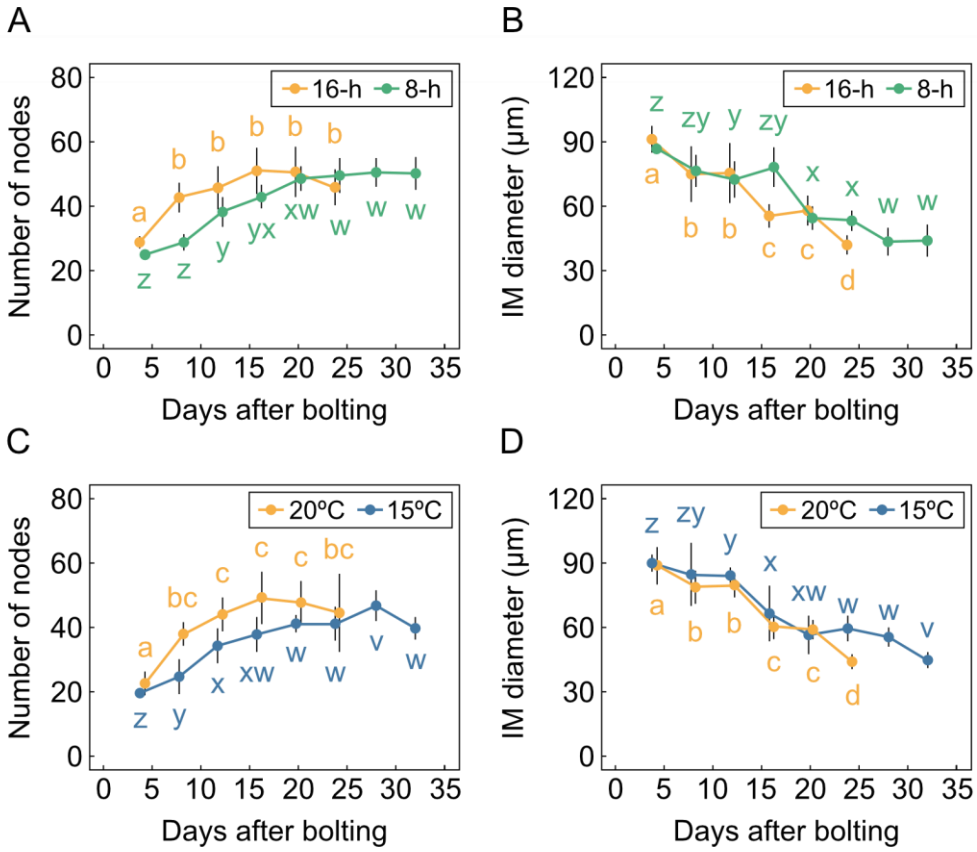

Figure 3.6. IM lifespan is controlled by day length and temperature

A-B. Effect of day length on IM lifespan. Cumulative number of reproductive nodes (i.e., fruits, flowers and unopened floral primordia) (**A**) and IM diameter (**B**) of the primary inflorescence at different time points after bolting in plants grown under 8 or 16 hours of light per day (22ºC, 120 µmol m^{-2} s^{-1}) (N=6-12). **C-D.** Effect of temperature on IM lifespan. Cumulative number of reproductive nodes (i.e., fruits, flowers and unopened floral primordia) (**C**) and IM diameter (**D**) of the primary inflorescence at different time points after bolting in plants grown at 20ºC or 15ºC (16-h day length, 120 µmol m^{-2} s^{-1}) (N=4-7). Different letters indicate statistical differences between time points within each environmental condition (ANOVA, Tukey HSD test, P<0.05).

For both experiments, the maximum number of reproductive nodes produced by the IM was similar in both treatments. However, this maximum was achieved earlier in the 16-hour day length compared with the 8-hour one (**Figure 3.6A**) and at

20ºC compared with 15ºC (**Figure 3.6C**). In addition, the size of the IM decreased at earlier time points in the 16-hour day length and in 20ºC compared with the 8-hour day length and 15ºC, respectively (**Figure 3.6B**, **Figure 3.6D**). This demonstrates that increases in both day length and temperature accelerate the rate at which the IM produces floral primordia, leading to an earlier IM arrest and, ultimately, a shorter inflorescence duration. That the size of the IM gradually decreases during flowering has been described before (Wang et al., 2020). While this was also found here under all conditions, the decrease in size of the IM started earlier at longer day lengths (**Figure 3.6B**) and warmer temperatures (**Figure 3.6D**). Taken together, these results support the idea that the effects of both ambient temperature and day length on inflorescence arrest operate at the IM level.

3.3.6. An Active IM is Necessary for Photo-thermal Regulation of Inflorescence Arrest

Knowing that temperature and day length regulate inflorescence arrest (**Figure 3.1**, **Figure 3.5**), an additional question was whether plants are responsive to light and temperature during the whole duration of flowering. To test this, plants were transferred from a 16-hour daylength to a 8-hour one late into flowering (approximately 16 days after flowering). Interestingly, inflorescence duration did not differ between transferred and control plants (**Figure 3.7A**), suggesting that sensitivity to day length is lost at some point during flowering. To narrow down the approximate time for this, a follow-up experiment was set up in which plants were originally grown in a 16-h daylength. Next, subsets of plants were transferred to an 8-h daylength 0, 4, 8, 12 or 16 days after bolting. Plants transferred from 16- to 8-h day lengths at bolting showed an inflorescence duration twice longer than control plants which remained at 16-h day length (**Figure 3.7C**), in accordance with previous

results (**Figure 3.5A**). Increasingly later transfers showed a progressive reduction in inflorescence duration, which was shorter the longer plants stayed in 16-h day length. Changes in duration to day length were found up to 12 days after bolting, but not in plants transferred later (**Figure 3.7C**). In agreement with prior observations that day length does not impact inflorescence fruit set, the number of fruits per inflorescence was not affected by photoperiod transfers (**Figure 3.7D**).

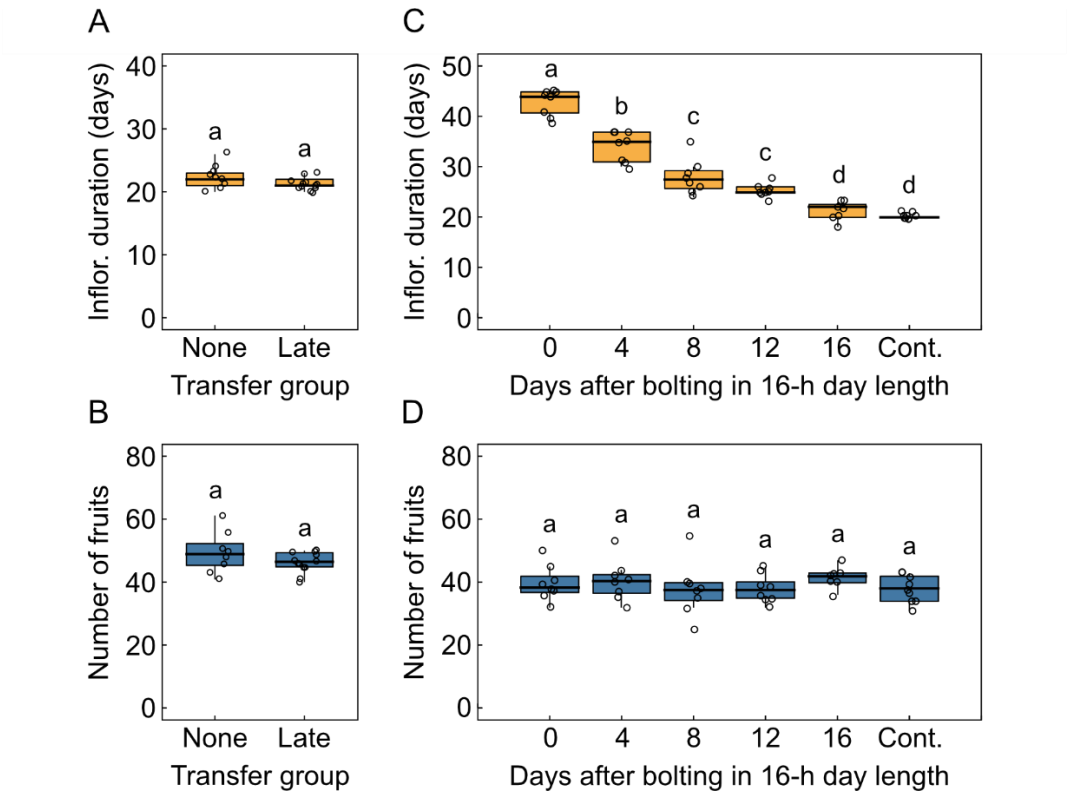

Figure 3.7. Sensitivity to day length is lost during inflorescence development

A-B. Effect of a late day length transfer on inflorescence arrest. Inflorescence duration (**A**) and number fruits per inflorescence (**B**) in plants grown in 16-h day length ('none') or transferred to 8-h day length approximately 16 days after bolting ('late') (22ºC, 120 µmol m^{-2} s^{-1}) (N=9-12). Different letters indicate statistical differences (Student's t test, P<0.05). **C-D.** Effect of variable day length transfers on inflorescence arrest. Inflorescence duration (**C**) and number fruits per inflorescence (**D**) in plants transferred from 16-h day length to 8-h day length 0-, 4-, 8-, 12- or 16-days post bolting (22ºC, 120 µmol m^{-2} s^{-1}) (N=8-9). Control plants were not transferred to 8-h day length. Different letters indicate statistical differences (Kruskal-Wallis rank sum test, pairwise Wilcoxon test with Benjamini and Hochberg correction, P<0.05).

While plants grown under a 16-h daylength typically arrest ~20 days after bolting, they undergo IM arrest earlier, ~16 days after bolting (**Figure 3.6A**). The data presented here shows that sensitivity to day length is lost approximately 16 days after flowering, which corresponds with the timing of IM arrest. This suggests that an active IM is necessary for the response to day length at the end-of-flowering, which further supports the idea that response to day length occurs at the IM level .

3.3.7. Nutrient Availability Impacts Inflorescence Arrest

Other than light and temperature, soil resources are key environmental signals that impact plant growth. Specifically, soil and nutrient availability represent factors with clear effects on reproductive development in plants (Poorter et al., 2012; Vidal et al., 2014). To characterize the general effect of soil resources on inflorescence arrest, a first experiment was carried out where plants were grown in three different pot volumes: 500, 100 and 50 ml. Inflorescence arrest and fruit number were recorded at the end-of-flowering for each pot volume. Interestingly, a reduction in pot size led to a decrease in both inflorescence duration and fruit number (**Figure 3.8A**, **Figure 3.8B**). While the differences in inflorescence duration between plants grown in 50 ml- and 100 ml-pots were not statistically significant, the effect of soil volume on inflorescence arrest was evident in plants grown in 500 ml-pots (**Figure 3.8A**), and the number of fruits per inflorescence was consistently affected by pot volume in all three treatments (**Figure 3.8B**).

These effects could be attributed to three main sources, as the size of the pot determines the physical space for rooting, the availability of water and that of nutrients (Poorter et al., 2012). To test whether nutrient availability specifically impacts inflorescence arrest, a new experiment was carried out where plants were grown in 100 ml-pots filled with either compost (100% compost) or a 1:1 mixture of

compost and sand (50% compost). Upon inspection of the inflorescence duration and fruit set in these two treatments, it is clear that nutrient availability impacts inflorescence arrest and fruit number (**Figure 3.8C**, **Figure 3.8D**).

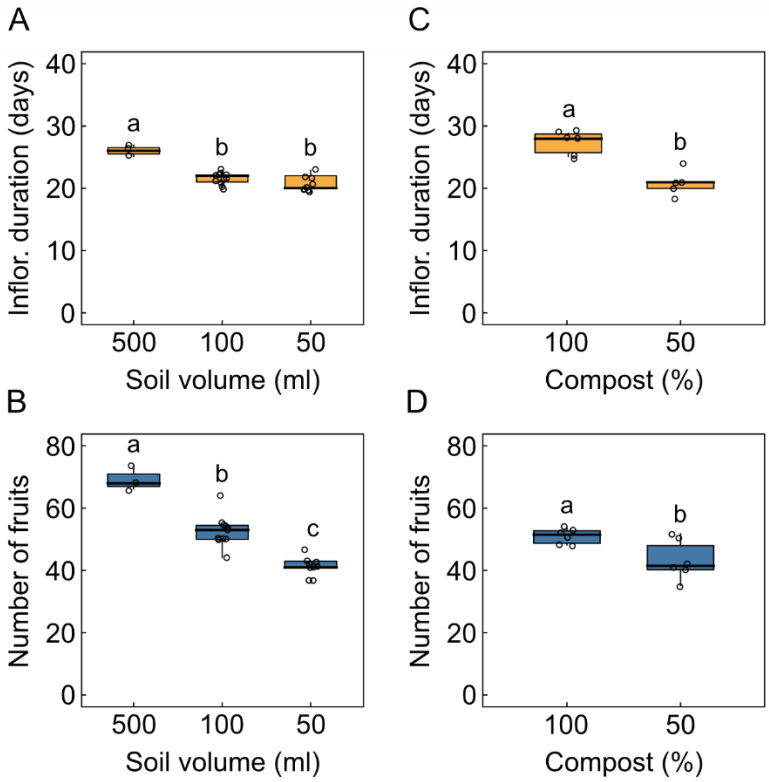

Figure 3.8. Soil and nutrient availability impact inflorescence arrest and yield

A-B. Inflorescence duration (**A**) and number of fruits per inflorescence (**B**) in plants grown in 500-, 100- or 50-ml pots (22ºC, 16-h day length, 100 µmol m^{-2} s^{-1}) (N=3-11). **C-D.** Inflorescence duration (**C**) and number of fruits per inflorescence (**D**) in plants grown in 100% compost or 50% compost (50% sand) (N=6-7). Different letters indicate statistical differences between conditions (for A and B: ANOVA, Tukey HSD test, $P<0.05$; for C: Wilcoxon test, $P<0.05$; for D: Student's t test, $P<0.05$).

Similarly to the observations using smaller pots, inflorescences from plants grown with less compost arrested earlier and produced less fruits, suggesting that the effect of pot size on inflorescence arrest is at least partially caused by a reduction in nutrient availability in smaller pots. While the effect of nutrients on the end-of-flowering in *A. thaliana* has not been examined before, the existing literature on the

onset of flowering shows that a limitation in nutrient availability accelerates floral transition in the accession Col-0 (Pigliucci and Schlichting, 1995; Vidal et al., 2014). Taking this into account, the results presented here suggest that nutrient availability acts in a manner similar to day length and temperature, i.e., the same stimuli that promote the transition into flowering also accelerate inflorescence arrest.

Other than nutrients, another possible source for the effect of decreasing pot size on inflorescence arrest (**Figure 3.8A**) is a reduction water availability. This raised the question as to whether soil water content affects the duration of flowering. To test this, a new experiment was conducted in which plants were grown in 100 ml-pots, in standard substrate, and supplied with either a high or a low water treatment. Interestingly, a reduction in water supply accelerated the transition into flowering, which is consistent with published literature (Stock et al., 2015) (**Figure 3.9A**). In contrast, inflorescences from plants grown under lower water availabilities arrested later (**Figure 3.9B**), despite having produced less fruits (**Figure 3.9C**). However, a repetition of the same experiment revealed no significant differences in any of these traits in response to water availability (**Figure 3.9D**, **Figure 3.9E**, **Figure 3.9F**), questioning the reliability of the previous data. This disagreement could be related to the difficulty in controlling soil water content. The methodology chosen for these experiments, based on previous literature (Stock et al., 2015), consisted on watering pots with differing volumes of water every other day, i.e., 15 ml for the low water treatment and 35 ml for the high water treatment. The problem with this approach is that, other than the water supply, soil water content depends on the amount of water evaporated from the soil, which can be highly variable between experiments. Future research addressing this question would benefit from using a different approach, such as controlling for water content by weighing the pots on every watering day, a technique that has been utilized to study plant responses to water (de Ollas et al., 2019). Taking into account how sensitive inflorescence arrest is to the environment, that flowering time is marginally affected by water availability (Stock et al., 2015), and

that genes that underlie flowering time also play a role in water response (Lovell et al., 2013), it is reasonable to hypothesize that water availability could impact end-of-flowering, although the results presented here do not clearly support this idea.

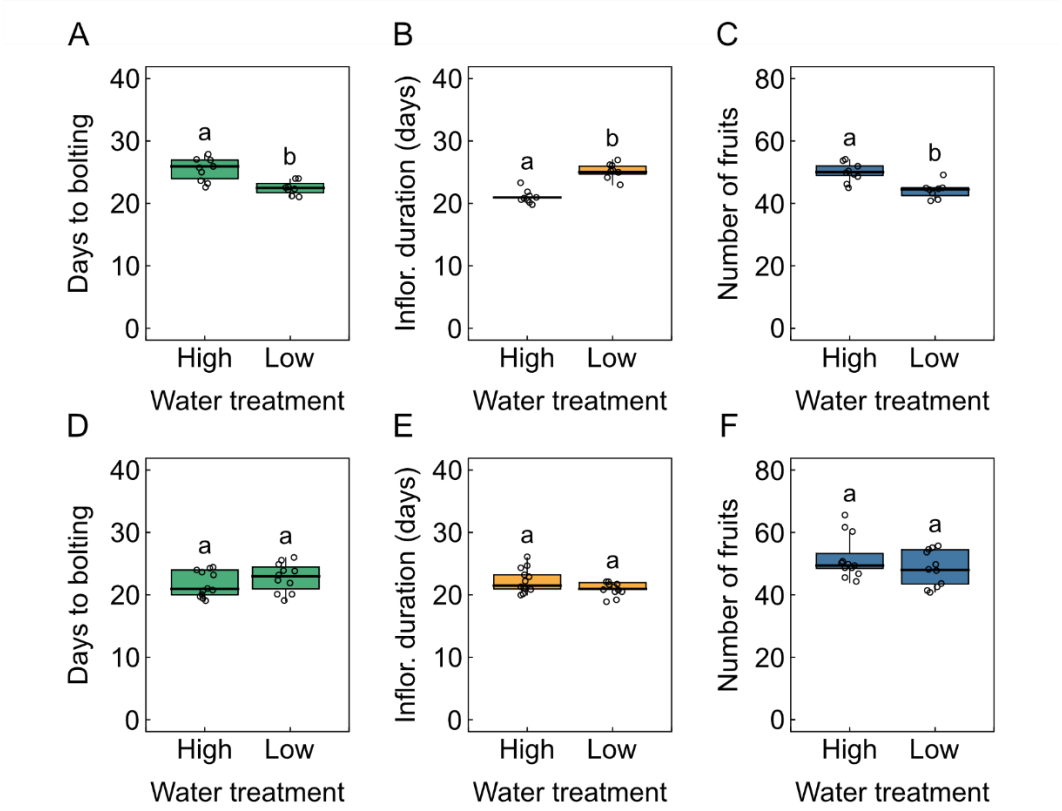

Figure 3.9. Water supply does not have a clear effect on inflorescence arrest

A-C. Days to bolting (**A**), inflorescence duration (**B**) and number of fruits per inflorescence (**C**) in plants grown under high (35 ml H_2O every other day) or low (15 ml H_2O every other day) water regimes (22ºC, 16-h day length, 120 µmol m^{-2} s^{-1}) (N=8). **D-F**. Days to bolting (**D**), inflorescence duration (**E**) and number of fruits per inflorescence (**F**) in plants exposed to the same water treatments in a repeated experiment (N=12).

3.3.8. Nitrate Availability Controls Inflorescence Meristem Arrest

While the impact of water supply on inflorescence arrest remains unresolved, it was clear that nutrient availability plays a role in the control of end-of-flowering, with a reduction in compost leading to earlier inflorescence arrest (**Figure 3.8C**). This effect could be attributed to numerous nutrients, however, nitrogen (N) represented an attractive candidate for various reasons. Nitrogen is one of the essential macronutrients for plant growth and development, as well as a pivotal str (Sanagi et al., 2021) and, in contrast to other elements like phosphorus (P), a reduction in N availability leads to earlier flowering (Kant et al., 2011; Lin and Tsay, 2017). Given that nitrate (NO_3^-) is the major form of N used by plants, a new experiment was designed to test the effect of nitrate availability on inflorescence arrest. Plants were grown in a nutrient-free substrate, composed of a 1:1 (v/v) mixture of vermiculite and sand, and weekly supplied with either standard or NO_3^--limiting media, and inflorescence duration and fruit number were recorded. The effect of NO_3^- availability on inflorescence architecture was evident (**Figure 3.10A**), with plants grown under lower nitrate supplies showing a reduction in both inflorescence duration and fruit number (**Figure 3.10B**, **Figure 3.10C**). This suggested that N limitation accelerates inflorescence arrest, similarly to warm temperatures and long days.

Furthermore, it was hypothesized that the reduced inflorescence duration of N-limited plants would be due to an earlier IM arrest. To test this, plants were grown in either standard or NO_3^--limiting media and IM activity was monitored during flowering. The results showed that the IM arrests earlier in N-limiting conditions, where it produces a smaller number of reproductive nodes (**Figure 3.10D**, **Figure 3.10E**). Taking everything together, it was concluded that N availability regulates inflorescence arrest by tuning the duration of IM lifespan and that a limitation in N accelerates IM arrest similarly to warm temperatures and long day lengths.

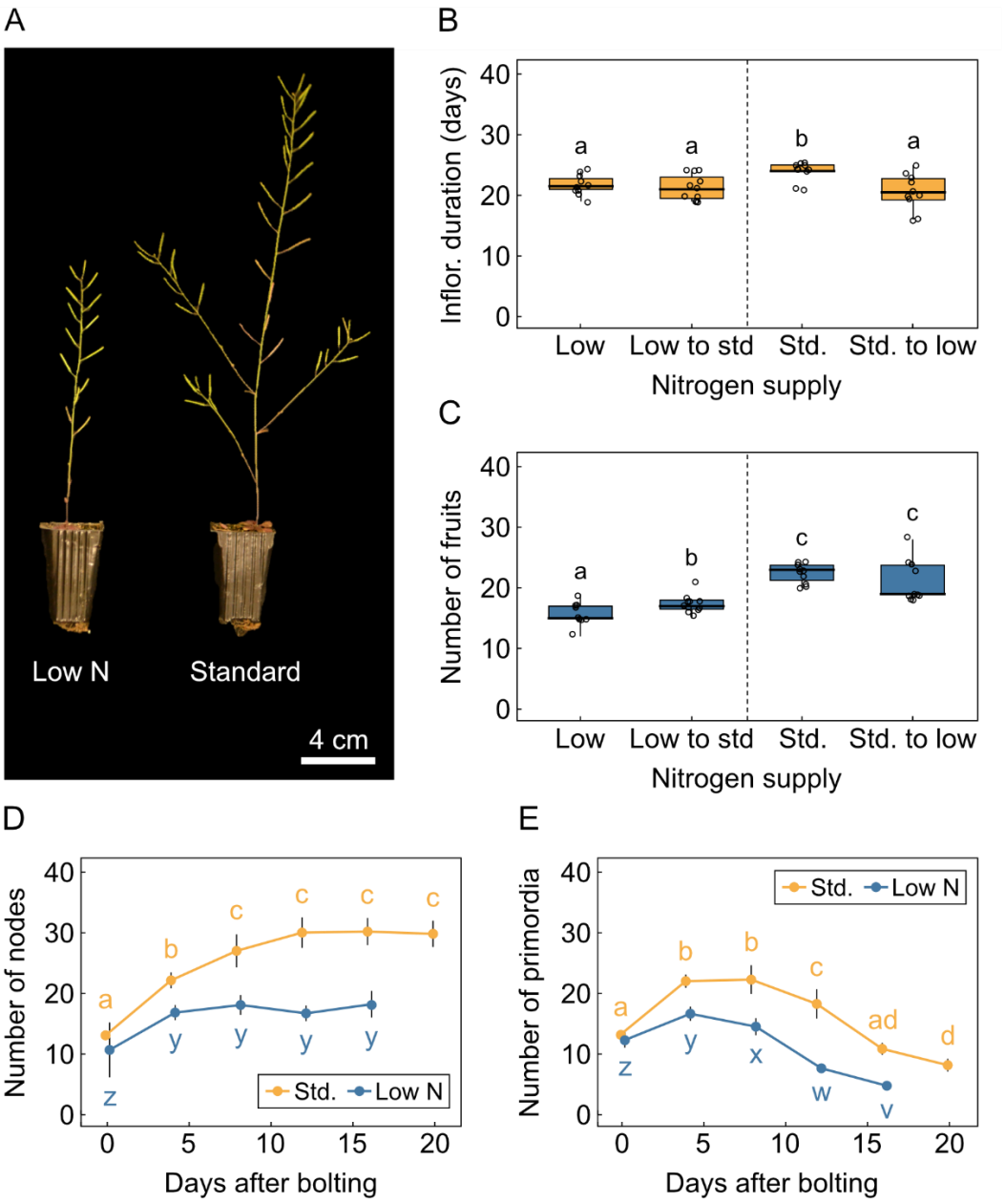

Figure 3.10. Nitrogen availability controls inflorescence arrest and yield

A. Photograph of plants supplied with standard (right) or low N growth media (left). **B-C.** Inflorescence duration (**B**) and number of fruits per inflorescence (**C**) in plants grown on standard N supply, low N supply, or transferred between the two at bolting (22ºC, 16-h day length, 120 µmol m^{-2} s^{-1}) (N=9-10). Different letters indicate statistical differences between conditions (Kruskal-Wallis rank sum test, pairwise Wilcoxon test with Benjamini and Hochberg correction, $P<0.05$). **D-E.** Cumulative number of reproductive nodes (**D**) and number of unopened floral primordia (**E**) of the primary inflorescence at different time points after bolting in plants grown on standard N supply or low N supply (N=7-8).

Figure 3.10. (Continuation)

Different letters indicate statistical differences between time points within each environmental condition (ANOVA, Tukey HSD test, P<0.05).

That N availability impacts inflorescence arrest is not surprising taking into account that its described role in controlling the timing of floral transition. Indeed, it affects the expression of key flowering genes (Vidal et al., 2014) and, recently, N availability was linked to the transcriptional regulation of the photoperiod pathway gene *CONSTANS* (*CO*). In N-limiting conditions, *CO* expression is up-regulated, leading to an activation of *FT*, which triggers earlier flowering (Sanagi et al., 2021). It is possible that the same signalling cascade takes place at the end-of-flowering, a hypothesis that should be properly inspected in any future work aiming to understand the molecular basis of this process.

3.3.9. Plant Density but not Neighbour Identity Controls Arrest

A final goal of this chapter was to explore the effect of biotic factors on inflorescence arrest. Plant-plant interaction was chosen as a case study, and a first experiment was carried out where plants were grown in 100-ml pots under two contrasting densities: one plant per pot or four plants per pot. Upon measurement of inflorescence duration and fruit set, it was found that plant density significantly affected both traits, with plants grown in crowded scenarios showing a shorter inflorescence duration (**Figure 3.11A**) and lower fruit number (**Figure 3.11B**). These results are not surprising taking into account that nutrient availability is a factor controlling inflorescence arrest (**Figure 3.8**, **Figure 3.10**). Under higher densities, competition among plants sharing the same pot likely leads to a greater limitation in nutrient availability for each plant, which in turn affects their reproductive outcome. Thus, plant density could be regulating the timing of arrest by directly limiting the

nutrient supply for plants sharing the same pot. It should be noted that the observed phenotypes could also arise as a consequence of shading, which acts through a molecular mechanism mediated by *PHYTOCHROME B* (*PHYB*) (Goyal et al., 2016).

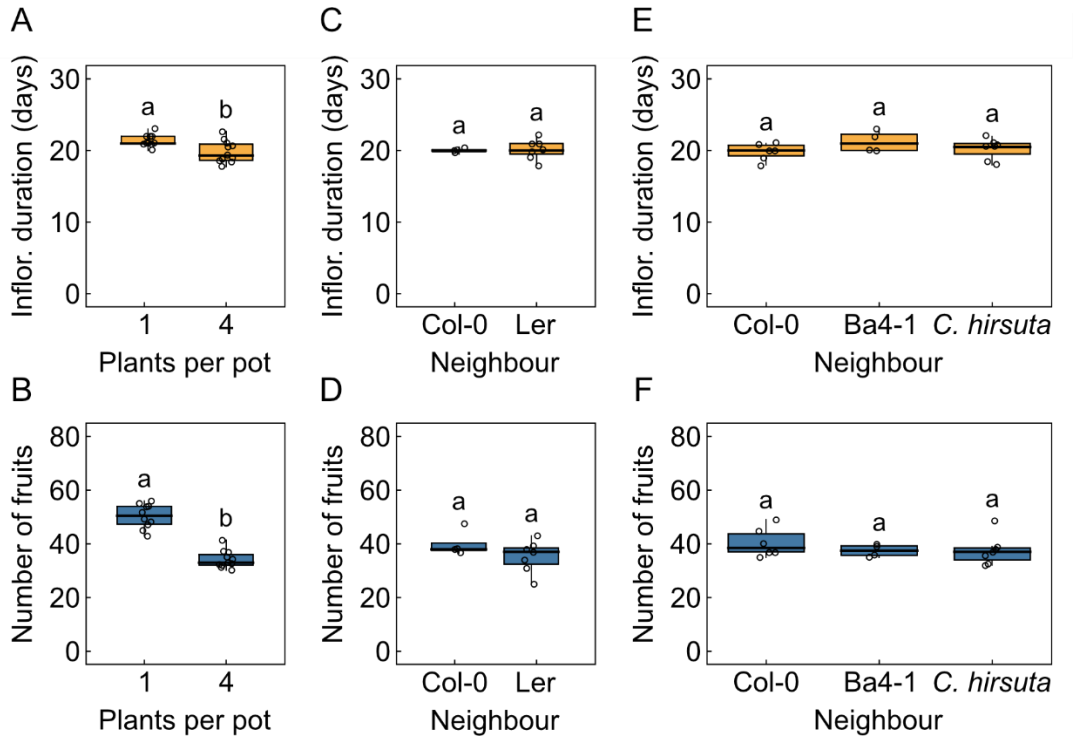

Figure 3.11. Plant density but not neighbour identity controls arrest

A-B. Inflorescence duration (**A**) and number of fruits per inflorescence (**B**) in Col-0 plants grown at a density of 1 per pot or 4 per pot (N=10-11). **C-D.** Inflorescence duration (**C**) and number of fruits per inflorescence (**D**) in Col-0 plants grown in the same pot as a neighbouring Col-0 or Ler plant (N=4-7). **E-F.** Inflorescence duration (**E**) and number of fruits per inflorescence (**F**) in Col-0 plants grown in the same pot as a neighbouring Col-0, Bå4-1 or *Cardamine hirsuta* plant (N=4-7). Different letters indicate statistical differences between groups (for A-C: Student's t test, $P<0.05$; for D: Wilcoxon test, $P<0.05$; for E and F: ANOVA, Tukey HSD test, $P<0.05$).

Next, it was questioned whether the identity of the neighbouring plant would affect end-of-flowering. There is evidence that neighbour identity affects plant responses at different levels of development, with plants grown with close relatives ('kin') displaying cooperative behaviour (Bilas et al., 2021). To test whether neighbour

identity affect the response of *A. thaliana* to neighbouring plants, Col-0 plants were grown in couples with either a neighbouring Col-0 or Ler plant, and inflorescence duration and fruit set were measured. To minimize shading-related effects, plants were sown sufficiently apart from each other within the pot. Interestingly, the identity of the neighbour did not significantly affect inflorescence arrest in the focal Col-0 plant (**Figure 3.11C**), although the number of fruits per inflorescence was slightly reduced with a neighbour Ler plant (**Figure 3.11D**). However, these little differences could be due to the accessions Col-0 and Ler being very close phylogenetically and, indeed, the Ler accession is thought to have originated directly from Col-0 (Rédei, 1992). Taking this into account, it is possible that the focal Col-0 plants are also perceiving Ler as 'kin', leading to no differences in response in comparison with a Col-0 neighbour.

To further expand on this, a new experiment was set up to test the response of Col-0 to more distant neighbours, including the Swedish accession Bå4-1 and the species *Cardamine hirsuta*. Again, no differences were found in either inflorescence duration (**Figure 3.11E**) or fruit set (**Figure 3.11F**) among Col-0 plants growing with different neighbours. Taken together, these data suggest the effect of plant density on inflorescence arrest is independent of the identity of the neighbour and that crowding imposes a limitation on the nutrient availability that ultimately affects both inflorescence duration and fruit set in *A. thaliana*.

3.4. Conclusions

The data presented here demonstrates that inflorescence arrest in *A. thaliana* is environmentally regulated. A number of environmental cues affect the timing of inflorescence arrest, including ambient temperature, vernalization, day length, nutrient (and, specifically, nitrate) availability and plant density. Generally speaking,

conditions that are known to accelerate the transition to flowering were also shown to promote inflorescence arrest, e.g., long days and warmer temperatures. This suggests that the transition in and out of flowering has the same genetic basis in *A. thaliana*, something that will be further explored in the following chapters.

In addition to this, it has been demonstrated that environmental signals regulate inflorescence arrest at the IM level by controlling the rate of production of floral primordia and the timing of meristematic arrest. In accordance with this, an active IM is needed to for plants to appropriately respond to environmental changes that occur during flowering. Altogether, these results point towards a model in which the perception of different environmental cues converges on the same pathways that underlie arrest of the IM. This would be analogous to the environmental control of floral transition, where different external inputs sensed through distinct pathways ultimately control the expression and/or stability of a handful of floral integrators.

While these results shade much light on the environmental control of the end-of-flowering, future research would highly benefit from a more detailed study of some of the evaluated signals. Particularly, although a novel role for vernalization in accelerating inflorescence arrest has been identified, the question remains as to how this is achieved at both the physiological and molecular levels. Here, it has also been suggested that plant density impacts arrest, but it would be beneficial to thoroughly assess these effects, which could arise from either shading or below-ground plant-plant communication. Lastly, all of the experiments carried out throughout this chapter have evaluated plant responses to non-stressful conditions. However, the question remains as to how these environmental stimuli affect arrest in sub-optimal scenarios, such as drought or heat stress. Thus, moving forward, it would be interesting to explore how the effects described here translate during plant stress.

Chapter 4: Molecular Basis of Inflorescence Meristem Arrest in *A. thaliana*

4.1. Introduction

While the end-of-flowering has been largely overlooked over the years, recent interest in the topic has led to several publications that provide insight into the genetic regulation of this process. Whole-transcriptome profiling of arrested meristems in *A. thaliana* suggests that arrest represents a quiescent state of the IM, with arrested IMs showing a transcriptomic signature that is resemblant of dormant axillary buds (Wuest et al., 2016). This is in accordance with the fact that arrested IMs can be reactivated when exposed to certain stimuli such as the removal of fruits (Hensel et al., 1994).

It is likely that the decline in the activity of the IM is related to the meristem identity marker *WUSCHEL* (*WUS*), as previously reported (Balanzà et al., 2018; Wang et al., 2020; Wuest et al., 2016). In short, *WUS* is a widely known homeodomain transcription factor that maintains the stem cell pool of the meristem. *WUS* expression is undetectable in arrested IMs (Wang et al., 2020; Wuest et al., 2016), suggesting that WUS activity may be crucial for the IM to maintain its proliferative state. Recently, the first genetic pathway that regulates IM arrest, the *FRUITFUL-APETALA 2* (*FUL-AP2*) pathway, was identified (Balanzà et al., 2018). Briefly, the authors proposed that the MADS-box transcription factor FUL directly represses the expression of AP2 and AP2-like genes, which are in turn activators of *WUS*. In addition to FUL, *miR172*, which accumulates over time in an age-dependent manner (Wu et al., 2009), also represses AP2-like genes, which allows for ageing to be integrated into the end-of-flowering (Balanzà et al., 2018; Martínez-Fernández et

al., 2020). Ectopic induction of *AP2* expression in arrested IMs is sufficient to reactivate meristematic activity, causing a whole-transcriptome remodelling that includes repression of stress response, induction of cytokinin (CK) responsiveness and repression of senescence, among others (Martínez-Fernández et al., 2020).

Hormonal signaling has also been showed to be important for the control of the end-of-flowering (Balanzà et al., 2023), and auxin was one of the first hormones to be implicated in the regulation of arrest. Evidence for this comes from the observation that auxin transport from fruits accelerates inflorescence arrest, and mutants disrupted in auxin transport arrest later than wild-type plants (Ware et al., 2020). According to the current model, auxin export from fruits disrupts auxin transport from the IM, leading to arrest of the developing floral primordia through undescribed molecular mechanisms. In accordance with this, auxin transport in the apex gradually decreases during flowering (Goetz et al., 2021). Cytokinin has also been characterized as a hormone with a key role in controlling the end-of-flowering. Low levels of CK in the IM correlate with a decrease in proliferative activity (Merelo et al., 2022; Walker et al., 2023), suggesting that a decline in CK underlies IM arrest. Accordingly, mutants with enhanced CK responsiveness arrest later than wild-type plants (Bartrina et al., 2017; Walker et al., 2023) and CK application can reactivate arrested IMs (Merelo et al., 2022). It has been proposed that CK signaling interacts with the FUL-AP2 pathway (Merelo et al., 2022) and a possible mechanism for this is through AP2-mediated repression of the negative regulators of CK signaling from the *KISS ME DEADLY* (*KMD*) family, *KMD2* and *KMD4* (Balanzà et al., 2023). However, these ideas still need to be formally validated. In addition to auxin and CK, other hormones have been associated with IM arrest, including abscisic acid (ABA), jasmonic acid (JA). Arrested IMs show an up-regulation of ABA-related genes (Wuest et al., 2016), many of which are targets of AP2 (Martínez-Fernández et al., 2020). Similar to ABA, JA has been proposed as a promoter of arrest based on the end-of-

flowering phenotype of mutants disrupted in JA synthesis and perception (Caldelari et al., 2011; J. Kim et al., 2013).

Despite of the growing body of information regarding the genetic and molecular regulation of the end-of-flowering, there is still much left to uncover. Specifically, our understanding of how environmental stimuli are integrated into the decision to stop flowering is very limited. Given that both floral transition and arrest constitute transitions in the plant cycle, it is possible that similar molecular factors play a role in both processes, and thus, knowledge on the environmental control of flowering may prove useful in better understanding the control of arrest (González-Suárez et al., 2020). Still, no significant research has been done in assessing the potential role of relevant flowering time genes in the integration of environmental inputs into the inflorescence arrest developmental programme. The gene *FLOWERING LOCUS T* (*FT*) is a central integrator during floral transition and recent preliminary results from the Bennett lab suggests that it may also have a key role during arrest. Thus, *FT* provides a compelling candidate for the genetic regulation of environmental plasticity during end-of-flowering.

4.2. Aims

Based on the lack of information surrounding the genetic basis of arrest, the aim of this chapter is to identify factors that control arrest at the molecular level, as well as its response to environmental signals. To achieve this, the specific goals are:

1) To identify genes that underlie the environmental control of arrest.
2) To characterize the role of the floral integrator *FT* during arrest.
3) To identify downstream targets of *FT*.

4.3. Results and Discussion

4.3.1. Strigolactone and Cytokinin Signaling Regulate Arrest

Phytohormones are key in regulating plant development and hormonal signaling has been previously associated with arrest in *A. thaliana* (Balanzà et al., 2023). Specifically, auxin, cytokinin (CK) and strigolactone (SL) have known roles in the regulation of reproductive architecture in response to soil signals such as N availability (Vega et al., 2019). Thus, it was hypothesized that these hormones would also participate in the control of inflorescence arrest. To test this, a range of *A. thaliana* mutants were screened for differences in the timing of inflorescence arrest and fruit set relative to wild-type. These included mutants deficient in genes involved in the signalling of two hormones, cytokinin (*ARR1*, *ARR3*, *ARR4*, *ARR5*, *ARR6*, *ARR7*, *ARR15*) and strigolactone (*MAX4*, *D14*, *SMXL6*, *SMXL7*, *SMXL8*) , which were all grown under standard conditions (22ºC, 16-h day length). Only two of the mutants showed an inflorescence duration significantly different to wild-type: the CK pathway sextuple mutant *arr3,4,5,6,7,15* and the SL signalling triple mutant *smxl6,7,8* (**Figure 4.1A**). In both cases, inflorescence duration was statistically longer than wild-type, and the fruit set was greater (**Figure 4.1B**).

The *arr3,4,5,6,7,15* sextuple mutant is impaired in 6 out of 11 type-B *Arabidopsis* response regulators (ARRs). Type-B ARRs participate in the last step of CK signaling and are responsible for mediating the primary response to CK at the transcriptional level (Zubo and Schaller, 2020). While the sextuple mutant showed an inflorescence duration significantly longer than wild-type, the *arr1-4* single mutant did not, suggesting that there is functional redundancy among ARRs during end-of-flowering. Overall, this suggests that ARRs and, more generally speaking, CK responsiveness, is necessary for timely inflorescence arrest. While CK had been proposed to have a role in arrest (Merelo et al., 2022; Walker et al., 2023), the specific

role of ARRs had not been explored before. It is interesting to note that, although *A. thaliana* contains 11 ARRs, only three of them, i.e., *ARR1*, *ARR10* and *ARR12*, have typically been implicated in the physiological response to CK (Ishida et al., 2008). This raises the question as to whether this is also the case during end-of-flowering, and future research investigating the specific contribution of individual ARRs to the CK pathway during arrest may shed light into this.

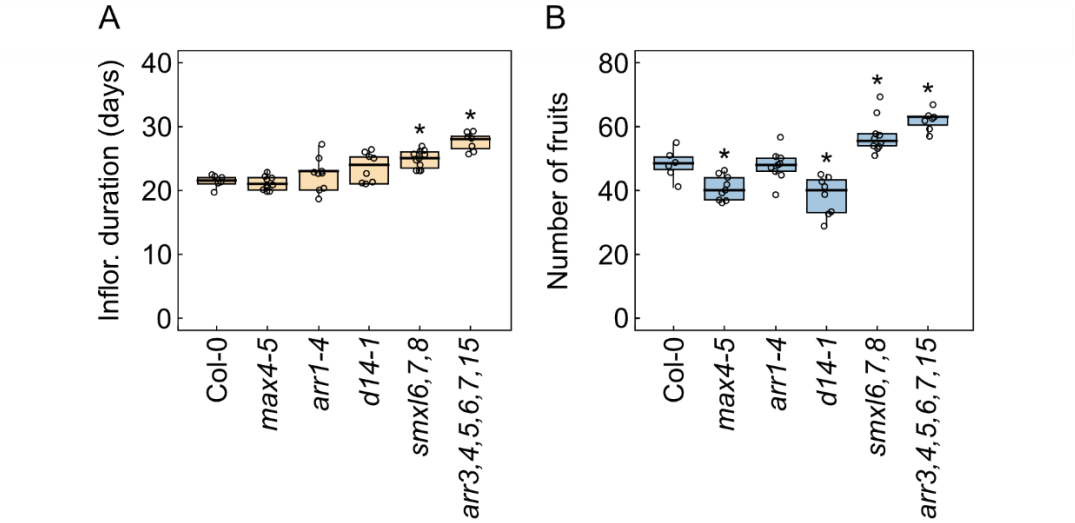

Figure 4.1. Cytokinin and strigolactone signaling control inflorescence arrest

Inflorescence duration (**A**) and number of fruits per inflorescence (**B**) in mutants deficient in cytokinin or strigolactone signaling (N=6-10). Asterisks indicate statistical differences between the mutant and wild-type (ANOVA, Tukey HSD test, P<0.05).

The *smxl6,7,8* triple mutant is impaired in 3 genes from the *SUPPRESSOR OF MAX 2-LIKE* (*SMXL*) family, which have redundant functions in the SL signaling pathway (Bennett and Leyser, 2014). During SL signaling, strigolactone physically binds to the receptor DWARF 14 (D14), triggering a conformational change that allows D14 to interact with an ubiquitination complex, as well as with SMXL proteins. As a consequence of this, SMXL proteins are ubiquitinated and later degraded, which ultimately triggers downstream responses to SLs (Marzec and Brewer, 2019). Since SMXLs act as repressors of SL-responsive genes, the *smxl6,7,8* mutant is expected

to show phenotypes opposite to those of other SL pathway mutants, and it is interesting to note that this is the case for the inflorescence fruit set (**Figure 4.1B**), suggesting a potential broad role for SL in the control of IM arrest. Still, this does not translate in substantial changes in inflorescence duration (**Figure 4.1A**), with only the *smxl6,7,8* triple mutant showing significant differences when compared to wild-type.

4.3.2. The Photoperiod Pathway Controls Inflorescence Arrest

Results from the previous chapter had demonstrated that inflorescence duration is environmentally controlled, with a particularly important role of day length, temperature and nitrogen (N) availability in regulating inflorescence arrest (see Chapter 3). Thus, it was hypothesized that known genes that underlie the perception of these signals and its integration into flowering would play a role in the end-of-flowering. To test this, a new mutant screening was carried out by growing plants in standard conditions (22ºC, 16-h day length) and recording inflorescence duration and fruit set. The genotypes selected included mutants deficient in genes involved in temperature-regulated flowering (*FLM*, *FLC*, *SVP*), light-regulated flowering (*GI*, *CO*, *PHYA*) or both (*ELF3*, *ELF4*, *PHYB*, *FT*, *TSF, PIF4*). All genotypes were grown in standard conditions (22ºC, 16-h day length), and both inflorescence duration and fruit set were recorded.

All mutants impaired in components of the photoperiod pathway (*co-2*, *gi-4*, *ft-10*, *tsf-1* and *ft-1*) showed an inflorescence duration statistically longer than wild-type controls (**Figure 4.2A**), suggesting that this pathway is involved in the regulation of inflorescence arrest. Briefly, the photoperiod pathway controls flowering through a chain of regulatory events that converges in the transcriptional activation of the floral integrator *FT* (Song et al., 2015; Srikanth and Schmid, 2011). Both GIGANTEA (GI) and CONSTANS (CO) fall upstream of FT in this pathway (Turck et al., 2008), and

TWIN SISTER OF FT (TSF) is a close paralog of FT that also promotes flowering (Wickland and Hanzawa, 2015). It is likely that the phenotypes observed in both *co-2* and *gi-4* are partially dependent on FT, however, FT-independent effects are also expected considering that the disruption in inflorescence duration in the Ler background is much more severe in these mutants compared to *ft-1* (**Figure 4.2A**). It is interesting to note that the increased inflorescence duration did not necessarily lead to a greater fruit production, with both *tsf-1* and *co-2* having the same number of fruits than wild-type and *ft-1*, an even smaller fruit set (**Figure 4.2B**).

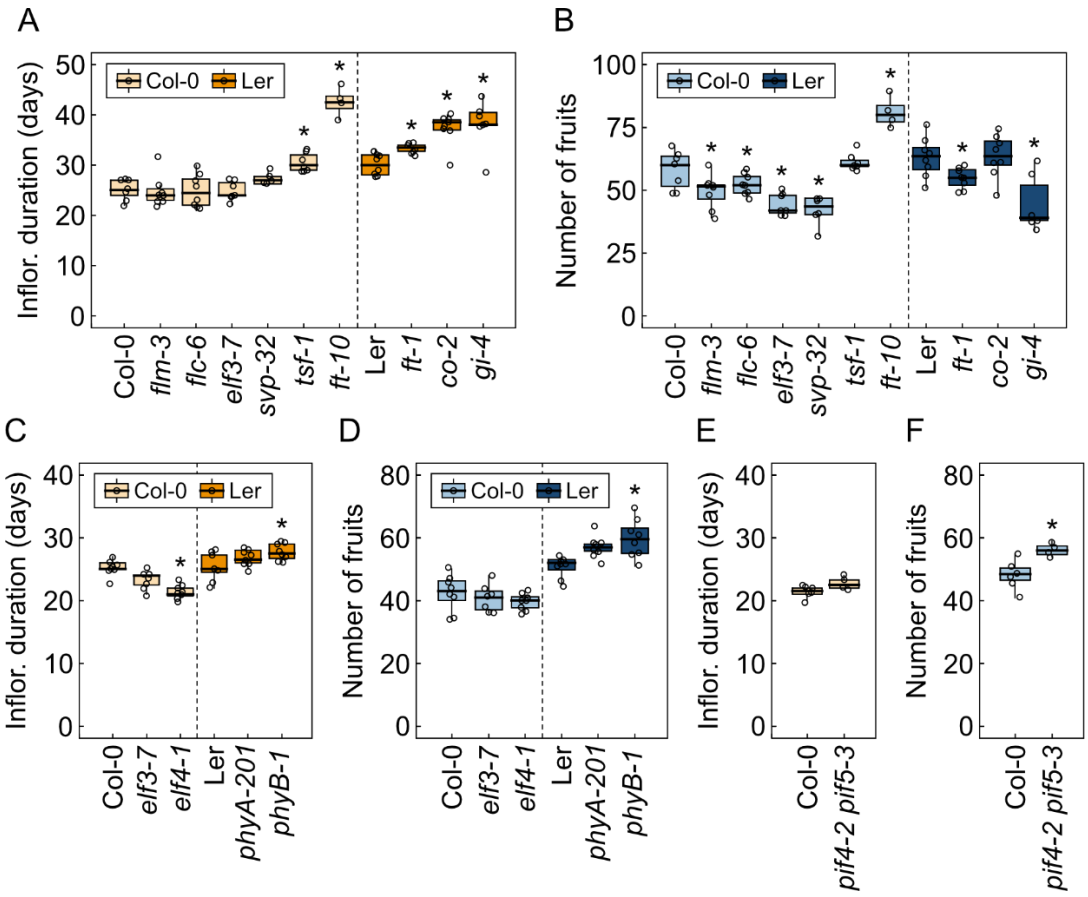

Figure 4.2. Screening of light and temperature perception mutants

Inflorescence duration (**A**, **C**, **E**) and number of fruits per inflorescence (**B**, **D**, **F**) in a series of mutants deficient in light and/or temperature perception (N=4-10). Asterisks indicate statistical differences between the mutant and the corresponding wild-type (Col-0 or Ler) (ANOVA, Tukey HSD test, P<0.05). The data in panels A and B was collected by Catriona H. Walker.

Only one of the phytochrome mutants, *phyB-1*, showed an inflorescence duration significantly different to wild-type (**Figure 4.2C**). PHYTOCHROME B (PHYB) is considered both a thermostat and a photoreceptor, and is involved in the combined perception of light and temperature through a pathway that includes the transcription factors *PHYTOCHROME INTERACTING FACTOR 4* (*PIF4*) and *PIF5* (Jung et al., 2016; Xu and Zhu, 2021). It has multifaceted roles in gene regulatory networks and, thus, it can act as both an activator and repressor of flowering (Susila et al., 2018). A separate inspection of the *pif4-2 pif5-3* double mutant revealed no significant differences in inflorescence duration compared to wild-type (**Figure 4.2E**), suggesting that PHYB does not control arrest through this pathway. As PHYB also promotes the degradation of CO (Valverde et al., 2004), it is possible that its role in arrest is through direct regulation of CO protein stability. However, greater CO levels in the *phyB-1* mutants should lead to an earlier inflorescence arrest, as CO seems to accelerate inflorescence arrest (**Figure 4.2A**). Instead, the inflorescence duration of *phyB-1* is longer than wild-type, suggesting that its role in this regulatory network is more complicated and properly understanding it would require further investigation.

Intriguingly, none of the mutants deficient in the perception of ambient temperature (*flm-3*, *flc-6*, *elf3-7*, *elf4-1* and *svp-32*) showed significant differences in inflorescence duration compared to wild-type, with the exception of *elf4-1*, whose duration was slightly shorter (**Figure 4.2A**, **Figure 4.2C**). Although not statistically significant, *elf3-7* also had a slightly shorter inflorescence duration. Both EARLY FLOWERING 3 (ELF3) and 4 (ELF4) are involved in the perception of temperature, as well as circadian regulation and light signalling (Doyle et al., 2002; Zhao et al., 2021). While they are functionally distinct (Doyle et al., 2002), they both impact flowering by transcriptionally and post-transcriptionally regulating GI (Zhao et al., 2021) and, in turn, affecting CO and FT levels. ELF3 facilitates the degradation of GI protein (Yu et al., 2008), while ELF4 decreases its activity by preventing its association with the promoter of target genes (Kim et al., 2012; Y. Kim et al., 2013).

Additionally, they both act as direct transcriptional repressors of *GI* (Ezer et al., 2017; Huang and Nusinow, 2016). As clear negative regulators of GI, and taking into account that GI is necessary for timely inflorescence arrest (**Figure 4.2A**), it is likely that both ELF3 and ELF4 regulate arrest in a GI-dependent manner. This is consistent with the shorter duration of *elf3-7* and *elf4-1* mutants (**Figure 4.2C**), which are expected to have greater GI levels.

4.3.3. The Ambient Temperature Pathway Regulates Arrest Responses to Warm but not Cold Temperature

Considering the great impact of temperature on arrest (see Chapter 3), it was surprising not to find any differences in inflorescence duration compared to wild-type among any of the mutants deficient in the ambient temperature pathway (i.e., *flm-3*, *flc-6* and *svp-32*). It was then hypothesized that, although not necessary for timely arrest at 22ºC, the ambient temperature pathway may be important for the environmental plasticity of the end-of-flowering. To test this, a subset of mutants deficient in the ambient temperature pathway were grown at two different temperatures, 20ºC and 27ºC (16-h day length for both), and their inflorescence durations and fruit sets were recorded. With the exception of the wild-type, none of the genotypes showed differences in duration between the two temperatures (**Figure 4.3A**). This strongly suggests that the ambient temperature pathway is required to modulate inflorescence duration in response to temperature. However, the number of fruits per inflorescence was reduced at higher temperatures in all the genotypes (**Figure 4.3B**), suggesting that additional factors play a role in regulating the rate of flower opening, i.e., florochron, in response to temperature.

Aside from warmth, which accelerates inflorescence arrest, cold temperatures delay the timing of arrest (see Chapter 3). Thus, it was questioned

whether cold response is also mediated by the ambient temperature pathway. In an attempt to answer this, the same set of mutants were grown at either 20ºC or 15ºC (16-h day length) until end-of-flowering, and inflorescence duration and fruit set were recorded. Surprisingly, all of the mutants extended their inflorescence duration in the cold similarly to wild-type (**Figure 4.3C**). This led to the conclusion that the ambient temperature pathway is not necessary for the regulation of arrest by cold, and that its function is restricted to warm temperatures.

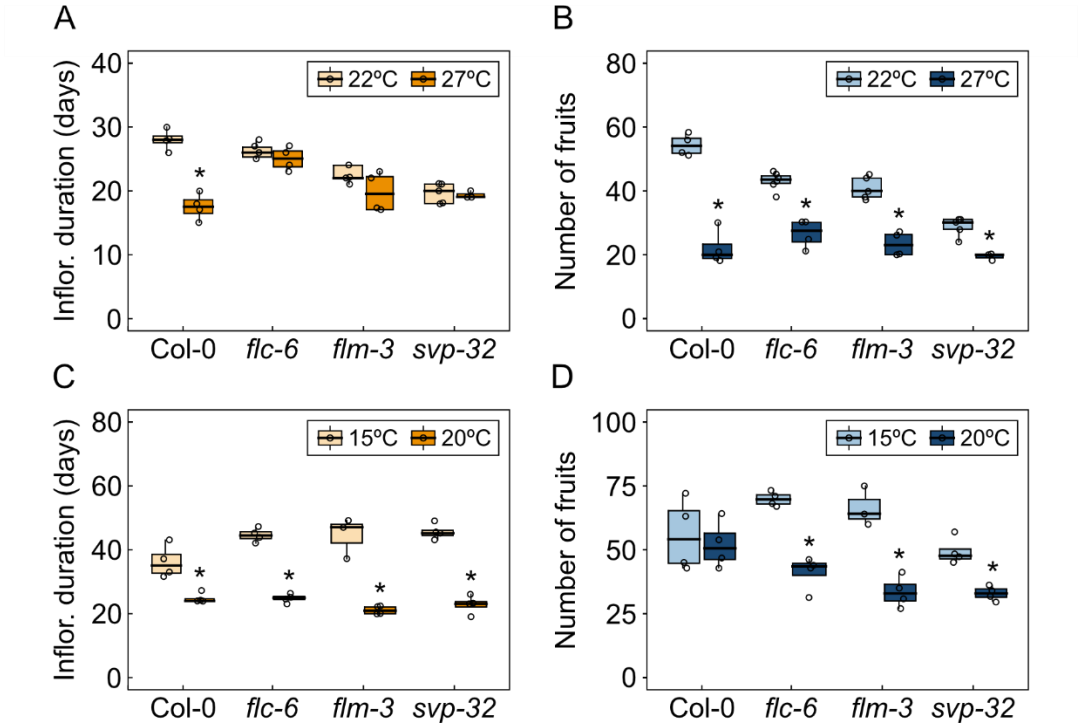

Figure 4.3. The ambient temperature pathway is necessary for arrest responses to warm but not cold temperatures

A-B. Inflorescence duration (**A**) and number of fruits per inflorescence (**B**) in mutants deficient in the ambient temperature pathway grown at 22ºC or 27ºC (N=3-6). **C-D.** Inflorescence duration (**C**) and number of fruits per inflorescence (**D**) in mutants deficient in the ambient temperature pathway grown at 15ºC or 20ºC (N=3-4). Asterisks indicate statistical differences between temperatures and within each genotype (Student's t test, $P<0.05$).

The three ambient temperature pathway genes *SHORT VEGETATIVE PHASE* (*SVP*), *FLOWERING LOCUS C* (*FLC*) and *FLOWERING LOCUS M* (*FLM*) are direct transcriptional repressors of the floral activator *FT* (Capovilla et al., 2017, 2015; Lee et al., 2013). Although none of the mutants showed any interesting phenotypes in the previous screening (**Figure 4.2A**, **Figure 4.2C**), the results presented here suggest that the ambient temperature pathway is important for the environmental plasticity of arrest, and necessary for appropriate responses to warm temperatures. Taking into account that the photoperiod pathway, which seems key for the control of inflorescence arrest (**Figure 4.2A**), also acts upstream of *FT*, it is tempting to hypothesize that *FT* acts as an environmental integrator during arrest, where both temperature and light signals converge to regulate the timing of inflorescence arrest. Indeed, *FT* is a known integrator of these signals during floral transition (Bratzel and Turck, 2015; Turck et al., 2008; Wickland and Hanzawa, 2015), which further supports this idea.

In light of these results, the question remains as to how arrest responses to cold temperatures are regulated, if not by the ambient temperature pathway. Most of the known thermosensors in *A. thaliana* have been identified in warm temperatures, with not as many known to have a role in cold (Brightbill and Sung, 2022). It is possible that the regulation of arrest by cold is mediated by genes that were not considered in this experiment. For instance, PHYB is a regulator of signals that participate in cold acclimation processes, including PIF4 and PIF5 (Jiang et al., 2020), which raises the possibility that the PHYB-PIF pathway underlies responses to cold during end-of-flowering. Another possible explanation is that this regulation occurs directly at the *FT* level. In the cold, the FT protein binds to cell membranes, which limits its mobility (Susila et al., 2021). FT acts as a promoter of arrest (**Figure 4.2A**) and the role of FT as a floral activator largely depends on FT protein produced in the leaves translocating to the meristem (Corbesier et al., 2007). Thus, cold-

induced retention of FT in the leaves could explain the delay in arrest seen in cold temperatures without the need for additional upstream regulators.

4.3.4. *FLOWERING LOCUS T* is a Key Regulator of IM Arrest

Most of the mutants that exhibited an inflorescence duration significantly different to wild-type, particularly those involved in photoperiod and/or temperature perception, seemed to be disrupted in molecular pathways that converge in the floral integrator *FT*. Thus, it was hypothesized that *FT* would be a central component of the molecular process that underlies IM arrest and its response to the environment, and new experiments were designed to further explore this idea. Compared with the difference in inflorescence duration between Col-0 and the *ft-10* mutant (~20 days), the *ft-1* mutant only arrested slightly later than its Ler wild-type (**Figure 4.2A**). Thus, the mutants and corresponding wild-types were grown again in standard conditions (22ºC, 16-h day length) to validate these observations. In this new experiment, the inflorescence duration of *ft-1* was much longer leading to differences against the wild-type that were comparable to those of *ft-10* (**Figure 4.4A**). In agreement with this, both mutants produced more fruits per inflorescence than wild-type plants (**Figure 4.4B**). Additionally, analysis of a heterozygous line, obtained by crossing Col-0 and *ft-10* mutants, demonstrated that a single functional copy of *FT* is sufficient to rescue the *ft-10* phenotype and, thus, for timely inflorescence arrest (**Figure 4.4A**).

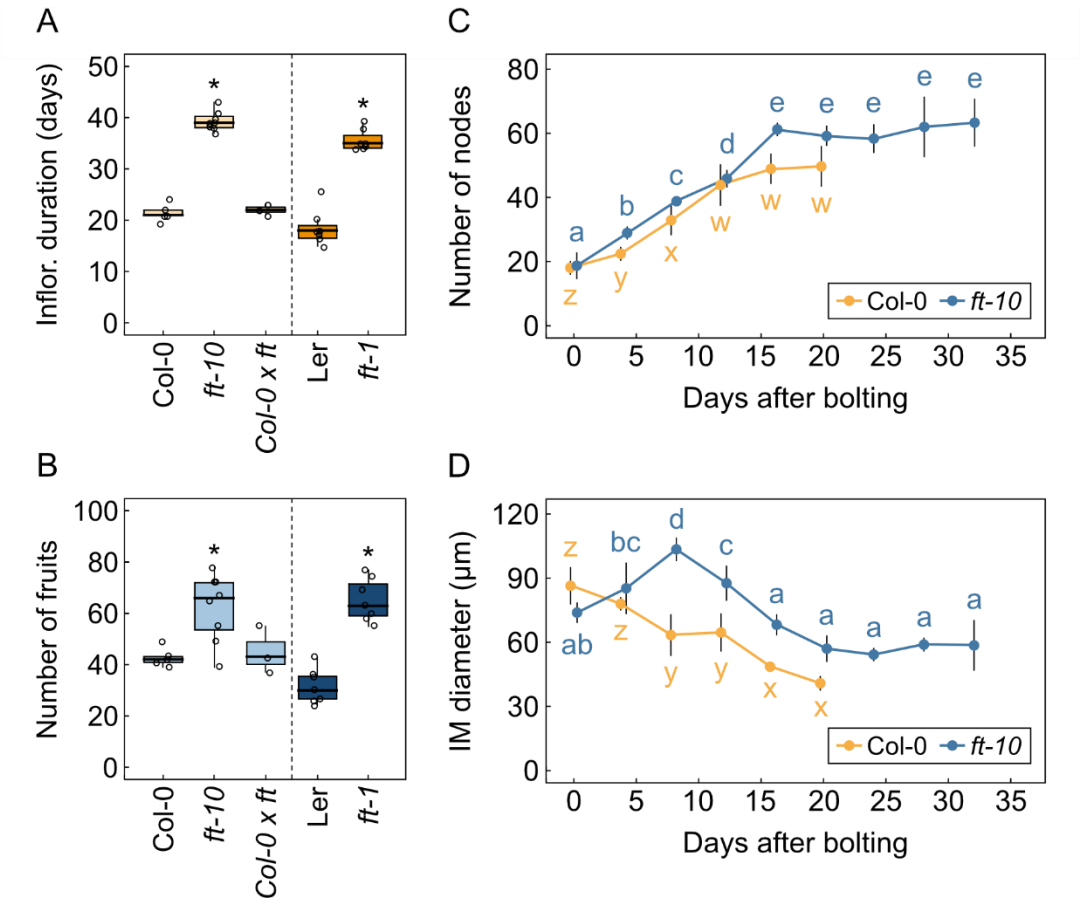

Figure 4.4. FT is necessary for timely arrest of the inflorescence meristem

A-B. Inflorescence duration (**A**) and number of fruits per inflorescence (**B**) in *ft* knock-out mutants and the heterozygous Col-0 x *ft-10* (N=3-8). Different colours indicate different genetic background (light yellow and blue: Col-0; dark yellow and blue: Ler). Asterisks indicate statistical differences between the mutant and the corresponding wild-type (ANOVA, Tukey HSD test, P<0.05). **C-D.** Cumulative number of reproductive nodes (i.e., fruits, flowers and unopened floral primordia) (**C**) and IM diameter (**D**) of the primary inflorescence at different time points after bolting in *ft-10* and wild-type Col-0 (N=3-8). Different letters indicate statistical differences between time points within each genotype (ANOVA, Tukey HSD test, P<0.05).

Temperature and day length control inflorescence arrest by regulating the activity of the IM (see Chapter 3). Based on this, it was questioned whether *FT* controls arrest of the IM specifically. To test this, the *ft-10* mutant was grown in standard conditions (22ºC, 16-h day length) and its IM was dissected in a time-course

manner to record the number of floral primordia produced during flowering. While Col-0 stopped producing new reproductive organs ~12 days after bolting, the *ft-10* mutant continued to do so for ~4 more days (**Figure 4.4C**). In addition to this, the size of the IM in *ft-10* was consistently greater than that of the wild-type at all time points, and started decreasing ~8 days later (**Figure 4.4D**). Taken together, these results suggest that functional *FT* is necessary for timely IM arrest, raising the possibility that day length and temperature control over IM arrest is FT-dependent. It is worth noting that, unlike changes in temperature or day length (see Chapter 3), the lack of functional *FT* did not affect the rate of production of floral primordia (**Figure 4.4C**), which is probably controlled through FT-independent mechanisms.

4.3.5. *FT* is Necessary for Arrest Responses to Warm Temperature

Based on the phenotype of the *ft-10* mutant, and the established role of *FT* in integrating light and temperature inputs during floral transition, it was hypothesized that *FT* would be necessary for the environmental control of arrest. To test this idea, three separate experiments were conducted to examine the effect of warm and cold temperature, as well as day length, on the *ft-10* mutant. While wild-type plants showed a reduction in inflorescence duration at warm temperatures, *ft-10* mutants did not (**Figure 4.5A**), and arrested with the same number of fruits per inflorescence regardless of the temperature (**Figure 4.5B**). In contrast, *ft-10* mutants were able to respond to both cold temperatures (**Figure 4.5C**, **Figure 4.5D**) and day length (**Figure 4.5E**, **Figure 4.5F**) in a manner roughly similar to wild-type.

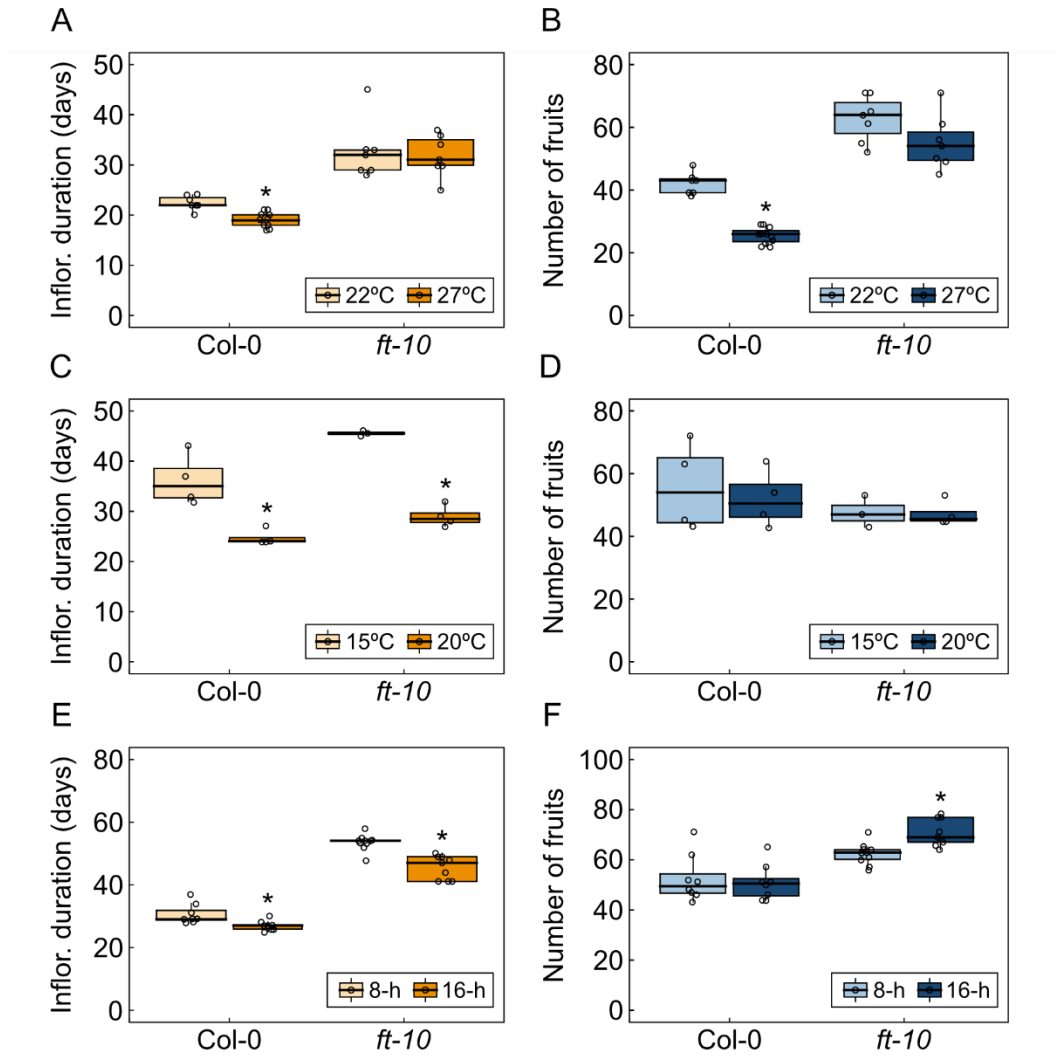

Figure 4.5. FT is necessary for environmental plasticity of arrest in the warmth

A-B. Effect of warm temperature on the *ft-10* mutant. Inflorescence duration (**A**) and number of fruits per inflorescence (**B**) in plants grown at 22ºC or 27ºC (N=12). **C-D.** Effect of cold temperature on the *ft-10* mutant. Inflorescence duration (**C**) and number of fruits per inflorescence (**D**) in plants grown at 15ºC or 20ºC (N=3-4). **E-F.** Effect of day length on the *ft-10* mutant. Inflorescence duration (**E**) and number of fruits per inflorescence (**F**) in plants grown at 8-h or 16-h day length (N=9-12). Asterisks indicate statistical differences between conditions and within each genotype (Student's t test, $P<0.05$).

Taken together, these results suggest that *FT* is essential for the plasticity of arrest in response to warm temperature, but not necessarily for the response to cold or day length. Components of the ambient temperature pathway (i.e., *SVP*, *FLM*, *FLC*) were previously shown to be necessary for the response to warm temperature (**Figure 4.3A**) and, in light of the new information, it is likely that this is FT-dependent. Indeed, SVP and proteins from the FLC clade, to which both FLC and FLM belong, are known to form regulatory complexes that transcriptionally repress *FT* (Capovilla et al., 2017). In contrast, neither the ambient temperature pathway nor FT seem to mediate the response to cold during end-of-flowering. Thermosensory processes are poorly understood at cold temperatures in *A. thaliana*, with the few known pathways usually including FT as a central component (Brightbill and Sung, 2022). Given the lack of clear alternative candidates for the response to cold during end-of-flowering, future research targeting this question could benefit from more general approaches such as a screening of EMS-mutagenized seeds in search for genotypes that are disrupted in the response to cold during end-of-flowering.

Finally, these results suggest that FT is also not necessary for arrest responses to day length. While *ft-10* mutants had inflorescence durations consistently longer than wild-type plants in both 8-h and 16-h day lengths, arrest was still accelerated at longer day lengths (**Figure 4.5E**). This suggests that the plasticity of arrest in response to day length is mediated by alternative mechanisms, and a promising alternative is that it is controlled through the photoperiod pathway independently of FT. Recently, a new role for the photoperiod pathway gene *CO* in regulating seed size has been identified (Yu et al., 2023). According to the proposed model, *CO* can directly repress the transcription of *AP2* in the seeds through a photoperiod-sensitive pathway. It is possible that this novel CO-AP2 regulatory hub also acts in the IM, and its potential implication in the control of arrest, as well as its response to changes in day length, should be formally investigated.

4.3.6. Transcriptional Activation of *FT* Underlies IM Arrest

During floral transition, the photoperiod and ambient temperature pathways trigger the conversion of the apical meristem to an IM through signaling cascades that lead to a transcriptional up-regulation of *FT* (Srikanth and Schmid, 2011). Thus, it was hypothesized that regulation of *FT* at the transcriptional level could also underlie IM arrest. To test this, a new experiment was designed to characterize the expression dynamics of *FT* during flowering in a time-course manner. Wild-type Col-0 plants were grown in standard conditions (22ºC, 16-h day length) and samples of different tissues (i.e., leaves, siliques and IMs) were harvested every 4 days after bolting for quantification of *FT* mRNA levels via RT-qPCR. In addition to the sampling, time-course dissections of the IM were performed to determine the approximate time of IM arrest, which occurred ~12-16 days after bolting in this experiment (**Figure 4.6A**).

Interestingly, *FT* expression in both rosette and cauline leaves was up-regulated at later points in flowering, leading to a peak of expression ~12-16 days after bolting, after which *FT* mRNA levels substantially decreased (**Figure 4.6B**). In fruits, *FT* expression did not show significant changes during flowering (**Figure 4.6C**). However, *FT* mRNA levels in the IM increased slightly ~12 days after bolting, and even more so at very late time points, ~20 days after bolting (**Figure 4.6D**). *FT* expression in the leaves is known to increase over time during the vegetative phase, and to reach an expression peak prior to floral transition (Song et al., 2015). However, expression dynamics of *FT* at later time points have been largely overlooked (Liu et al., 2014). The results presented here indicate that *FT* expression in the leaves shows a previously uncharacterized second peak of expression approximately 2 weeks after bolting (**Figure 4.6B**), which coincides with the timing of IM arrest (**Figure 4.6A**). This suggests that a transcriptional activation of *FT* in the leaves could be associated with IM arrest. In addition, it is interesting to note that *FT* expression is induced in arrested

IMs at late time points (**Figure 4.6D**), raising the possibility that *FT* could have an additional role in maintaining the dormant state of arrested meristems.

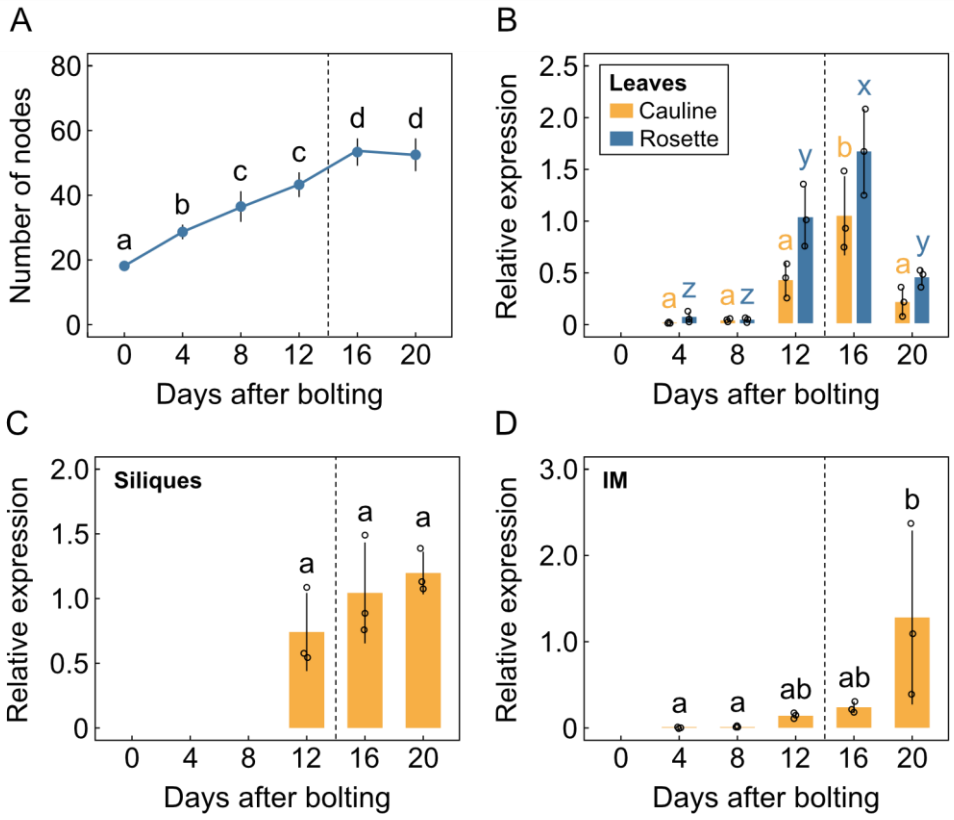

Figure 4.6. Global *FT* expression increases during flowering

A. Cumulative number of reproductive nodes (i.e., fruits, flowers and unopened floral primordia) produced during flowering in the population of wild-type plants used for RT-qPCR. **B-D.** Expression dynamics of the *FT* transcript in leaves (**B**), siliques (**C**) and the IM (**D**) during flowering (N=3). Transcript levels are normalized to *UBC9* and then referred to the day at which the maximum *FT* level was achieved, which was 16 days post-bolting. Different letters indicate statistical differences between time points (ANOVA, Tukey HSD test, P<0.05). The dashed line indicates approximate timing of IM arrest.

In any case, these data indicate that *FT* expression peaks at the same time points at which the IM arrests. Thus, it was speculated that the transcriptional up-regulation of *FT* could trigger IM arrest. To further validate this idea, a transgenic construct containing the *FT* coding sequence driven by the constitutive CaMV 35S

promoter and fused to a rat glucocorticoid receptor (GR) was introduced into the Col-0 background. Due to the 35S promoter, the resulting line over-expresses *FT*. However, due to the GR fusion, the FT protein is excluded from the nucleus unless a steroid hormone such as dexamethasone (DEX) is added to the growth media, rendering the transgenic FT inactive in the absence of DEX. It was hypothesized that a DEX-induced *FT* over-expression during early development would accelerate IM arrest. To test this, a set of 6 independent lines bearing the *35S:FT-GR* construct were grown in sterile conditions on either standard growth media (ATS) or DEX-supplemented media, and both the flowering time and number of reproductive nodes were recorded. While the presence of DEX did not have any effect on flowering time in Col-0, it significantly promoted it in most of the transgenic lines (**Figure 4.7A**). An ectopic over-expression of *FT* early in development is expected to cause an acceleration of flowering (Kardailsky et al., 1999; Kobayashi et al., 1999), which was found here for 3 of the lines, i.e., L-2, L-4 and L-7. All the transgenic lines but one showed a lower number of reproductive nodes per inflorescence at the end-of-flowering in DEX-supplemented media (**Figure 4.7B**). Indeed, most of the plants bearing a transgenic *35S:FT-GR* showed visual signs of early senescence when grown with DEX (**Figure 4.7C**) but not in control media (**Figure 4.7D**), likely due to the acceleration in end-of-flowering. Altogether, these results suggest that an ectopically-induced over-expression of *FT* during early development accelerates IM arrest and support the idea that a transcriptional activation of *FT* underlies arrest at the meristematic level.

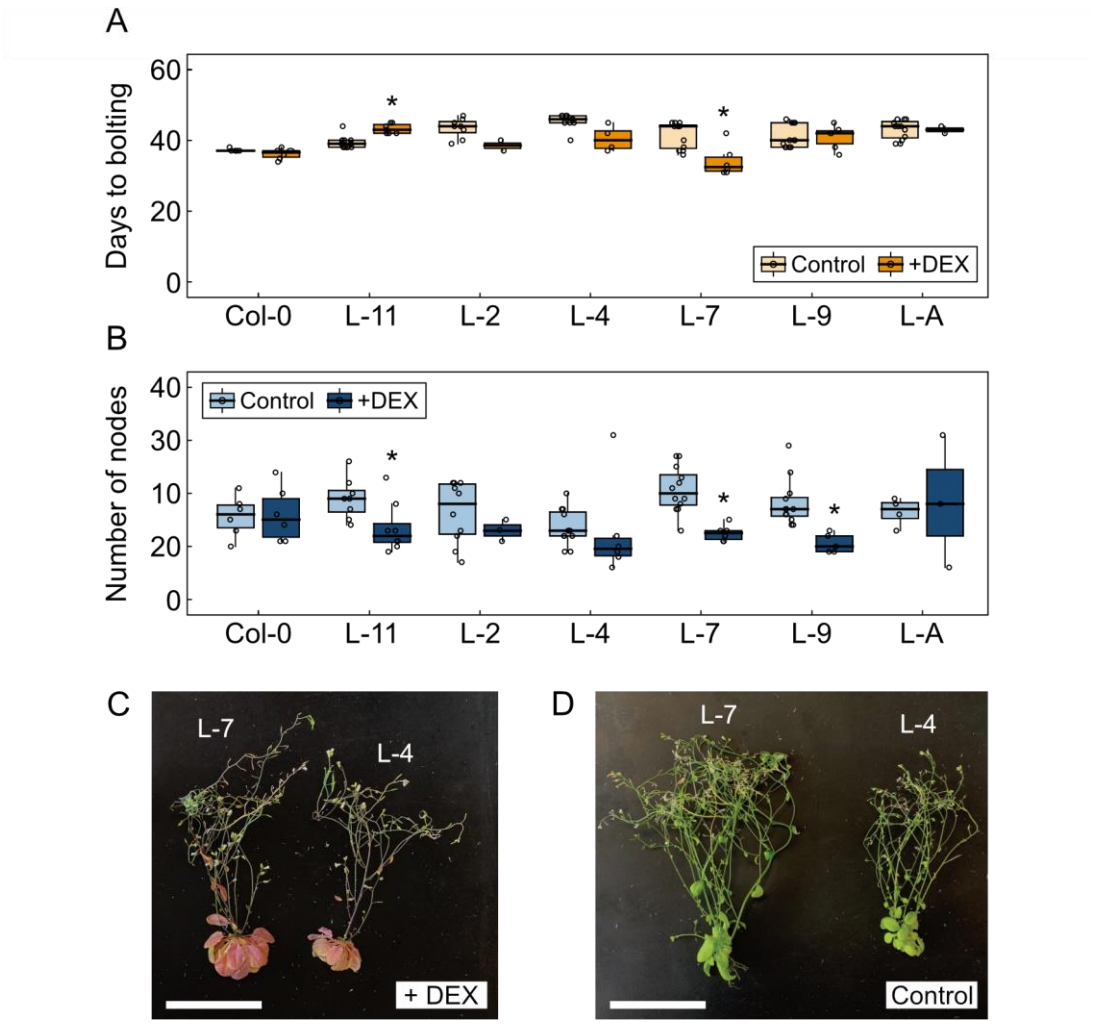

Figure 4.7. Ectopic over-expression of *FT* accelerates IM arrest

A-B. Flowering time, measured in days to bolting (**A**), and final number of reproductive nodes per inflorescence (**B**) in *35S:FT-GR* lines (N=3-12). Asterisks indicate statistical differences between control and DEX-supplemented media for each genotype (Student's t test, P<0.05). **C-D.** Photographs showing the phenotype of *35S:FT-GR* lines grown in DEX-supplemented (**C**) or control (**D**) media. Scale bar represents 5 cm.

Previously, it had been noted that the environmental plasticity of arrest is FT-dependent, particularly in response to ambient temperature (**Figure 4.5**). Knowing that the expression of gradually *FT* increases during flowering (**Figure 4.6**) and that transcriptional up-regulation of *FT* triggers IM arrest (**Figure 4.7**), it was hypothesized that temperature could impact arrest by modulating *FT* expression levels. To test this,

a new experiment was conducted in which plants were grown at 20ºC until bolting. Next, a subset of plants was transferred to 15ºC, while the others were maintained at 20ºC, and rosette leaves were harvested for both temperatures 8 and 16 days after bolting for the quantification of *FT* mRNA levels through RT-qPCR. In plants grown at 20ºC, *FT* expression was up-regulated as early as 8 days after bolting, whereas it stayed at lower levels all throughout the experiment for plants grown at 15ºC (**Figure 4.8**). Generally speaking, *FT* levels increased gradually at both temperatures, but they did so more slowly at 15ºC. Both cold and warm temperatures are known to affect *FT* expression during the vegetative phase (Blázquez et al., 2003; Thines et al., 2014), which ultimately affects flowering time. The results presented here suggest that ambient temperature continues to affect *FT* expression after floral transition, and raises the possibility that regulation at the transcriptional level underlies the environmental plasticity of arrest, particularly in response to warm temperatures.

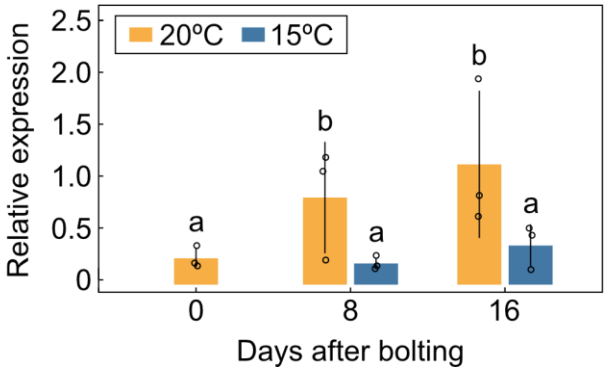

Figure 4.8. *FT* expression during flowering is affected by temperature

Relative expression of *FT* in rosette leaves at different time points after bolting in plants grown at 20ºC or 15ºC (N=3). Transcript levels are normalized to *UBC9* and then referred to the day at which the maximum *FT* level was achieved, which was 16 days post-bolting in 20ºC. Different letters indicate statistical differences between time points and/or temperatures (ANOVA, Tukey HSD test, P<0.05).

4.3.7. Identification of Transcriptional Targets Downstream of FT

The data presented throughout this chapter strongly supported a role for *FT* in the control of inflorescence arrest, but the question remained as to what could be the molecular mechanism underlying this. Prior to flowering, FT synthesized in the leaves is transported through the phloem to the SAM (Corbesier et al., 2007). In the SAM, FT physically interacts with the transcription factor FD (Abe et al., 2005), forming a protein complex that can induce the transcription of important floral identity genes such as *APETALA 1* (*AP1*) or *FUL* (Wigge et al., 2005). Thus, during the beginning of flowering, FT acts mainly by transcriptionally regulating downstream genes. Based on this, it was hypothesized that FT also functions as a transcriptional regulator during IM arrest. To further explore this idea, and with the ultimate goal of identifying potential target genes for FT during end-of-flowering, a new experiment was designed to track changes in the whole transcriptome of IMs in *ft-10* and wild-type plants during meristematic arrest. IMs of both genotypes were sampled at two different time points during flowering, i.e., 4 and 12 days after bolting. The sampling points were chosen to reflect an active stage when the IM is still proliferative in both wild-type and *ft-10* and an arrested stage when the IM of the wild-type has already undergone arrest, but that of *ft-10* has not (**Figure 4.4C**). Finally, samples were used for RNA extraction and standard RNA sequencing (Genewiz, Azenta Life Sciences).

Principal Component Analysis (PCA) was used to reduce the dimensionality of the RNA-Seq data and facilitate a preliminary exploratory analysis. The first principal component (PC1), which accounts for 51% of the variance, allowed to clearly differentiate the second time point in the wild-type, corresponding to arrested IMs, from the rest of the samples (**Figure 4.9A**). This suggests that there are substantial differences at the whole-transcriptome level between arrested wild-type IMs and active IMs from either wild-type of *ft-10* plants. Indeed, the differences between the rest of the samples were much less pronounced, especially considering

the highly similar values in both PC1 and PC2 for most samples from the first time point. Hierarchical clustering, which was used to group the samples based on their general similarities, seemed to validate these observations. Samples from arrested IMs form a cluster distinctly separated from the rest of the samples (**Figure 4.9B**). In addition, samples from both genotypes for the first time point seem to cluster together. Finally, samples from *ft-10* for the second time point, while seemingly forming their own group, fall closer to earlier samples of active IMs than to arrested wild-type IMs, which is expected given that *ft-10* IMs are still proliferative at this stage.

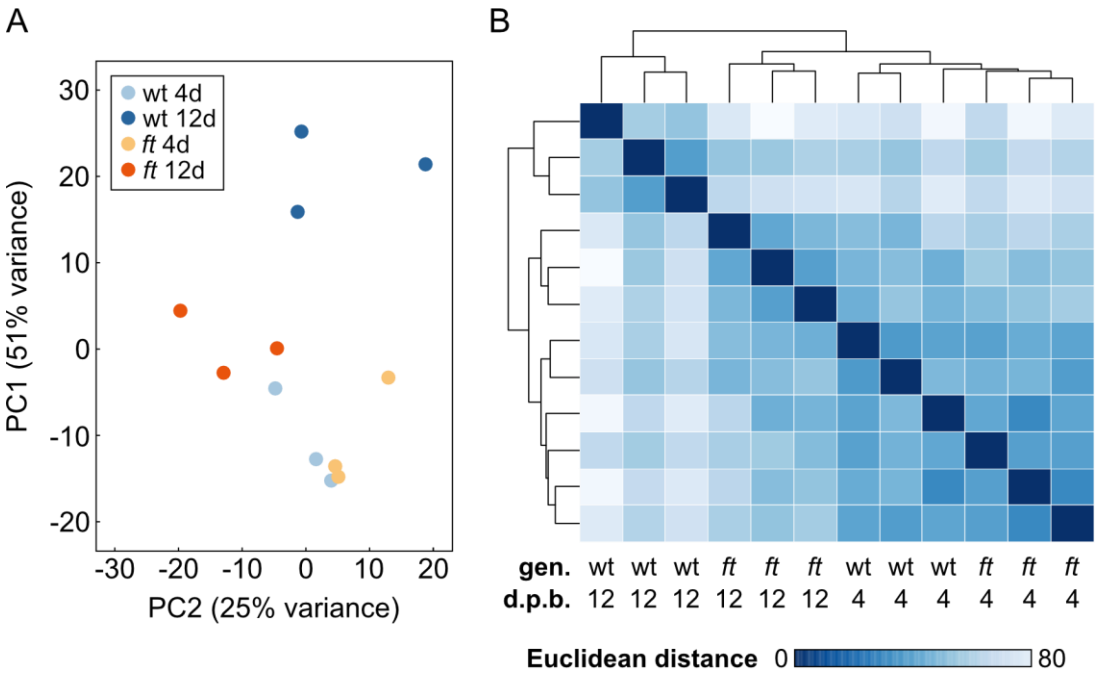

Figure 4.9. Exploratory analysis of the *ft-10* RNA-Sequencing data

A. Principal Component Analysis (PCA) performed on the VST-transformed read counts. **B.** Heat map and hierarchical clustering of the sample-to-sample Euclidean distances calculated using the VST-transformed read counts. The genotype (gen.) and days post bolting (d.p.b.) corresponding to each sample are indicated at the bottom. wt: wild-type (Col-0). *ft*: *ft-10*. 4/12d: 4/12 days post bolting.

Next, a statistical analysis was performed to identify genes for which the expression over time is significantly affected by the genotype. A total of 2,634 genes

(~10% of all quantified genes) were found to be differentially expressed over time between wild-type and *ft-10*. In other words, these are genes for which their wild-type expression dynamic is disrupted in the *ft-10* mutant. To better understand these differentially expressed genes (DEGs), unsupervised classification was used to group them into clusters with similar expression patterns. The number of clusters was set to 4 based on the minimum centroid distance criterion (**Figure 4.10A**), and the number of genes assigned to each cluster was quantified (**Figure 4.10B**).

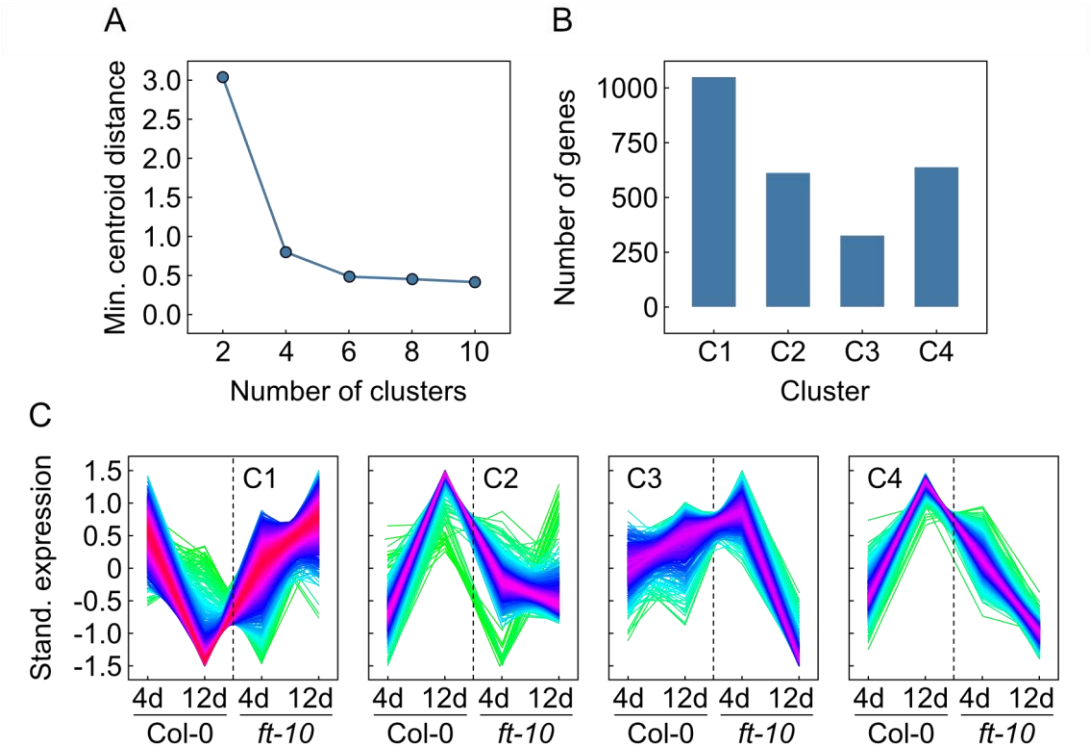

Figure 4.10. Summary of results for the clustering of genes differentially expressed in *ft-10*

A. Effect of the number of clusters on the minimum centroid distance between the cluster centroids. The optimal number of clusters is considered that after which the minimum centroid distance declines more slowly. **B.** Number of genes assigned to each of the four clusters. **C.** Standardized gene expression of genes belonging to each cluster (C1-C4). The colour represents membership to the cluster (yellow and green correspond to genes with low membership value, red and purple correspond to genes with high membership value).

Based on their expression profile in wild-type plants (**Figure 4.10C**), DEGs can be classified in 3 major types (**Table 4.1**). The vast majority of genes, including types A and B, are either down- or up-regulated, respectively, from 4 to 12 days post bolting in wild-type IMs, but not in *ft-10*. Thus, these are of special interest as they may play a relevant role during wild-type IM arrest and could also fall downstream of FT. On the other hand, type C corresponds to a small group of genes that do not change between 4 and 12 days post bolting in wild-type IMs. While these are differentially expressed in *ft-10* compared to wild-type, their transcriptomic profile in wild-type plants suggest that they may not be relevant targets of FT in the context of IM arrest.

Table 4.1. Types of genes differentially expressed in *ft-10*

Type	Cluster	Description	Number	Examples
A	C1	Down-regulated in wild-type (during IM arrest) but not in *ft-10*	1,053 (**40%**)	*SVP*, *CAL*, *AHK4, CYCB2;3, STM…*
B	C2 C4	Up-regulated in wild-type (during IM arrest) but not in *ft-10*	1,254 (**48%**)	*MAX1*, *KNU, HB-3*, *HB51*…
C	C3	Stable in wild-type (during IM arrest) but not in *ft-10*	327 (**12%**)	*AP2*, *TFL1*, *CKX1*…

To better visualize the expression pattern of each cluster, standardized read counts of a random sample of genes per cluster were plotted as a heat map (**Figure 4.11A-D**, top left). Additionally, membership scores provided by the unsupervised classification method used for clustering (Mfuzz) were used to select a representative gene per cluster (**Figure 4.11A-D**, top right), and Gene Ontology (GO) enrichment analysis was performed separately on each cluster to gain a better insight of the biological significance of these expression groups (**Figure 4.11A-D**, bottom).

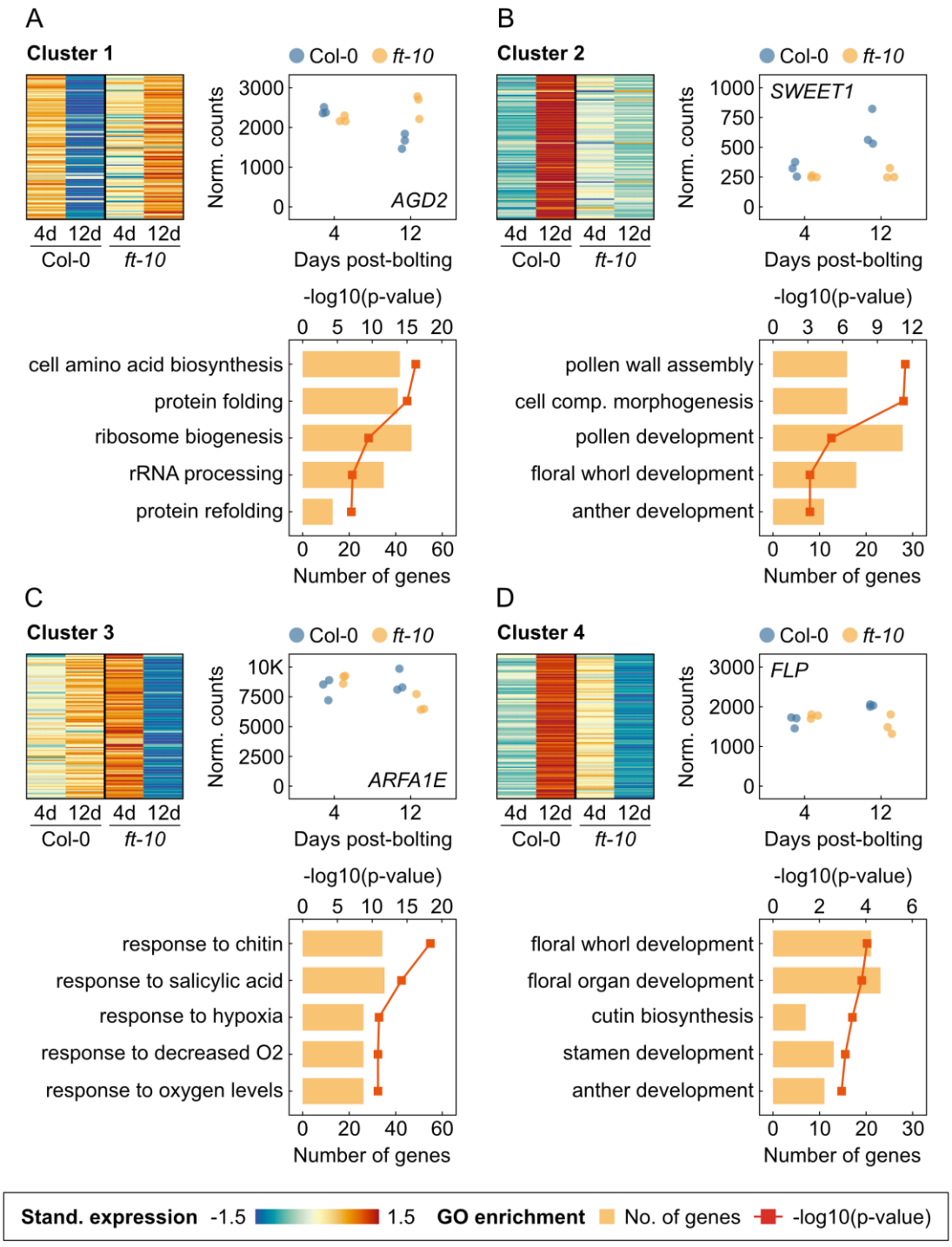

Figure 4.11. Clustering of genes differentially expressed in *ft-10*

Each cluster is visualized in a separate panel (**A-D**). Each panel includes a heat map showing the expression of random sample of 100 genes from the cluster (top left), the expression profile of a representative gene (top right) and the top 5 enriched GO terms (bottom). For heat maps, expression is in standardized DESeq2-normalized counts. For individual gene graphs, it is in non-standardized DESeq2-normalized counts. For GO enrichment results, the p-value and number of genes are shown.

Genes from cluster 1, which are down-regulated in wild-type IMs (type A), were significantly enriched in GO terms associated with amino acid biosynthesis, as well as protein synthesis and folding. An interesting gene identified within this group is the histidine kinase *ARABIDOPSIS HISTIDINE KINASE 4* (*AHK4*), which is a known cytokinin (CK) receptor (Yamada et al., 2001). Homologues of *AHK4*, *ARABIDOPSIS HISTIDINE KINASE 2* (*AHK2*) and *3* (*AHK3*), have been implicated in the control of end-of-flowering before (Bartrina et al., 2017), and current models of IM arrest propose that repression of CK signaling in the meristem is necessary for arrest (Merelo et al., 2022), which is consistent with the decline in *AHK4* expression seen in arrested wild-type IMs in this dataset. Interestingly, this raises the possibility that FT functions during IM arrest by modulating CK signaling, e.g., through transcriptional down-regulation of *AHK4*, either directly or indirectly. In any case, further investigation would be required to validate this idea, as well as to gain a full understanding of the interactions between FT and CK signaling during IM arrest.

Genes from clusters 2 and 4, which are up-regulated in wild-type IMs (type B), were enriched in GO terms related mainly to flower and pollen development, among others. A number of genes found within these clusters are regulators of the homeodomain transcription factor *WUS*, e.g., *FANTASTIC FOUR 2* (*FAF2*), *KNUCKLES* (*KNU*), *ARR12* or *HOMEOBOX 3* (*HB-3*), among others. Given that *WUS* is a well-characterized regulator of stem cell maintenance in shoot apices, and a decline in WUS activity is associated with IM arrest (Balanzà et al., 2018; Goetz et al., 2021; Merelo et al., 2022), it is also possible that FT signaling controls IM arrest through fine-tuning *WUS* levels. Indeed, the FUL-AP2 pathway, which is an important player in the control of IM arrest, also converges in the control of WUS (Balanzà et al., 2018). Another example of an interesting gene belonging to this group is the homeodomain transcription factor *HOMEOBOX 53* (*HB53*), which promotes abscisic acid accumulation during bud dormancy (González-Grandío et al., 2017). Recently, HB53 has been characterized as a main contributor to IM arrest (Sánchez-Gerschon

et al., 2023). This makes HB53 an interesting candidate gene for the downstream effect of FT in arrest, an hypothesis that would require careful investigation.

A limitation of the whole-transcriptome profiling as an approach to identify downstream targets of FT during arrest lies in the fact that DEGs may have been pooled out simply because IMs in the *ft-10* mutant are proliferative at both time points. Thus, it is unclear with the information that is currently available which DEGs are causative for the phenotype of *ft-10* mutants, and which are a consequence of *ft-10*'s extended IM lifespan. Still, this dataset offers a compelling list of candidate genes which will direct future research efforts to better understand downstream effects of FT signaling during IM arrest. Specifically, DEGs annotated with GO terms related to 'meristem development' (GO:0048507) are of particular interest for any further studies, as they constitute genes with established roles in the regulation of meristem maintenance. A complete list of such DEGs, along with a brief description of their molecular function, is included in **Supplementary Table 1**.

4.4. Conclusions

Throughout this chapter, different approaches have been used to better understand the genetic regulation of arrest. The results presented here strongly suggest that flowering time genes, which are important in the regulation of the onset of flowering, also play a role during end-of-flowering. In particular, the photoperiod pathway, which includes genes such as *GI*, *CO* and *FT*, has been showed to be necessary for timely inflorescence arrest. Additionally, it has been demonstrated that the ambient temperature pathway, which includes the genes *SVP*, *FLM* and *FLC*, is essential for the environmental plasticity of arrest, specifically in response to warm temperatures. Lastly, although a more detailed study of them falls without the scope of this project, additional regulatory components have been identified to affect the

timing of arrest, including phytochrome B, type-B ARRs that participate in CK responses and the strigolactone signaling SMXL proteins.

This work has also allowed to characterize a novel role for the floral integrator *FT* as a central regulator of IM arrest. Not only is FT necessary for timely arrest of the IM, but also for the environmental plasticity of arrest in response to warmth. The results obtained here point towards a model in which transcriptional activation of *FT* triggers IM arrest. *FT* expression is regulated by environmental signals, and *FT* mRNA levels during flowering have been shown to vary depending on ambient temperature, suggesting that *FT* acts during end-of-flowering as a central integrator of environmental inputs. Through whole-transcriptome profiling of IMs, this work has led to the identification of potential downstream targets of FT during IM arrest. Although these would require further investigation, the data showed here suggest that FT may promote IM arrest in multiple ways, including through interactions with hormonal signaling pathways such as CK or ABA; or by indirectly fine-tuning the levels and/or activity of WUS, a key gene for meristem identity maintenance.

Due to time limitations, many of the molecular regulators identified throughout this chapter have not been explored in detail. Thus, future research would highly benefit from a closer look at genes that underlie light and hormonal signalling, including *PHYB*, *ELF*s, *SMXL*s and type-B ARRs, all of which seem to control the timing of arrest, to fully resolve their placement, if any, in the genetic network that regulates meristematic arrest. In addition, a key question that is left unanswered is how temperature and light information are integrated at the IM level, particularly in the cold, where *FT* does not seem to be necessary for temperature-dependent responses. Mathematical modelling, which has been previously used with success to investigate the role of *FT* during the floral transition (Kinmonth-Schultz et al., 2019), could be used in this context to study its function during arrest. Lastly, while the use of transcriptomics has facilitated the identification of potential downstream targets of

FT, further experiments are required to further validate their function, including a phenotypic assessment of any effects due to their knock-down or over-expression. In addition, chromatin immunoprecipitation (ChIP) approaches could help elucidate whether the transcriptional dynamics observed are due to a direct regulation by *FT*.

Chapter 5: Natural Variation of Inflorescence Arrest in *A. thaliana*

5.1. Introduction

Inevitably, the study of any biological process in a model species is influenced by the genetic background in which it is being analysed. Most research on the end-of-flowering comes from analysis of common laboratory accessions of *A. thaliana*, Col-0 and Ler (Balanzà et al., 2018; Hensel et al., 1994; Walker et al., 2023; Wang et al., 2020; Ware et al., 2020), with not many studies assessing arrest in less common genotypes (Miryeganeh, 2020; Miryeganeh et al., 2018). Because of this, mechanisms underlying the control of arrest that have been identified so far may only be important in certain genetic backgrounds. This limitation can be overcome by exploiting naturally-occurring populations as a source of genetic variation (Page and Grossniklaus, 2002). The study of natural variation not only uncovers the allelic diversity of key regulators of a biological process in nature, but also increases our overall understanding of the process itself (Jasinski et al., 2012; Weigel, 2012). In this sense, *A. thaliana* is an excellent model to study natural variation for multiple reasons. Firstly, extensive genomic information is available for a great number of natural accessions (Alonso-Blanco et al., 2016; Seren et al., 2017; Weigel, 2012). Secondly, it has a worldwide distribution which covers diverse environments, which has likely led to distinct selective pressures acting over time (Wilczek et al., 2009). Lastly, it is a predominantly selfing plant and, as a consequence, natural accessions are expected to be practically homozygous inbred lines (Page and Grossniklaus, 2002; Weigel, 2012).

There are various different techniques which can be used to identify polymorphisms that underlie natural variation. A common method involves crossing two accessions with distinctly extreme phenotypes in the trait of interest. This creates additional genetic and phenotypic variation, which can be utilised to better understand the genetic basis of the trait (Fujisaki et al., 2004; Hegarty, 2012; Rohde et al., 2004). After selfing of the resulting hybrid (F1), simply looking at the second generation of offspring (F2) from such cross can reveal valuable information about the inheritance of the phenotype that is being examined (Parker et al., 2016; Strange et al., 2011). If the F2 population is large enough, and sufficiently diverse at the genetic level, it can also be used to map potential genes that underlie this inheritance (Jasinski et al., 2012).

However, natural variation in biological processes is usually quantitative. Quantitative traits, of which flowering time is a good example, are typically controlled by multiple quantitative trait loci (QTLs). This adds a new layer of complexity to the study of natural variation, and a number of different techniques can be used to identify QTLs that associate with variability in the trait of interest (Doerge, 2002). A popular approach is based on recombinant inbred lines (RILs). RILs are produced by not only crossing two parental accessions but also subsequently inbreeding the resulting hybrid through repeated selfing over several generations (Page and Grossniklaus, 2002). While the development of RILs is time-consuming, they provide excellent tools for the mapping of QTLs as they contain different stable combinations of alleles from the parental genomes (Brachi et al., 2010; Jasinski et al., 2012; Swarup et al., 1999). Another approach commonly used to investigate natural variation is through genome-wide association studies (GWAS). World-wide research efforts had led to the genomic sequencing of over 1,000 natural accessions of *A. thaliana* (Alonso-Blanco et al., 2016), often making it possible to simply screen these genotypes and associate phenotypic variation to underlying genomic polymorphisms with enough resolution, eliminating the need for development of mapping populations.

Previously, the natural variation in *A. thaliana* has been exploited to better understand the regulation of flowering, in many cases leading to the novel identification of floral regulators (Weigel, 2012). However, information about variation in end-of-flowering among different accessions of *A. thaliana* is still lacking, raising the question as to whether inflorescence arrest occurs differently in genotypes other than Col-0 and Ler and, if so, what the genetic causes for such differences could be.

5.2. Aims

The general goal of this chapter is to characterize the natural variation in end-of-flowering and, particularly, inflorescence duration, among different accessions of *A. thaliana*. Specifically, the two main aims are as follows.

1) To examine the natural variation in end-of-flowering in *A. thaliana*.
2) To characterize potential genetic causes for such natural variation, if any.

5.3. Results and Discussion

5.3.1. End-of-flowering Traits Show Variation Among Accessions

In a first attempt to better understand the natural variation in end-of-flowering, a total of 69 accessions of *A. thaliana* were vernalized and grown in standard conditions (20ºC, 16-h day length) until the end-of-flowering. At this point, plants were harvested and 11 different traits related to fruit yield and reproductive architecture were recorded. All traits showed variability among the natural accessions that were examined, with the number of fruits per primary inflorescence and plant height being the least variable and the number of tertiary inflorescences, the most (**Table 5.1**).

Table 5.1. Summary statistics for end-of-flowering traits

Mean, standard deviation (SD) and coefficient of variation (CV) of the traits recorded at end-of-flowering for 69 *A. thaliana* accessions. PI: Primary Inflorescence. SI: Secondary Inflorescence, which branches out of the PI. TI: Tertiary Inflorescence, which branches out of a SI.

Trait	Unit	Mean	SD	CV
Fruits per PI	Number	51.7	10.1	20
PI length	mm	251.1	63.6	25
Number of SIs	Number	7.3	2.2	30
Fruits per SI	Number	27.0	6.4	24
SI length	mm	192.6	51.4	27
Number of TIs	Number	1.6	3.2	200
Fruits per TI	Number	8.2	3.7	45
TI length	mm	54.9	26.7	49
Plant height	mm	396.3	78.5	20
Internode length	mm	26.2	12.8	50
Total fruits	Number	259.9	85.7	33

The number of fruits per primary inflorescence was particularly interesting in the context of this research, as inflorescence fruit set is generally linked to inflorescence duration (see Chapter 3). Col-0 produced an average of 47 fruits per inflorescence, which was expected for these growth conditions. However, there was a substantial variability in this trait within the panel of accessions, with other genotypes ranging from 35 (No-0) to 80 (Tottarp-2) fruits per inflorescence (**Figure 5.1A**). There was also remarkable variability in the final number of fruits produced across the whole plant (**Figure 5.1B**), and it was questioned whether this could be directly associated to the performance of individual inflorescences. However, these variables were poorly correlated (r = 0.30) and a simple linear model including the two, although statistically significant, did not provide a good fitting for the data (R^2 = 0.05, P < 0.05) (**Figure 5.1C**); suggesting that whole-plant fruit set is not a direct reflection of the fruit number of individual inflorescences.

The onset of flowering, and various traits associated with it, has been extensively studied in different accessions of *A. thaliana* (Brachi et al., 2010), but the end-of-flowering has only been investigated in the commonly used accessions Col-0 and Ler. Thus, the dataset generated here provides a very valuable tool for the study of the natural variation of several end-of-flowering traits. This is especially relevant taking into account that one of the only yield-related traits that is currently available in public databases such as Arapheno (Seren et al., 2017) is the total number of fruits across the whole plant (Vasseur et al., 2018). When comparing this with the data quantified here, it was noted that, even though the results for standard accessions like Col-0 and Ler were similar, the total number of fruits obtained in this experiment was consistently higher for most other accessions (**Figure 5.1D**). While certain variability is expected across experiments, these disagreements may suggest that the phenotypic information about the end-of-flowering that is currently available could be enriched and expanded, potentially leading to the discovery of new regulatory genes through genomic analyses such as GWAS.

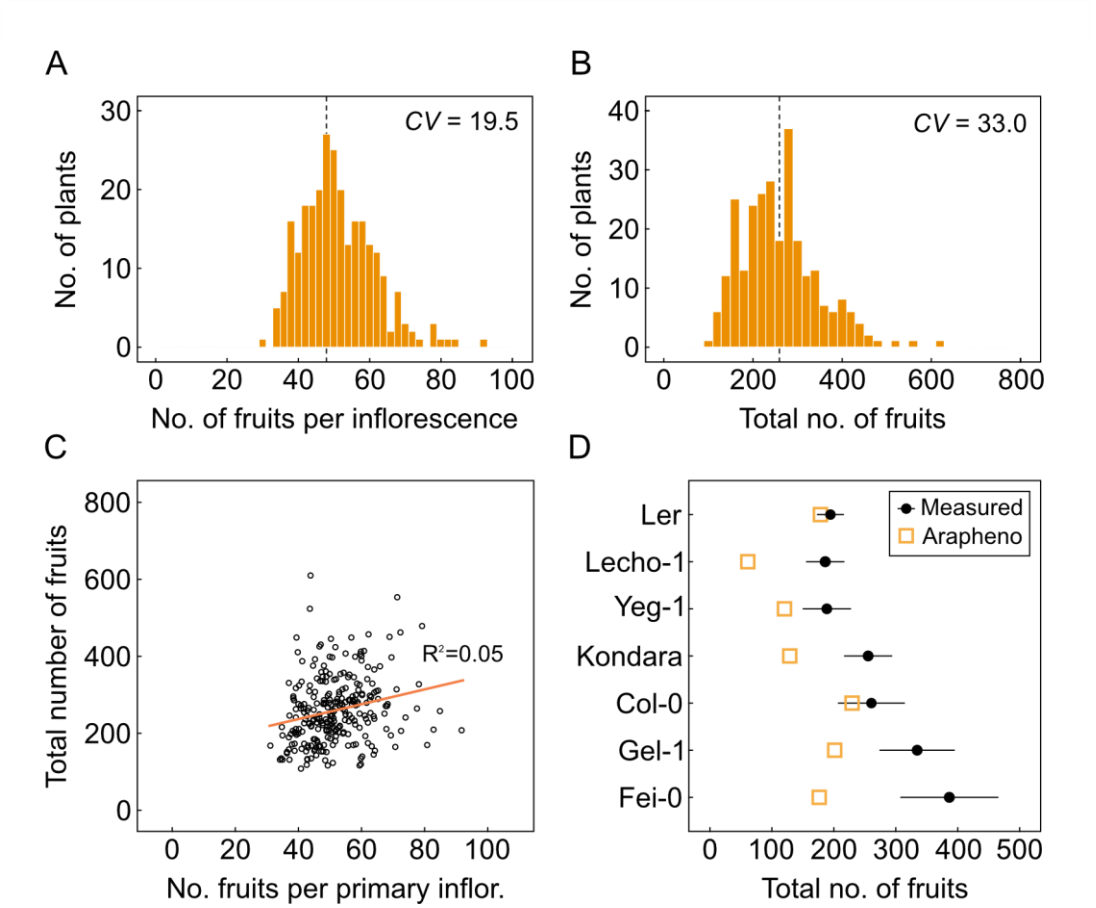

Figure 5.1. Variation in end-of-flowering traits among *A. thaliana* accessions

A-B. Histograms depicting the distribution of the number of fruits per inflorescence (**A**) and total number of fruits (**D**) in plants from 69 natural accessions of *A. thaliana* (N=3-4). The coefficient of variation (CV) of the trait is indicated in each graph. The dashed line indicates the average for the reference accession Col-0. **C.** Relationship between the number of fruits per primary inflorescence and the total number of fruits. The solid line represents the best fit for a linear model calculated by the least squares approach. **D.** Comparison between the total number of fruits measured in this experiment and the data available in the database Arapheno, from Vasseur *et al.*, 2018. The circles indicate the average, and the lines indicate the standard deviation.

Typically, GWAS analyses in *A. thaliana* are based on information ranging from hundreds to thousands of accessions. Thus, it would be preferable to assess a wider range of genotypes before implementing genomic analyses, which was not possible here due to time constraints. Still, in an attempt to identify potential causative SNPs that may underlie natural variation in end-of-flowering traits, GWAS was conducted using the information on the 69 accessions that were evaluated in this experiment for one trait, i.e., the number of fruits per primary inflorescence. Only one statistically significant peak was detected in chromosome 3 (**Figure 5.2**). The QTL was located in the region ~1 kb upstream of a gene encoding an F-box protein (AT3G49040). The biological function of the gene is unknown, but F-box proteins have been implicated in numerous processes that are key for plant development, including hormone signaling and light perception (Kuroda et al., 2002). This raises the possibility that the QTL identified may play a role in the genetic regulation of inflorescence arrest although, as mentioned before, extending this study to a greater number of natural accessions may both increase the robustness of this finding as well as help identify other potential regulators.

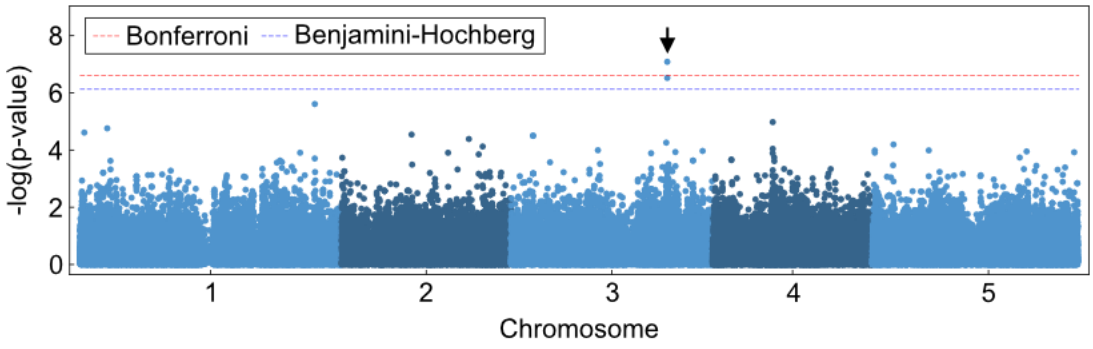

Figure 5.2. GWAS of the number of fruits per primary inflorescence

Manhattan plot showing the results for the genome-wide association study (GWAS) performed using the data on number of fruits per primary inflorescence for 69 accessions of *A. thaliana*. Dashed lines indicate cutoff p-values for statistical significance (red: Bonferroni, blue: Benjamini-Hochberg). The arrow highlights the single significant QTL identified in this test.

5.3.2. Inflorescence Duration Shows Natural Variation

Despite the broad need for a better characterization of end-of-flowering in different *A. thaliana* accessions, the main focus of this research is on inflorescence duration. Thus, a new strategy was implemented to investigate natural variation in inflorescence arrest using a small subset of 38 accessions. Three consecutive screenings were carried out using the standard accession Col-0 as an internal control. In all cases, accessions were grown in standard conditions (22ºC, 16-h day length), and inflorescence duration and fruit number were recorded. Similarly to other end-of-flowering traits, the results showed that there is considerable variability in inflorescence duration among natural accessions, with the majority of accessions showing an inflorescence duration statistically different to Col-0 (**Figure 5.3A**). There was also remarkable variation in the number of fruits per primary inflorescence (**Figure 5.3B**), which was expected based on the previous screening (**Figure 5.1A**). Inflorescence duration and fruit set were somewhat correlated ($r = 0.55$), and a simple linear model with duration as a predictor of fruit number was statistically significant ($P<0.05$, $R^2 = 0.3$). However, it is important to note that longer inflorescence durations did not necessarily lead to greater fruit numbers, e.g., in Rd-0 or Bla-2, showing the limitations of fruit number as an indicator of inflorescence duration.

Based on whether statistical differences relative to Col-0 exist, accessions were classified into 3 categories: early-arresting (18%), Col-like (42%) or late-arresting (40%). Interestingly, most genotypes had a duration similar to or longer than Col-0, with only a handful arresting earlier. No specific trend was found when considering the geographic origin of the accessions (**Figure 5.4A**), with late-arresting phenotypes being found in areas from different climatic regions such as the Iberian Peninsula, Sweden or Tajikistan. In accordance with this, no significant latitudinal clines were detected for either of the two traits that were assessed (**Figure 5.4B**, **Figure 5.4C**).

Figure 5.3. Accessions of *A. thaliana* show variation in inflorescence duration

Inflorescence duration (**A**) and number of fruits per inflorescence (**B**) in 38 natural accessions of *A. thaliana* (N=5-12). All measurements are relative to the Col-0 internal control. Asterisks indicate statistical differences between any accession and Col-0 (ANOVA, Tukey HSD test, $P<0.05$).

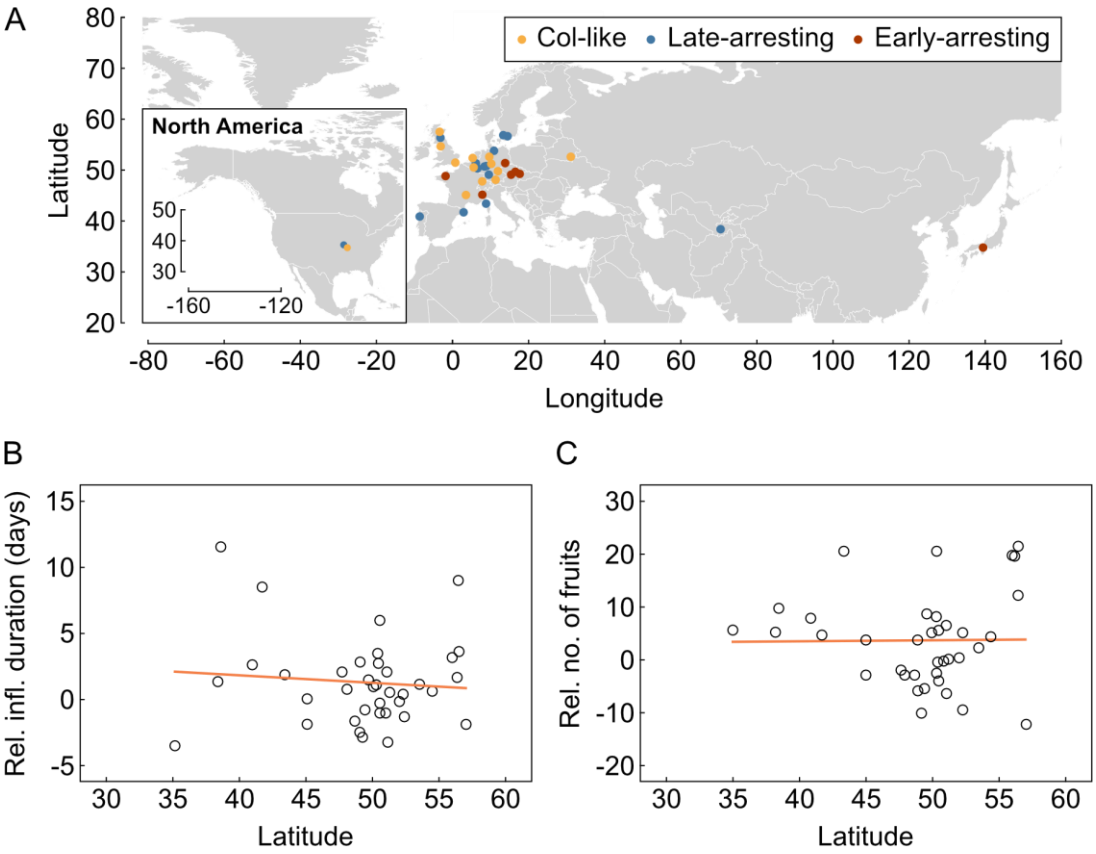

Figure 5.4. Geographic distribution of inflorescence arrest phenotypes

A. Geographic distribution of the 39 *A. thaliana* accessions screened, classified by their inflorescence duration relative to Col-0. **B-C.** Relationship between inflorescence duration (**B**) and the number of fruits per inflorescence (**C**) with latitude. The solid line represents the best fit for a linear model calculated by the least squares approach.

In light of the results obtained here, it may be necessary to assess a wider range of natural accessions before drawing any conclusions regarding the diversity of inflorescence arrest in *A. thaliana*. The observed lack of association between the geographical origin of the accessions and their end-of-flowering phenotypes could be due to human disturbance, which has been a key factor determining the geographical distribution and population structure of *A. thaliana* (Sharbel et al., 2000; Shirsekar et al., 2021). It has been proposed that, following the last glacial period, *A. thaliana* colonized central and Northern Europe from Mediterranean refugia (Sharbel et al.,

2000). In contrast, the colonization of North America is relatively recent and, based on the high similarity between Col-0 and individuals from Germany, it is believed that American accessions of *A. thaliana* may have originated in or near Germany (Rédei, 1992; Shirsekar et al., 2021). It is interesting to note that most late-arresting accessions come from regions that could have acted as Pleistocene refugia during the last glaciation, such as the Iberian Peninsula, Italy and the Norwegian coast (Sharbel et al., 2000) (**Figure 5.4A**). Again, while any inferences from these data are speculative at this stage, it is tempting to hypothesize that late arrest could be the ancestral phenotype, from which shorter inflorescence duration may have arose independently due to different selective pressures.

Two late-arresting accessions, i.e., Bå4-1 and Kondara, were of particular interest for their considerably long inflorescence durations (**Figure 5.3A**). Both also produced a significantly greater number of fruits per inflorescence (**Figure 5.3B**). However, they had somewhat distinct phenotypes in that Kondara was both late-flowering and late-arresting, while Bå4-1 was only late-arresting (**Table 5.2**). It was hypothesized that the phenotypic differences observed between these two genotypes and Col-0 would be due to genetic differences among the accessions, and further research effort was directed to explore this idea.

Table 5.2. Summary statistics for relevant traits in Bå4-1 and Kondara

Sample size (N), mean, standard deviation (SD) and range for three different traits (bolting time, inflorescence duration and inflorescence fruit set) are shown for each accession, Col-0, Bå4-1 and Kondara.

Genotype	N	Bolting (days)			Inf. duration (days)			Fruits (number)		
		Mean	SD	Range	Mean	SD	Range	Mean	SD	Range
Col-0	21	**23**	5	17-30	**23**	2	20-26	**45**	4	38-54
Bå4-1	9	**26**	4	21-30	**31**	4	27-36	**66**	10	56-83
Kondara	7	**44**	5	37-51	**36**	2	33-38	**56**	3	50-59

5.3.3. Genetic Basis of Inflorescence Duration in Bå4-1

To better understand the inheritance of inflorescence duration in the late-arresting accession Bå4-1, an F2 population was derived from a cross between it and the standard accession Col-0. Next, a total of 205 individuals from said F2 population were grown in standard conditions (22ºC, 16-h day length) and their inflorescence duration and fruit set were recorded. Although the F2 was expected to combine the difference in traits between the two parental accessions, most plants showed inflorescence durations and fruit sets within the range of the Col-0 parental or lower, with very few individuals within the Bå4-1 range being recovered (**Figure 5.5**).

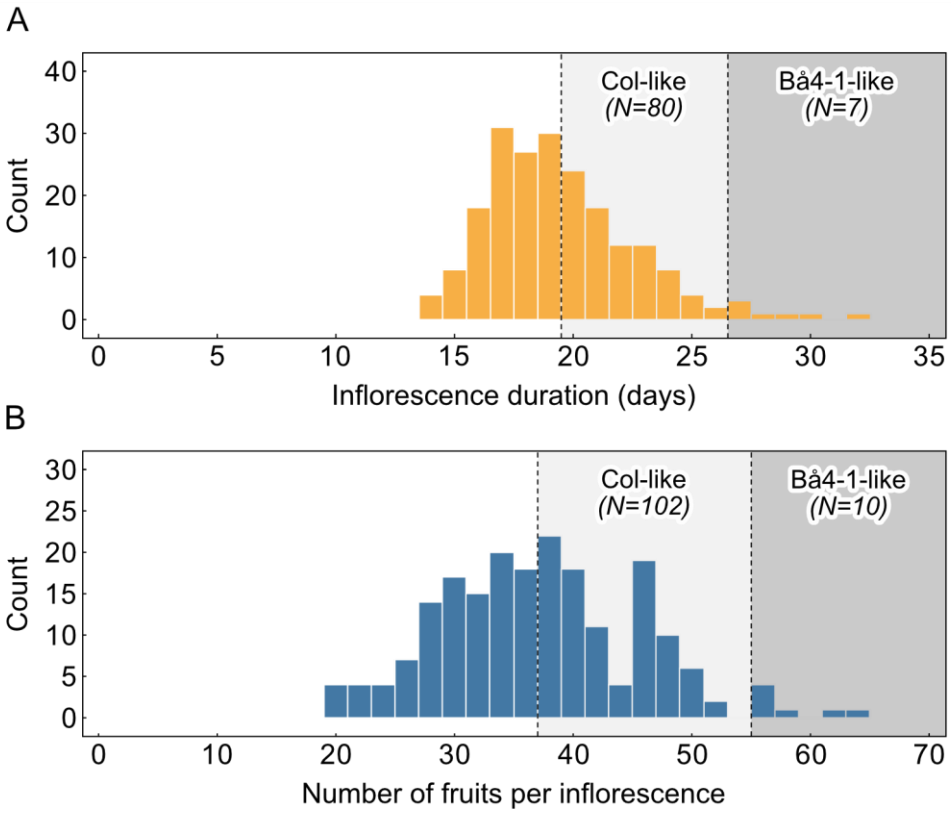

Figure 5.5. Inflorescence arrest traits in the Bå4-1 x Col-0 F2 population

Histograms depicting the distribution of inflorescence duration (**A**) and number of fruits per inflorescence (**B**) in the F2 population of Bå4-1 x Col-0 individuals (N=205). The grey areas highlight the range of values for the Col-0 and Bå4-1 parentals.

These results suggest that the inheritance of inflorescence arrest in Bå4-1 is complex, and that multiple loci underlie the differences observed between the end-of-flowering phenotypes of Bå4-1 and Col-0. An approach based on the development of recombinant inbred lines (RILs) may be suitable for the study of the genetic regulation of this trait, for which this F2 would be a starting point. However, and due to time constraints, no further work was done with this cross in the context of this project. Interestingly, for the Bå4-1 x Col-0 F2 population, inflorescence duration was highly correlated with the number of fruits per primary inflorescence (r = 0.80), and a linear model with duration as a predictor of fruit set provided a good fit for the data ($P<0.05$, $R^2 = 0.6$). This could indicate that these traits are affected by the same or closely linked loci, which would make the Bå4-1 x Col-0 hybrid relevant to better understand not only inflorescence duration but also its impact on fruit number .

5.3.4. Genetic Basis of Inflorescence Duration in Kondara

In order to investigate the inheritance of inflorescence arrest in the second late-arresting accession of interest, Kondara, a different cross was performed between Kondara and Col-0. After selfing for one generation, an F2 population was derived from said cross and a total of 168 F2 individuals from it were grown in standard conditions (22ºC, 16-h day length) to record their inflorescence duration and fruit set. In contrast to the Bå4-1 x Col-0 cross, the Kondara x Col-0 F2 population showed a very high variation in inflorescence durations. Approximately 45% and 10% of plants had a duration reminiscent of the Col-0 and Kondara parents, respectively, with the remaining showing either an intermediate between the two (30%) or extremely long (5%) or short (10%) durations (**Figure 5.6A**).

Overall, there was a continuous distribution of values for both of the traits assessed (**Figure 5.6A**, **Figure 5.6B**), which is expected for quantitative traits like

these. Again, inflorescence duration and primary inflorescence fruit number were highly correlated (r = 0.84) and a linear model with duration as a predictor of fruit number provided a good fit for the data ($P<0.05$, $R^2 = 0.7$), suggesting that both traits are probably affected by the same or similar loci. Considering the rich diversity of phenotypes observed, this F2 population could be suitable for the mapping of QTLs associated with inflorescence duration and fruit set in its current state (Doerge, 2002), and, indeed, examples of F2 populations being used for genetic mapping of flowering-related traits can be found in the literature (Fu et al., 2022; Takagi et al., 2013).

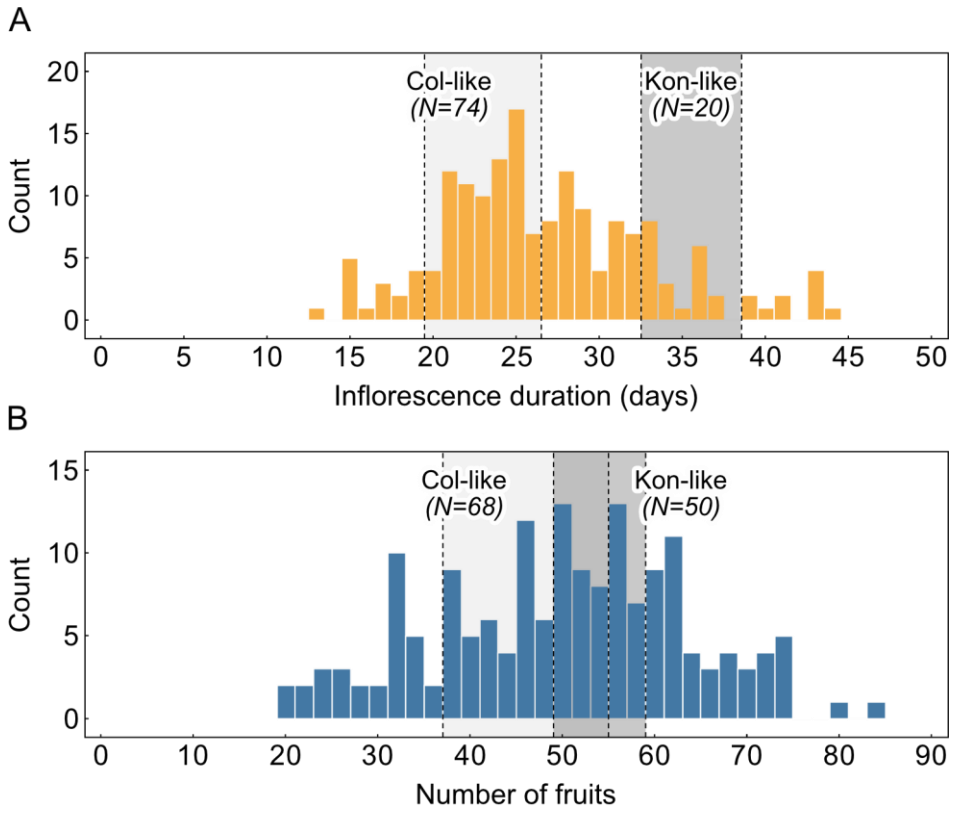

Figure 5.6. Inflorescence arrest traits in the Kondara x Col-0 F2 population

Histograms depicting the distribution of inflorescence duration (**A**) and number of fruits per inflorescence (**B**) in the F2 population of Kondara x Col-0 individuals (N=168). The grey areas highlight the range of values for the Col-0 and Kondara parentals.

It is interesting to note that some of the recovered individuals in the F2 showed extreme inflorescence durations (**Figure 5.6A**) and primary inflorescence fruit numbers (**Figure 5.6B**), a phenomenon known as transgressive segregation (Fu et al., 2022). This is likely due to the combination of alleles from the Col-0 and Kondara parentals giving rise to genotypes that outperform either, which is expected in hybrids generated from a cross such as this (Hegarty, 2012). This could suggest that both traits are polygenic and, thus, controlled by multiple loci, and it is also possible that additional interactions exist between the underlying genes. To further investigate the inheritance of inflorescence arrest in Kondara, more specific techniques should be applied to map the QTLs that are associated with the traits of interest. Nevertheless, general patterns can be described from the available data. Considering the range of inflorescence durations observed in the parentals (**Table 5.2**), a phenotypic ratio of approximately 9:4:3 can be found in the F2 population, where ~55% individuals show Col-like duration of shorter, ~30% show intermediate duration between the parentals and ~15% show Kondara-like duration or longer. This inheritance tentatively suggests that inflorescence duration is controlled by two loci with recessive epistasis. In this scenario, two genes with complete dominance would control inflorescence duration. However, due to the epistasis, when one of the genes is homozygous recessive, it would mask the phenotype of the other, which may be the cause for a much smaller portion of late-arresting individuals in the F2 (**Figure 5.6A**).

Based on these observations, it was hypothesized that inflorescence duration in the Kondara x Col-0 cross is controlled by two loci. To test this, seeds were collected from 4 late-arresting individuals from the F2, all of which had an inflorescence duration longer than 40 days. These seeds were germinated and grown, also in standard conditions (22ºC, 16-h day length), to assess the distribution of inflorescence duration in the F3 generation. It was expected that, if the trait was controlled by 2 loci, all of the F2 individuals selected would be homozygous for both

genes. Thus, all of their offspring should be late-arresting and no F3 individuals with a duration shorter than Kondara should be recovered. However, the results obtained contradict these expectations, with the offspring of two F2 late-arresting plants showing both Col-like and Kondara-like durations (**Figure 5.7C**, **Figure 5.7D**) and the offspring from the other two showing an inflorescence duration predominantly Col-like (**Figure 5.7A**, **Figure 5.7B**). Thus, the two-gene hypothesis was rejected and it was concluded that inflorescence duration is likely a complex trait controlled by multiple QTLs.

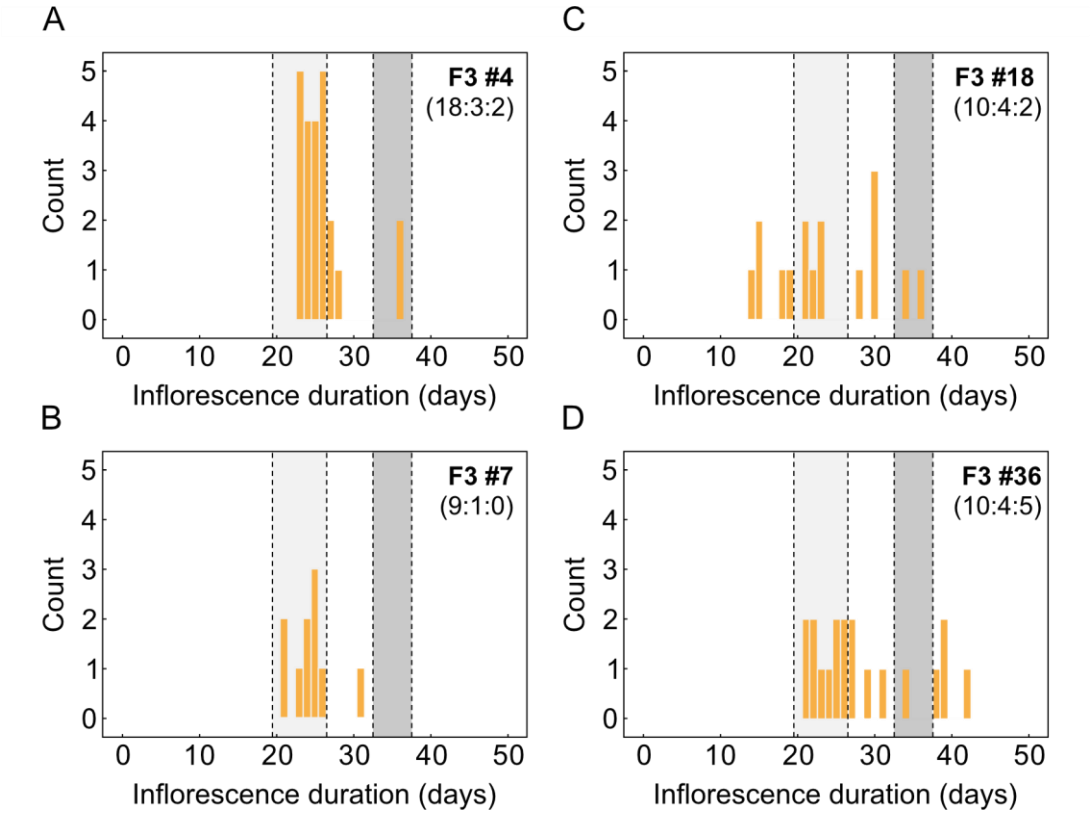

Figure 5.7. Inflorescence duration in Kondara x Col-0 F3 generation

Histograms depicting the distribution of inflorescence duration in the F3 generation of the Kondara x Col-0 cross (N=12-24). Each panel corresponds to the offspring of a different F2 individual that exhibited a late-arresting phenotype, #4 (**A**), #7 (**B**), #18 (**C**) and #36 (**D**). The light and dark grey area highlights the range of values for the Col-0 and Kondara parentals, respectively.

As previously mentioned, mapping the QTLs associated with the variation in inflorescence duration would require appropriate quantitative genetics techniques. Assuming that the Kondara x Col-0 F2 generation is diverse enough to be used as a mapping population, which seems to be the case, it may be possible to perform QTL mapping directly on the F2 (Fu et al., 2022; Takagi et al., 2013). Different tools are available for this, but a classic approach would involve the use of molecular markers such as single-nucleotide polymorphisms (SNPs) to detect areas of genetic variation among the F2 individuals. This would allow to construct a genetic map, after which statistical analyses would be used to identify QTLs. Lastly, further experiments would be required to further validate the role of the genes identified (Doerge, 2002). Due to time constraints, QTL mapping felt outside the scope of this project, and two alternative approaches were chosen to identify candidate genes associated with the variation of inflorescence arrest between Kondara and Col-0. On the one hand, a bioinformatic analysis was carried out using publicly available data to identify variation at the genomic level between the two accessions. On the other hand, arrest was characterized in Kondara at the whole-transcriptome level.

5.3.5. Analysis of Genomic Variation in Kondara and Col-0

Genomic variation information for a number of *A. thaliana* accessions is available through public databases (Alonso-Blanco et al., 2016), including for the late-arresting accession Kondara. A variant call format (VCF) file summarizing the genomic differences between Col-0 and Kondara was downloaded and used to identify genes that could underlie the control of inflorescence duration in Kondara. This file contains information for all single nucleotide polymorphisms (SNPs) observed between the two accessions of interest. In a first attempt to narrow down the list of candidate genes, the functional effects of each genomic variant were predicted using the software snpEff (Cingolani et al., 2012). Most variants were

associated with low or moderate effects, such as changes in promoter regions or synonymous mutations, with only ~1% of the SNPs being associated with severe impacts on coding regions, including the gain or loss of a stop codon. It was hypothesized that phenotypic differences between Col-0 and Kondara would be due to high impact SNPs affecting coding genomic regions and, as such, any genomic variants with predicted effects that were moderate or less impactful were filtered out. The resulting list of candidates was reduced to 890 unique genes for which high impact variants were found in Kondara. It had been previously noted that a wide range of genes function in both the control of floral transition and arrest (see Chapter 4), and thus, a last filter was applied based on the assumption that genes underlying arrest would have a known role in reproductive development. This was done by filtering any genes that were annotated with a GO term related to 'reproduction' (GO:0000003), after which only 58 genes were left (**Table 5.3**).

Several known regulators of flowering can be found among the final list of candidate genes. One that is worth mentioning is *TWIN SISTER OF FT* (*TSF*), which is a paralog of *FLOWREING LOCUS T* (*FT*) (Wickland and Hanzawa, 2015), a floral integrator which has already been showed to regulate arrest and its environmental plasticity in Col-0 (see Chapter 4). In addition, genes that regulate floral transition upstream of *FT*, such as *JUMONJI 14* (*JMJ14*) (Lu et al., 2010), are also found among the genes mutated in Kondara. Other interesting candidates include regulators of floral identity genes, such as *EARLY FLOWERING 9* (*ELF9*) or *BLADE ON PETIOLE 1* (*BOP1*), and genes implicated in hormonal signaling, namely auxin and cytokinin. All of these constitute regulators that are potentially causative for the differences in inflorescence arrest observed between Kondara and Col-0. As such, future research may benefit from studying them in closer detail to further validate their role, if any, during end-of-flowering, for which a possible first step would be to characterize inflorescence duration in Col-0 mutants lacking these genes.

Table 5.3. Candidate genes underlying inflorescence arrest in Kondara identified through genomic analysis

Genes annotated with a GO term related to 'reproduction' for which a high impact SNP was detected in Kondara. The predicted effect of the SNP and a description of the gene are shown. **Sg**: Stop gained, **Sl**: Stop lost, **St**: Start lost, *Sa*: Splice acceptor variant, *Sd*: Splice donor variant, *In*: intron variant, *Sr*: splice region variant.

Symbol	Gene ID	SNP	Description
ABCG9	AT4G27420	**Sl**	ABC-2 type transporter
ALY1	AT5G27610	*Sd*, *In*	RNA-binding protein
ANN5	AT1G68090	**Sl**, *Sr*	Calcium-binding protein, involved in pollen development
AOG1	AT5G57790	**Sl**	Unknown molecular function
ARR20	AT3G62670	**Sl**, *Sr*	Response regulator, involved in CK signaling
AT1G11280	AT1G11280	*Sa*, *In*	S-locus lectin protein kinase
AT1G15165	AT1G15165	**Sg**	RING/FYVE/PHD zinc finger protein
AT1G16570	AT1G16570	**Sg**	UDP-Glycosyltransferase, involved in floral organ development
AT1G18940	AT1G18940	**Sl**, *Sr*	Nodulin-like protein
AT1G27385	AT1G27385	*Sd*, *In*	Phosphoribosylformylglycinamidine synthase
AT1G36050	AT1G36050	**Sg**	Endoplasmic reticulum vesicle transporter
AT1G49870	AT1G49870	*Sa*, *In*	Myosin-2 heavy chain-like protein
AT1G61490	AT1G61490	**Sg**	S-locus lectin protein kinase
AT2G17670	AT2G17670	*Sd*, *In*	Tetratricopeptide repeat-like protein
AT3G02060	AT3G02060	**Sl**	DEAD/DEAH box helicase
AT3G05060	AT3G05060	*Sa*, *In*	Pre RNA processing ribonucleoprotein
AT3G12915	AT3G12915	*Sd*, *In*	Ribosomal protein S5/Elongation factor G/III/V
AT3G46480	AT3G46480	*Sd*, *In*	2-oxoglutarate and Fe(II)-dependent oxygenase
AT4G00980	AT4G00980	**Sg**	Zinc knuckle (CCHC-type) protein
AT4G16745	AT4G16745	**Sl**	Exostosin family protein
AT4G23860	AT4G23860	*Sa*, *In*	PHD finger protein
AT5G39770	AT5G39770	*Sa*, *In*	
AT5G44495	AT5G44495	**Sl**, *Sr*	
AT5G49440	AT5G49440	**Sg**	
AT5G52975	AT5G52975	**Sl**	Protein of unknown function
AT5G55180	AT5G55180	**Sl**	

Symbol	Gene ID	SNP	Description
AT5G57700	AT5G57700	**St**	
AT5G64790	AT5G64790	**St**	
AT5G67411	AT5G67411	**Sl**, *Sr*	GRAS family transcription factor
BOP1	AT3G57130	*Sa, In*	Promotes floral meristem fate, targets AP1 and AGL24, required for expression of *LFY* and *AP1*
BUPS2	AT2G21480	**St**	Receptor-like protein kinase, involved in pollen tube growth
CAM2	AT2G41110	*Sd, In*	Calmodulin
DAU1	AT5G02390	**Sg**	Protein of unknown function
DTX33	AT1G47530	**Sl**	MATE efflux protein
EAF1A	AT3G24880	*Sa, In*	Helicase, DNA-binding
ELF9	AT5G16260	*Sd, In*	RNA binding protein, involved in the timing of flowering, upstream regulator of *a*
FBXL	AT5G22720	*Sa*, *In*	F-box protein
HRD3B	AT1G73570	*Sd*, *In*	HCP-like protein
JMJD5	AT3G20810	*Sa, In*	Histone demethylase, represses FT
JMJ14	AT4G20400	**Sg**	Histone demethylase, represses floral transition
KNAT2	AT1G70510	**Sl**	Homeobox gene, involved in carpel development
LBD27	AT3G47870	**Sl**	LOB protein, involved in pollen development
MCC1	AT3G02980	**Sl**, *Sr*	Involved in meiosis
MEE25	AT2G34850	*Sa*, *In*	NAD(P)-binding Rossmann-fold protein
MEE38	AT3G43160	**Sg**	Maternal effect embryo arrest 38
MEE57	AT4G13610	**Sg**	DNA methyltransferase
MIK2	AT4G08850	**Sl**	Leucine-rich repeat receptor-like kinase
MTERF26	AT4G19650	*Sd*, *In*	Mitochondrial transcription termination factor
NS1	AT4G17300	*Sa*, *In*	Class II aminoacyl-tRNA and biotin synthetase
NUC1	AT1G48920	**Sg**	Nucleolin, involved in rRNA processing
pBRP2	AT3G29380	**Sg**	Cyclin-like protein
PLC2	AT3G08510	*Sa*, *In*	Phospholipase, involved in auxin signaling
SEIPIN3	AT2G34380	**Sg**	Putative adipose-regulatory protein
SHP1	AT3G58780	*Sd*, *In*	Transcription factor, involved in fruit dehiscence
SUS2	AT5G49190	*Sa*, *In*	Sucrose synthase
TBL16	AT5G20680	*Sa*, *In*	Protein of unknown function
TSF	AT4G20370	**Sg**	PEBP protein, homolog of FT, floral promoter
UNE4	AT2G12940	**Sl**	Basic-leucine zipper transcription factor

5.3.6. Whole-Transcriptome Profiling of Arrest in Kondara

As mentioned before, in addition to the genomic analysis, a transcriptomic approach was chosen to better understand inflorescence arrest in Kondara. Similarly to what was previously done to investigate the role of *FT* in inflorescence arrest (see Chapter 4), an experiment was designed to characterize differences between Col-0 and Kondara during IM arrest at the whole-transcriptome level. To do so, both Col-0 and Kondara plants were grown in standard conditions (20ºC, 16-h day length) until flowering. Next, IMs from both genotypes were harvested 4 and 12 days after bolting. At the second time point, it was expected that IMs from Col-0 would be arrested (see Chapter 4), while those of Kondara would still be proliferative, given the extended inflorescence duration of Kondara plants (**Figure 5.3A**, **Table 5.2**). The harvested IM samples were used for RNA extraction and, then, submitted for RNA-Sequencing.

An initial exploratory analysis of the RNA-Seq results revealed that IMs from Col-0 and Kondara are substantially different to one another at the whole-transcriptome level. The first principal component (PC1) in the PCA, which accounts for a 65% of the variance in the data, allowed to clearly distinguish between the two genotypes (**Figure 5.8A**). Interestingly, younger IMs differed from older IMs in Col-0, but not in Kondara. This is comparable to results obtained previously for the *ft-10* mutant, in which the IM arrests later than in Col-0 wild-types (see Chapter 4), and suggests that the transcriptomic profile of proliferative IMs is maintained for longer in Kondara. Accordingly, hierarchical clustering clearly differentiated arrested IMs from Col-0 from the rest of the samples, while proliferative IMs from Col-0 fall closer to IMs from Kondara (**Figure 5.8B**). Generally speaking, it is clear that the whole-transcriptome remodelling observed in Col-0 between 4 and 12 days is absent in Kondara, raising the possibility that genes that fail to up- or down-regulate between the two time points in Kondara are responsible for its late-arresting phenotype.

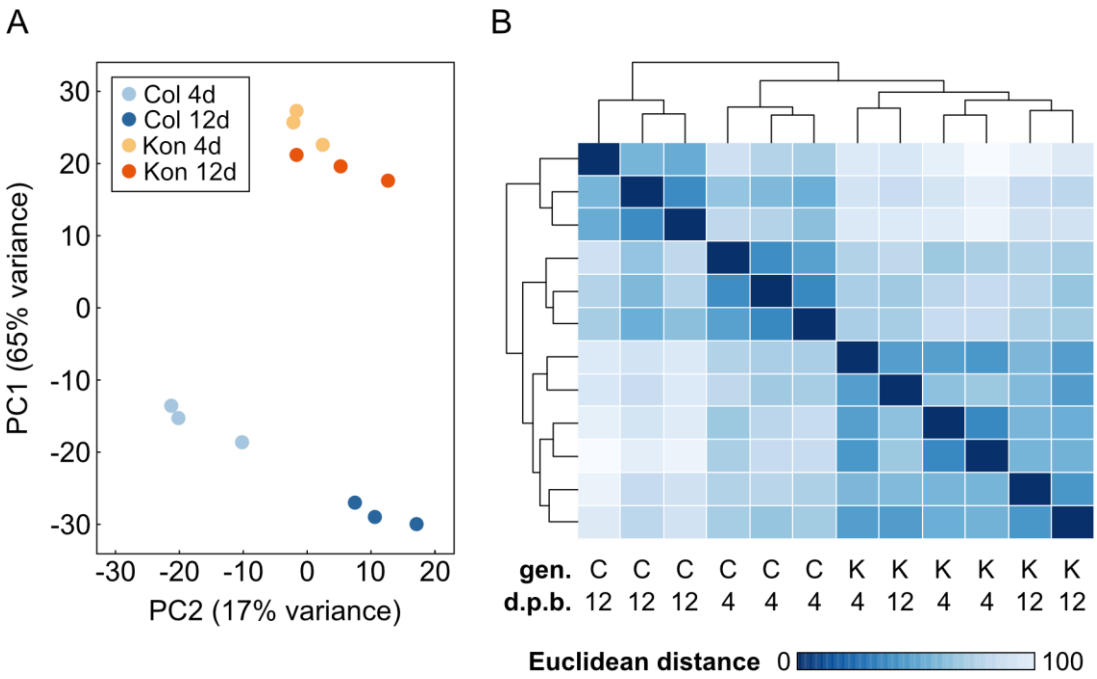

Figure 5.8. Exploratory analysis of the Kondara RNA-Sequencing data

A. Principal Component Analysis (PCA) performed on the VST-transformed read counts. Col: Col-0. Kon: Kondara. 4/12d: 4/12 days post bolting. **B.** Heat map and hierarchical clustering of the sample-to-sample Euclidean distances calculated using the VST-transformed read counts. The genotype (gen.) and days post bolting (d.p.b.) corresponding to each sample are indicated at the bottom. C: Col-0. K: Kondara.

A statistical test was carried out to identify genes for which their temporal expression pattern is significantly different between Kondara and Col-0. As a result, a total of 1,760 differentially expressed genes (DEGs) were pulled out. The number of DEGs was much lower than those previously identified for the *ft-10* mutant (see Chapter 4), but the majority (~70%) overlapped with DEGs identified for *ft-10* (**Figure 5.9A**). To better visualize the expression pattern of DEGs, an unsupervised clustering algorithm was used to classify genes into expression groups. Based on the minimum centroid criterion, the optimal number of clusters was estimated to be 3, and there was a fairly equal distribution of genes assigned to each cluster (**Figure 5.9B**).

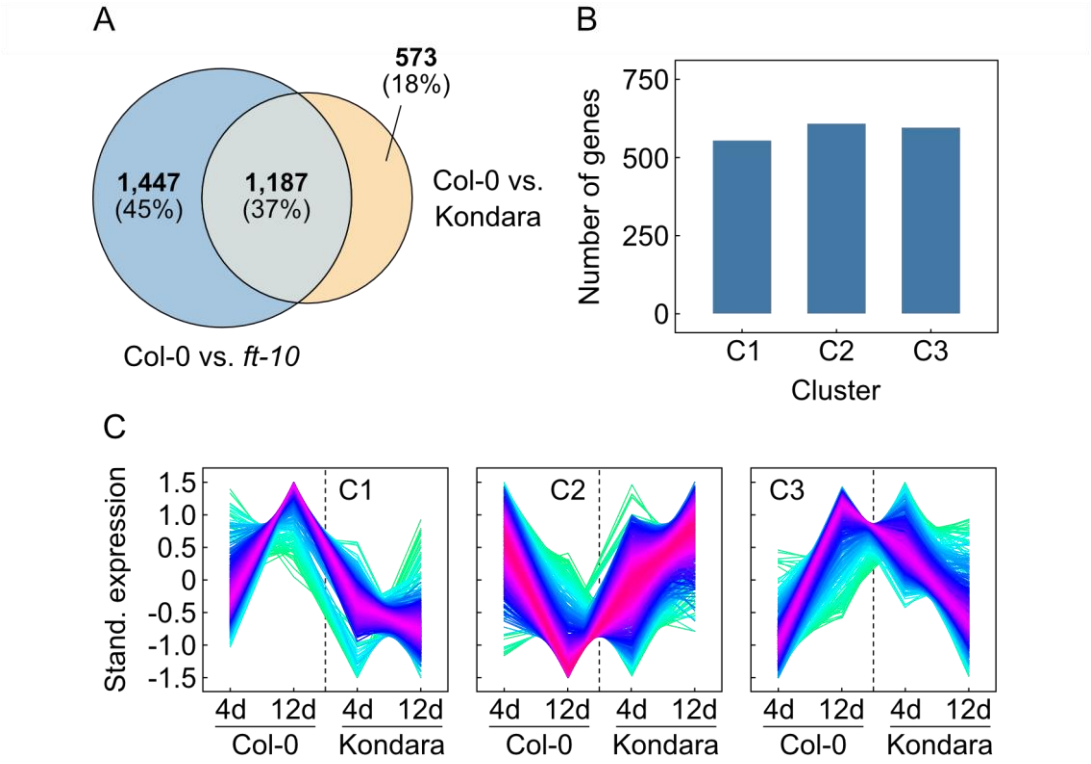

Figure 5.9. Clustering of genes differentially expressed in Kondara

A. Venn diagram highlighting the numbers of DEGs identified for Kondara and the *ft-10* mutant (see Chapter 4). **B.** Number of genes assigned to each of the four clusters. **C.** Standardized gene expression of genes belonging to each cluster (C1-C3). The colour represents membership to the cluster (yellow and green correspond to genes with low membership value, red and purple correspond to genes with high membership value).

Based on the average expression profile for each cluster (**Figure 5.9C**), two types of DEGs can be distinguished, i.e., genes that are up-regulated during IM arrest in Col-0 but not in Kondara (type I), which correspond to the majority of DEGs, and genes that are down-regulated during IM arrest in Col-0 but not in Kondara (type II) (**Table 5.4**). Next, GO term enrichment was performed on each class separately to obtain a general idea of the biological processes in which DEGs may participate. Genes from type I, which are up-regulated during IM arrest, were enriched in GO terms related to pollen and flower development, as well as trehalose and lignin metabolism. In contrast, genes from type II, which are down-regulated during arrest,

were enriched in GO terms associated with amino acid biosynthesis, response to hypoxia and metabolism of glucose, chlorophyll and lysine, among others. Most of these processes had been previously associated with IM arrest in Col-0 wild-type (see Chapter 4), suggesting that downstream mechanisms that mediate arrest are common among different accessions of *A. thaliana*.

Table 5.4. Types of genes differentially expressed in Kondara

Type	Cluster	Description	Number	Examples
I	C1 C3	Up-regulated in Col-0 (during IM arrest) but not in Kondara	1,150 (**65%**)	*CAL*, *MAX1*, *FL3*, *AP2*, *FAF2*…
II	C2	Down-regulated in Col-0 (during IM arrest) but not in Kondara	610 (**35%**)	*AP1*, *FAF4*, *TAR2, SPL10, FLC…*

It was hypothesized that relevant regulatory genes for IM arrest would have known functions in the control of meristem development, and so any genes annotated with the GO term 'meristem development' (GO:0048507) were filtered as particularly interesting candidates for further studies (**Supplementary Table 2**). Not only did many of these overlap with candidates for downstream targets of FT (see Chapter 4), but they also showed similarities in their expression profile between Kondara and the *ft-10* mutant (**Figure 5.10**). Among these, some examples that are worth mentioning are regulators of meristem identity, such as *FANTASTIC FOUR 2* (*FAF2*) and *4* (*FAF4*) and *APETALA 2* (*AP2*). Both FAF2 and FAF4 repress the expression of *WUSCHEL* (*WUS*) (Wahl et al., 2010), which is necessary for the maintenance of meristems. In this analysis, they were placed in different groups, with *FAF2* being up-regulated during arrest and *FAF4*, down-regulated. This suggests that complex regulatory interactions act upstream of *WUS* during IM arrest in Col-0, and that these could be underlying the longer inflorescence duration of Kondara. AP2 is another known repressor of *WUS* expression (Huang et al., 2017; Würschum et al., 2006). Previously, it has been proposed that a decline in *AP2* levels in the IM during

flowering could lead to arrest in a WUS-dependent manner (Balanzà et al., 2018). However, the data presented here challenge this idea as *AP2* expression in the IM of Col-0 plants seems to be up-regulated, albeit only slightly, during arrest (**Figure 5.10A**, **Table 5.4**). Taken together, these results prompt a formal re-examination of the role of meristem identity genes during IM arrest, with a focus on regulators of *WUS*, which has been shown to be relevant during end-of-flowering (Balanzà et al., 2018; Wang et al., 2020).

Other additional genes of interest pooled out as regulators of meristem development which are differentially expressed between Kondara and Col-0 include the floral identity genes *APETALA 1* (*AP1*) and *CAULIFLOWER* (*CAL*) (**Figure 5.10D**, **Figure 5.10E**), both of which are functionally redundant transcription factors with key roles during flower development (Ó'Maoiléidigh et al., 2014). The floral repressor *FLOWERING LOCUS C* (*FLC*) is also found among these genes. FLC plays a key role in preventing floral transition in non-vernalized winter accessions of *A. thaliana*. Here, *FLC* transcript levels were much higher in Kondara than in Col-0 during flowering, which was expected as Kondara is a winter accession (Johanson et al., 2000) and plants were not vernalized during this experiment. However, upon closer examination, *FLC* levels barely changed from 4 to 12 days after bolting in Col-0 (**Figure 5.10B**), which does not support a role for FLC during IM arrest. Finally, some genes involved in hormonal synthesis were found after the filtering, including for strigolactone, e.g., *MORE AXILLARY GROWTH 1* (*MAX1*); and auxin, e.g., *TRYPTOPHAN AMINOTRANSFERASE RELATED 2* (*TAR2*) (**Figure 5.10G**, **Figure 510I**). Both auxin (Ware et al., 2020) and strigolactone (see Chapter 4) have been implicated with inflorescence arrest before, so it is also possible that differences in hormonal biosynthesis or signaling between Kondara and Col-0 underlies the differing inflorescence durations found between both accessions.

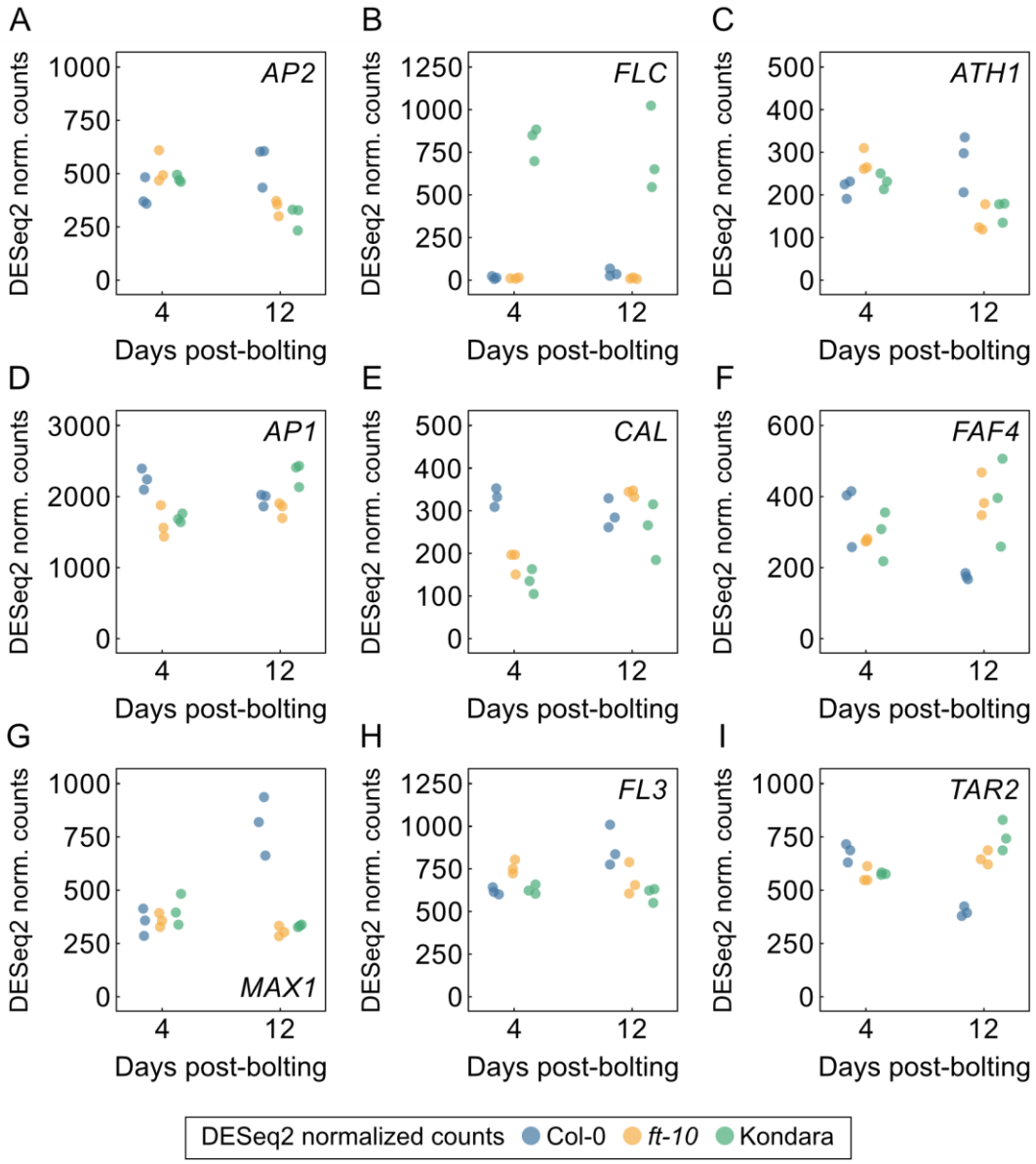

Figure 5.10. Comparison between DEGs of interest between Kondara and *ft-10*

Expression profile of a selection of genes annotated with the GO term 'meristem development' (GO:0048507) differentially expressed between Kondara and Col-0.

It should be noted that the RNA-Seq study conducted here does not provide a definite answer to the genetic cause of the differences observed in inflorescence duration between Col-0 and Kondara. However, differences in gene expression can reflect genetic variation between different accessions, and may be associated with polymorphisms at the genomic level (Doerge, 2002). Thus, the list of DEGs identified

for Kondara through RNA-Seq was compared against the list of genes for which high impact SNPs had been detected in the genomic analysis (see 5.3.5), and the 45 genes that overlapped between the two were extracted (**Supplementary Table 3**). None of the previous examples, such as *FAF2*, *FAF4* or *AP2*, were found among these genes, suggesting that differences in their expression between Kondara and Col-0 has other causes, such as lower impact polymorphisms, e.g., in promoter regions. An interesting example of an overlapping gene between the two datasets is *ARR20*, a type-B response regulator that participates in cytokinin signaling (Zubo and Schaller, 2020). Previously, a sextuple mutant lacking several type-B ARRs was reported to have impaired inflorescence duration (see Chapter 4), and cytokinin has an established role during early arrest (Merelo et al., 2022; Walker et al., 2023). Thus, as previously mentioned, it would be beneficial to investigate the specific involvement of the CK signaling pathway in *A. thaliana*. In light of these results, *ARR20* specifically proves a good candidate to explain differential responsiveness to cytokinin that may be relevant during IM arrest in different accessions. Lastly, another gene worth mentioning is *TREHALOSE PHOSPHATE SYNTHASE 11* (*TPS11*), which encodes an enzyme involved in the metabolism of trehalose 6-phosphate (T6P) (Singh et al., 2011). Generally speaking, GO terms related to trehalose metabolism were enriched among genes up-regulated during IM arrest in Col-0, and T6P participates in a pathway that has been recently proposed to participate in IM arrest (Goetz et al., 2021). During early IM arrest, the expression of the T6P synthase *TREHALOSE PHOSPHATE SYNTHASE 1* (*TPS1*) is down-regulated, leading to a reduction in the T6P pathway (Goetz et al., 2021). In contrast to *TPS1*, which has a trehalose synthase (TPS) domain, *TPS11* has both a TPS and a trehalose phosphatase (TPP) domain (Singh et al., 2011), suggesting that its role during IM arrest may be more complex. However, due to the limited information available on the role of the T6P pathway during arrest, it is difficult to draw any more conclusions at this stage.

5.4. Conclusions

The data presented throughout this chapter shows that there is natural variation in end-of-flowering among different accessions of *A. thaliana* and highlights the need for a better characterization of traits associated with it in accessions other than the commonly used Col-0 and Ler. A screening of multiple phenotypes performed in over 60 accessions has demonstrated that techniques such as GWAS can be utilized to map QTLs associated to relevant traits, including primary inflorescence fruit number, although a greater sample size would be required to draw final conclusions. However, the number of accessions included has proved insufficiently high and, thus, future research would benefit from expanding on this study to identify genes that underlie processes associated to the end-of-flowering. A subset of accessions was used to investigate variation in inflorescence duration specifically, which led to the identification of late-arresting genotypes such as Bå4-1 and Kondara. A detailed genetic study of both revealed that inflorescence duration is a quantitative and polygenic trait, likely subject to complex genetic inheritance. Two different F2 mapping populations were developed by crossing Col-0 to either Bå4-1 and Kondara. These can be used in further research for the development of RILs through repeated selfing over generations and, in turn, RILs can be utilized to map QTLs associated with inflorescence duration in these accessions.

Lastly, two independent analyses were performed to better understand the regulation of end-of-flowering in the late-arresting accession Kondara, based on the genomic and transcriptomic variation between Kondara and Col-0. These led to the identification of candidate genes which, subject to further validation, could be responsible for the differences in inflorescence duration between these genotypes. Some relevant examples include genes that participate in the control of meristem maintenance and floral organogenesis, hormonal synthesis and sugar signaling, specifically the trehalose 6-phosphate pathway. It should be noted that, while these

constitute interesting candidates, further experiments are required to fully validate and elucidate their functions, if any, during arrest. Particularly, a phenotypic assessment of mutants disrupted in these genes may support their suggested function in controlling arrest. Additionally, an interesting question is to what extent the extended duration of Kondara is *FT*-dependent, as the majority of DEGs identified overlapped between Kondara and the *ft-10* mutant, something that could be further explored through genomic and bioinformatic approaches.

Chapter 6: Effect of Parental Ageing on Offspring Production in *A. thaliana*

6.1. Introduction

As has been shown before, inflorescence arrest can have drastic impacts on the reproductive output of *A. thaliana*. Indeed, environmental and genetic factors determine the duration of the reproductive phase and, ultimately, the number of fruits that plants are able to produce (see Chapters 3-5). Aside from this, very little is known about the effect of end-of-flowering on offspring production in *A. thaliana*, although work on other species suggest that the production of seeds is variable throughout the reproductive phase (Lenser et al., 2018; Schmidt et al., 2020). In fact, it is not uncommon to observe changes in development as a consequence of ageing during a plant's lifespan, a phenomenon named heteroblastic development (Allsopp, 1967). In the vegetative phase, for instance, leaves show morphological differences depending on the age at which they were formed (Tsukaya et al., 2000; Wang et al., 2019). This age-dependent modulation of development can be important for coordinating different biological processes in plants (Cartolano et al., 2015), but it has barely been explored in the context of end-of-flowering.

Heteroblastic development is thought to be controlled autonomously, through a mechanism that allows plant age to be integrated into the developmental programme (Forster and Bonser, 2009; Tsukaya et al., 2000). In *A. thaliana*, age is perceived through the ageing pathway, a regulatory hub where two miRNAs have a leading role, *miR156* and *miR172*. During earlier development, when the plant is the youngest, *miR156* levels are the highest. As plant age increases and, particularly, after the onset of flowering, *miR156* begins to decrease and *miR172* gradually

increases (Wang, 2014). This balance between *miR156* and *miR172* acts as a time-keeping mechanism that tracks plant age and can modulate development through transcriptional regulation of target genes (Cartolano et al., 2015). Interestingly, there is evidence that ambient temperature regulates the ageing pathway upstream of *miR172* (Jung et al., 2012), suggesting that environmental signals could affect the way in which age is perceived by the plant. In fact, the concept of photo-thermal time, which combines the passing of time with information of light and temperature exposure, has been widely used with success to predict the timing of key developmental transitions in plants (Kirby, 1995; Masle et al., 1989). It is thus possible that the perception of plant age is affected by the environment, although the specific molecular basis of this remains to be characterized.

Regardless of the underlying genetic background, the existing literature supports the idea that ageing affects seed production, and that this is dependent on the environment. Recent work on *A. thaliana* and its close relative *Brassica nigra* shows that fertility changes during flowering in an age-dependent manner (Dogra and Dani, 2019). Fruits located at the bottom of the inflorescence, which are produced early during flowering, are smaller and contain fewer seeds. Halfway through flowering, fertility increases, with fruits showing bigger size and a greater number of seeds. Finally, fruits located at the top of the inflorescence, which are produced when the plant is the oldest, contain less seeds. Additionally, parental age seems to also affect the viability of the seed, which increases towards the top of the inflorescence (Dogra and Dani, 2019). A likely explanation for the age-dependent decline in fertility is that older parents undergo senescence and, thus, are under suboptimal conditions, which limits their ability to direct resources to offspring production. A lower number of seeds per fruit at the top of the inflorescence could reduce the competition among seeds, rendering them bigger and, as a consequence, more viable. In accordance with this, both parental age and position along the inflorescence have been reported to influence seed size (House et al., 2010), and a known trade-off exists between

seed quantity and seed size (Dogra and Dani, 2019; Manning et al., 2009). Furthermore, environmental factors impact both traits either directly or indirectly by affecting the resources that the mother plant has access to (Manning et al., 2009; Roach and Wulff, 1987).

The effect of parental age on offspring seed size is not trivial, as seed size is directly linked to fitness potential (House et al., 2010). Generally, bigger seeds are more likely to germinate and give rise to seedlings with better survival (Krannitz et al., 1991; Manning et al., 2009; Westoby et al., 1997). An interesting question arising from this is whether parental age affects the performance of the next generation of plants. Works on several animal species have reported that older parents tend to produce shorter-lived descendants which reproduce earlier, a phenomenon known as the Lansing effect (Lansing, 1947; Monaghan et al., 2020; Noguera et al., 2018). In plants, evidence supporting the existence, or lack thereof, of a Lansing effect is scarce. In pine trees, the age of the mother plant affects the size of the seeds, but it has no influence on the survival of seedlings (Pardos et al., 2022). Similarly, in aquatic duckweed plants, which usually reproduce asexually, parental age impacts certain aspects of the offspring but not their survival (Barks and Laird, 2015), suggesting that parental age does not affect offspring longevity in the plant kingdom.

6.2. Aims

The main aim of this chapter is to characterize the effect of parental age on offspring production in *A. thaliana*. To achieve this, the specific goals are as follows.

1) To assess the effect of parental age on seed production and quality.
2) To determine the transgenerational effects of parental ageing.
3) To determine if environmental signals, specifically temperature, have any effects on the age-dependent control of offspring production.

6.3. Results and Discussion

6.3.1. Parental Age Affects Offspring Production

As a first step towards characterizing the effect of parental age on offspring production, a set of 5 different accessions of *A. thaliana* were grown in standard conditions (22ºC, 16-h day length). These included genotypes with different inflorescence durations (see Chapter 5): two with intermediate durations (Col-0 and Ler), one with a short duration (Kyoto) and two with long durations (Kondara and Bå4-1). Plants were grown until end-of-flowering and, after fruit ripening, seed samples were collected from individual fruits placed at different positions along the inflorescence. These were then used to measure two traits related to offspring production, i.e., the number of seeds per fruit and the average seed area (recorded from photographs taken from above and used as a proxy for seed size).

Both seed number and size showed clear changes depending on the position of the source fruit within the inflorescence. In Col-0, seed number was minimal at the bottom-most part of the inflorescence, increased at the middle and decreased again towards the top (**Figure 6.1A**), which is consistent with previous observations of fruit lengths along the inflorescence (Dogra and Dani, 2019). The decline in seed number towards the top of the inflorescence could be attributed to a lower control of the ageing parent over the allocation of resources to the reproductive organs, as the top-most fruits are produced when the mother plant is the oldest. Indeed, signs of cellular senescence, such as a greater vacuolation (Rhinn et al., 2019), start to be observed in reproductive tissues after arrest of the inflorescence meristem (IM) (Wang et al., 2020), suggesting that processes related to whole-plant death could be initiated during the late reproductive phase.

Due to the limited amount of resources that the parent can allocate to offspring production, a trade-off between seed size and number often determines the

characteristics of the fruits that are produced, with less fertile fruits typically containing bigger seeds (Dogra and Dani, 2019; Manning et al., 2009). Previously, it had been speculated that seed from less fertile fruits located at the top of the inflorescence would have reduced competition for resources and, thus, show a bigger size (Dogra and Dani, 2019). However, the data presented here clearly shows that the reduction in seed number seen in the top-most fruits does not lead to a bigger seed size (**Figure 6.1**). Instead, seeds decrease in size from the bottom to the top of the inflorescence proportionally to the age of the parent. This pattern is clear even in the bottom-most fruits, which are produced days prior to arrest and the onset of senescence (Wang et al., 2020), suggesting that, although age-dependent, the heteroblastic effect on seed size is not a consequence of either of these processes. A possible alternative is that seed size is controlled by molecular time-keeping mechanisms such as the ageing pathway, which operate during the whole lifespan of the plant (Wu et al., 2009). Since the ageing pathway has already been implicated with the control of IM arrest (Balanzà et al., 2018), it would be interesting to also explore its potential involvement in the regulation of offspring production.

For the most part, age-dependent patterns observed for both seed size and number were conserved across different accessions of *A. thaliana* (**Figure 6.1C**-**J**). Both Kondara and Bå4-1, although having an inflorescence duration twice as long as Col-0, presented roughly the same type of heteroblastic development with the number of seeds per fruit showing a bell-shaped curve (**Figure 6.1G**, **Figure 6.1I**) and seed size decreasing along the inflorescence (**Figure 6.1H**, **Figure 6.1J**). This was also the case for Kyoto, which has a significantly shorter inflorescence duration (**Figure 6.1E**, **Figure 6.1F**). Taken together, these results demonstrate that seed production and the characteristics of the offspring seed change during flowering in an age-dependent manner, and that this is conserved across different accessions of *A. thaliana*.

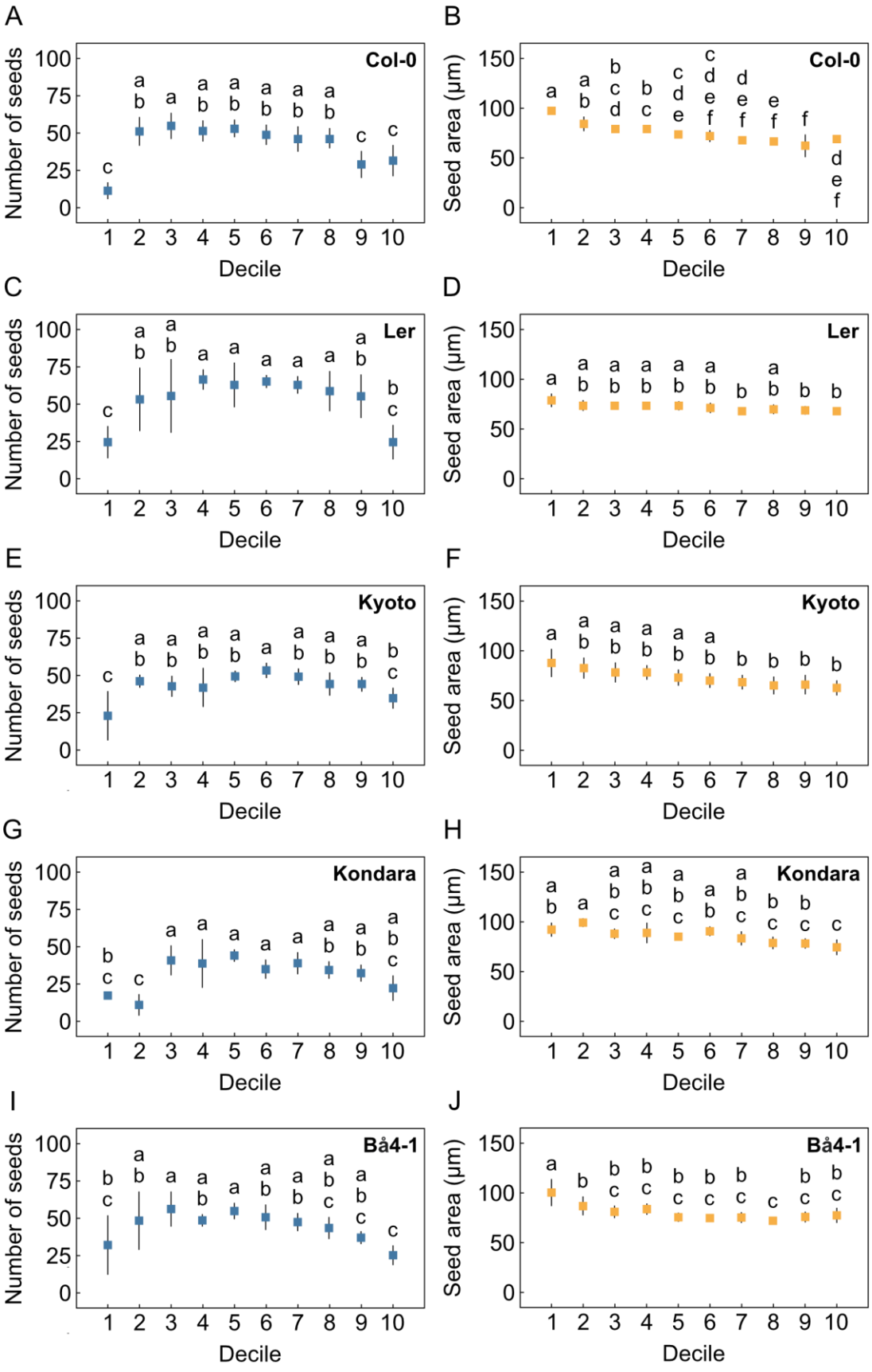

Figure 6.1. Parental age affects offspring production in *A. thaliana*

Figure 6.1. (Continuation)

Number of seeds per fruit and average seed area in fruits placed at different positions along the inflorescence in plants from the Col-0 (**A**-**B**), Ler (**C**-**D**), Kyoto (**E**-**F**), Kondara (**G**-**H**) and Bå4-1 (**I**-**J**) accessions (N=6-7). Positions are classified into deciles such that decile 1 corresponds to the bottom-most fruits and 10, to the top-most fruits. Different letters indicate statistical differences between deciles (ANOVA, Tukey HSD test, $P<0.05$).

6.3.2. Parental Age Has Limited Transgenerational Effects

Size has been shown to affect not only the survival of the seed itself (House et al., 2010) but also that of the future plant (Krannitz et al., 1991; Manning et al., 2009; Westoby et al., 1997). Thus, it was hypothesized that the observed effect of parental age on seed size (**Figure 6.1**) could affect the performance of the next generation of plants. To test this, a new experiment was designed in which seeds collected from different positions along the inflorescences of Col-0 plants (**Figure 6.1B**) were grown in standard conditions (22ºC, 16-h day length) and 6 different developmental traits related to survival, fitness and yield were measured for each offspring group (**Figure 6.2**). Interestingly, almost no differences were observed for any of the measured traits. The duration of the vegetative phase (**Figure 6.2A**), as well as that of the reproductive phase (**Figure 6.2B**), and, ultimately, the lifespan of the offspring (**Figure 6.2C**) were similar regardless of the position of the source fruit in the inflorescence of the mother plant. Similarly, there were no significant differences in fruit set (**Figure 6.2D**, **Figure 6.2E**) or biomass (**Figure 6.2F**).

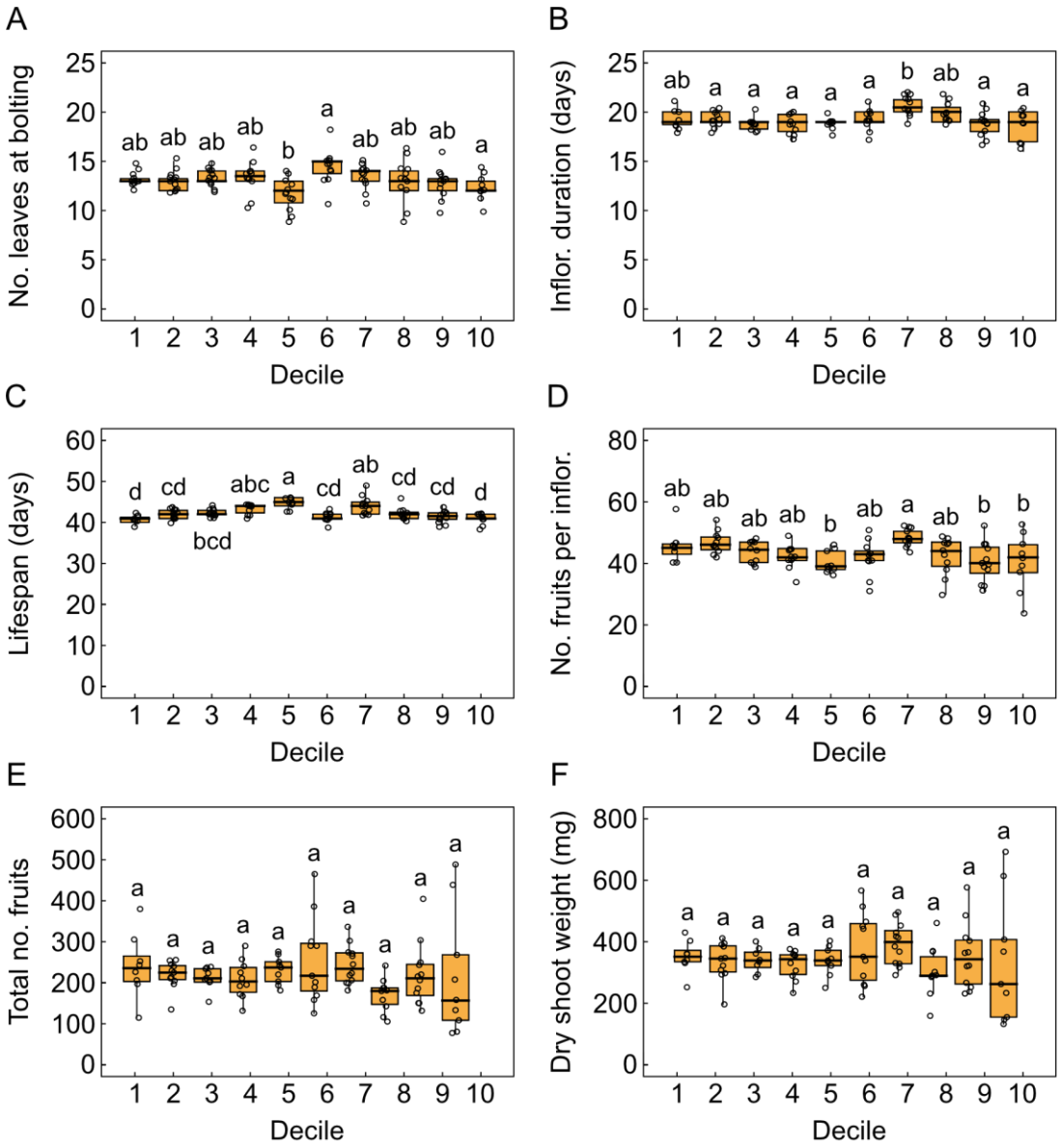

Figure 6.2. Transgenerational effects of parental age are limited

Number of leaves at bolting (**A**), inflorescence duration (**B**), plant lifespan (**C**), number of fruits per inflorescence (**D**), total number of fruits (**E**) and final shoot biomass (**F**) in plants germinated from seeds belonging to different positions across the inflorescence of Col-0 parentals (N=9-12). The position of the source seed within the parental inflorescence is classified into deciles such that decile 1 corresponds to the bottom-most positions and 10, to the top-most. Different letters indicate statistical differences between offspring groups (ANOVA, Tukey HSD test, P<0.05).

These results suggest that, although parental age impacts the size of the seed (**Figure 6.1**), it has little to no effect on the performance of the future generation of

plants (**Figure 6.2**). This is in accordance with work on pine trees (Pardos et al., 2022) and duckweeds (Barks and Laird, 2015), where parental age affects certain aspects of the offspring but not its survival. Taken together, these data support the idea that the Lansing effect does not apply to the plant kingdom, where ageing of the mother plant seems to have limited transgenerational effects. In *A. thaliana*, it is likely that these are restricted to early plant development. Here, it has been shown that at least seed size is affected by the age of the parent (**Figure 6.1**). As seed size directly impacts germination potential and vigour of the seedlings in several species (Murali, 1997; van Mölken et al., 2005), it is likely that this maternal age-dependent control has implications for the early establishment of seedlings, although this remains to be tested. Recent research has reported roles for different flowering time genes in the control of seed size (Yu et al., 2023; Zhang et al., 2020). Given the importance of these in controlling inflorescence arrest of the mother plant, it is possible that they could also underlie the parental control over offspring production. Thus, it would be interesting to test their role, if any, in establishing the heteroblastic patterns of development described here, as well as the implications of this for the germination and the establishment of young seedlings.

6.3.3. Parental Control is Partially Temperature-dependent

Considering that parental age controls seed number and size (**Figure 6.1**), and taking into account that environmental factors affect inflorescence arrest (see Chapter 3), it was questioned whether the effect of parental age on offspring production is influenced by the environment experienced by the mother plant. To test this, plants were grown at 3 different temperatures, i.e., 15ºC, 20ºC and 25ºC. After end-of-flowering, seed number and size were recorded for ripened fruits placed at different positions across the inflorescence. Fruit length, which has been proposed as a proxy for fertility (Dogra and Dani, 2019), was also measured. Both fruit length

(**Figure 6.3A**) and the number of seeds per fruit (**Figure 6.3B**) showed a bell-shaped pattern across the inflorescence, whereas seed size gradually decreased with parental age in all temperatures (**Figure 6.3C**), as expected from previous results. In addition, temperature had a clear negative effect on all traits, with higher temperatures consistently leading to a reduction in fruit length, seed size and number.

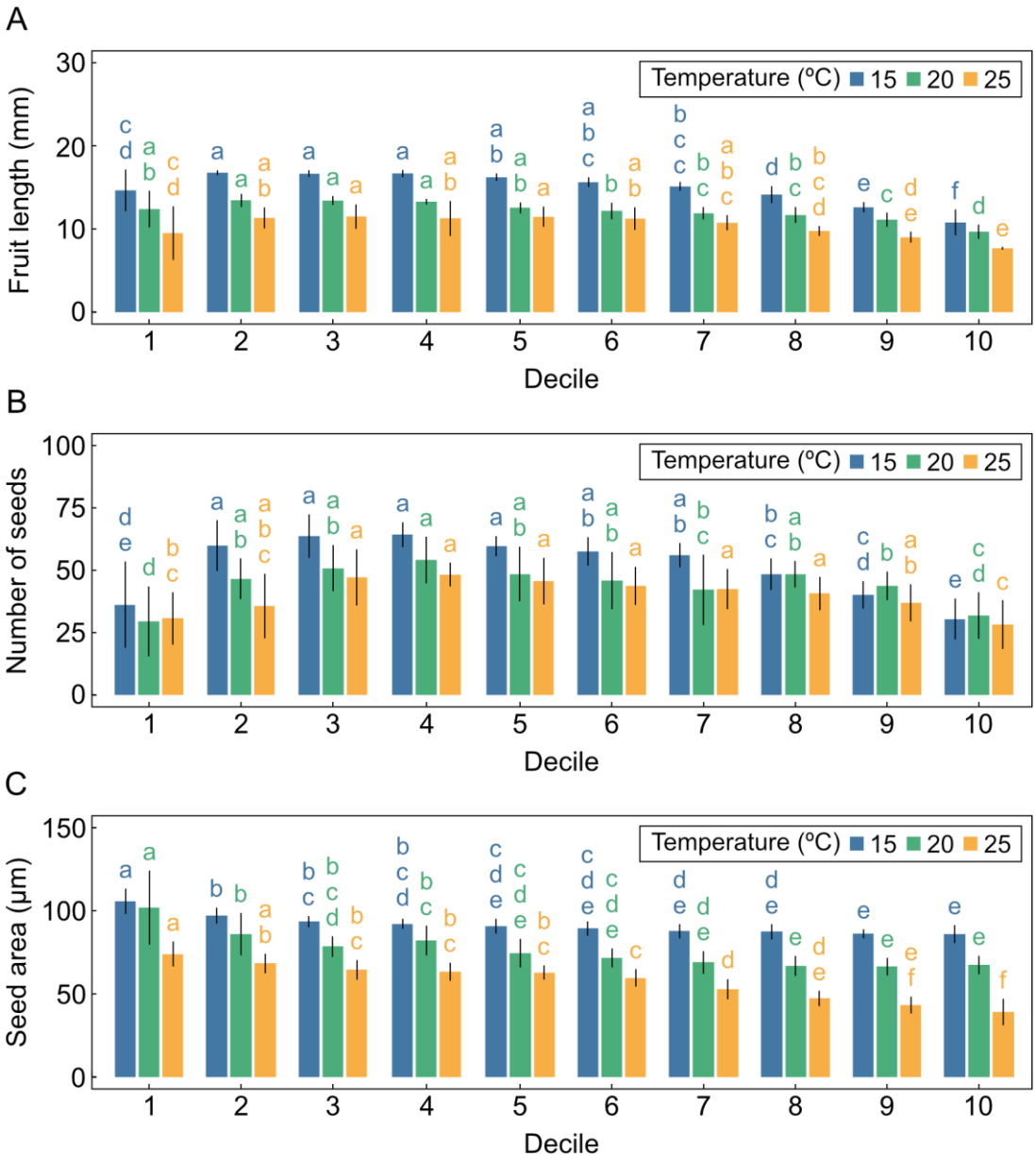

Figure 6.3. Parental control of offspring production is temperature-dependent

Fruit length (**A**), number of seeds per fruit (**B**) and average seed area (**C**) in fruits placed at different positions along the inflorescence in Col-0 plants grown at 15ºC, 20ºC or 25ºC (N=3-5).

Figure 6.3. (Continuation)

Positions are classified into deciles such that decile 1 corresponds to the bottom-most fruits and 10, to the top-most fruits. Different letters indicate statistical differences between deciles for each temperature (ANOVA, Tukey HSD test, $P<0.05$). All data was collected by Tom Lock.

These results also indicate that there is interaction between temperature and parental age during offspring production, as age-dependent effects were affected by the temperature experienced by the parent. For both fruit length and seed number, the differences among positions across the inflorescence were generally subtler in higher temperatures (**Figure 6.3A**, **Figure 6.3B**), suggesting that an increase in temperature diminishes the effect of parental age on fertility. This was not the case for seed size, which showed a clear age-dependent decline in all temperatures tested (**Figure 6.3C**), indicating that the control of seed size by parental age is largely independent from that of temperature. Seed number and size affect one another through trade-off mechanisms (Dogra and Dani, 2019; Manning et al., 2009), however, the data presented here demonstrates that these traits may also be controlled independently, leading to differential responses to environmental signals such as temperature.

The case of seed number was particularly interesting, as it hinted at the existence of feed-back mechanisms between parental age and temperature. If parental age affects the way in which temperature influences offspring production, a question arising from this is at what point during reproductive development temperature control operates. To shed light into this, a new experiment was designed where plants were grown at 20ºC until bolting. Next, subsets of plants were transferred to 25ºC after 0, 4, 8, 12 or 16 days of flowering. Finally, at the end of the experiment, length was recorded for ripened fruits from different positions along the inflorescence. Fruit length was chosen over seed number as a proxy for fertility to

facilitate data collection and based on the fact that a good correlation between the two was previously observed (r = 0.7, R^2 = 0.5) (**Figure 6.3**).

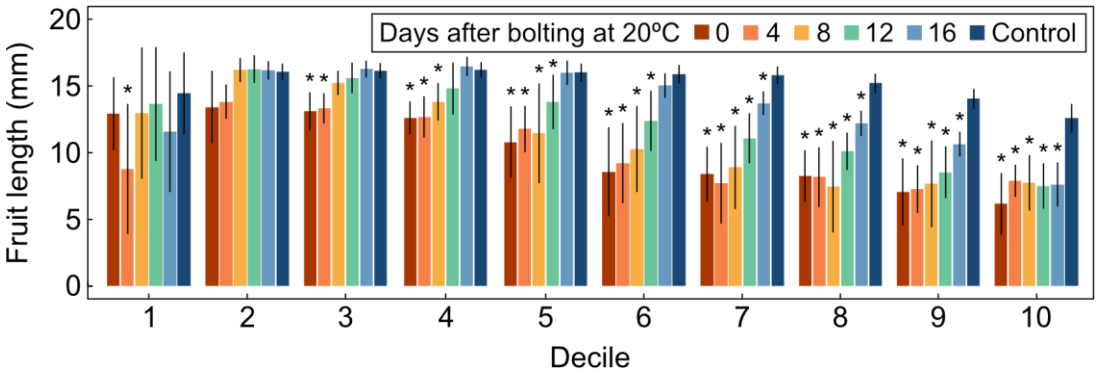

Figure 6.4. Temperature experienced during fruit development affects fertility

Length of fruits placed at different positions along the inflorescence in plants transferred from 20ºC to 25ºC 0, 4, 8, 12, or 16 days after bolting (N=4). Control plants remained at 20ºC during the whole experiment. Positions are classified into deciles such that decile 1 corresponds to the bottom-most fruits and 10, to the top-most fruits. Asterisks indicate statistical differences between any transfer group and control plants (ANOVA, Tukey HSD test, P<0.05).

The relationship between parental age and fruit length followed a bell-shaped curve for all temperature groups (**Figure 6.4**). In addition, plants transferred to 25ºC immediately after bolting showed reduced fruit lengths for all positions across the inflorescence, as expected. These were almost identical to those of plants transferred after 4 days of flowering. Since flower opening began approximately 5 days after bolting at 20ºC, neither of these groups had opened flowers at the time of transfer, suggesting that temperature experienced by young floral primordia does not have a significant effect on fertility. In agreement with this, all temperature groups that had opened flowers and/or fruits at the time of transfer showed fruit lengths similar to control plants for at least some of the deciles. Plants transferred after 8, 12 and 16 days of flowering started showing differences to the control after the third, fourth and sixth decile, respectively. Based on this, it can be concluded that temperature during

flower and fruit development determines fertility, with little effect of previous temperature experienced during the initiation of floral primordia.

These results reveal a complex picture for the environmental control of offspring production, with temperature affecting reproductive output at different stages throughout flowering. During early reproductive development, temperature experienced by the mother plant affects the timing of inflorescence arrest and, thus, the number of fruits produced (see Chapter 3). Later on, temperature experienced by the developing fruits impacts their own fertility (**Figure 6.4**). It is currently unclear how the environmental control of seed development is regulated at the molecular level, but it is likely that the underlying mechanism operates at the fruit or seed levels, in contrast to the temperature-dependent regulation of arrest, which is at the IM level. Previously, temperature experienced by the mother plant during seed development has been shown to affect seed germination (Chen et al., 2014; Roach and Wulff, 1987). This process is at least partially mediated by the floral integrator FLOWERING LOCUS T (FT) (Chen et al., 2014), which has been previously shown to regulate IM arrest, raising the possibility that FT signaling also participates in the control of offspring production by the mother plant, ultimately serving as a link between parental end-of-flowering and the development of offspring seeds.

6.3.4. *FT* Mediates Parental Control of Offspring Production and its Interaction with Temperature

Taking into account that *FT* participates in the parental control of seed dormancy (Chen et al., 2014), it was hypothesized that the observed effects of both parental age and temperature on offspring production would be mediated by *FT*. To test this, *ft-10* mutants were grown at either 15ºC, 20ºC or 25ºC and, after end-of-flowering, offspring production was characterized in ripened fruits. Higher

temperatures reduced both fruit length (**Figure 6.5A**) and seed number (**Figure 6.5B**) in *ft-10* in a manner similar to wild-type (**Figure 6.3**), suggesting that temperature-mediated regulation of fertility is *FT*-independent. Contrary to wild-type, which showed a clear effect of parental age on fertility, *ft-10* mutants only exhibited minor significant changes in fruit length and seed number with parental age. In both cases, the characteristic increase in fertility observed at the middle of the inflorescence was absent for most temperatures and fruits from different positions were very similar. Additionally, while higher temperatures reduced the impact of age on fertility in wild-type, this was not the case for *ft-10*, suggesting that although *FT* is not necessary for the control of fertility by temperature, it is somewhat required for the interaction between temperature and parental age.

The role of *FT* in controlling offspring production was clearer when considering seed size, as *ft-10* mutants failed to respond to either temperature or parental age (**Figure 6.5C**). A subtle effect of parental age was noticeable in plants grown at 20ºC, but the gradual reduction in seed size along the inflorescence was almost completely lacking at both 15ºC and 25ºC. These results point towards the idea that *FT* could be required for appropriate responses to both temperature and parental age at the seed level, adding a new layer of complexity to the role of *FT*, which not only controls fruit production (see Chapter 4) but also key characteristics of the offspring seeds such as their dormancy levels (Chen et al., 2014) and, as shown here, their size. The precise mechanism by which *FT* controls seed size still remains to be described. Recently, a role for an homolog of *FT*, *TERMINAL FLOWER 1* (*TFL1*) in regulating seed size has been characterized in detail (Zhang et al., 2020). In short, TFL1 produced in the seeds mediates cellularization of the endosperm through stabilization of the transcription factor ABA INSENSITIVE 5 (ABI5), which has well-described roles in seed development (Skubacz et al., 2016). TFL1 and FT have antagonistic roles during plant development and they compete for the binding to the same target genes (Zhu et al., 2020). Thus, it is possible that FT produced in

the seeds controls their size through the same molecular pathway as TFL1, although this would require appropriate testing, which falls outside of the scope of this project.

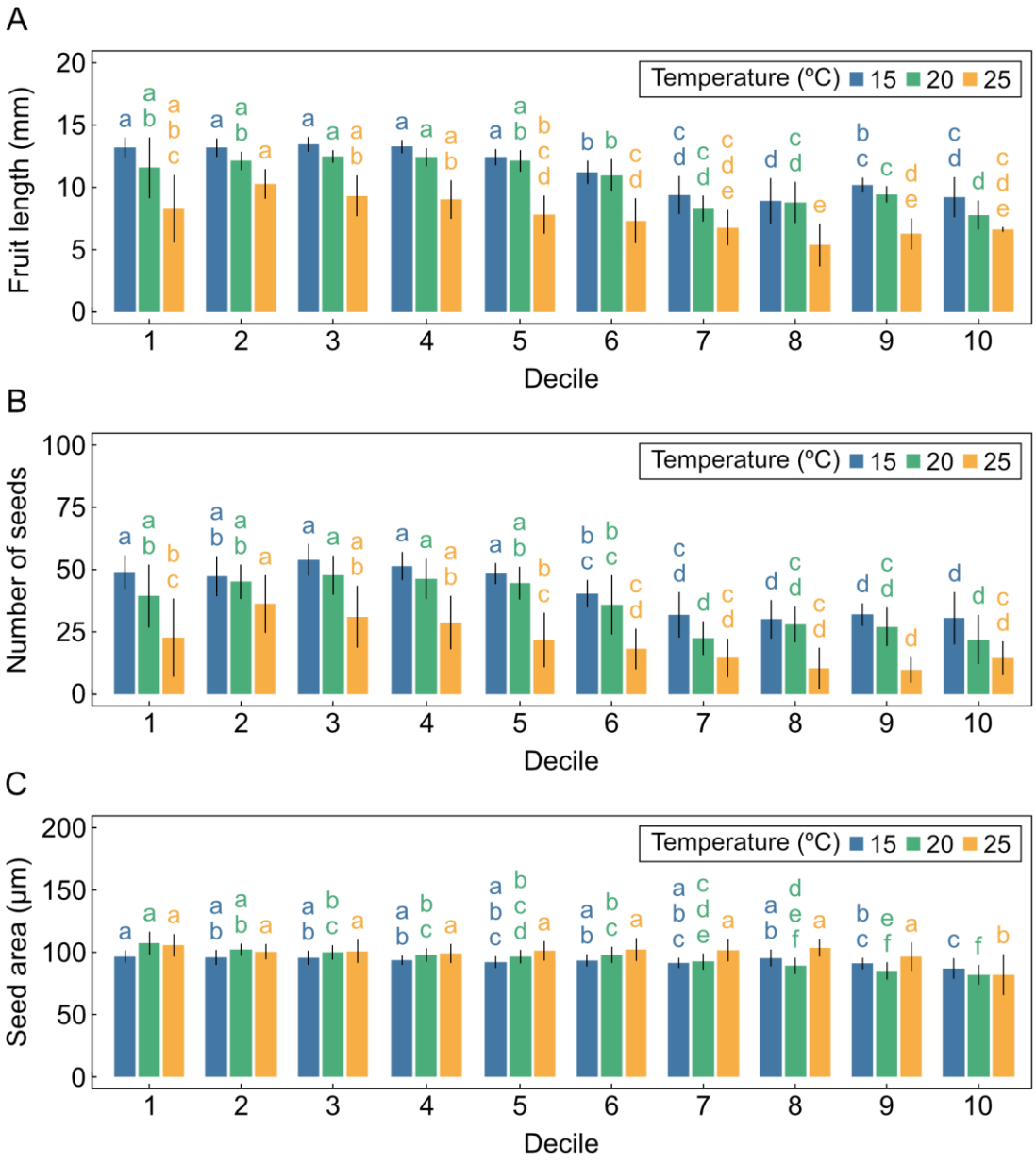

Figure 6.5. *FT* mediates the control of offspring production by parental age

Fruit length (**A**), number of seeds per fruit (**B**) and average seed area (**C**) in fruits placed at different positions along the inflorescence in *ft-10* mutants grown at 15ºC, 20ºC or 25ºC (N=3-4). Positions are classified into deciles such that decile 1 corresponds to the bottom-most fruits and 10, to the top-most fruits. Different letters indicate statistical differences between deciles for each temperature (ANOVA, Tukey HSD test, P<0.05). All data was collected by Tom Lock.

The lack of age-dependent changes in offspring production in the *ft-10* mutant hints at a previously uncharacterized role of *FT* during seed development. To further validate these results, and to discard any background-specific effects, a new experiment was carried out where two different mutants lacking *FT* were grown at either 20ºC or 25ºC, one in the Col-0 background, i.e., *ft-10*, and another in the Ler background, i.e., *ft-1*. After end-of-flowering, ripened fruits from different positions across the inflorescence were harvested and their length was recorded. As expected, fruit length was affected by both parental age and temperature in wild-type plants, and higher temperatures tended to mitigate the age-dependent effects in both accessions (**Figure 6.6A**, **Figure 6.6C**).

In agreement with previous results, *ft-10* and *ft-1* mutants also showed a consistent reduction in fruit length at higher temperatures (**Figure 6.6B**, **Figure 6.6D**), further demonstrating that *FT* is not necessary for the regulation of fertility by temperature. In contrast, both mutants were impaired in the distribution of fruits across the inflorescence. Wild-type plants showed a clear increase in fruit lengths in the middle of the inflorescence at both 20ºC and 25ºC, whereas *ft* mutants lacked this characteristic pattern and exhibited fruits of very similar lengths. At 25ºC, the usual bell-shaped effect of parental age on fruit length was completely disrupted in the *ft* mutants, which showed unusually long fruits at the top of the inflorescence (**Figure 6.6B**, **Figure 6.6D**). These observations seem to further support the idea that *FT* mediates responses to age during offspring production. It is important to note that there are discrepancies between these data and that from the previous experiment (**Figure 6.5**), particularly for *ft-10* mutants grown at 25ºC. However, the lack of an age-dependent effect on fertility in *ft* mutants was obvious in both cases.

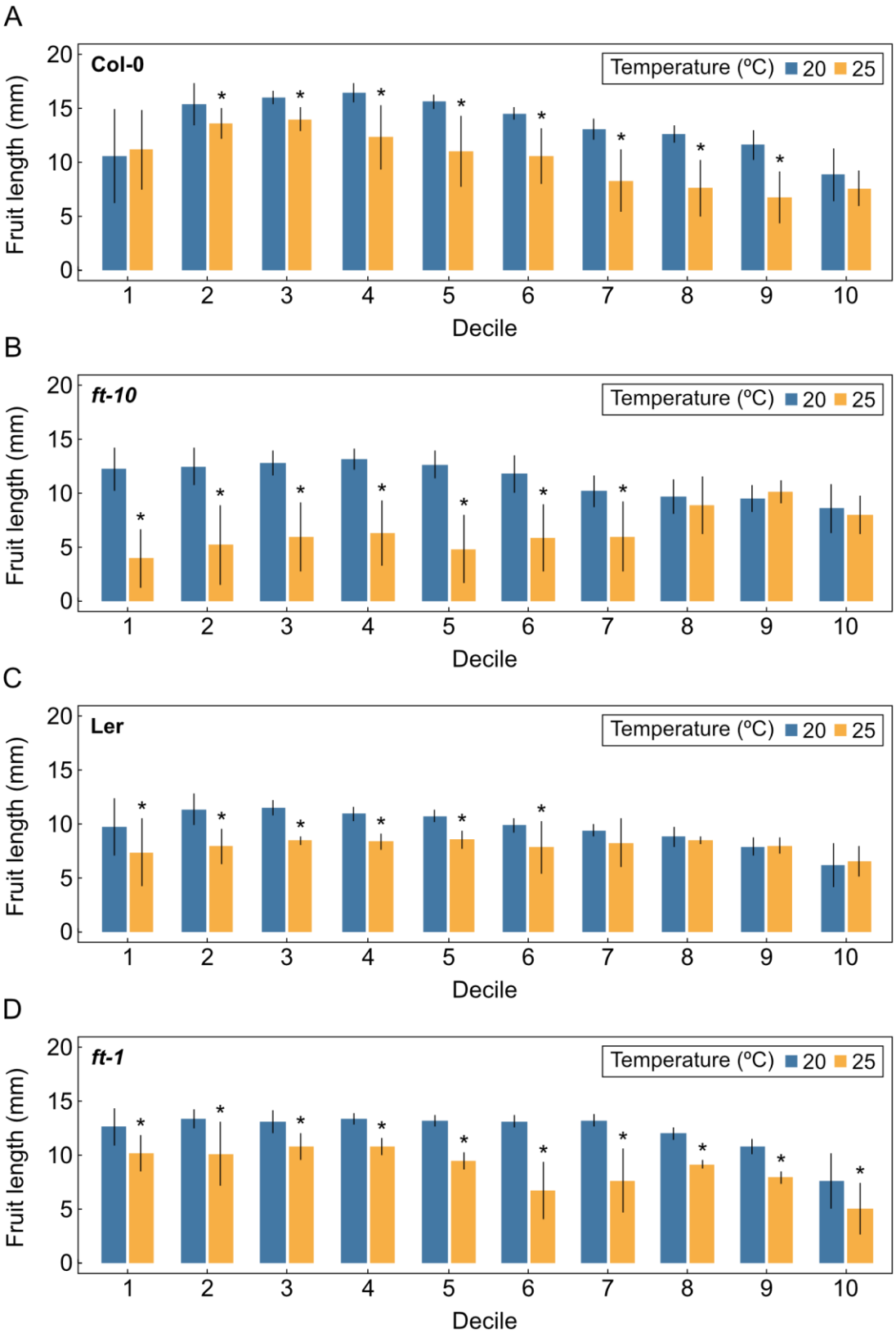

Figure 6.6. *FT* is necessary for the control of fertility by age but not temperature

A-B. Length of fruits placed at different positions along the inflorescence of wild-type (**A**) and *ft* mutants (**B**) in the Col-0 background grown at 20ºC or 25ºC (N=4).

Figure 6.6. (Continuation)

C-D. Length of fruits placed at different positions along the inflorescence of wild-type (**C**) and *ft* mutants (**D**) in the Ler background grown at 20ºC or 25ºC (N=4). Positions are classified into deciles such that decile 1 corresponds to the bottom-most fruits and 10, to the top-most fruits. Asterisks indicate statistical differences between temperatures for each decile (Student's t test, $P<0.05$).

6.3.5. Transcriptional Regulation of *FT* May Underlie Parental Control of Offspring Production

Knowing that *FT* is involved in the interaction between parental age and temperature, it was questioned how this process is regulated at the molecular level. During end-of-flowering, temperature affects arrest of the IM by modulating the expression of *FT* in the leaves (see Chapter 4). In the fruits, *FT* expression has been previously shown to be controlled by temperature (Chen et al., 2014), thus, it was hypothesized that a mechanism based on the transcriptional regulation of *FT* in the fruits could control offspring production. To test this, plants were grown at either 15ºC, 20ºC or 25ºC and, after inflorescence arrest, fruits from the bottom, middle and top of the inflorescence were harvested and used for the quantification of *FT* expression by RT-qPCR. *FT* mRNA was undetectable in fruits from the bottom and middle of the inflorescence, both of which were fully ripened. Conversely, it was possible to quantify *FT* transcript levels in the top-most fruits, all of which were still developing at the time of harvest. In these, temperature showed a clear effect on *FT* levels, with higher temperatures up-regulating *FT* expression in a manner similar to the induction of *FT* by warmth that occurs in the leaves prior to flowering (Blázquez et al., 2003; Thines et al., 2014) (**Figure 6.7**).

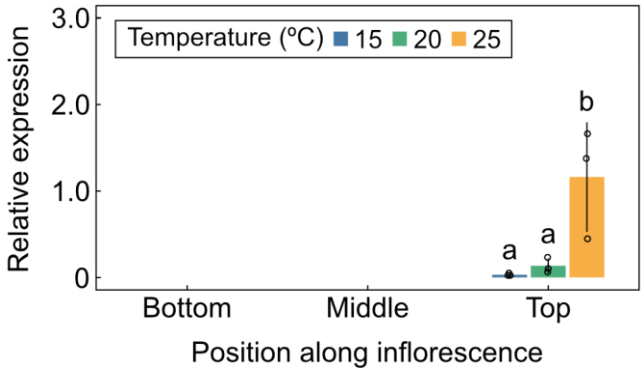

Figure 6.7. Temperature regulates *FT* expression in developing fruits

FT expression in fruits placed at different positions along the inflorescence of plants exposed to 15ºC, 20ºC or 25ºC (N=3). Transcript levels are normalized to *UBC9* and then referred to the temperature at which the maximum *FT* level was achieved, which was 25ºC. Different letters indicate statistical differences between temperatures (ANOVA, Tukey HSD test, P<0.05).

Temperature-dependent regulation of *FT* in the fruits has been previously reported and is a key step in a molecular pathway that integrates the temperature experienced by the parental with the dormancy of the offspring seeds (Chen et al., 2014). Here, it has been demonstrated that *FT* is expressed only in developing fruits. Based on the existing literature, it is likely that the detected *FT* mRNA is produced specifically in the vascular bundles of the silique (Liu et al., 2014). FT synthesized in the phloem of the fruit could then affect offspring production by either translocating to the seeds to act locally or through indirect mechanisms, as *FT* is not expressed in the seeds themselves (Chen et al., 2014). Since *FT* mRNA is also produced in various other organs during development (see Chapter 4), it is also possible that FT from sources other than the fruits participates in this process, given its mobile nature. Either way, *FT* expression seems to be under tight control by temperature and parental age, suggesting that the integration of both cues on the development of seeds occurs at the transcriptional level. The *35S:FT-GR* line developed previously (see Chapter 4) was used to further validate this idea. To recap, this line is in the Col-

0 background but contains a transgenic *35S:FT-GR* that allows for an overexpression of *FT* in the presence of the steroid hormone dexamethasone (DEX). If transcriptional regulation of *FT* underlies the parental control of seed development, it was hypothesized that ectopically inducing an overexpression of *FT* would disrupt the effect of parental age on offspring production. To test this, an experiment was carried out where *35S:FT-GR* and wild-type plants were grown in standard conditions (20ºC, 16-h day length). Approximately 10 days after bolting, three secondary inflorescences from each plant were tagged. One was treated with DEX, another with a control solution and the last one was left untreated. Plants were then kept until end-of-flowering and, finally, fruit length was recorded at different positions along the inflorescence for each treatment.

No effect of the DEX application was observed for either of the genotypes (**Figure 6.8A**, **Figure 6.8B**), suggesting that an overexpression of FT does not have any significant effects on fertility. However, inflorescences treated with DEX did not present any differences in fruit number either (**Figure 6.8C**, **Figure 6.3D**), which is unexpected as *35S:FT-GR* plants were previously shown to increase their production of fruits in the presence of DEX (see Chapter 4). There are various possible causes for these discrepancies. The method followed for the treatment of DEX, as well as the concentration used (1 mM), has been successfully used before (Crawford et al., 2010), but it is possible that it needs to be optimized for the study of seed development. The concentration of DEX used previously for the *35S:FT-GR* line was in fact much lower (10 µM), but it was supplied in the growth media, so it was available during the whole life cycle (see Chapter 4). Here, DEX was mixed into lanolin and applied to the base of the inflorescence, but it is possible that this local induction of *FT* at the bottom of the inflorescence is insufficient to affect either inflorescence arrest or offspring production. Thus, it would be beneficial to test different concentrations of DEX and methods of application before drawing final conclusions. Another possible explanation is that secondary inflorescences are not an appropriate unit of study for

this experiment. Upon closer examination of the results, changes in fruit length across the inflorescence were surprisingly subtle and almost lacking in both *35S:FT-GR* and wild-type (**Figure 6.8A**, **Figure 6.8B**), suggesting that heteroblastic development is less noticeable in the secondary branches compared to the primary inflorescence (**Figure 6.3A**). Hence, future research would probably benefit from focusing on the primary inflorescence, where the effect of parental age on fruit length is much clearer.

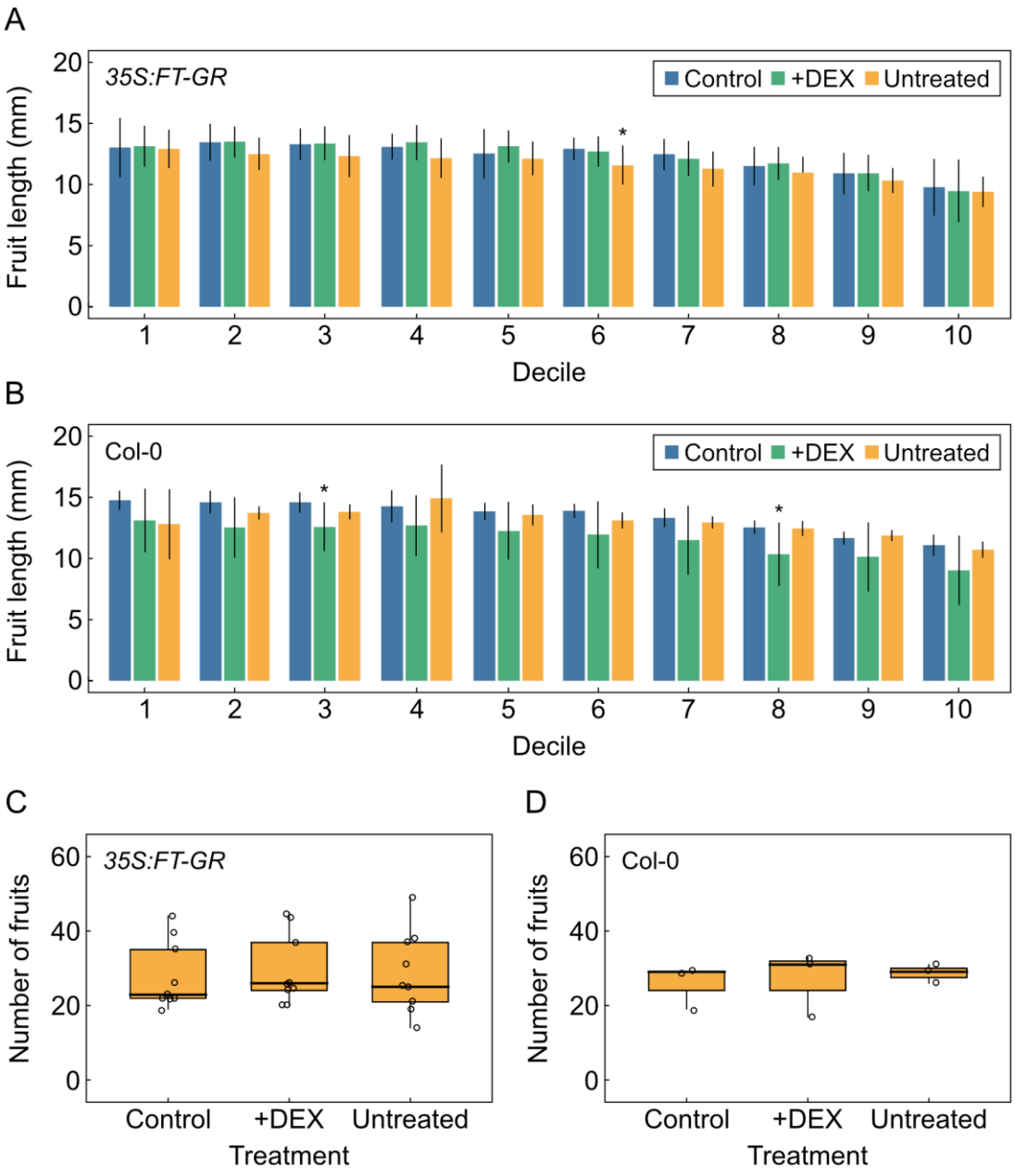

Figure 6.8. Ectopic overexpression of *FT* does not affect offspring production

Figure 6.8. (Continuation)

A-B. Length of fruits placed at different positions along the inflorescence in transgenic *35S:FT-GR* (**A**) or wild-type Col-0 (**B**) plants (N=3-6). Inflorescences were either treated with a control solution, with a DEX-supplemented solution or left untreated. Positions are classified into deciles such that decile 1 corresponds to the bottom-most fruits and 10, to the top-most fruits. Asterisks indicate statistical differences against the control for each decile (ANOVA, Tukey HSD test, P<0.05). **C-D.** Number of fruits per inflorescence in inflorescences from each treatment in transgenic *35S:FT-GR* (**C**) or wild-type Col-0 (**D**) (N=3-9). Different letters indicate statistical differences between treatments (ANOVA, Tukey HSD test, P<0.05).

6.4. Conclusions

The data presented throughout this chapter strongly supports that offspring production is influenced by parental age. The number of seeds per fruit is the lowest at the start of flowering, increases during mid-flowering, and declines later, when the mother plant is the oldest. In addition, seed size decreases proportionally to the age of the parent. Both of these effects are highly conserved across different natural accessions of *A. thaliana*, and they seem largely independent from the processes of arrest and senescence. Interestingly, although parental age impacts seed production and seed size, it has no effect on the performance or longevity of the future generation of plants.

Classically, the effect of plant age on the morphology of organs has been attributed to an autonomous control independent of the environment. However, the results obtained here demonstrates that environmental signals such as temperature not only affect offspring production independently but also crosstalk with parental age, influencing the way ageing is integrated into the development of seeds. Both of these are at least partially mediated by the floral integrator *FT*, which is necessary for appropriate responses of offspring production to both parental age and temperature. Altogether, these results highlight *FT*'s multifaceted nature during

flowering, as not only does it control inflorescence arrest and the number of fruits produced, as previously shown, but also the quantity and size of seeds, ultimately exerting a complete control over the final reproductive output.

The main question arising from these data, which is left unanswered here, is how *FT* regulates seed size and seed number. A possibility mentioned throughout the text is that an interplay between *FT* and its homolog *TFL1* could underlie these processes, however, this remains to be formally assessed. In addition, environmental signals other than temperature could affect the age-dependent control of seed production, none of which have been explored to date. Thus, future research would benefit from an inspection of the potential interactions between age and other environmental stimuli, such as day length and nutrients.

Chapter 7: Comparative Study of the End-of-Flowering in the Plant Kingdom

7.1. Introduction

During the last decade, interest in the end-of-flowering has increased significantly, leading to a good characterization of inflorescence arrest and its genetic regulation. However, with very few exceptions, research revolving around the end-of-flowering has focused on *A. thaliana* (Balanzà et al., 2023), whereas non-model species have been largely overlooked. As has been shown throughout this thesis and in the published literature, end-of-flowering has clear implications for the reproductive output of plants. Thus, the study of processes that underlie arrest in non-model species is key for better understanding the factors that determine reproductive output in plants, something of particular importance in the case of crops and species of commercial interest. The main challenge associated with this lies in the fact that an astonishing diversity of growth habits and inflorescence types exist in the plant kingdom (Prusinkiewicz et al., 2007), with not all species having the same reproductive development. Like many other members of the Brassicaceae family, *A. thaliana* forms indeterminate inflorescences, in which the inflorescence meristem (IM) remains undifferentiated during the whole lifespan of the plant (Ratcliffe et al., 1998; Weberling, 1992). However, other species, including crops such as tomato (*Solanum lycopersicum*) or onion (*Allium cepa*), have determinate inflorescences, where the IM eventually acquires floral identity, turning into a terminal flower (Benlloch et al., 2007; Caselli et al., 2020; Ratcliffe et al., 1998).

As processes related to arrest have been described primarily for *A. thaliana*, it is currently unclear whether arrest mechanisms are conserved among species with

indeterminate inflorescences. Furthermore, *A. thaliana* is a monocarpic plant, i.e., it undergoes a single reproductive episode, after which it dies. This raises the question as to how end-of-flowering operates in perennials and polycarpic species, which experience multiple reproductive events during their lifetime. Work on *Arabis alpina*, a perennial from the Brassicaceae, demonstrates that individual inflorescences die back at the end of each reproductive phase (Vayssières et al., 2020). This suggests that inflorescence arrest may be conserved in the Brassicaceae family, with additional mechanisms operating in perennial members which mediate the transitions between reproductive and vegetative phases. However, a detailed analysis of end-of-flowering in the Brassicaceae is still necessary to determine whether other aspects of arrest and, particularly, its environmental control are conserved in this plant family.

Outside of the Brassicaceae, very little is known about processes that underlie inflorescence arrest. Grasses from the Poaceae family, such as hexaploid wheat (*Triticum aestivum*), present an interesting system to study end-of-flowering as they have reproductive architectures very different to that of *A. thaliana*. In wheat, inflorescences are organized in specialized structures named spikes, which are determinate (Caselli et al., 2020; Kirby and Appleyard, 1984). The spike meristem produces a variable number of spikelet meristems (SMs) before differentiating itself into a terminal SM (Benlloch et al., 2007; Bradley et al., 1997; Caselli et al., 2020). In each spikelet, the indeterminate SM initiates a number of floret meristems, typically 10-12, before ceasing its proliferative activity (Bonnett, 1936; Sadras and Slafer, 2012). While all initiated SMs hold the potential to become fertile florets, only 1-4 tend to do so (Fischer, 1984), with the remaining undergoing a degenerative process based on cellular autophagy (Glick et al., 2010). Taking all of this into account, end-of-flowering in wheat likely relies on two separate developmental transitions. First, the differentiation of the spike meristem into a terminal SM causes arrest at the spike level. Later, individual SMs undergo an uncharacterized arrest process that is reminiscent of IM arrest in *A. thaliana*, as in both cases the meristem is indeterminate

and inflorescences arrest with a cluster of undeveloped floral primordia (Hensel et al., 1994).

Despite the importance of spikelet arrest in determining yield in wheat, the exact mechanisms underlying SM arrest and the subsequent abortion of florets are largely unknown (Backhaus et al., 2023), although they are thought to be genetically and environmentally controlled (Bonnett, 1966; Caselli et al., 2020). Two of the major environmental factors that control spikelet development are temperature and day length, which impact the duration of early reproductive development and, ultimately, the number of surviving florets (Slafer and Rawson, 1994). Furthermore, floret death can be promoted by conditions that accelerate growth and development, as faster developmental rates cause sugar starvation, which in turn triggers floret autophagy (Ghiglione et al., 2008). Accordingly, factors such shading (Stockman et al., 1983) or nitrogen availability (Ferrante et al., 2013), which affect assimilate production and consumption, are known to impact spikelet and floret development.

Very little is known about the molecular basis of SM arrest in wheat, as most of the published research has focused on the genetic regulation of arrest at the spike level, i.e., the formation of the terminal spikelet. Interestingly, wheat homologs of *FLOWERING LOCUS T* (*FT*) have been associated with both the transition into flowering (Bratzel and Turck, 2015; Finnegan et al., 2018; Yan et al., 2006) and the formation of the terminal spikelet (Dixon et al., 2018; Gauley and Boden, 2021). This raises the possibility that the function of *FT*-like genes during end-of-flowering (see Chapter 4) may be conserved in the plant kingdom. Indeed, the genetic network controlling the timing of flowering and, particularly, the role of *FT* as a floral promoter, is largely conserved in plants (Benlloch et al., 2007; Turck et al., 2008; Wickland and Hanzawa, 2015). However, further research is still required to fully understand the role of *FT*-like genes in both spike meristem arrest in wheat, as well as their potential implication in the regulation of SM arrest, which has not been explored yet.

7.2. Aims

The general aim of this chapter was to characterize end-of-flowering and its response to the environment in species other than *A: thaliana*. Specifically, the proposed goals were as follows.

1) To characterize inflorescence arrest in two species from the Brassicaceae, *Olimarabidopsis pumila* and *Capsella rubella*.
2) To assess the effect of environmental cues on inflorescence arrest in *O. pumila* and *C. rubella*.
3) To characterize inflorescence arrest in a species from the Poaceae family, hexaploid wheat (*Triticum aestivum*).
4) To assess the effect of environmental cues on inflorescence arrest in wheat.
5) To assess the natural variation in inflorescence arrest in wheat.

7.3. Results and Discussion

7.3.1. Inflorescence Arrest is Conserved in the Brassicaceae

As a first step towards understanding end-of-flowering outside *A. thaliana*, a first experiment was carried out to characterize arrest in other species from the Brassicaceae family. Two species from different genera, *Olimarabidopsis pumila* and *Capsella rubella*, were grown in standard conditions (20ºC, 16-h day length) until flowering, after which the number of flowers and fruits was counted every two days for the primary inflorescence. For both species, inflorescence development was very similar to that of *A. thaliana*, with new flowers opening every day in the primary inflorescence at a constant rate of ~3.6 and ~4.4 flowers per day in *O. pumila* and *C. rubella*, respectively. Approximately 3 weeks after the beginning of flowering, flower opening stopped in the primary inflorescence a manner similar to *A. thaliana*, while secondary inflorescences continued to flower for some additional time (**Figure 7.1A**, **Figure 7.1B**). A closer inspection of the apex of arrested inflorescences also revealed a clear cluster of arrested buds surrounding the IM (**Figure 7.1C**, **Figure 7.1D**).

End-of-flowering in members of the Brassicaceae other than *A. thaliana* has never been investigated before, however, the results presented here suggest that inflorescence arrest is conserved within this family. Like *A. thaliana*, *O. pumila* and *C. rubella* are annual species (Hintz et al., 2006; Hoffmann et al., 2010), but the perennial *A. alpina* has been attributed similar end-of-flowering phenotypes (Vayssières et al., 2020), suggesting that inflorescence arrest is not limited to monocarpic species. An interesting question arising from this is whether the genetic regulation of end-of-flowering is also conserved in the Brassicaceae. As the genetic pathways controlling the onset of flowering are highly conserved in plants (Benlloch et al., 2007; Turck et al., 2008; Wickland and Hanzawa, 2015), and given that genes underlying floral transition also regulate arrest (see Chapter 4), it is tempting to

hypothesize that flowering time genes may have conserved functions in the regulation of both flowering and end-of-flowering in the Brassicaceae, although this would require further validation.

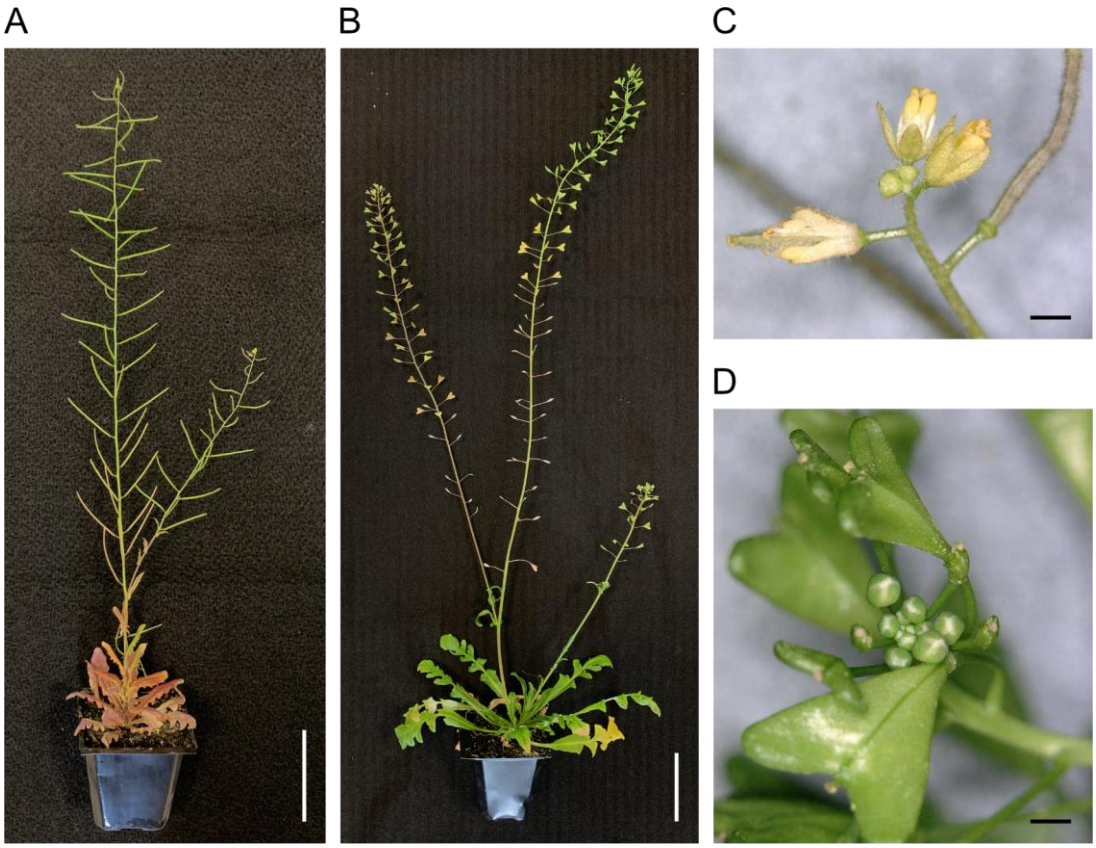

Figure 7.1. Inflorescence arrest phenotype in *Olimarabidopsis* and *Capsella*

A-B. Photographs of *Olimarabidopsis pumila* (**A**) and *Capsella rubella* (**B**) at the end-of-flowering. White scale bars are 5 cm. **C-D.** Close-up view of the cluster of arrested buds in *O. pumila* (**C**) and *C. rubella* (**D**). Black scale bars are 1 mm.

7.3.2. Arrest in the Brassicaceae is Environmentally-Regulated

Knowing that inflorescence arrest is conserved among the Brassicaceae (**Figure 7.1**), and that this is a process under tight environmental control in *A. thaliana* (see Chapter 3), it was hypothesized that environmental signals would also impact arrest in other species from the Brassicaceae family. A new experiment was designed to test this, where *O. pumila* and *C. rubella* were either grown in standard conditions

(20ºC, 16-h day length), at cold temperatures (15ºC, 16-h day length) or on low nutrients. For the latter, plants were also grown in standard conditions (20ºC, 16-h day length) but on a 1:1 (v/v) mixture of compost and sand instead of compost. In all cases, plants were grown until flowering, and inflorescence duration and fruit set were measured for each environmental setup and species.

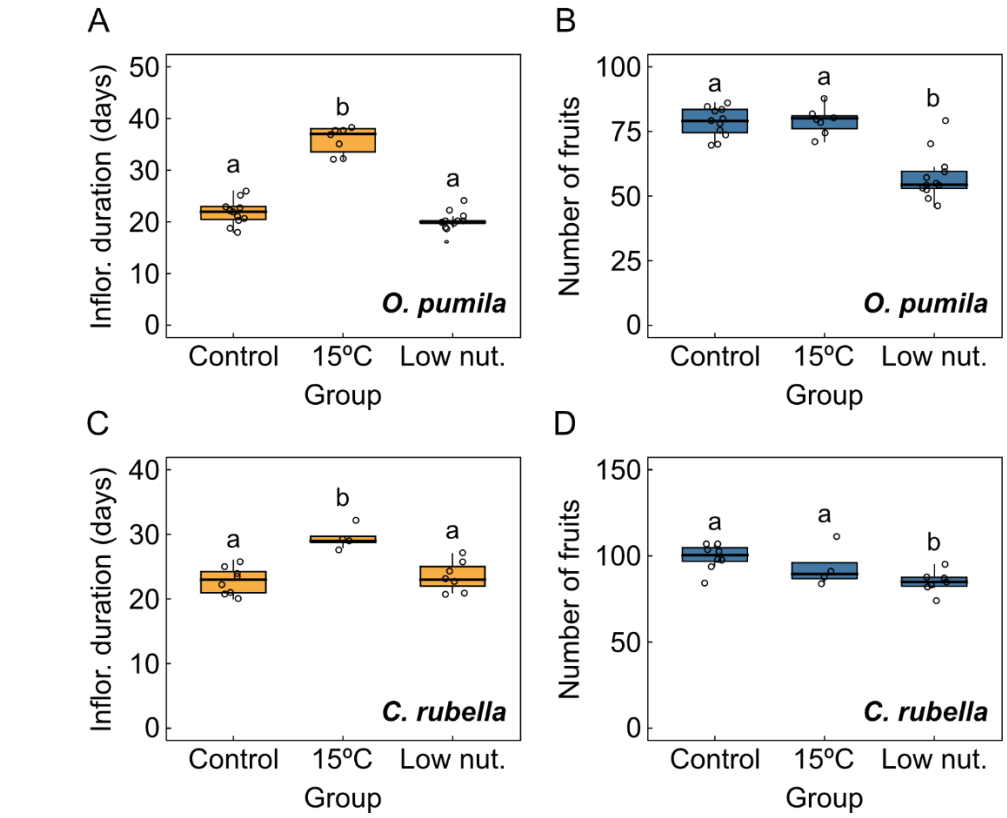

Figure 7.2. Environmental signals control arrest in the Brassicaceae

A-B. Inflorescence duration (**A**) and number of fruits per inflorescence (**B**) in *O. pumila* plants grown in control conditions, at 15ºC or in low nutrients (N=7-12). **C-D.** Inflorescence duration (**C**) and number of fruits per inflorescence (**D**) in *C. rubella* plants grown in control conditions, at 15ºC or in low nutrients (N=4-8). Different letters indicate statistical differences (ANOVA, Tukey HSD test, P<0.05).

Both temperature and nutrient availability affected inflorescence arrest in *O. pumila* in distinct ways (**Figure 7.2A**, **Figure 7.2B**). In the cold, inflorescences showed a longer duration but produced the same number of fruits as in the warmth.

The opposite was observed for the effect of nutrient availability, as there were little differences in inflorescence duration under low nutrients, but the number of fruits per inflorescence was reduced. The same was true for *C. rubella*, which showed a longer inflorescence duration in the cold (**Figure 7.2C**) a reduced inflorescence fruit set on low nutrients (**Figure 7.2D**). In both cases, the observed responses closely matched those previously observed for *A. thaliana* (see Chapter 3). Taken together, these data suggest that temperature and nutrient availability affect both inflorescence arrest and the rate of flower opening, i.e., florochron, in species from the Brassicaceae.

In *A. thaliana*, environmental conditions that trigger the transition into flowering, such as warm temperatures, also tend to promote inflorescence arrest (see Chapter 3). For other species from the Brassicaceae, the environmental control of flowering time is not as well characterized. However, increases in temperature have been described to accelerate the onset of flowering in *O. pumila* (Hoffmann et al., 2010) and *C. rubella* (Choi et al., 2019), demonstrating that the dual role of temperature as a regulator of both flowering and arrest may be a common feature of the Brassicaceae, many of which are adapted to the same climatic regions (Hintz et al., 2006; Hoffmann et al., 2010).

7.3.3. Parental Age Affects Seed Production in the Brassicaceae

Another key feature of reproductive development in *A. thaliana* is the control of offspring production by parental age, which has been previously described (see Chapter 6). Here, it was hypothesized that this age-dependent regulation would be conserved in the Brassicaceae family. To test this, *O. pumila* and *Capsella bursa-pastoris* plants were grown in standard conditions (22ºC, 16-h day length). Next, fruits were sampled from different positions along their inflorescences, and both the number of seeds per fruit as well as the average seed size were recorded.

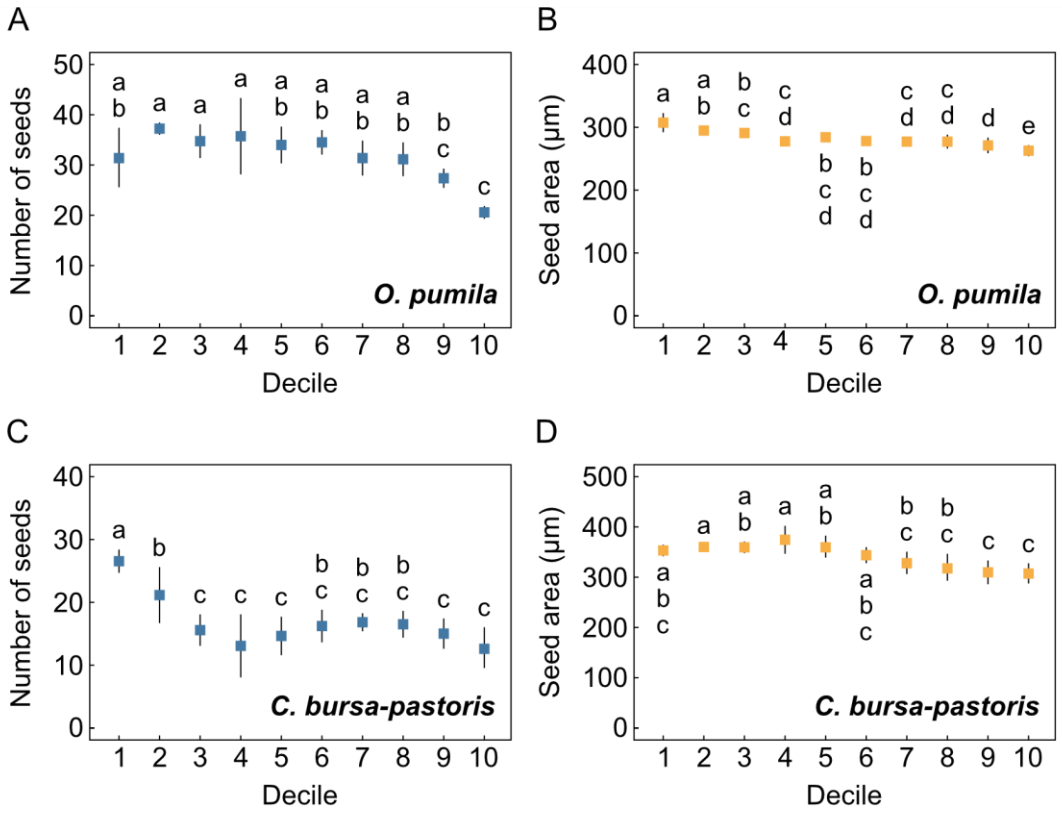

Figure 7.3. Parental age affects offspring production in the Brassicaceae

A-B. Number of seeds per fruit (**A**) and average seed area (**B**) at different positions across the inflorescence of *O. pumila* plants (N=4). **C-D.** Number of seeds per fruit (**C**) and average seed area (**D**) at different positions across the inflorescence of *C. bursa-pastoris* plants (N=4). Fruits are classified into deciles such that decile 1 corresponds to the bottom-most fruits and 10, to the top-most fruits. Different letters indicate statistical differences between deciles (ANOVA, Tukey HSD test, $P<0.05$).

For both species, age had a clear impact on the number and size of the seeds produced. Fruits from the bottom and middle of the inflorescence contained more seeds, whereas those from the top-most part of the inflorescence (produced when the mother plant was the oldest) showed the minimum number of seeds (**Figure 7.3A**, **Figure 7.3C**). In contrast, seed area gradually decreased from the bottom to the top of the inflorescence, in a manner proportional to the age of the mother plant (**Figure 7.3B**, **Figure 7.3D**). These results closely match those previously obtained for *A. thaliana*, where the number of seeds per fruit is maximum at the middle of the

inflorescence, and seed area consistently decreases with plant age (see Chapter 6). The only notable difference was observed for *C. bursa-pastoris*, which shows a distinctly high fertility in the fruits from the bottom-most part of the inflorescence, which had the maximum number of seeds (**Figure 7.3C**). This suggests that *C. bursa-pastoris* invests a greater proportion of resources in the fruits that are produced first, possibly as a consequence of selective pressures to which *A. thaliana* and *O. pumila* may not have been exposed. In any case, the bell-shaped effect of parental age on seed number is still seen for fruits produced later, i.e., from deciles 4 onwards, suggesting that parental age impacts offspring production similarly in different species of the Brassicaceae family.

7.3.4. Spikelet Removal Increases Productivity in Wheat

Wheat inflorescences, i.e., spikelets, are assembled in spikes, the development of which is characterized by two key transitions at the meristematic level, i.e., the conversion of the spike meristem into a terminal spikelet meristem (SM) (Caselli et al., 2020; Kirby and Appleyard, 1984) and, subsequently, the arrest of the SM at the spikelet level (Bonnett, 1936; Sadras and Slafer, 2012). Similarly to inflorescence meristems (IM) of *A. thaliana*, SMs are indeterminate and, after arrest, they are surrounded by a cluster of rudimentary floral primordia (Hensel et al., 1994; Kirby and Appleyard, 1984). Based on these similarities, it was hypothesized that spikelet arrest in wheat could be analogous to inflorescence arrest in *A. thaliana* and, ultimately, that it would be controlled by similar regulatory mechanisms.

One of the firstly identified elements controlling inflorescence arrest was the presence of developing fruits, and surgically removing fruits from inflorescences of *A. thaliana* has been proved to extend inflorescence duration in several occasions (Balanzà et al., 2018; Hensel et al., 1994; Ware et al., 2020). Thus, it was questioned

whether developing reproductive structures also promote arrest in wheat. To test this, *cv.* Mulika wheat plants were grown in standard conditions (22ºC, 16-h day length) and, prior to flowering, they were assigned to three different treatment groups. One was left untreated, another was subjected to the surgical removal of 2-3 spikelets from the main spike and the last served as an experimental control, where a surgical cut was made in the shoot to expose the main spike, but no spikelets were removed (see Chapter 2). At the end of the experiment, spike length, the number of spikelets per spike and the number of florets per spikelet were recorded for each treatment group.

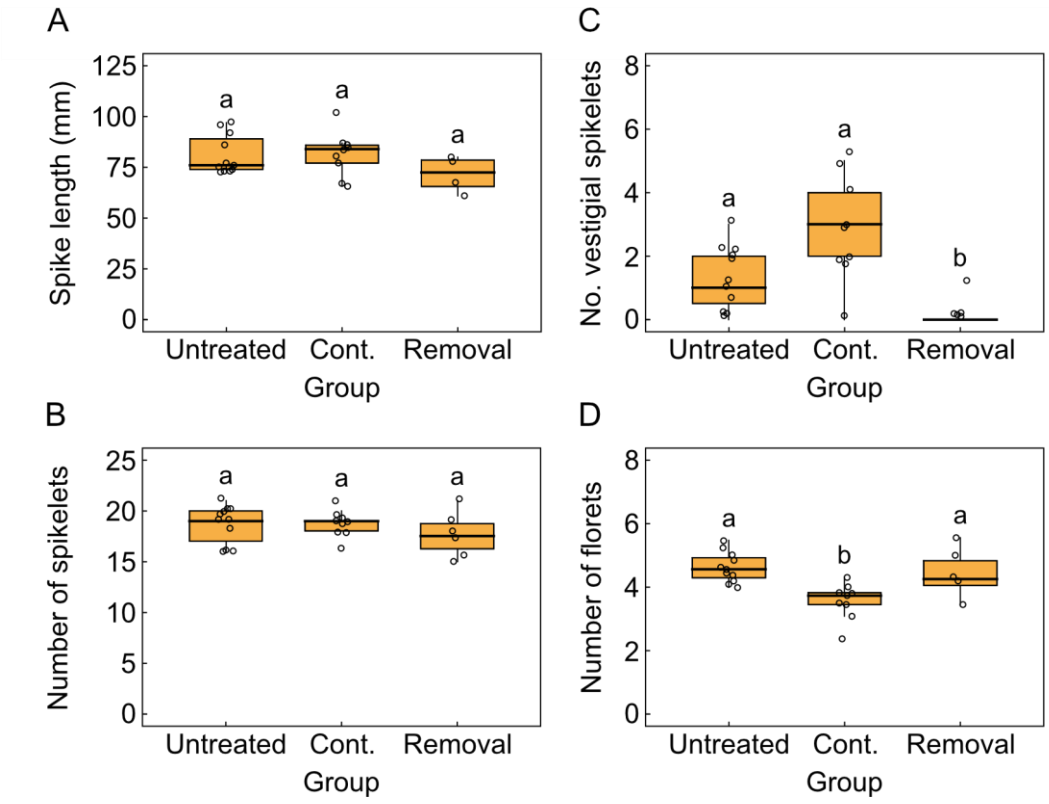

Figure 7.4. Spikelet removal impacts arrest of the surviving spikelets

Average spike length (**A**), number of initiated spikelets per spike (**B**) number of vestigial spikelets per spike (**C**) and number of florets per spikelet (**D**) in plants from different treatment groups (N=6-9). The treatment was either a surgical cut in the main tiller ('control'), a surgical removal of 2-3 spikelets per spike ('removal'). Different letters indicate statistical differences between conditions (for A-B: Kruskal-Wallis rank sum test, pairwise Wilcoxon test with Benjamini and Hochberg correction, $P<0.05$; for D: ANOVA, Tukey HSD test, $P<0.05$).

Neither spike length (**Figure 7.4A**) nor the number of initiated spikelets per spike (**Figure 7.4B**) were affected by the spikelet removal, which was expected as the spike meristem had already differentiated into a terminal spikelet at the time of treatment. However, visible differences were observed between the spikelets produced by treated and untreated plants, particularly at the bottom of the spike. In wheat, basal spikelets are typically vestigial and tend not to produce fertile florets (Backhaus et al., 2023). Strikingly, almost none of the spikelets from treated plants were vestigial (**Figure 7.4C**), suggesting that removal of some spikelets increases the productivity of the remaining ones. In accordance with this, compared to untreated plants, the average number of florets per spikelet was significantly lower in control spikes but not in treated ones (**Figure 7.4D**). Altogether, these results demonstrate that removal of developing spikelets increases the productivity of the remaining ones. It is possible that this is due to a delay in SM arrest, which would result in more florets being initiated in the surviving spikelets. Nonetheless, an alternative explanation is that spikelet removal improves floret survival in the remaining spikelets without affecting SM arrest.

7.3.5. Arrest in Wheat is Controlled by Environmental Signals

While the environmental regulation of reproductive development has been extensively studied at the spike level, spikelet and floret development have been less investigated. As both spike and spikelet arrest possibly contribute to end-of-flowering in wheat, a series of experiments were designed to test the effect of different environmental signals on them. First, *T. aestivum cv*. Cadenza plants were grown in either standard conditions (20ºC, 16-h day length), at a cold temperature (15ºC, 16-h day length) or on low nutrients, i.e., in a 1:1 (v/v) mixture of compost and sand. At the end of the experiment, mature spikes were harvested and phenotyped.

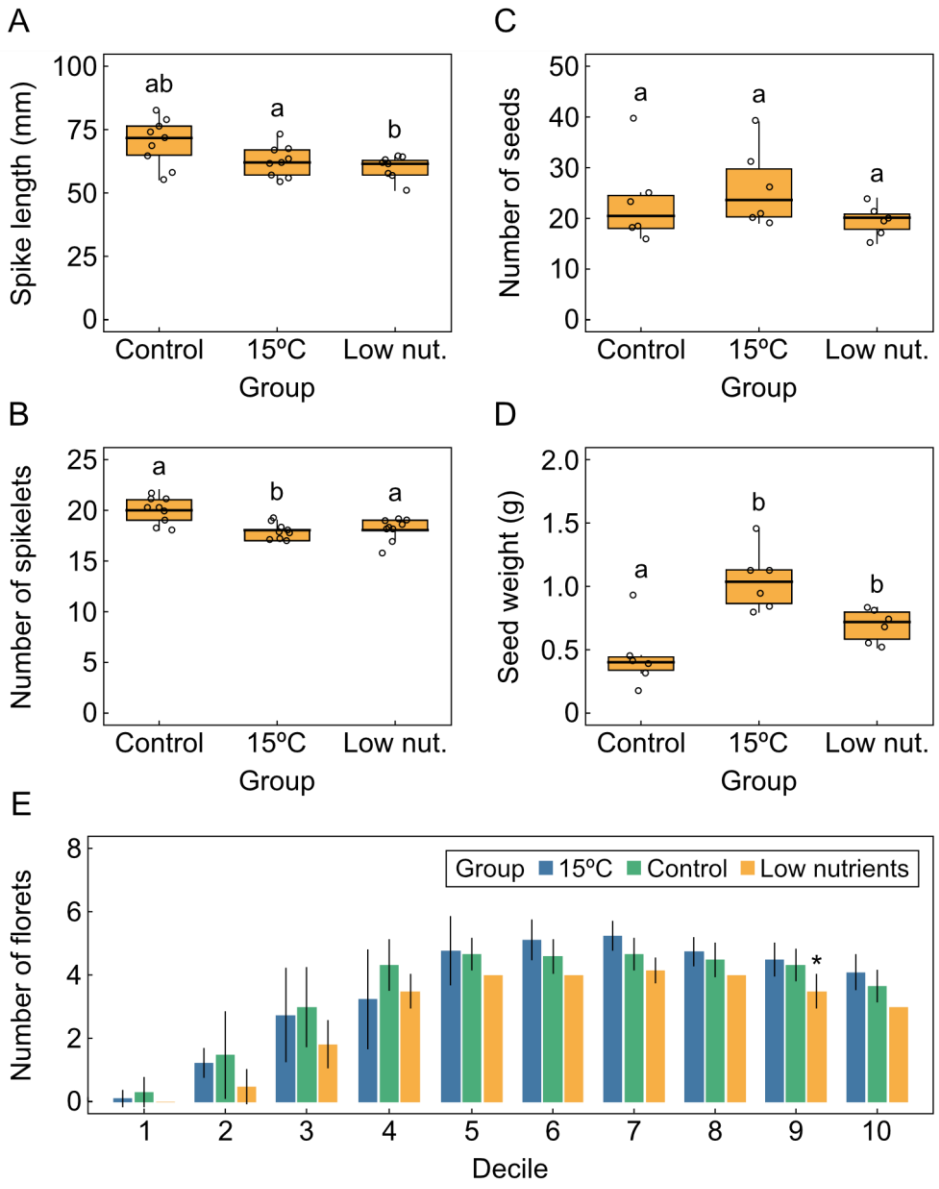

Figure 7.5. Temperature and nutrient supply control spike and spikelet arrest

A-D. Average spike length (**A**), number of spikelets per spike (**B**) number of seeds per spike (**C**) and seed weight per spike (**D**) in plants grown in control conditions, at 15ºC or in low nutrients (N=9). Different letters indicate statistical differences (for A and C-D: ANOVA, Tukey HSD test, $P<0.05$; for B: Kruskal-Wallis rank sum test, pairwise Wilcoxon test with Benjamini and Hochberg correction, $P<0.05$). **E.** Number of florets per spikelet at different positions across the spike in plants grown in control conditions, at 15ºC or in low nutrients (N=3). Positions are classified into deciles such that decile 1 corresponds to the bottom-most spikelets and 10, to the top-most spikelets. Asterisks indicate statistical differences against the control for each decile (ANOVA, Tukey HSD test, $P<0.05$).

Spike length (**Figure 7.5A**) and the number of spikelets per spike (**Figure 7.5B**) were slightly reduced in the cold and in low nutrients. This is not surprising as both temperature and nutrient availability are known to impact the number of spikelets in a similar manner in other wheat cultivars (Halse and Weir, 1974; Nerson et al., 1990; Slafer and Rawson, 1994). While the differences in spikelet number did not translate into different grain numbers (**Figure 7.5C**), seeds were significantly heavier in both cold temperatures and low nutrients (**Figure 7.5D**). Altogether, these observations suggest that both temperature and nutrient availability control arrest at the spike level, ultimately affecting the number of initiated spikelets but without any clear impact on the number of produced seeds.

To assess the effect of these environmental signals on spikelet arrest, individual spikelets were recovered from the mature spikes and used to record the number of surviving florets per spikelet. As there are large differences in the number of florets along the spike (Bonnett, 1966), this was done for different spikelet positions from the bottom to the top of the spike. Albeit not statistically significant, the number of florets per spikelet was consistently higher in plants exposed to cold temperatures and lower in plants exposed to low nutrients (**Figure 7.5E**). Interestingly, this resembles the effect of the same cues in species from the Brassicaceae family (see Chapter 3 and **Figure 7.2**), supporting the idea that spikelet arrest may be regulated in a manner similar to inflorescence arrest in *A. thaliana*.

The effect of day length on both spike and spikelet arrest was assessed in a separate experiment, where plants were grown in standard conditions (22ºC, 16-h day length). Apices from the main tiller were dissected every 3 days and, upon detection of floral transition (i.e., at the double ridge stage, when the vegetative meristem is converted into a spike meristem), a subset of plants were transferred to an 8-h day length. At the end of the experiment, mature spikes were collected and the number of spikelets per spike and florets per spikelet, recorded. At the spike level,

plants grown under longer day lengths unexpectedly produced a greater number of spikelets (**Figure 7.6A**). In photoperiod-sensitive wheat cultivars such as *cv.* Cadenza, shorter day lengths delay the formation of the terminal spikelet, extending the spike meristem lifespan (Stefany, 1993) and typically leading to a greater number of spikelets (Rahman and Wilson, 1978; Rawson, 1971). While the timing of terminal spikelet formation was not appropriately recorded for this experiment, dissection of the apices at various points after the transfer confirmed that terminal spikelets were produced later in the shorter day lengths (data not shown). Thus, the reduction in spikelets under the 8-h day length is likely not caused by a shorter spike duration but rather by a slower rate of SM initiation, possibly caused by the sudden reduction in light exposure in transferred plants.

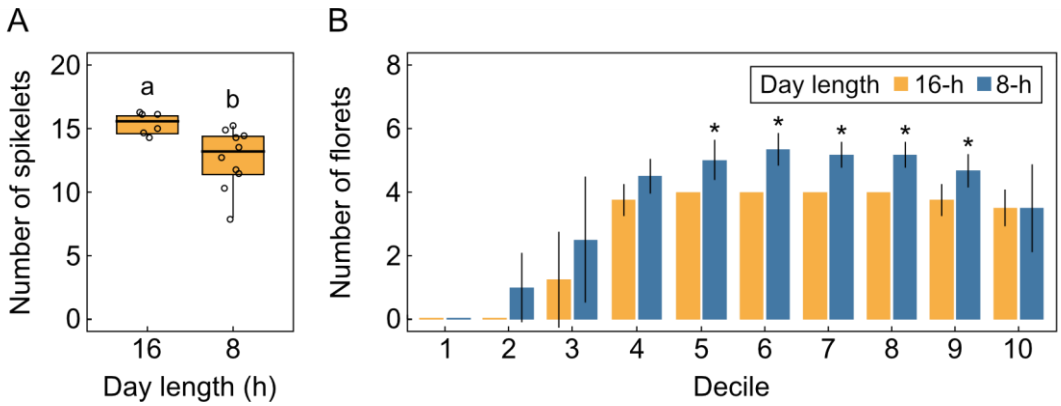

Figure 7.6. Day length controls spike and spikelet arrest

A. Number of spikelets per spike in plants grown under 8 or 16 h of light per day (N=6-10). Different letters indicate statistical differences between conditions (Student's t test, P<0.05). **B.** Number of florets per spikelet at different positions across the spike in plants grown under 8 or 16 h of light per day (N=3). Positions are classified into deciles such that decile 1 corresponds to the bottom-most spikelets and 10, to the top-most spikelets. Asterisks indicate statistical differences between conditions for each decile (Student's t test, P<0.05).

At the spikelet level, a shorter day length consistently increased the number of florets for most spikelet positions (**Figure 7.6B**). This is in accordance with previous reports that day length affects the duration of floret development, which can maximize floret survival (Basavaraddi et al., 2021; Serrago et al., 2008). The greater number of surviving florets per spikelet observed here could be due to either an extended SM lifespan, potentially leading to a greater number of initiated florets, or a higher survival of florets without changes in the number of initiated primordia. The former would resemble responses previously described for *A. thaliana*, where short days delay the timing of IM arrest (see Chapter 3), although further work would be required to better understand at what level day length controls spikelet development.

As nutrient availability regulates arrest at the spikelet (**Figure 7.5E**) and, to a lesser extent, at the spike (**Figure 7.5B**) levels; and given that that nitrogen (N) is a key regulator of arrest in *A. thaliana* (see Chapter 3), a last experiment was designed to test the effect of N supply on both spike and spikelet arrest in wheat. Plants were grown in nutrient-free substrate, i.e., a 1:1 (v/v) mixture of vermiculite and sand, and weekly supplied with either standard or NO_3^-limiting growth media until spikes were produced and fully matured, at which point spikelets and florets were counted. N supply had a clear effect on the number of spikelets per spike, with NO_3^--limited plants producing less spikelets (**Figure 7.7A**). Previously, N limitation has been shown to reduce the rate of SM initiation and the number of spikelets (Longnecker et al., 1993; Whingwiri and Kemp, 1980), which is in accordance with the data presented here. Additionally, plants grown with a low N supply showed a clear reduction in the number of florets per spikelet for all spikelet positions (**Figure 7.7B**), suggesting that N limitation also affects spikelet arrest and/or floret survival. Field experiments with durum wheat (*T. durum*) demonstrate that low N availability can both accelerate arrest of the SM and increase floret death (Ferrante et al., 2013). Hence, it is very likely that N supply also affects spikelet development at both the SM and floret levels in *T. aestivum*.

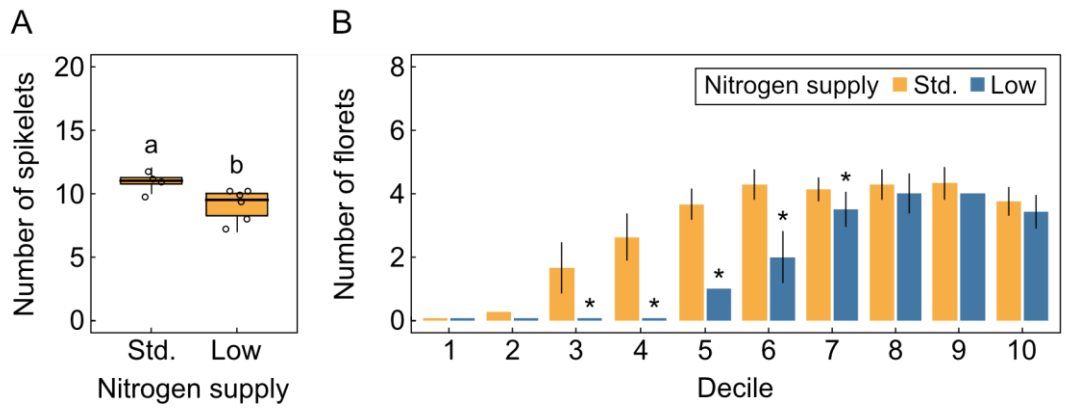

Figure 7.7. Nitrogen availability controls spike and spikelet arrest

A. Number of spikelets per spike in plants grown on standard or low nitrogen supply (N=4-6). Different letters indicate statistical differences between conditions (Student's t test, P<0.05). **B.** Number of florets per spikelet at different positions across the spike in plants grown on standard or low nitrogen supply (N=6). Positions are classified into deciles such that decile 1 corresponds to the bottom-most spikelets and 10, to the top-most spikelets. Asterisks indicate statistical differences between conditions for each decile (Student's t test, P<0.05).

Taken together, these results demonstrate that spikelet and floret production are environmentally regulated in *T. aestivum*, likely through an environmental control over both spike and spikelet arrest. At the spikelet level, developmental responses to the environment are similar to those previously described for *A. thaliana* (see Chapter 3), with flowering-promotive signals such as warmer temperatures, higher nutrient availabilities and longer day lengths reducing the number of florets, either through an acceleration of SM arrest or a reduction in floret death.

7.3.6. Natural Variation of End-of-flowering in Wheat

Modern cultivated wheat corresponds to elite cultivars which are the result of years of breeding, a process that has led to the loss of substantial genetic variety (Cseh et al., 2021). In contrast, wheat landraces present a source of rich genetic

variability which is key for better understanding the genetic basis of biologically relevant processes (Cseh et al., 2021; Frankin et al., 2020), including end-of-flowering. Taking this into account, a set of 37 different wheat landraces were screened for differences in either the number of spikelets per spike, as a proxy for spike arrest, or the number of florets per middle spikelet, as a proxy for spikelet arrest. To do this, plants were grown in standard conditions (22ºC, 16-h day length) until flowering and, once spikes were fully matured, they were harvested and phenotyped.

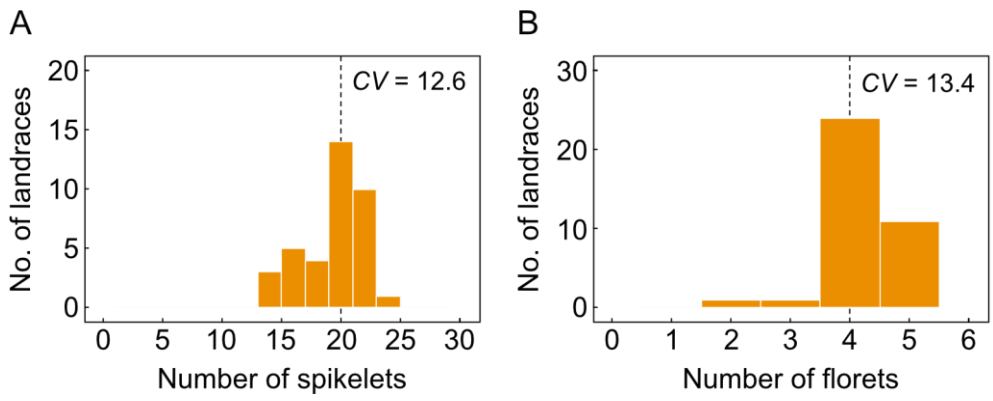

Figure 7.8. Variation in spikelet and floret number among wheat landraces

A-B. Histograms depicting the distribution of the number of spikelets per spike (**A**) and number of florets per middle spikelet (**B**) in 37 wheat landraces (N=3). The coefficient of variation (CV) of the trait is indicated in each graph. The dashed line indicates the average for the reference accession Cadenza.

Both the number of spikelets and florets showed differences among landraces, although the variability was relatively low for both traits (**Figure 7.8**). This was particularly evident in the latter, with almost all landraces showing either 4 or 5 florets per spikelet (**Figure 7.8B**). While wheat typically only maintains 1-4 florets per spikelet (Fischer, 1984), the lack of variability in this set of landraces suggests that floret survival is under strong genetic control. Thus, it is possible that although differences may exist in spikelet duration and SM arrest between different landraces, they could be masked by the highly conserved patterns of floret death. Ultimately,

future research may benefit from tracking the dynamics of floret initiation and death over time by dissecting spikelets in a time-course manner, which would reveal differences in SM duration among different wheat genotypes.

As previously mentioned, spikelets from different positions along the spike show differences in the number of surviving florets (Bonnett, 1966). Particularly, basal spikelets tend to be vestigial with no fertile florets, which causes a dramatic loss of reproductive potential (Backhaus et al., 2023). To account for these spatial differences in spikelet productivity, the number of surviving florets was recorded for different spikelet positions in the panel of 37 wheat landraces. Interestingly, despite the middle spikelets producing a similar number of florets regardless of the genotype (**Figure 7.8B**), more phenotypic differences were noted among the landraces when assessing other spikelet positions (**Figure 7.9**). All spikes presented a lanceolate morphology, with less florets per spikelet at the bottom and top, which is typical of wheat spikes. However, for ~25% of the landraces, e.g., 016 and 046, a higher proportion of spikelets from the bottom part of the spike were vestigial, with no surviving florets. Concurrently, the decrease in productivity that is usually seen in the top-most spikelet positions was less pronounced or absent in these landraces, which is not surprising as trade-offs are known to exist between different yield components in wheat (Reynolds et al., 2009). The lower number of florets in the basal spikelets could be due to a reduced initiation of floral meristems at these positions or, more likely, to a higher rate of floret abortion, which has been previously linked to the loss of potential in vestigial spikelets (Backhaus et al., 2023). In any case, the results presented here demonstrate that there is natural variation in spike morphology among wheat landraces, particularly when considering spikelet productivity at different positions.

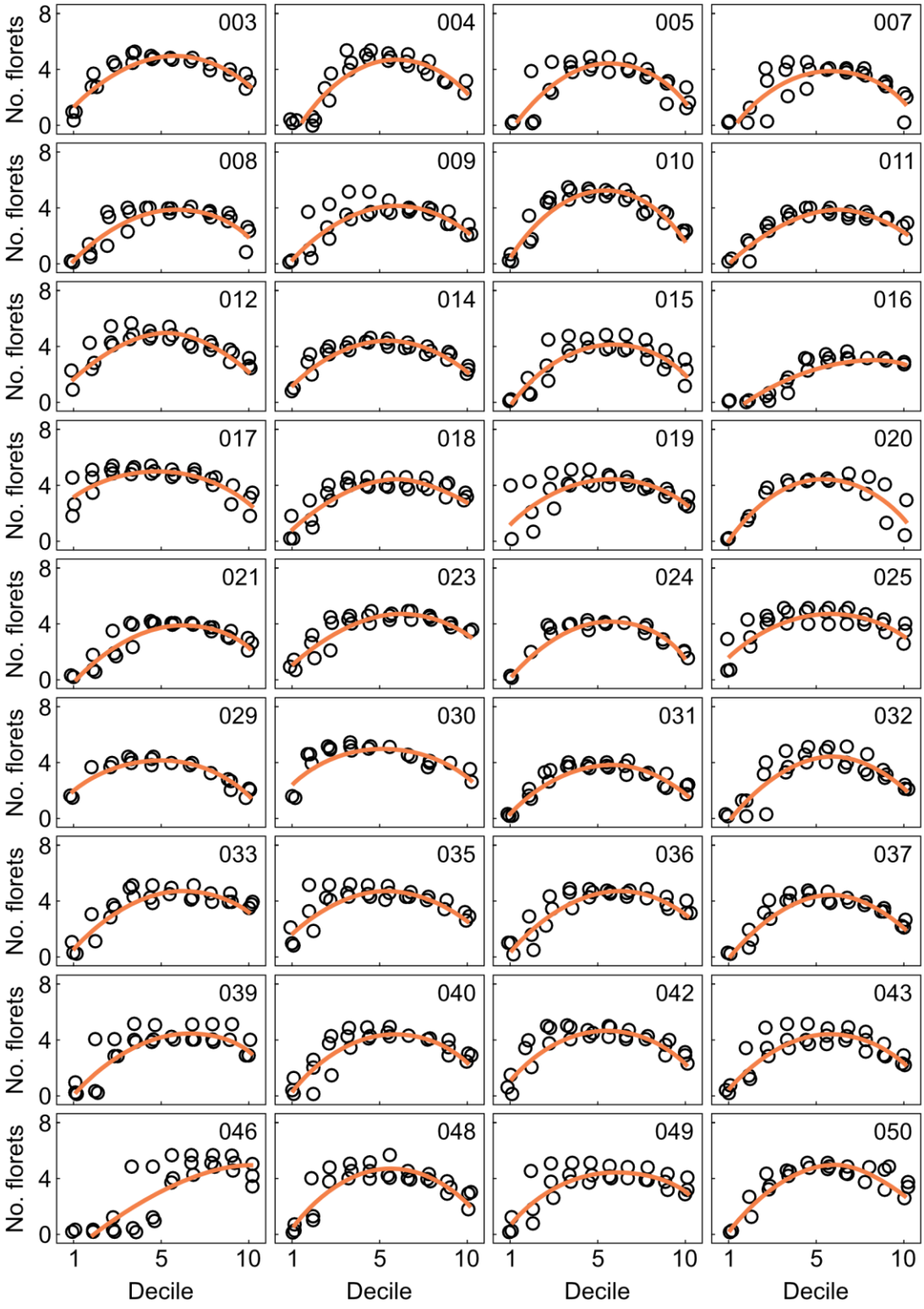

Figure 7.9. Spatial distribution of florets across the spike in wheat landraces

Number of florets per spikelet at different positions across the spike in 37 wheat landraces (N=3). Positions are classified into deciles such that decile 1 corresponds to the bottom-most spikelets and 10, to the top-most spikelets. The orange line represents the best fit for a linear quadratic model.

7.3.7. Natural Variation of Spikelet Meristem Arrest in Wheat

Previously, very little variation was observed in the number of florets per spikelet among wheat landraces (**Figure 7.8B**), but it was unclear whether differences exist in the timing of SM arrest as these could be masked by a highly conserved pattern of floret death. It was hypothesized that SM duration shows natural variation in wheat and two different landraces, i.e., 004 and 023, were used in an experiment aimed to test this. The genotypes were chosen based on their differences in the number of surviving florets for spikelets from different positions along the spike. While 004 produces spikes with a more lanceolate morphology, spikelets from 023 are more similar to each other, with very little differences in floret number between the middle at the top (**Figure 7.9**). Plants from both genotypes were grown in standard conditions (22ºC, 16-h day length) and the apex of their main stem was sampled every 5-10 days. At each sampling, the number of initiated florets was counted for spikelets from different positions along the spike, i.e., bottom, middle and top; and, at the end of the experiment, the final number of spikelets and florets per spikelet were also recorded.

Both the number of spikelets (**Figure 7.10A**) and florets (**Figure 7.10B**) confirmed the previous observations that neither of these traits show substantial differences between the two landraces, and that spikelet productivity is affected by the position in the spike in a distinct manner for each genotype. For all spikelet positions, floret initiation began earlier in 004, but the SM was active for ~5 days longer when compared to 023 (**Figure 7.10C**). With the exception of SMs from the middle spikelets, the total number of initiated florets was comparable between the two landraces, suggesting that SMs from 023, despite exhibiting a shorter lifespan, initiate florets at a higher rate. Floret death also showed differences depending on both the genotype and spikelet position. Altogether, these results demonstrate that there are differences between landraces in SM arrest and activity, as well as in floret

survival. Not only does this show that natural variation exists at the end-of-flowering level in wheat but also it prompts to exploit the genetic diversity present in landraces to pinpoint the underlying genetic regulation of these processes. As the final number of fertile florets produced in wheat spikes likely depends on both SM arrest and floret death, future research would highly benefit from implementing an approach that would allow for the characterization of both, such as the one presented here.

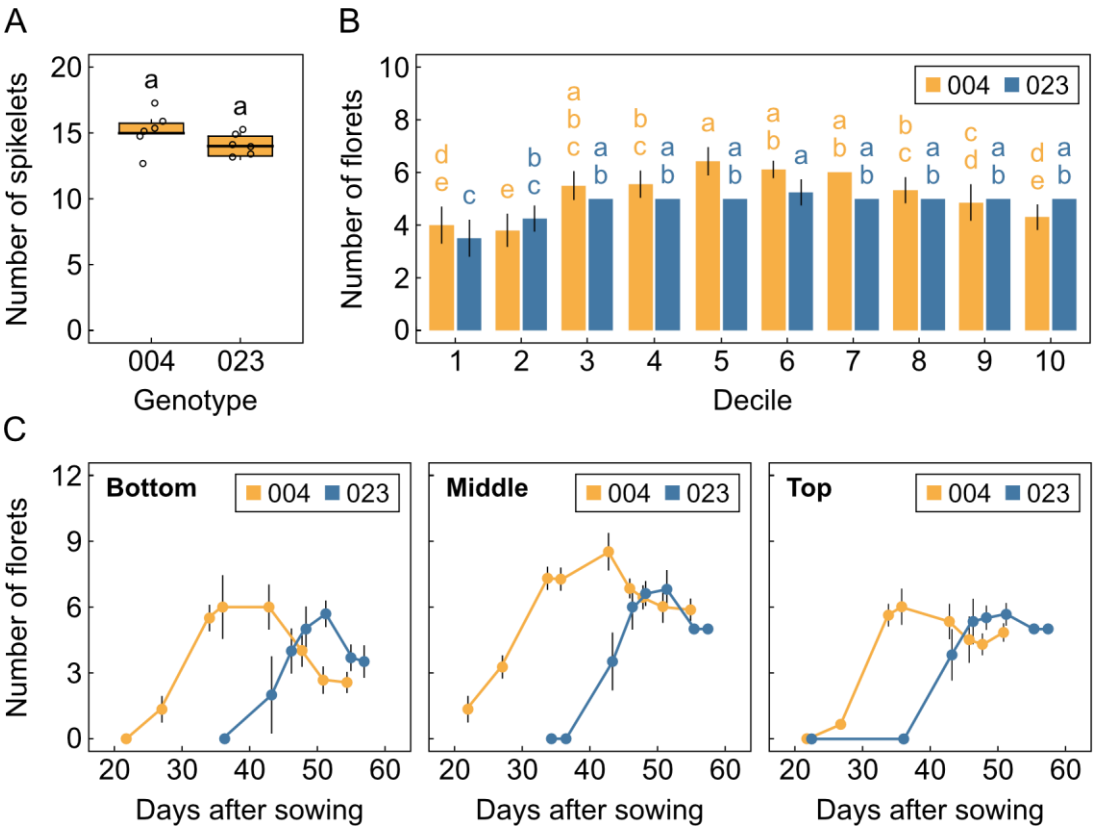

Figure 7.10. Spikelet duration shows variation among wheat landraces

A. Number of spikelets per spike in plants from the 004 and 023 genotypes (N=6). Different letters indicate statistical differences between conditions (Student's t test, P<0.05). **B.** Number of florets per spikelet at different positions across the spike in 004 and 023 plants (N=3). Positions are classified into deciles such that decile 1 corresponds to the bottom-most spikelets and 10, to the top-most spikelets. Different letters indicate statistical differences between deciles for each temperature (ANOVA, Tukey HSD test, P<0.05). **C.** Cumulative number of florets per spikelet at different time points after sowing in spikelets from three different positions (N=3). Bottom, middle and top correspond to the first, fifth and tenth decile, respectively.

7.4. Conclusions

Throughout this chapter, different species have been used in an attempt to shed some light into the conservation of the end-of-flowering in the plant kingdom. The results presented here strongly suggest that inflorescence arrest is conserved in the Brassicaceae family, to which *A. thaliana* belongs. Other annual Brassicaceae species, such as *O. pumila* and *C. rubella*, produce inflorescences that arrest with a terminal cluster of undeveloped floral primordia, a process that is also controlled by environmental cues, including temperature and nutrient availability.

In hexaploid wheat (*T. aestivum*), a member of the Poaceae family, end-of-flowering is brought about by two sequential processes: first, the arrest of the spike, which terminates the production of spikelets; and lastly, the arrest of individual spikelets, which terminates the production of florets. While both are environmentally controlled, spikelet arrest is morphologically and developmentally more similar to inflorescence arrest from *A. thaliana*, suggesting that these could be analogous processes. In accordance, spikelet productivity is also negatively impacted by flowering-promotive signals and the development of other reproductive structures. However, the study of spikelet arrest is challenged by the subsequent death of initiated florets, which can mask the effect of arrest on the number of surviving florets. This, clearly demonstrated by the data shown here, evidences the need for alternative approaches that allow for the combined characterization of both. The molecular signals controlling spikelet arrest are still largely unknown, but the results presented here demonstrate that the genetic diversity present in wheat landraces could be exploited to identify the genetic regulation of these processes.

A key question arising from research concerns the genetic regulation of arrest in species other than *A. thaliana*. Knowing that inflorescence arrest is a common process within the Brassicaceae family, it would be interesting to explore its genetic control and, particularly, to assess whether known regulators of arrest such as *FT* or

FUL are functionally conserved during end-of-flowering in this plant family. In the case of wheat, facing these questions would require an extensive molecular investigation, especially considering that some of these genes have undergone multiple duplications (Bennett and Dixon, 2021). Thus, future research would benefit from a deeper analysis of the processes of spikelet termination and floret abortion in wheat broadly at a molecular level. For instance, using the approaches described towards the end of the chapter to characterize spikelet arrest in a wider range of wheat landraces may help reveal QTLs that underlie the timing of arrest in wheat.

Chapter 8: General Discussion

8.1. Inflorescence Meristem (IM) Arrest is Regulated by Environmental Signals in *A. thaliana*

As a monocarpic species, *A. thaliana* experiences a single reproductive event throughout its life cycle (Thomas, 2013). This begins with floral transition, i.e., the conversion of the vegetative meristem into an inflorescence meristem (IM), and ends with inflorescence arrest, a process characterized by the interruption of both the IM's proliferative activity as well as the development of the youngest floral primordia (González-Suárez et al., 2020; Hensel et al., 1994). Although previously understudied, research into the end-of-flowering has gained traction in the last decade, resulting in a good understanding of its genetic and hormonal regulation (Balanzà et al., 2023). In contrast, the effect of the environment on this developmental transition has been largely overlooked, despite the key role of environmental signals in controlling the onset of flowering.

The data presented throughout this thesis unequivocally demonstrates that the timing of inflorescence arrest is tightly controlled by the environment. Environmental signals that impact flowering in *A. thaliana* also affected inflorescence arrest, including temperature (**Figure 3.1**), vernalization (**Figure 3.3**), day length (**Figure 3.5**) and nutrient availability (**Figure 3.8**, **Figure 3.10**, **Figure 3.11**). Interestingly, environmental conditions that are classically known as flowering-promotive accelerated the timing of inflorescence arrest, particularly warm temperatures (Blázquez et al., 2003) and long day lengths (Melzer et al., 2008). Vernalization, i.e., the exposure to a long span of cold, only affected inflorescence duration in winter accessions of *A. thaliana* (**Figure 3.3**), suggesting that meeting the

vernalization requirement in these genotypes not only accelerates floral transition (Lempe et al., 2005) but also arrest. In the rapid-cycling accession Col-0, which is insensitive to vernalization, environmental experience during flowering seemed to be the main driver of inflorescence arrest, with little effect of the temperature and/or day length experienced during the vegetative phase (**Figure 3.2**, **Figure 3.5**). Nutrient availability also had a clear impact on inflorescence duration (**Figure 3.8**, **Figure 3.10**, **Figure 3.11**). Nutrient-limiting conditions, which are known to promote floral transition (Pigliucci and Schlichting, 1995; Vidal et al., 2014), accelerated the timing of inflorescence arrest (**Figure 3.8**), and this seemed to be at least partially attributable to the availability of nitrogen (N) (**Figure 3.10**). In contrast, environmental cues with less clear roles in the control of flowering time, such as light intensity (**Figure 3.4**), water availability (**Figure 3.9**) or the identity of neighbouring plants (**Figure 3.11**) did not show any effect on the timing of inflorescence arrest. Taken together, these results demonstrate that environmental signals affect floral transition and inflorescence arrest in a similar manner, and suggest that the regulation of these processes may be tightly linked (**Figure 8.1**).

The environmental control of inflorescence arrest takes places at the IM level. Accordingly, warm temperatures (**Figure 3.6**), long days (**Figure 3.6**) and low N supply (**Figure 3.10**) shortened inflorescence duration by accelerating IM arrest. Furthermore, an active IM was necessary for the response to many environmental cues during the end-of-flowering (**Figure 3.7**). During flowering, the IM is known to gradually decrease in size (Walker et al., 2023; Wang et al., 2020), a phenomenon that has been associated with arrest at the cellular level (Merelo et al., 2022). Here, IM size has also been shown to decline faster under arrest-promoting signals (**Figure 3.6**), suggesting that they may control arrest by acting upstream of the molecular processes that underlie the mitotic inactivation of stem cells (Merelo et al., 2022; Wuest et al., 2016).

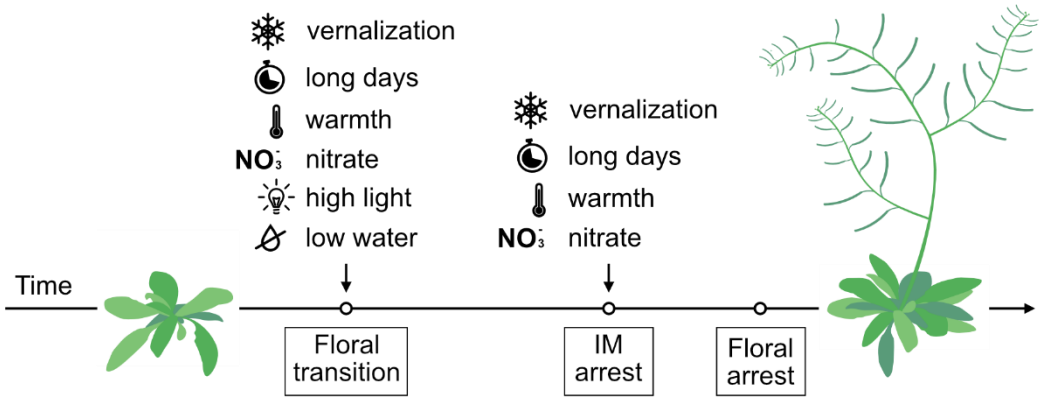

Figure 8.1. Environmental signals control both floral transition and arrest

Diagram depicting the relevant developmental milestones during the reproductive phase of *A. thaliana* (bottom) and the effect of environmental stimuli on them (top). Arrows indicate promotive effects.

8.2. Environmental Control of IM Arrest is Regulated at the Genetic Level

Prior to flowering, up to seven molecular pathways control the perception of environmental and endogenous inputs, and their impact on the timing of floral transition (Quiroz et al., 2021; Song et al., 2015; Srikanth and Schmid, 2011). Two of these participate in the regulation of flowering by temperature, i.e., the ambient temperature pathway (Capovilla et al., 2015) and the vernalization pathway (Kim and Sung, 2014); and a third mediates the regulation by day length, i.e., the photoperiod pathway (Song et al., 2015; Srikanth and Schmid, 2011). Interestingly, many of the components implicated in these pathways are necessary for timely inflorescence arrest (**Figure 4.2**), for the response to the environment during arrest (**Figure 4.3**), or for both (**Figure 4.2**, **Figure 4.5**); suggesting that floral transition and end-of-flowering are genetically controlled by similar processes.

Mutants disrupted in either *GIGANTEA* (*GI*) or *CONSTANS* (*CO*), which are key components of the photoperiod pathway, showed inflorescence durations longer than wild-type plants (**Figure 4.2**), suggesting that GI and CO are promoters of arrest.

Both of them are transcriptional activators of the floral integrator *FLOWERING LOCUS T* (*FT*) (Song et al., 2015; Srikanth and Schmid, 2011), which also promotes inflorescence arrest (**Figure 4.2**), suggesting that this process is FT-dependent. In accordance with this, other genes that participate in light signalling upstream of *FT*, such as *EARLY FLOWERING 4* (*ELF4*) (Zhao et al., 2021) and *PHYTOCHROME B* (*PHYB*) (Valverde et al., 2004), are also necessary for timely inflorescence arrest (**Figure 4.2**). As the expression of *CO* and, ultimately, *FT* is induced by long days (Turck et al., 2008), these results raised the possibility that the photoperiod pathway may mediate the previously described acceleration of IM arrest by long day lengths (**Figure 3.5**). However, this does not seem to be the case given that mutants lacking a functional copy of *FT* are still able to modulate inflorescence duration in response to day length (**Figure 4.5**). Thus, the photoperiod pathway probably controls the response to day length independently of FT, e.g., through direct transcriptional repression of *APETALA 2* (*AP2*) (Yu et al., 2023), a known activator of the meristem identity gene *WUSCHEL* (*WUS*), which is key for the maintenance of IMs (Balanzà et al., 2018; Wang et al., 2020).

The inflorescence duration of mutants impaired in genes from the thermosensory pathway, such as *FLOWERING LOCUS M* (*FLM*), *FLOWERING LOCUS C* (*FLC*) and *SHORT VEGETATIVE PHASE* (*SVP*), did not differ from wild-type plants in standard conditions (**Figure 4.2**). However, contrary to wild-type, none of the mutants accelerated arrest in response to warm temperature (**Figure 4.3**), suggesting that they mediate temperature control during end-of-flowering. Both FLM and FLC interact with SVP forming repressive complexes that down-regulate the expression of *FT*, a process that is temperature-sensitive (Capovilla et al., 2017, 2015; Lee et al., 2013). Given that inflorescence duration in mutans disrupted in *FT* did not respond to warm temperature either (**Figure 4.5**), it is likely that the thermosensory pathway mediates the acceleration of IM arrest by temperature (**Figure 3.5**) in an FT-dependent manner.

8.3. FT is a Central Regulator of IM Arrest

The photoperiod and thermosensory pathways, which underlie the control of flowering by day length and temperature, respectively, converge in the regulation of FT (Capovilla et al., 2015; Song et al., 2015), which has long been described as a central integrator of environmental signals during floral transition (Bratzel and Turck, 2015; Turck et al., 2008). Here, it has been demonstrated that FT continues to integrate environmental inputs after floral transition, and that this process is fundamental for timely inflorescence arrest and its response to the environment. Mutants disrupted in the *FT* locus exhibited a longer inflorescence duration when compared to wild-type independently of the genetic background (**Figure 4.2**, **Figure 4.4**), suggesting that FT promotes inflorescence arrest. Specifically, FT has been shown to induce arrest at the IM level (**Figure 4.4**) through a mechanism based on its transcriptional up-regulation during later stages of flowering (**Figure 4.6**, **Figure 4.7**). Not only is *FT* necessary for timely IM arrest but also for the response to warm temperatures during end-of-flowering (**Figure 4.5**), where it probably acts downstream of the thermosensory pathway, as previously suggested. Temperature is known to affect the expression of *FT* prior to flowering (Blázquez et al., 2003; Thines et al., 2014) and, here, it has been shown that this transcriptional regulation continues after floral transition in different tissues, including leaves (**Figure 4.8**) and developing fruits (**Figure 6.7**). This points towards a working model in which the transcriptional activation of *FT* under warm temperatures, mediated by the thermosensory pathway, accelerates IM arrest, leading to a shorter inflorescence duration and reduced fruit production.

FT is a phosphatidylethanolamine binding protein able to act as a transcriptional regulator by partnering with the transcription factor FD. During floral transition, the FT-FD complex induces the expression of floral identity genes such as *AP1* and *FUL* (Abe et al., 2005; Wigge et al., 2005). While the downstream targets of

FT during end-of-flowering still remain unknown, the transcriptomic profile of *ft-10* mutants presented here points towards promising candidates, including the cytokinin (CK) receptor *ARABIDOPSIS HISTIDINE KINASE 4* (*AHK4*) and several regulators of *WUS* (**Table 4.1**). Two homologs of *AHK4*, i.e., AHK2 and AHK3, have previously been implicated in the control of IM arrest (Bartrina et al., 2017), and IM arrest is characterized by a decline in CK signaling (Merelo et al., 2022; Walker et al., 2023). Thus, it is possible that FT triggers arrest by transcriptionally repressing *AHK4*, either directly, after complexing with FD, or indirectly. An alternative explanation is that FT affects the activity of the meristem regulator *WUS* by fine-tuning the expression of its upstream regulators, many of which fail to be up-regulated during IM arrest in *ft-10* mutants, e.g., *FANTASTIC FOUR 2* (*FAF2*) or *KNUCKLES* (*KNU*). A decline in *WUS* has been consistently associated with IM arrest, and is believed to underlie the mitotic arrest of stem cells (Balanzà et al., 2018; Goetz et al., 2021; Merelo et al., 2022; Wang et al., 2020). Therefore, it is likely that FT signaling converges in the regulation of WUS similarly to the age and CK pathways (Balanzà et al., 2018; Merelo et al., 2022). Although it is currently unclear how this may be achieved, the proposed target genes presented here offer interesting candidates for future research aiming to unravel the mechanism that controls IM arrest downstream of FT (**Figure 8.2**).

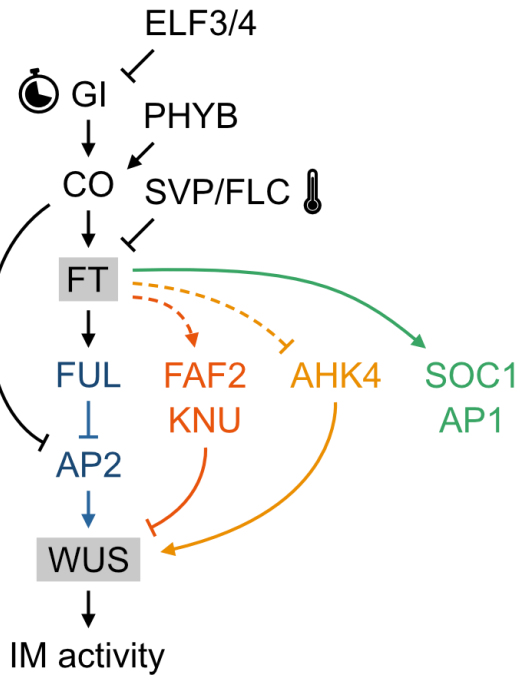

Figure 8.2. Proposed model for the environmental control of IM arrest

Diagram depicting the proposed model for the genetic network that underlies IM arrest responses to temperature and day length in *A. thaliana*. Day length and temperature can be perceived by the photoperiod and thermosensory pathways at the GI and SVP/FLC levels, respectively. Environmental cues are then integrated by FT or through FT-independent mechanisms, including the transcriptional regulation of AP2 by CO. FT can promote IM arrest through four main mechanisms, i.e., via the age pathway by promoting FUL (blue), by up-regulating upstream repressors of WUS (orange), in a CK-dependent manner by repressing the CK receptor AHK4 (yellow) or by directly upregulating floral identity genes (green). Arrows indicate transcriptional or post-transcriptional activation and blunt-ended arrows indicate repression.

8.4. Parental Age and Environmental Signals Jointly Control Offspring Production

Environmental conditions experienced by *A. thaliana* during flowering not only affected the timing of IM arrest but also the number of fruits produced (**Figure 3.1**, **Figure 3.4**, **Figure 3.8**, **Figure 3.10**, **Figure 3.11**). While this demonstrated that arrest has a clear impact on the reproductive output of plants, it was not clear whether

environmental signals specifically affected the production of seeds, a process that is known to be under the control of ageing (Dogra and Dani, 2019). In this thesis, a series of experiments were conducted to better understand the effect of both ageing and temperature on offspring production. Parental age has been shown to control both the quantity of seeds produced and their size independently of the genetic background (**Figure 6.1**). Seed number was maximal in fruits from the middle of the inflorescence and decreased in the top-most and bottom-most fruits, suggesting that fertility peaks mid-flowering, which is in accordance with previous reports (Dogra and Dani, 2019). On the other hand, seed size gradually decreased from the bottom to the top of the inflorescence in a manner proportional to the age of the parent. These phenomena are unlikely to depend on the processes of IM arrest and senescence, both of which begin at later stages in development (Wang et al., 2020). Instead, they may be controlled by the ageing pathway, which participates in the perception of age throughout the plant's life cycle (Cartolano et al., 2015; Wang, 2014). Furthermore, it is likely that the parental control of seed size and number operates similarly in other angiosperms, as the same age-dependent patterns were observed in two other species from the Brassicaceae family, *Capsella rubella* and *Olimarabidopsis pumila* (**Figure 7.3**). Interestingly, despite the clear impact of parental age on seed size, there was no significant effect of parental ageing on the performance or longevity of the future generation of plants (**Figure 6.2**). This observation adds to a growing body of literature which suggests that, in contrast to animals (Lansing, 1947; Monaghan et al., 2020; Noguera et al., 2018), parental age has little influence on offspring survival in plants (Barks and Laird, 2015; Pardos et al., 2022).

In addition to parental age, temperature clearly affected seed number and size, with higher temperatures negatively impacting both (**Figure 6.3**). Interestingly, the results presented here strongly suggest that temperature and parental age interact with one another during offspring production, and that this is, at least partially, mediated by FT (**Figure 6.5**, **Figure 6.6**). This is particularly true for the control of

seed size, which is both temperature-sensitive and FT-dependent. Whilst further work is required to determine the molecular basis of this process, it is likely that the integration of temperature and age takes place at fruit or seed levels (**Figure 6.4**). It is possible that this mechanism is based on the transcriptional regulation of *FT*, similarly to what has been described for IM arrest. Accordingly, *FT* expression in the fruits is up-regulated at higher temperatures (**Figure 6.7**). *TERMINAL FLOWER 1* (*TFL1*), a homolog of *FT*, has been shown to control seed size through a well-described molecular pathway (Zhang et al., 2020). Given that TFL1 and FT compete for the binding to the same target genes (Zhu et al., 2020), it is possible that FT synthesized in the seeds in a temperature-dependent manner controls seed size through the same route, although this remains to be tested.

8.5. Inflorescence Arrest Shows Variation Among Natural Accessions of *A. thaliana*

Most of the research on end-of-flowering in *A. thaliana* has been based on the commonly used laboratory accessions Col-0 and Ler (Balanzà et al., 2018; Hensel et al., 1994; Walker et al., 2023; Wang et al., 2020; Ware et al., 2020), with very little attention put into less common genotypes (Miryeganeh, 2020; Miryeganeh et al., 2018). Here, a screening of 69 natural accessions of *A. thaliana* has demonstrated that there is remarkable variability in several traits associated with the end-of-flowering, including inflorescence duration (**Figure 5.1**, **Figure 5.3**). Interestingly, there was not a clear association between the geographic origin of the accessions and their end-of-flowering phenotype, although most late-arresting genotypes were from areas that acted as refugia during the last glaciation (Sharbel et al., 2000) (**Figure 5.4**). This raises the possibility that a long inflorescence duration could be the ancestral phenotype, from which earlier-arresting phenotypes would

have evolved. However, assessing a wider range of genotypes may help validate this idea and shed more light into the evolution of the end-of-flowering.

The natural allelic diversity present among naturally-occurring populations of *A. thaliana* has been exploited before to better understand the genetic regulation of different biological processes, including flowering (Weigel, 2012). Knowing that there is natural variation in inflorescence arrest (**Figure 5.3**), the same approaches could be used to identify the underlying regulatory loci. To demonstrate this, a genome-wide association study (GWAS) has been conducted using the data for the number of fruits per primary inflorescence, although the results suggest that a greater number of accessions may be required before drawing any conclusions (**Figure 5.2**). Alternatively, quantitative trait loci (QTLs) responsible for the phenotype of late-arresting accessions such as Bå4-1 and Kondara could be mapped using recombinant inbred lines (RILs), a suitable approach for the study of quantitative traits. Crosses between Col-0 and Bå4-1, as well as between Col-0 and Kondara have been developed and characterized here as a first step towards this end (**Figure 5.5**, **Figure 5.6**, **Figure 5.7**). Additionally, genomic and transcriptomic analyses carried out in the late-arresting accession Kondara led to the identification of candidate genes for the regulation of IM arrest (**Table 5.3**, **Table 5.4**). Many of these showed expression profiles similar to *ft-10* mutants during end-of-flowering (**Figure 5.10**), suggesting that common molecular mechanisms may underlie late IM arrest in both of these genotypes.

8.6. Environmental Control of Inflorescence Arrest is Conserved in the Plant Kingdom

Despite recent advances in the study of arrest in *A. thaliana*, the developmental processes underlying end-of-flowering in other species have been, for the most part, unexplored. Here, it has been demonstrated that inflorescence

arrest is conserved in the Brassicaceae family, with species such as *O. pumila* and *C. rubella* showing arrest phenotypes similar to *A. thaliana* (**Figure 7.1**). Inflorescences from another perennial from the Brassicaceae, *Arabis alpina*, are known to arrest in a similar manner (Vayssières et al., 2020), suggesting that processes that underlie IM arrest and floral arrest are common among Brassicaceae species, whether annual or perennial. Moreover, inflorescence arrest has been shown to be environmentally-controlled in other Brassicaceae species similarly to *A. thaliana*, with warm temperature accelerating arrest and low nutrient availability affecting the number of fruits produced per inflorescence (**Figure 7.2**). In both *O. pumila* and *C. rubella*, an increase in temperature also accelerates floral transition (Choi et al., 2019; Hoffmann et al., 2010), suggesting that the dual role of temperature as a promoter of both the onset and the end of flowering is also conserved among members of the Brassicaceae.

These findings shed light on the regulation of arrest in indeterminate inflorescences, in which the IM remains undifferentiated throughout the plant's lifetime (Ratcliffe et al., 1998; Weberling, 1992). However, end-of-flowering in species with determinate inflorescences, which includes many crops (Benlloch et al., 2007; Caselli et al., 2020), is much less understood. In this context, hexaploid wheat (*Triticum aestivum*) offers an excellent biological system for the study of end-of-flowering, as its reproductive arrest is characterized by at least three distinct developmental milestones. First, the spike meristem, which produces spikelet meristems (SMs), differentiates into a terminal spikelet (Caselli et al., 2020; Kirby and Appleyard, 1984). Later, the SMs, which initiate floret primordia, arrest in a manner that is reminiscent of IM arrest in *A. thaliana* (Bonnett, 1936; Sadras and Slafer, 2012). Finally, after arrest of the SM, several floret primordia interrupt their development and degenerate through a process based on cellular autophagy (Fischer, 1984; Glick et al., 2010), which resembles floral arrest in *A. thaliana* (Hensel et al., 1994). The results presented in this thesis strongly suggest that SM arrest in

T. aestivum is analogous to IM arrest. Accordingly, the production of florets is sensitive to the development of other reproductive structures (**Figure 7.4**) and environmental signals. Specifically, warm temperature (**Figure 7.5**), low nutrient availability (**Figure 7.5**, **Figure 7.7**) and long days (**Figure 7.6**), all of which regulate spike development in wheat (Basavaraddi et al., 2021; Halse and Weir, 1974; Nerson et al., 1990; Serrago et al., 2008; Slafer and Rawson, 1994), negatively impacted the number of florets per spikelet.

These observations demonstrate that environmental signals control spikelet arrest and raise the possibility that they do so by fine-tuning the lifespan of the SM, similarly to the regulation of IM in *A. thaliana*. However, the study of SM arrest in *T. aestivum* presents several challenges. Differently to species from the Brassicaceae, most of the reproductive development in *T. aestivum* occurs before the emergence of the inflorescences, which hinders phenotyping of plants. In addition, the final number of florets is a trait under strong genetic control (**Figure 7.8**), which suggests that it is not a good indicator of SM duration. Nevertheless, a pilot experiment carried out here clearly demonstrates that there is variation in SM duration among different wheat landraces (**Figure 7.10**), even though these present a similar final number of surviving florets (**Figure 7.9**). Similarly to natural accessions of *A. thaliana*, landraces of *T. aestivum* are remarkably diverse at the genetic level (Cseh et al., 2021; Frankin et al., 2020) and, thus, further exploiting this allelic richness would shed light into the genetic basis of end-of-flowering in wheat. Along with floret degeneration, SM arrest is a key determinant of floret number (**Figure 7.10**), which in turn affects reproductive potential. Therefore, better understanding both of these processes is a critical step towards designing effective strategies for the improvement of productivity in cultivated wheat.

8.7. Concluding Remarks

In this thesis, several genetic and molecular biology approaches have been utilized to characterize the environmental regulation of end-of-flowering, a process that has been largely overlooked over the years. The work presented here clearly demonstrates that end-of-flowering is under tight genetic and environmental control and that this is conserved to some degree within angiosperms. Whilst the genetic basis of this process is still not fully resolved, this research sheds light into the signals that mediate the response to the environment. Furthermore, it shows that both the beginning of flowering and the end of it are under control by similar genetic mechanisms and identifies a novel role for *FT* as a dual promoter of both floral transition and inflorescence arrest.

The environmental control of the end-of-flowering is only beginning to be understood, but the results and tools developed here will be key to direct future research efforts aiming to better understand this process in *A. thaliana* and other flowering species. This is particularly critical considering the current scenario, where rising global temperatures threaten to impact flowering in crop species and compromise agricultural output. The research presented here demonstrates that this increase in temperatures could not only shorten the reproductive period of flowering plants but also reduce their fruit yield and seed size. Thus, further exploring the genetic and molecular bases of the end-of-flowering and its response to the environment is a pivotal step towards achieving food security in the coming years, for which this thesis presents a key starting point.

References

Abe, M., Kobayashi, Y., Yamamoto, S., Daimon, Y., Yamaguchi, A., Ikeda, Y., Ichinoki, H., Notaguchi, M., Goto, K., Araki, T., 2005. FD, a bZIP protein mediating signals from the floral pathway integrator FT at the shoot apex. Science 309 (5737), 1052–1056. https://doi.org/10.1126/science.1115983

Aikawa, S., Kobayashi, M.J., Satake, A., Shimizu, K.K., Kudoh, H., 2010. Robust control of the seasonal expression of the Arabidopsis FLC gene in a fluctuating environment. Proceedings of the National Academy of Sciences 107 (25), 11632–11637. https://doi.org/10.1073/pnas.0914293107

Allsopp, A., 1967. Heteroblastic development in vascular plants. Advances in Morphogenesis 6, 127–171. https://doi.org/10.1016/b978-1-4831-9953-5.50008-1

Alonso-Blanco, C., Andrade, J., Becker, C., Bemm, F., Bergelson, J., Borgwardt, K.M., Cao, J., Chae, E., Dezwaan, T.M., Ding, W., Ecker, J.R., Exposito-Alonso, M., Farlow, A., Fitz, J., Gan, X., Grimm, D.G., Hancock, A.M., Henz, S.R., Holm, S., Horton, M., Jarsulic, M., Kerstetter, R.A., Korte, A., Korte, P., Lanz, C., Lee, C.-R., Meng, D., Michael, T.P., Mott, R., Muliyati, N.W., Nägele, T., Nagler, M., Nizhynska, V., Nordborg, M., Novikova, P.Y., Picó, F.X., Platzer, A., Rabanal, F.A., Rodriguez, A., Rowan, B.A., Salomé, P.A., Schmid, K.J., Schmitz, R.J., Seren, Ü., Sperone, F.G., Sudkamp, M., Svardal, H., Tanzer, M.M., Todd, D., Volchenboum, S.L., Wang, C., Wang, G., Wang, X., Weckwerth, W., Weigel, D., Zhou, X., 2016. 1,135 Genomes Reveal the Global Pattern of Polymorphism in Arabidopsis thaliana. Cell 166 (2), 481–491. https://doi.org/10.1016/j.cell.2016.05.063

Anders, S., Huber, W., 2010. Differential expression analysis for sequence count data. Genome Biology 11, R106. https://doi.org/10.1186/gb-2010-11-10-r106

Appendino, M.L., Slafer, G.A., 2004. Earliness per se and its dependence upon temperature in diploid wheat lines differing in the major gene Eps-Am1 alleles. The Journal of Agricultural Science, 141 (2): 149-154. https://doi.org/10.1017/S0021859603003472

Ausin, I., Alonso-Blanco, C., Martinez-Zapater, J.-M., 2004. Environmental regulation of flowering. International Journal of Developmental Biology 49, 689–705. https://doi.org/10.1387/ijdb.052022ia

Backhaus, A.E., Griffiths, C., Vergara-Cruces, A., Simmonds, J., Lee, R., Morris, R.J., Uauy, C., 2023. Delayed development of basal spikelets in wheat explains their increased floret abortion and rudimentary nature. Journal of Experimental Botany 74 (17), 5088-5103. https://doi.org/10.1093/jxb/erad233

Baerenfaller, K., Massonnet, C., Hennig, L., Russenberger, D., Sulpice, R., Walsh, S., Stitt, M., Granier, C., Gruissem, W., 2015. A long photoperiod relaxes energy management in Arabidopsis leaf six. Current Plant Biology 2, 34–45. https://doi.org/10.1016/j.cpb.2015.07.001

Balanzà, V., Martínez-Fernández, I., Ferrándiz, C., 2014. Sequential action of FRUITFULL as a modulator of the activity of the floral regulators SVP and SOC1. Journal of Experimental Botany 65 (4), 1193–1203. https://doi.org/10.1093/jxb/ert482

Balanzà, V., Martínez-Fernández, I., Sato, S., Yanofsky, M.F., Ferrándiz, C., 2019. Inflorescence Meristem Fate Is Dependent on Seed Development and FRUITFULL in Arabidopsis thaliana. Frontiers in Plant Science 10, 1622. https://doi.org/10.3389/fpls.2019.01622

Balanzà, V., Martínez-Fernández, I., Sato, S., Yanofsky, M.F., Kaufmann, K., Angenent, G.C., Bemer, M., Ferrándiz, C., 2018. Genetic control of meristem arrest and life span in Arabidopsis by a FRUITFULL-APETALA2 pathway. Nature Communications 9, 565. https://doi.org/10.1038/s41467-018-03067-5

Balanzà, V., Merelo, P., Ferrándiz, C., 2023. Flowering also has to end: knowns and unknowns of reproductive arrest in monocarpic plants. Journal of Experimental Botany 74 (14), 3951–3960. https://doi.org/10.1093/jxb/erad213

Balasubramanian, S., Sureshkumar, S., Lempe, J., Weigel, D., 2006. Potent Induction of Arabidopsis thaliana Flowering by Elevated Growth Temperature. PLOS Genetics 2, e106. https://doi.org/10.1371/journal.pgen.0020106

Barks, P.M., Laird, R.A., 2015. Senescence in duckweed: age-related declines in survival, reproduction and offspring quality. Functional Ecology 29 (4), 540–548. https://doi.org/10.1111/1365-2435.12359

Bartrina, I., Jensen, H., Novák, O., Strnad, M., Werner, T., Schmülling, T., 2017. Gain-of-Function Mutants of the Cytokinin Receptors AHK2 and AHK3 Regulate Plant Organ Size, Flowering Time and Plant Longevity. Plant Physiol. 173 (3), 1783–1797. https://doi.org/10.1104/pp.16.01903

Basavaraddi, P.A., Savin, R., Bencivenga, S., Griffiths, S., Slafer, G.A., 2021. Wheat Developmental Traits as Affected by the Interaction between Eps-7D and Temperature under Contrasting Photoperiods with Insensitive Ppd-D1 Background. Plants 10 (3), 547. https://doi.org/10.3390/plants10030547

Bawa, K.S., Kang, H., Grayum, M.H., 2003. Relationships among time, frequency, and duration of flowering in tropical rain forest trees. American Journal of Botany 90 (6), 877–887. https://doi.org/10.3732/ajb.90.6.877

Benett, T., Dixon, L., 2021. Asymmetric expansions of FT and TFL1 lineages characterize differential evolution of the EuPEBP family in the major angiosperm lineages. BMC Biology 19: 181. https://doi.org/10.1186/s12915-021-01128-8

Bennett, T., Leyser, O., 2014. Strigolactone signalling: standing on the shoulders of DWARFs. Current Opinion in Plant Biology 22, 7–13. https://doi.org/10.1016/j.pbi.2014.08.001

Bennett, T., Sieberer, T., Willett, B., Booker, J., Luschnig, C., Leyser, O., 2006. The Arabidopsis MAX Pathway Controls Shoot Branching by Regulating Auxin Transport. Current Biology 16 (6), 553–563. https://doi.org/10.1016/j.cub.2006.01.058

Benjamini, Y., Hochberg, Y., 1995. Controlling the False Discovery Rate: A Practical and Powerful Approach to Multiple Testing. Journal of the Royal Statistical Society: Series B (Methodological) 57 (1), 289–300. https://doi.org/10.1111/j.2517-6161.1995.tb02031.x

Benlloch, R., Berbel, A., Serrano-Mislata, A., Madueno, F., 2007. Floral Initiation and Inflorescence Architecture: A Comparative View. Annals of Botany 100 (3), 659–676. https://doi.org/10.1093/aob/mcm146

Bentley, A.R., Horsnell, R., Werner, C.P., Turner, A.S., Rose, G.A., Bedard, C., Howell, P., Wilhelm, E.P., Mackay, I.J., Howells, R.M., Greenland, A., Laurie, D.A., Gosman, N., 2013. Short, natural, and extended photoperiod response in BC2F4 lines of bread wheat with different photoperiod-1 (Ppd-1) alleles. Journal of Experimental Botany 64 (7): 1783-1793. 10.1093/jxb/ert038

Berardini, T.Z., Reiser, L., Li, D., Mezheritsky, Y., Muller, R., Strait, E., Huala, E., 2015. The arabidopsis information resource: Making and mining the “gold standard” annotated reference plant genome. genesis 53 (8), 474–485. https://doi.org/10.1002/dvg.22877

Bergonzi, S., Albani, M.C., Ver Loren van Themaat, E., Nordström, K.J.V., Wang, R., Schneeberger, K., Moerland, P.D., Coupland, G., 2013. Mechanisms of age-dependent response to winter temperature in perennial flowering of Arabis alpina. Science 340 (6136), 1094–1097. https://doi.org/10.1126/science.1234116

Bertani, G., 1951. Studies on lysogenesis I: The Mode of Phage Liberation by Lysogenic Escherichia coli. Journal of Bacteriology 62 (3), 293–300. https://doi.org/10.1128/jb.62.3.293-300.1951

Bilas, R.D., Bretman, A., Bennett, T., 2021. Friends, neighbours and enemies: an overview of the communal and social biology of plants. Plant, Cell & Environment 44 (4), 997–1013. https://doi.org/10.1111/pce.13965

Blázquez, M.A., Ahn, J.H., Weigel, D., 2003. A thermosensory pathway controlling flowering time in Arabidopsis thaliana. Nature Genetics 33, 168–171. https://doi.org/10.1038/ng1085

Bonnett, O.T., 1966. Inflorescences of Maize, Wheat, Rye, Barley, and Oats: Their Initiation and Development. University of Illinois, College of Agriculture, Agricultural Experiment Station.

Bonnett, O.T., 1936. The development of the wheat spike. Journal of Agricultural Research 53, 445–451.

Brachi, B., Faure, N., Horton, M., Flahauw, E., Vazquez, A., Nordborg, M., Bergelson, J., Cuguen, J., Roux, F., 2010. Linkage and Association Mapping of Arabidopsis thaliana Flowering Time in Nature. PLOS Genetics 6 (5), e1000940. https://doi.org/10.1371/journal.pgen.1000940

Bradley, D., Ratcliffe, O., Vincent, C., Carpenter, R., Coen, E., 1997. Inflorescence commitment and architecture in Arabidopsis. Science 275 (5296), 80–83. https://doi.org/10.1126/science.275.5296.80

Brand, U., Fletcher, J.C., Hobe, M., Meyerowitz, E.M., Simon, R., 2000. Dependence of stem cell fate in Arabidopsis on a feedback loop regulated by CLV3 activity. Science 289 (5479), 617–619. https://doi.org/10.1126/science.289.5479.617

Bratzel, F., Turck, F., 2015. Molecular memories in the regulation of seasonal flowering: from competence to cessation. Genome Biology 16, 192. https://doi.org/10.1186/s13059-015-0770-6

Bray, N.L., Pimentel, H., Melsted, P., Pachter, L., 2016. Near-optimal probabilistic RNA-seq quantification. Nature Biotechnology 34, 525–527. https://doi.org/10.1038/nbt.3519

Brightbill, C.M., Sung, S., 2022. Temperature-mediated regulation of flowering time in Arabidopsis thaliana. aBIOTECH 3, 78–84. https://doi.org/10.1007/s42994-022-00069-2

Caldelari, D., Wang, G., Farmer, E.E., Dong, X., 2011. Arabidopsis lox3 lox4 double mutants are male sterile and defective in global proliferative arrest. Plant Molecular Biology 75, 25–33. https://doi.org/10.1007/s11103-010-9701-9

Cao, Y., Xiao, Y., Huang, H., Xu, J., Hu, W., Wang, N., 2016. Simulated warming shifts the flowering phenology and sexual reproduction of Cardamine hirsuta under different Planting densities. Scientific Reports 6, 27835. https://doi.org/10.1038/srep27835

Capovilla, G., Schmid, M., Posé, D., 2015. Control of flowering by ambient temperature. Journal of Experimental Botany 66 (1), 59–69. https://doi.org/10.1093/jxb/eru416

Capovilla, G., Symeonidi, E., Wu, R., Schmid, M., 2017. Contribution of major FLM isoforms to temperature-dependent flowering in Arabidopsis thaliana. Journal of Experimental Botany 68 (18), 5117–5127. https://doi.org/10.1093/jxb/erx328

Carrasco, B., Retamales, J.B., Quiroz, K., Garriga, M., Caligari, P.D.S., Garcia-Gonzales, R., 2013. Inter Simple Sequence Repeat Markers Associated with Flowering Time Duration in the Chilean Strawberry (Fragaria chiloensis). Journal of Agricultural Science and Technology 15 (6), 1195–1207.

Cartolano, M., Pieper, B., Lempe, J., Tattersall, A., Huijser, P., Tresch, A., Darrah, P.R., Hay, A., Tsiantis, M., 2015. Heterochrony underpins natural variation in Cardamine hirsuta leaf form. Proceedings of the National Academy of Sciences 112 (33), 10539–10544. https://doi.org/10.1073/pnas.1419791112

Caselli, F., Zanarello, F., Kater, M.M., Battaglia, R., Gregis, V., 2020. Crop reproductive meristems in the genomic era: a brief overview. Biochemical Society Transactions 48 (3), 853–865. https://doi.org/10.1042/BST20190441

Chen, M., MacGregor, D.R., Dave, A., Florance, H., Moore, K., Paszkiewicz, K., Smirnoff, N., Graham, I.A., Penfield, S., 2014. Maternal temperature history activates Flowering Locus T in fruits to control progeny dormancy according to time of year. Proceedings of the National Academy of Sciences 111 (52), 18787–18792. https://doi.org/10.1073/pnas.1412274111

Cheng, Y.-J., Shang, G.-D., Xu, Z.-G., Yu, S., Wu, L.-Y., Zhai, D., Tian, S.-L., Gao, J., Wang, L., Wang, J.-W., 2021. Cell division in the shoot apical meristem is a trigger for miR156 decline and vegetative phase transition in *Arabidopsis*. Proceedings of the National Academy of Sciences 118 (46): e2115667118. https://doi.org/10.1073/pnas.2115667118

Choi, B., Jeong, H., Kim, E., 2019. Phenotypic plasticity of Capsella bursa-pastoris (Brassicaceae) and its effect on fitness in response to temperature and soil moisture. Plant Species Biology 34 (1), 5–10. https://doi.org/10.1111/1442-1984.12227

Cingolani, P., Platts, A., Wang, L.L., Coon, M., Nguyen, T., Wang, L., Land, S.J., Lu, X., Ruden, D.M., 2012. A program for annotating and predicting the effects of single nucleotide polymorphisms, SnpEff. Fly 6, 80–92. https://doi.org/10.4161/fly.19695

Clough, S.J., Bent, A.F., 1998. Floral dip: a simplified method for Agrobacterium - mediated transformation of Arabidopsis thaliana. The Plant Journal 16 (6), 735–743. https://doi.org/10.1046/j.1365-313x.1998.00343.x

Cockram, J., Jones, H., Leigh, F.J., O'Sullivan, D., Powell, W., Laurie, D.A., Greenland, A.J., 2007. Control of flowering time in temperate cereals: genes, domestication and sustainable productivity. Journal of Experimental Botany 58 (6), 1231-1244. https://doi.org/10.1093/jxb/erm042

Collani, S., Neumann, M., Yant, L., Schmid, M., 2019. FT Modulates Genome-Wide DNA-Binding of the bZIP Transcription Factor FD. Plant Physiology 180 (1), 367–380. https://doi.org/10.1104/pp.18.01505

Corbesier, L., Vincent, C., Jang, S., Fornara, F., Fan, Q., Searle, I., Giakountis, A., Farrona, S., Gissot, L., Turnbull, C., Coupland, G., 2007. FT Protein Movement Contributes to Long-Distance Signaling in Floral Induction of Arabidopsis. Science 316 (5827), 1030–1033. https://doi.org/10.1126/science.1141752

Cortés-Flores, J., Hernández-Esquivel, K.B., González-Rodríguez, A., Ibarra-Manríquez, G., 2017. Flowering phenology, growth forms, and pollination syndromes in tropical dry forest species: Influence of phylogeny and abiotic factors. American Journal of Botany 104 (1), 39–49. https://doi.org/10.3732/ajb.1600305

Crawford, S., Shinohara, N., Sieberer, T., Williamson, L., George, G., Hepworth, J., Müller, D., Domagalska, M.A., Leyser, O., 2010. Strigolactones enhance competition between shoot branches by dampening auxin transport. Development 137 (17), 2905–2913. https://doi.org/10.1242/dev.051987

Cseh, A., Poczai, P., Kiss, T., Balla, K., Berki, Z., Horváth, Á., Kuti, C., Karsai, I., 2021. Exploring the legacy of Central European historical winter wheat landraces. Scientific Reports 11, 23915. https://doi.org/10.1038/s41598-021-03261-4

Czechowski, T., Stitt, M., Altmann, T., Udvardi, M.K., Scheible, W.-R., 2005. Genome-wide identification and testing of superior reference genes for transcript normalization in Arabidopsis. Plant Physiology 139 (1): 5-17. https://doi.org/10.1104/pp.105.063743

de Ollas, C., Segarra-Medina, C., González-Guzmán, M., Puertolas, J., Gómez-Cadenas, A., 2019. A customizable method to characterize Arabidopsis thaliana transpiration under drought conditions. Plant Methods 15, 89. https://doi.org/10.1186/s13007-019-0474-0

Dixon, L.E., Farré, A., Finnegan, E.J., Orford, S., Griffiths, S., Boden, S.A., 2018. Developmental responses of bread wheat to changes in ambient temperature following deletion of a locus that includes FLOWERING LOCUS T1. Plant, Cell & Environment 41 (7), 1715–1725. https://doi.org/10.1111/pce.13130

Doerge, R.W., 2002. Mapping and analysis of quantitative trait loci in experimental populations. Nature Reviews Genetics 3, 43–52. https://doi.org/10.1038/nrg703

Dogra, H., Dani, K.G.S., 2019. Defining features of age-specific fertility and seed quality in senescing indeterminate annuals. American Journal of Botany 106 (4), 604–610. https://doi.org/10.1002/ajb2.1265

Domagalska, M.A., Leyser, O., 2011. Signal integration in the control of shoot branching. Nature Reviews Molecular Cell Biology 12, 211–221. https://doi.org/10.1038/nrm3088

Dorji, T., Hopping, K.A., Meng, F., Wang, S., Jiang, L., Klein, J.A., 2020. Impacts of climate change on flowering phenology and production in alpine plants: The importance of end of flowering. Agriculture, Ecosystems & Environment 291, 106795. https://doi.org/10.1016/j.agee.2019.106795

Doyle, M.R., Davis, S.J., Bastow, R.M., McWatters, H.G., Kozma-Bognár, L., Nagy, F., Millar, A.J., Amasino, R.M., 2002. The ELF4 gene controls circadian rhythms and flowering time in Arabidopsis thaliana. Nature 419, 74–77. https://doi.org/10.1038/nature00954

Ezer, D., Jung, J.-H., Lan, H., Biswas, S., Gregoire, L., Box, M.S., Charoensawan, V., Cortijo, S., Lai, X., Stöckle, D., Zubieta, C., Jaeger, K.E., Wigge, P.A., 2017. The evening complex coordinates environmental and endogenous signals in Arabidopsis. Nature Plants 3, 17087. https://doi.org/10.1038/nplants.2017.87

Feng, P., Guo, H., Chi, W., Chai, X., Sun, X., Xu, X., Ma, J., Rochaix, J.-D., Leister, D., Wang, H., Lu, C., Zhang, L., 2016. Chloroplast retrograde signal regulates flowering. Proceedings of the National Academy of Sciences 113 (38), 10708–10713. https://doi.org/10.1073/pnas.1521599113

Fernández, V., Takahashi, Y., Le Gourrierec, J., Coupland, G., 2016. Photoperiodic and thermosensory pathways interact through CONSTANS to promote flowering at high temperature under short days. The Plant Journal 86 (5), 426–440. https://doi.org/10.1111/tpj.13183

Ferrante, A., Savin, R., Slafer, G.A., 2013. Floret development and grain setting differences between modern durum wheats under contrasting nitrogen availability. Journal of Experimental Botany 64 (1), 169–184. https://doi.org/10.1093/jxb/ers320

Ferreira, M.J., Silva, J., Pinto, S.C., Coimbra, S., 2023. I Choose You: Selecting Accurate Reference Genes for qPCR Expression Analysis in Reproductive Tissues in *Arabidopsis thaliana*. Biomolecules 13: 463. https://doi.org/10.3390/biom13030463

Finnegan, E.J., Ford, B., Wallace, X., Pettolino, F., Griffin, P.T., Schmitz, R.J., Zhang, P., Barrero, J.M., Hayden, M.J., Boden, S.A., Cavanagh, C.A., Swain, S.M., Trevaskis, B., 2018. Zebularine treatment is associated with deletion of FT-B1 leading to an increase in spikelet number in bread wheat. Plant, Cell & Environment 41 (6), 1346–1360. https://doi.org/10.1111/pce.13164

Fischer, R.A., 1984. Growth and yield of wheat, in: Smith, W.H., Bante, S.J. (Eds.), Potential Productivity of Field Crops Under Different Environments, International Rice Research Institute. Los Baños, pp. 129–154.

Forster, M.A., Bonser, S.P., 2009. Heteroblastic development and the optimal partitioning of traits among contrasting environments in Acacia implexa. Annals of Botany 103 (1), 95–105. https://doi.org/10.1093/aob/mcn210

Francis, C., Gladstones, J., 1974. Relationships among rate and duration of flowering and seed yield components in subterranean clover (Trifolium subterraneum). Australian Journal of Agricultural Research 25 (3), 435–442. https://doi.org/10.1071/AR9740435

Frankin, S., Kunta, S., Abbo, S., Sela, H., Goldberg, B.Z., Bonfil, D.J., Levy, A.A., Avivi-Ragolsky, N., Nashef, K., Roychowdhury, R., Faraj, T., Lifshitz, D., Mayzlish-Gati, E., Ben-David, R., 2020. The Israeli–Palestinian wheat landraces collection: restoration and characterization of lost genetic diversity. Journal of the Science of Food and Agriculture 100 (11), 4083–4092. https://doi.org/10.1002/jsfa.9822

Fu, M., Qi, B., Li, S., Xu, H., Wang, Y., Zhao, Z., Yu, X., Pan, L., Yang, J., 2022. Detection of Hub QTLs Underlying the Genetic Basis of Three Modules Covering Nine Agronomic Traits in an F2 Soybean Population. Agronomy 12 (12), 3135. https://doi.org/10.3390/agronomy12123135

Fujisaki, K., Hagihara, F., Azukawa, Y., Kaido, M., Okuno, T., Mise, K., 2004. Identification and Characterization of the SSB1 Locus Involved in Symptom Development by Spring beauty latent virus Infection in Arabidopsis thaliana. MPMI 17 (9), 967–975. https://doi.org/10.1094/MPMI.2004.17.9.967

Gauley, A., Boden, S.A., 2021. Stepwise increases in FT1 expression regulate seasonal progression of flowering in wheat (Triticum aestivum). New Phytologist 229 (2), 1163–1176. https://doi.org/10.1111/nph.16910

Gentilucci, M., Burt, P., 2018. Using temperature to predict the end of flowering in the common grape (Vitis vinifera) in the Macerata wine region, Italy. Euro-Mediterranean Journal for Environmental Integration volumen 3, 38. https://doi.org/10.1007/s41207-018-0079-4

Ghiglione, H.O., Gonzalez, F.G., Serrago, R., Maldonado, S.B., Chilcott, C., Curá, J.A., Miralles, D.J., Zhu, T., Casal, J.J., 2008. Autophagy regulated by day length determines the number of fertile florets in wheat. The Plant Journal 55 (6), 1010–1024. https://doi.org/10.1111/j.1365-313X.2008.03570.x

Girden, E.R., 1992. ANOVA: Repeated measures, ANOVA: Repeated measures. Sage Publications, Inc, Thousand Oaks, CA, US.

Glick, D., Barth, S., Macleod, K.F., 2010. Autophagy: cellular and molecular mechanisms. The Journal of Pathology 221 (1), 3–12. https://doi.org/10.1002/path.2697

Goetz, M., Rabinovich, M., Smith, H.M., 2021. The role of auxin and sugar signaling in dominance inhibition of inflorescence growth by fruit load. Plant Physiology 187 (3), 1189–1201. https://doi.org/10.1093/plphys/kiab237

González-Grandío, E., Pajoro, A., Franco-Zorrilla, J.M., Tarancón, C., Immink, R.G.H., Cubas, P., 2017. Abscisic acid signaling is controlled by a BRANCHED1/HD-ZIP I cascade in Arabidopsis axillary buds. Proceedings of the National Academy of Sciences 114 (2), E245-E254. https://doi.org/10.1073/pnas.1613199114

González-Suárez, P., Walker, C.H., Bennett, T., 2020. Bloom and bust: understanding the nature and regulation of the end of flowering. Current Opinion in Plant Biology 57, 24–30. https://doi.org/10.1016/j.pbi.2020.05.009

Goyal, A., Karayekov, E., Galvão, V.C., Ren, H., Casal, J.J., Fankhauser, C., 2016. Shade promotes phototropism through phytochrome B-controlled auxin production. Current Biology 26 (24): 3280-3287. https://doi.org/10.1016/j.cub.2016.10.001

Halse, N., Weir, R., 1974. Effects of temperature on spikelet number of wheat. Australian Journal of Agricultural Research 25 (5), 687–695. https://doi.org/10.1071/AR9740687

Hegarty, M.J., 2012. Invasion of the hybrids. Molecular Ecology 21 (19), 4669–4671. https://doi.org/10.1111/j.1365-294X.2012.05720.x

Hensel, L.L., Nelson, M.A., Richmond, T.A., Bleecker, A.B., 1994. The Fate of Inflorescence Meristems Is Controlled by Developing Fruits in Arabidopsis. Plant Physiology 106 (3), 863–876. https://doi.org/10.1104/pp.106.3.863

Higuchi, Y., 2018. Florigen and anti-florigen: flowering regulation in horticultural crops. Breeding Science 68 (1), 109–118. https://doi.org/10.1270/jsbbs.17084

Hill, C.B., Li, C., 2016. Genetic Architecture of Flowering Phenology in Cereals and Opportunities for Crop Improvement. Frontiers in Plant Science 7. https://doi.org/10.3389/fpls.2016.01906

Hintz, M., Bartholmes, C., Nutt, P., Ziermann, J., Hameister, S., Neuffer, B., Theißen, G., 2006. Catching a “hopeful monster”: shepherd’s purse (Capsella bursa-pastoris) as a model system to study the evolution of flower development. Journal of experimental botany 57 (13), 3531–3542. https://doi.org/10.1093/jxb/erl158

Hisamatsu, T., King, R.W., 2008. The nature of floral signals in Arabidopsis. II. Roles for FLOWERING LOCUS T (FT) and gibberellin. Journal of Experimental Botany 59, 3821–3829. https://doi.org/10.1093/jxb/ern232

Hoffmann, M.H., Schmuths, H., Koch, C., Meister, A., Fritsch, R.M., 2010. Comparative Analysis of Growth, Genome Size, Chromosome Numbers and Phylogeny of Arabidopsis thaliana and Three Cooccurring Species of the Brassicaceae from Uzbekistan. Journal of Botany 2010, e504613. https://doi.org/10.1155/2010/504613

Horton, M.W., Hancock, A.M., Huang, Y.S., Toomajian, C., Atwell, S., Auton, A., Muliyati, N.W., Platt, A., Sperone, F.G., Vilhjálmsson, B.J., Nordborg, M., Borevitz, J.O., Bergelson, J., 2012. Genome-wide patterns of genetic variation in worldwide Arabidopsis thaliana accessions from the RegMap panel. Nature Genetics 44, 212–216. https://doi.org/10.1038/ng.1042

House, C., Roth, C., Hunt, J., Kover, P.X., 2010. Paternal effects in Arabidopsis indicate that offspring can influence their own size. Proceedings of the Royal Society B: Biological Sciences 277 (1695), 2885–2893. https://doi.org/10.1098/rspb.2010.0572

Huang, H., Nusinow, D.A., 2016. Into the Evening: Complex Interactions in the Arabidopsis Circadian Clock. Trends in Genetics 32 (10), 674–686. https://doi.org/10.1016/j.tig.2016.08.002

Huang, Z., Shi, T., Zheng, B., Yumul, R.E., Liu, X., You, C., Gao, Z., Xiao, L., Chen, X., 2017. APETALA2 antagonizes the transcriptional activity of AGAMOUS in regulating floral stem cells in Arabidopsis thaliana. New Phytologist 215 (3), 1197–1209. https://doi.org/10.1111/nph.14151

Ishida, K., Yamashino, T., Yokoyama, A., Mizuno, T., 2008. Three type-B response regulators, ARR1, ARR10 and ARR12, play essential but redundant roles in cytokinin signal transduction throughout the life cycle of Arabidopsis thaliana. Plant and Cell Physiology 49 (1), 47–57. https://doi.org/10.1093/pcp/pcm165

Jasinski, S., Lécureuil, A., Miquel, M., Loudet, O., Raffaele, S., Froissard, M., Guerche, P., 2012. Natural Variation in Seed Very Long Chain Fatty Acid Content Is Controlled by a New Isoform of KCS18 in Arabidopsis thaliana. PLOS ONE 7 (11), e49261. https://doi.org/10.1371/journal.pone.0049261

Jeuffroy, M.-H., Sebillotte, M., 1997. The end of flowering in pea: influence of plant nitrogen nutrition. European Journal of Agronomy 6 (1-2), 15–24. https://doi.org/10.1016/S1161-0301(96)02028-X

Jiang, B., Shi, Y., Peng, Y., Jia, Y., Yan, Y., Dong, X., Li, H., Dong, J., Li, J., Gong, Z., Thomashow, M.F., Yang, S., 2020. Cold-Induced CBF–PIF3 Interaction Enhances Freezing Tolerance by Stabilizing the phyB Thermosensor in Arabidopsis. Molecular Plant 13 (6), 894–906. https://doi.org/10.1016/j.molp.2020.04.006

Johanson, U., West, J., Lister, C., Michaels, S., Amasino, R., Dean, C., 2000. Molecular Analysis of FRIGIDA, a Major Determinant of Natural Variation in Arabidopsis Flowering Time. Science 290 (5490), 344–347. https://doi.org/10.1126/science.290.5490.344

Jones, H.E., Lukac, M., Brak, B., Martinez-Eixarch, M., Alhomedhi, A., Gooding, M.J., Wingen, L.U., Griffiths, S., 2017. Photoperiod sensitivity affects flowering duration in wheat. The Journal of Agricultural Science 155 (1), 32–43. https://doi.org/10.1017/S0021859616000125

Jung, J.-H., Domijan, M., Klose, C., Biswas, S., Ezer, D., Gao, M., Khattak, A.K., Box, M.S., Charoensawan, V., Cortijo, S., Kumar, M., Grant, A., Locke, J.C.W., Schäfer, E., Jaeger, K.E., Wigge, P.A., 2016. Phytochromes function as thermosensors in Arabidopsis. Science 354 (6314), 886–889. https://doi.org/10.1126/science.aaf6005

Jung, J.-H., Seo, P.J., Ahn, J.H., Park, C.-M., 2012. Arabidopsis RNA-binding Protein FCA Regulates MicroRNA172 Processing in Thermosensory Flowering. Journal of Biological Chemistry 287 (19), 16007–16016. https://doi.org/10.1074/jbc.M111.337485

Kant, S., Peng, M., Rothstein, S.J., 2011. Genetic regulation by NLA and microRNA827 for maintaining nitrate-dependent phosphate homeostasis in arabidopsis. PLOS Genetics 7 (3), e1002021. https://doi.org/10.1371/journal.pgen.1002021

Kardailsky, I., Shukla, V.K., Ahn, J.H., Dagenais, N., Christensen, S.K., Nguyen, J.T., Chory, J., Harrison, M.J., Weigel, D., 1999. Activation tagging of the floral inducer FT. Science 286 (5446), 1962–1965. https://doi.org/10.1126/science.286.5446.1962

Kays, S.J., Kultur, F., 2005. Genetic Variation in Jerusalem Artichoke (Helianthus tuberosus L.) Flowering Date and Duration. HortScience 40 (6), 1675–1678. https://doi.org/10.21273/HORTSCI.40.6.1675

Kim, D.-H., 2020. Current understanding of flowering pathways in plants: focusing on the vernalization pathway in Arabidopsis and several vegetable crop plants. Horticulture, Environment and Biotechnology 61, 209–227. https://doi.org/10.1007/s13580-019-00218-5

Kim, D.-H., Sung, S., 2014. Genetic and Epigenetic Mechanisms Underlying Vernalization. Arabidopsis Book 12, e0171. https://doi.org/10.1199/tab.0171

Kim, J., Dotson, B., Rey, C., Lindsey, J., Bleecker, A.B., Binder, B.M., Patterson, S.E., 2013. New Clothes for the Jasmonic Acid Receptor COI1: Delayed Abscission, Meristem Arrest and Apical Dominance. PLOS ONE 8 (4), e60505. https://doi.org/10.1371/journal.pone.0060505

Kim, Y., Lim, J., Yeom, M., Kim, H., Kim, J., Wang, L., Kim, W.Y., Somers, D.E., Nam, H.G., 2013. ELF4 regulates GIGANTEA chromatin access through subnuclear sequestration. Cell Reports 3 (3), 671–677. https://doi.org/10.1016/j.celrep.2013.02.021

Kim, Y., Yeom, M., Kim, H., Lim, J., Koo, H.J., Hwang, D., Somers, D., Nam, H.G., 2012. GIGANTEA and EARLY FLOWERING 4 in Arabidopsis exhibit differential phase-specific genetic influences over a diurnal cycle. Molecular Plant 5 (3), 678–687. https://doi.org/10.1093/mp/sss005

Kinmonth-Schultz, H.A., MacEwen, M.J.S., Seaton, D.D., Millar, A.J., Imaizumi, T., Kim, S.-H., 2019. An explanatory model of temperature influence on flowering through whole-plant accumulation of FLOWERING LOCUS T in Arabidopsis thaliana. in silico Plants 1 (1): diz006. https://doi.org/10.1093/insilicoplants/diz006

Kirby, E.J.M., 1995. Factors Affecting Rate of Leaf Emergence in Barley and Wheat. Crop Science 35 (1), cropsci1995.0011183X003500010003x. https://doi.org/10.2135/cropsci1995.0011183X003500010003x

Kirby, E.J.M., Appleyard, M., 1984. Cereal Development Guide. Arable Unit, National Agricultural Centre.

Kobayashi, Y., Kaya, H., Goto, K., Iwabuchi, M., Araki, T., 1999. A pair of related genes with antagonistic roles in mediating flowering signals. Science 286 (5446), 1960–1962. https://doi.org/10.1126/science.286.5446.1960

Kobayashi, Y., Weigel, D., 2007. Move on up, it's time for change: Mobile signals controlling photoperiod-dependent flowering. Genes & Development 21, 2371–2384. https://doi.org/10.1101/gad.1589007

Krannitz, P.G., Aarssen, L.W., Dow, J.M., 1991. The Effect of Genetically Based Differences in Seed Size on Seedling Survival in Arabidopsis Thaliana (brassicaceae). American Journal of Botany 78 (3), 446–450. https://doi.org/10.1002/j.1537-2197.1991.tb15207.x

Kruskal, W.H., Wallis, W.A., 1952. Use of Ranks in One-Criterion Variance Analysis. Journal of the American Statistical Association 47, 583–621. https://doi.org/10.1080/01621459.1952.10483441

Kudoh, H., 2019. Photoperiod–temperature phase lag: A universal environmental context of seasonal developmental plasticity. Development, Growth & Differentiation 61 (1), 5–11. https://doi.org/10.1111/dgd.12579

Kumar, L., E. Futschik, M., 2007. Mfuzz: A software package for soft clustering of microarray data. Bioinformation 2 (1), 5–7. https://doi.org/10.6026/97320630002005

Kuroda, H., Takahashi, N., Shimada, H., Seki, M., Shinozaki, K., Matsui, M., 2002. Classification and Expression Analysis of Arabidopsis F-Box-Containing Protein Genes. Plant and Cell Physiology 43 (10), 1073–1085. https://doi.org/10.1093/pcp/pcf151

Lansing, A.I., 1947. A transmissible, cumulative, and reversible factor in aging. Journal of Gerontology 2 (3), 228–239. https://doi.org/10.1093/geronj/2.3.228

Lee, J., Lee, I., 2010. Regulation and function of SOC1, a flowering pathway integrator. Journal of Experimental Botany 61 (9), 2247–2254. https://doi.org/10.1093/jxb/erq098

Lee, J.H., Ryu, H.-S., Chung, K.S., Posé, D., Kim, S., Schmid, M., Ahn, J.H., 2013. Regulation of temperature-responsive flowering by MADS-box transcription factor repressors. Science 342 (6158), 628–632. https://doi.org/10.1126/science.1241097

Lempe, J., Balasubramanian, S., Sureshkumar, S., Singh, A., Schmid, M., Weigel, D., 2005. Diversity of Flowering Responses in Wild Arabidopsis thaliana Strains. PLOS Genetics 1 (1), 109-118. https://doi.org/10.1371/journal.pgen.0010006

Lenhard, M., Bohnert, A., Jürgens, G., Laux, T., 2001. Termination of Stem Cell Maintenance in Arabidopsis Floral Meristems by Interactions between WUSCHEL and AGAMOUS. Cell 105 (6), 805–814. https://doi.org/10.1016/S0092-8674(01)00390-7

Lenser, T., Tarkowská, D., Novák, O., Wilhelmsson, P.K.I., Bennett, T., Rensing, S.A., Strnad, M., Theißen, G., 2018. When the BRANCHED network bears fruit: how carpic dominance causes fruit dimorphism in Aethionema. The Plant Journal 94 (2), 352–371. https://doi.org/10.1111/tpj.13861

Li, C., Lin, H., Dubcovsky, J., 2015. Factorial combinations of protein interactions generate a multiplicity of florigen activation complexes in wheat and barley. The Plant Journal 84 (1), 70-82. 10.1111/tpj.12960

Li, L., Li, X., Liu, Y., Liu, H., 2016. Flowering responses to light and temperature. Science China Life Sciences 59, 403–408. https://doi.org/10.1007/s11427-015-4910-8

Lifschitz, E., Ayre, B.G., Eshed, Y., 2014. Florigen and anti-florigen – a systemic mechanism for coordinating growth and termination in flowering plants. Frontiers in Plant Science 5, 465. https://doi.org/10.3389/fpls.2014.00465

Lin, Y.-L., Tsay, Y.-F., 2017. Influence of differing nitrate and nitrogen availability on flowering control in Arabidopsis. Journal of Experimental Botany 68 (10), 2603–2609. https://doi.org/10.1093/jxb/erx053

Liu, C., Thong, Z., Yu, H., 2009. Coming into bloom: the specification of floral meristems. Development 136 (20), 3379–3391. https://doi.org/10.1242/dev.033076

Liu, L., Farrona, S., Klemme, S., Turck, F.K., 2014. Post-fertilization expression of FLOWERING LOCUS T suppresses reproductive reversion. Frontiers in Plant Science 5, 164. https://doi.org/10.3389/fpls.2014.00164

Lomas, J., Burd, P., 1983. Prediction of the commencement and duration of the flowering period of citrus. Agricultural Meteorology 28 (4), 387–396. https://doi.org/10.1016/0002-1571(83)90014-6

Long, J.A., Moan, E.I., Medford, J.I., Barton, M.K., 1996. A member of the KNOTTED class of homeodomain proteins encoded by the STM gene of Arabidopsis. Nature 379, 66–69. https://doi.org/10.1038/379066a0

Longnecker, N., Kirby, E.J.M., Robson, A., 1993. Leaf Emergence, Tiller Growth, and Apical Development of Nitrogen-Dificient Spring Wheat. Crop Science 33 (1), cropsci1993.0011183X003300010028x. https://doi.org/10.2135/cropsci1993.0011183X003300010028x

Love, M.I., Huber, W., Anders, S., 2014. Moderated estimation of fold change and dispersion for RNA-seq data with DESeq2. Genome Biology 15, 550. https://doi.org/10.1186/s13059-014-0550-8

Lovell, J.T., Juenger, T.E., Michaels, S.D., Lasky, J.R., Platt, A., Richards, J.H., Yu, X., Easlon, H.M., Sen, S., McKay, J.K., 2013. Pleiotropy of FRIGIDA enhances the potential for multivariate adaptation. Proceedings of the Royal Society B: Biological Sciences 280 (1763), 20131043. https://doi.org/10.1098/rspb.2013.1043

Lu, F., Cui, X., Zhang, S., Liu, C., Cao, X., 2010. JMJ14 is an H3K4 demethylase regulating flowering time in Arabidopsis. Cell Research 20, 387–390. https://doi.org/10.1038/cr.2010.27

Luo, X., He, Y., 2020. Experiencing winter for spring flowering: A molecular epigenetic perspective on vernalization. Journal of Integrative Plant Biology 62 (1), 104–117. https://doi.org/10.1111/jipb.12896

Manning, P., Houston, K., Evans, T., 2009. Shifts in seed size across experimental nitrogen enrichment and plant density gradients. Basic and Applied Ecology 10 (4), 300–308. https://doi.org/10.1016/j.baae.2008.08.004

Martínez-Fernández, I., Menezes de Moura, S., Alves-Ferreira, M., Ferrándiz, C., Balanzà, V., 2020. Identification of Players Controlling Meristem Arrest Downstream of the FRUITFULL-APETALA2 Pathway. Plant Physiology 184 (2), 945–959. https://doi.org/10.1104/pp.20.00800

Marzec, M., Brewer, P., 2019. Binding or Hydrolysis? How Does the Strigolactone Receptor Work? Trends in Plant Science 24 (7), 571–574. https://doi.org/10.1016/j.tplants.2019.05.001

Masle, J., Doussinault, G., Farquhar, G.D., Sun, B., 1989. Foliar stage in wheat correlates better to photothermal time than to thermal time. Plant, Cell & Environment 12 (3), 235–247. https://doi.org/10.1111/j.1365-3040.1989.tb01938.x

Matsoukis, A., Kamoutsis, A., Chronopoulou-Sereli, A., 2018. Air temperature effect on end of flowering of Cirsium arvense (L.) Scop. in a mountainous region of Greece. Journal of Animal and Plant Sciences 28 (1), 100-106.

Melzer, S., Lens, F., Gennen, J., Vanneste, S., Rohde, A., Beeckman, T., 2008. Flowering-time genes modulate meristem determinacy and growth form in Arabidopsis thaliana. Nature Genetics 40, 1489–1492. https://doi.org/10.1038/ng.253

Meng, W.J., Cheng, Z.J., Sang, Y.L., Zhang, M.M., Rong, X.F., Wang, Z.W., Tang, Y.Y., Zhang, X.S., 2017. Type-B ARABIDOPSIS RESPONSE REGULATORs Specify the Shoot Stem Cell Niche by Dual Regulation of WUSCHEL. The Plant Cell 29 (6), 1357–1372. https://doi.org/10.1105/tpc.16.00640

Merelo, P., González-Cuadra, I., Ferrándiz, C., 2022. A cellular analysis of meristem activity at the end of flowering points to cytokinin as a major regulator of proliferative arrest in Arabidopsis. Current Biology 32 (4), 749-762.e3. https://doi.org/10.1016/j.cub.2021.11.069

Michaels, S.D., Amasino, R.M., 1999. FLOWERING LOCUS C Encodes a Novel MADS Domain Protein That Acts as a Repressor of Flowering. The Plant Cell 11 (5), 949–956. https://doi.org/10.1105/tpc.11.5.949

Miryeganeh, M., 2021. Senescence: The Compromised Time of Death That Plants May Call on Themselves. Genes 12 (2), 143. https://doi.org/10.3390/genes12020143

Miryeganeh, M., 2020. Synchronization of senescence and desynchronization of flowering in Arabidopsis thaliana. AOB PLANTS 12 (3), plaa018. https://doi.org/10.1093/aobpla/plaa018

Miryeganeh, M., Yamaguchi, M., Kudoh, H., 2018. Synchronisation of Arabidopsis flowering time and whole-plant senescence in seasonal environments. Scientific Reports 8, 10282. https://doi.org/10.1038/s41598-018-28580-x

Monaghan, P., Maklakov, A.A., Metcalfe, N.B., 2020. Intergenerational Transfer of Ageing: Parental Age and Offspring Lifespan. Trends in Ecology & Evolution 35 (10), 927–937. https://doi.org/10.1016/j.tree.2020.07.005

Murali, K.S., 1997. Patterns of Seed Size, Germination and Seed Viability of Tropical Tree Species in Southern India. Biotropica 29 (3), 271–279. https://doi.org/10.1111/j.1744-7429.1997.tb00428.x

Nagahama, A., Kubota, Y., Satake, A., 2018. Climate warming shortens flowering duration: a comprehensive assessment of plant phenological responses based on gene expression analyses and mathematical modeling. Ecological Research 33 (5), 1059–1068. https://doi.org/10.1007/s11284-018-1625-x

Nerson, H., Edelstein, M., Pinthus, M.J., 1990. Effects of N and P nutrition on spike development in spring wheat. Plant and Soil 124, 33–37. https://doi.org/10.1007/BF00010928

Noguera, J.C., Metcalfe, N.B., Monaghan, P., 2018. Experimental demonstration that offspring fathered by old males have shorter telomeres and reduced lifespans. Proceedings of the Royal Society B: Biological Sciences 285 (1874), 20180268. https://doi.org/10.1098/rspb.2018.0268

Notaguchi, M., Abe, M., Kimura, T., Daimon, Y., Kobayashi, T., Yamaguchi, A., Tomita, Y., Dohi, K., Mori, M., Araki, T., 2008. Long-Distance, Graft-Transmissible Action of Arabidopsis FLOWERING LOCUS T Protein to Promote Flowering. Plant and Cell Physiology 49 (11), 1645–1658. https://doi.org/10.1093/pcp/pcn154

O'Connor, K., González-Suárez, P., Dixon, L.E., 2020. Temperature Control of Plant Development. Annual Plant Reviews Online 3 (4), 563-606. https://doi.org/10.1002/9781119312994.apr0745

Ó'Maoiléidigh, D.S., Graciet, E., Wellmer, F., 2014. Gene networks controlling Arabidopsis thaliana flower development. New Phytologist 201 (1), 16–30. https://doi.org/10.1111/nph.12444

Page, D.R., Grossniklaus, U., 2002. The art and design of genetic screens: Arabidopsis thaliana. Nature Reviews Genetics 3, 124–136. https://doi.org/10.1038/nrg730

Pardos, M., Vázquez-Piqué, J., Benito, L., Madrigal, G., Alejano, R., Fernández, M., Calama, R., 2022. Does the Age of Pinus sylvestris Mother Trees Influence Reproductive Capacity and Offspring Seedling Survival? Forests 13 (6), 937. https://doi.org/10.3390/f13060937

Parker, N., Wang, Y., Meinke, D., 2016. Analysis of Arabidopsis Accessions Hypersensitive to a Loss of Chloroplast Translation. Plant Physiology 172 (3), 1862–1875. https://doi.org/10.1104/pp.16.01291

Pidkowich, M.S., Klenz, J.E., Haughn, G.W., 1999. The making of a flower: control of floral meristem identity in Arabidopsis. Trends in Plant Science 4 (2), 64–70. https://doi.org/10.1016/S1360-1385(98)01369-7

Pigliucci, M., Schlichting, C.D., 1995. Reaction Norms of Arabidopsis (Brassicaceae). III. Response to Nutrients in 26 Populations from a Worldwide Collection. American Journal of Botany 82 (9), 1117–1125. https://doi.org/10.1002/j.1537-2197.1995.tb11582.x

Poorter, H., Bühler, J., Van Dusschoten, D., Climent, J., Postma, J.A., 2012. Pot size matters: a meta-analysis of the effects of rooting volume on plant growth. Functional Plant Biology. 39 (11), 839. https://doi.org/10.1071/FP12049

Press, M.O., Lanctot, A., Queitsch, C., 2016. PIF4 and ELF3 Act Independently in Arabidopsis thaliana Thermoresponsive Flowering. PLOS ONE 11 (8), e0161791. https://doi.org/10.1371/journal.pone.0161791

Prusinkiewicz, P., Erasmus, Y., Lane, B., Harder, L.D., Coen, E., 2007. Evolution and Development of Inflorescence Architectures. Science 316 (5830), 1452–1456. https://doi.org/10.1126/science.1140429

Quiroz, S., Yustis, J.C., Chávez-Hernández, E.C., Martínez, T., Sanchez, M. de la P., Garay-Arroyo, A., Álvarez-Buylla, E.R., García-Ponce, B., 2021. Beyond the Genetic Pathways, Flowering Regulation Complexity in Arabidopsis thaliana. International Journal of Molecular Sciences 22 (11), 5716. https://doi.org/10.3390/ijms22115716

R Core Team, 2022. R: A language and environment for statistical computing.

Rahman, M.S., Wilson, J.H., 1978. Determination of spikelet number in wheat. III.* Effect of varying temperature on ear development. Australian Journal of Agricultural Research 29 (3), 459–467. https://doi.org/10.1071/ar9780459

Ratcliffe, O.J., Amaya, I., Vincent, C.A., Rothstein, S., Carpenter, R., Coen, E.S., Bradley, D.J., 1998. A common mechanism controls the life cycle and architecture of plants. Development 125 (9), 1609–1615. https://doi.org/10.1242/dev.125.9.1609

Rawson, H.M., 1971. An upper limit for spikelet number per ear in wheat as controlled by photoperiod. Australian Journal of Agricultural Research 22 (4), 537–546. https://doi.org/10.1071/ar9710537

Rédei, G.P., 1992. A heuristic glance at the past of Arabidopsis genetics, in: Methods in Arabidopsis Research. Singapore: World Scientific, pp. 1–15.

Reynolds, M., Foulkes, M.J., Slafer, G.A., Berry, P., Parry, M.A.J., Snape, J.W., Angus, W.J., 2009. Raising yield potential in wheat. Journal of Experimental Botany 60 (7), 1899–1918. https://doi.org/10.1093/jxb/erp016

Rhinn, M., Ritschka, B., Keyes, W.M., 2019. Cellular senescence in development, regeneration and disease. Development 146 (20), dev151837. https://doi.org/10.1242/dev.151837

Rivero, L., Scholl, R., Holomuzki, N., Crist, D., Grotewold, E., Brkljacic, J., 2014. Handling Arabidopsis Plants: Growth, Preservation of Seeds, Transformation, and Genetic Crosses, in: Sanchez-Serrano, J.J., Salinas, J. (Eds.), Arabidopsis Protocols, Methods in Molecular Biology. Humana Press, Totowa, NJ, pp. 3–25. https://doi.org/10.1007/978-1-62703-580-4_1

Roach, D.A., Wulff, R.D., 1987. Maternal Effects in Plants. Annual Review of Ecology and Systematics 18, 209–235. https://doi.org/10.1146/annurev.es.18.110187.001233

Rockwell, N.C., Su, Y.-S., Lagarias, J.C., 2006. Phytochrome structure and signaling mechanisms. Annual Review of Plant Biology 57, 837–858. https://doi.org/10.1146/annurev.arplant.56.032604.144208

Rohde, P., Hincha, D.K., Heyer, A.G., 2004. Heterosis in the freezing tolerance of crosses between two Arabidopsis thaliana accessions (Columbia-0 and C24) that show differences in non-acclimated and acclimated freezing tolerance. The Plant Journal 38 (5), 790–799. https://doi.org/10.1111/j.1365-313X.2004.02080.x

Royo, C., Dreisigacker, S., Alfaro, C., Ammar, K., Villegas, D., 2016. Effect of Ppd-1 genes on durum wheat flowering time and grain filling duration in a wide range of latitudes. The Journal of Agricultural Science 154, 612–631. https://doi.org/10.1017/S0021859615000507

Sadras, V.O., Slafer, G.A., 2012. Environmental modulation of yield components in cereals: Heritabilities reveal a hierarchy of phenotypic plasticities. Field Crops Research 127, 215–224. https://doi.org/10.1016/j.fcr.2011.11.014

Sanagi, M., Aoyama, S., Kubo, A., Lu, Y., Sato, Y., Ito, S., Abe, M., Mitsuda, N., Ohme-Takagi, M., Kiba, T., Nakagami, H., Rolland, F., Yamaguchi, J., Imaizumi, T., Sato, T., 2021. Low nitrogen conditions accelerate flowering by modulating the phosphorylation state of FLOWERING BHLH 4 in Arabidopsis. Proceedings of the National Academy of Sciences 118 (19), e2022942118. https://doi.org/10.1073/pnas.2022942118

Sánchez-Gerschon, V., Ferrándiz, C., Balanzà, V., 2023. HB21/40/53 promote inflorescence arrest through ABA accumulation at the end of flowering (preprint). bioRxiv. https://doi.org/10.1101/2023.04.20.537726

Satake, A., Kawagoe, T., Saburi, Y., Chiba, Y., Sakurai, G., Kudoh, H., 2013. Forecasting flowering phenology under climate warming by modelling the regulatory dynamics of flowering-time genes. Nature Communications 4, 2303. https://doi.org/10.1038/ncomms3303

Schmidt, J., Claussen, J., Wörlein, N., Eggert, A., Fleury, D., Garnett, T., Gerth, S., 2020. Drought and heat stress tolerance screening in wheat using computed tomography. Plant Methods 16, 15. https://doi.org/10.1186/s13007-020-00565-w

Schneider, C.A., Rasband, W.S., Eliceiri, K.W., 2012. NIH Image to ImageJ: 25 years of image analysis. Nature Methods 9, 671–675. https://doi.org/10.1038/nmeth.2089

Schoof, H., Lenhard, M., Haecker, A., Mayer, K.F., Jürgens, G., Laux, T., 2000. The stem cell population of Arabidopsis shoot meristems in maintained by a regulatory loop between the CLAVATA and WUSCHEL genes. Cell 100 (6), 635–644. https://doi.org/10.1016/s0092-8674(00)80700-x

Seren, Ü., 2018. GWA-Portal: Genome-Wide Association Studies Made Easy. Methods in Molecular Biology 1761, 303–319. https://doi.org/10.1007/978-1-4939-7747-5_22

Seren, Ü., Grimm, D., Fitz, J., Weigel, D., Nordborg, M., Borgwardt, K., Korte, A., 2017. AraPheno: a public database for Arabidopsis thaliana phenotypes. Nucleic Acids Research 45 (D1), D1054–D1059. https://doi.org/10.1093/nar/gkw986

Serrago, R.A., Miralles, D.J., Slafer, G.A., 2008. Floret fertility in wheat as affected by photoperiod during stem elongation and removal of spikelets at booting. European Journal of Agronomy 28 (3), 301–308. https://doi.org/10.1016/j.eja.2007.08.004

Shapiro, S.S., Wilk, M.B., 1965. An analysis of variance test for normality (complete samples). Biometrika 52 (3-4), 591–611. https://doi.org/10.1093/biomet/52.3-4.591

Sharbel, T.F., Haubold, B., Mitchell-Olds, T., 2000. Genetic isolation by distance in Arabidopsis thaliana: biogeography and postglacial colonization of Europe. Molecular Ecology 9 (12), 2109–2118. https://doi.org/10.1046/j.1365-294X.2000.01122.x

Shimizu, K.K., Kudoh, H., Kobayashi, M.J., 2011. Plant sexual reproduction during climate change: gene function in natura studied by ecological and evolutionary systems biology. Annals of Botany 108 (4), 777–787. https://doi.org/10.1093/aob/mcr180

Shirsekar, G., Devos, J., Latorre, S.M., Blaha, A., Queiroz Dias, M., González Hernando, A., Lundberg, D.S., Burbano, H.A., Fenster, C.B., Weigel, D., 2021. Multiple Sources of Introduction of North American Arabidopsis thaliana from across Eurasia. Molecular Biology and Evolution 38 (12), 5328–5344. https://doi.org/10.1093/molbev/msab268

Singh, V., Louis, J., Ayre, B.G., Reese, J.C., Shah, J., 2011. TREHALOSE PHOSPHATE SYNTHASE11-dependent trehalose metabolism promotes Arabidopsis thaliana defense against the phloem-feeding insect Myzus persicae. The Plant Journal 67 (1), 94–104. https://doi.org/10.1111/j.1365-313X.2011.04583.x

Skubacz, A., Daszkowska-Golec, A., Szarejko, I., 2016. The Role and Regulation of ABI5 (ABA-Insensitive 5) in Plant Development, Abiotic Stress Responses and Phytohormone Crosstalk. Frontiers in Plant Science 7, 1884. https://doi.org/10.3389/fpls.2016.01884

Slafer, G.A., Rawson, H.M., 1994. Does temperature affect final numbers of primordia in wheat? Field Crops Research 39 (2-3), 111–117. https://doi.org/10.1016/0378-4290(94)90013-2

Song, Y.H., 2016. The Effect of Fluctuations in Photoperiod and Ambient Temperature on the Timing of Flowering: Time to Move on Natural Environmental Conditions. Molecules and Cells 39 (10), 715–721. https://doi.org/10.14348/molcells.2016.0237

Song, Y.H., Shim, J.S., Kinmonth-Schultz, H.A., Imaizumi, T., 2015. Photoperiodic Flowering: Time Measurement Mechanisms in Leaves. Annual Review of Plant Biology 66, 441–464. https://doi.org/10.1146/annurev-arplant-043014-115555

Soundappan, I., Bennett, T., Morffy, N., Liang, Y., Stanga, J.P., Abbas, A., Leyser, O., Nelson, D.C., 2015. SMAX1-LIKE/D53 Family Members Enable Distinct MAX2-Dependent Responses to Strigolactones and Karrikins in Arabidopsis. Plant Cell 27 (11), 3143–3159. https://doi.org/10.1105/tpc.15.00562

Springthorpe, V., Penfield, S., 2015. Flowering time and seed dormancy control use external coincidence to generate life history strategy. eLife 4, e05557. https://doi.org/10.7554/eLife.05557

Srikanth, A., Schmid, M., 2011. Regulation of flowering time: all roads lead to Rome. Cellular and Molecular Life Sciences 68, 2013–2037. https://doi.org/10.1007/s00018-011-0673-y

Stefany, P., 1993. Vernalization requirement and response to day length in guiding development in wheat (report). CIMMYT.

Stock, A.J., McGoey, B.V., Stinchcombe, J.R., 2015. Water availability as an agent of selection in introduced populations of Arabidopsis thaliana: impacts on flowering time evolution. PeerJ 3, e898. https://doi.org/10.7717/peerj.898

Stockman, Y.M., Fischer, R.A., Brittain, E.G., 1983. Assimilate Supply and Floret Development Within the Spike of Wheat (Triticum aestivum L.). Functional Plant Biology 10 (6), 585–594. https://doi.org/10.1071/pp9830585

Strange, A., Li, P., Lister, C., Anderson, J., Warthmann, N., Shindo, C., Irwin, J., Nordborg, M., Dean, C., 2011. Major-Effect Alleles at Relatively Few Loci Underlie Distinct Vernalization and Flowering Variation in Arabidopsis Accessions. PLOS ONE 6 (5), e19949. https://doi.org/10.1371/journal.pone.0019949

Student, 1908. The Probable Error of a Mean. Biometrika 6 (1), 1–25.

Susila, H., Jin, S., Ahn, J.H., 2016. Light Intensity and Floral Transition: Chloroplast Says “Time to Flower!” Molecular Plant 9 (12), 1551–1553. https://doi.org/10.1016/j.molp.2016.10.013

Susila, H., Jurić, S., Liu, L., Gawarecka, K., Chung, K.S., Jin, S., Kim, S.-J., Nasim, Z., Youn, G., Suh, M.C., Yu, H., Ahn, J.H., 2021. Florigen sequestration in cellular membranes modulates temperature-responsive flowering. Science 373 (6559), 1137–1142. https://doi.org/10.1126/science.abh4054

Susila, H., Nasim, Z., Ahn, J., 2018. Ambient Temperature-Responsive Mechanisms Coordinate Regulation of Flowering Time. International Journal of Molecular Sciences 19 (10), 3196. https://doi.org/10.3390/ijms19103196

Swarup, K., Alonso-Blanco, C., Lynn, J.R., Michaels, S.D., Amasino, R.M., Koornneef, M., Millar, A.J., 1999. Natural allelic variation identifies new genes in the Arabidopsis circadian system. The Plant Journal 20 (1), 67–77. https://doi.org/10.1046/j.1365-313X.1999.00577.x

Takagi, H., Abe, A., Yoshida, K., Kosugi, S., Natsume, S., Mitsuoka, C., Uemura, A., Utsushi, H., Tamiru, M., Takuno, S., Innan, H., Cano, L.M., Kamoun, S., Terauchi, R., 2013. QTL-seq: rapid mapping of quantitative trait loci in rice by whole genome resequencing of DNA from two bulked populations. The Plant Journal 74 (1), 174–183. https://doi.org/10.1111/tpj.12105

Thines, B.C., Youn, Y., Duarte, M.I., Harmon, F.G., 2014. The time of day effects of warm temperature on flowering time involve PIF4 and PIF5. Journal of Experimental Botany 65 (4), 1141–1151. https://doi.org/10.1093/jxb/ert487

Thomas, H., 2013. Senescence, ageing and death of the whole plant. New Phytologist 197 (3), 696–711. https://doi.org/10.1111/nph.12047

Tsukaya, H., Shoda, K., Kim, G.-T., Uchimiya, H., 2000. Heteroblasty in Arabidopsis thaliana (L.) Heynh. Planta 210, 536–542. https://doi.org/10.1007/s004250050042

Tukey, J.W., 1949. Comparing Individual Means in the Analysis of Variance. Biometrics 5 (2), 99–114. https://doi.org/10.2307/3001913

Turck, F., Fornara, F., Coupland, G., 2008. Regulation and Identity of Florigen: FLOWERING LOCUS T Moves Center Stage. Annual Review of Plant Biology 59, 573–594. https://doi.org/10.1146/annurev.arplant.59.032607.092755

Valverde, F., Mouradov, A., Soppe, W., Ravenscroft, D., Samach, A., Coupland, G., 2004. Photoreceptor Regulation of CONSTANS Protein in Photoperiodic Flowering. Science 303 (5660), 1003–1006. https://doi.org/10.1126/science.1091761

van Berkel, K., de Boer, R.J., Scheres, B., ten Tusscher, K., 2013. Polar auxin transport: models and mechanisms. Development 140 (11), 2253–2268. https://doi.org/10.1242/dev.079111

van Mölken, T., Jorritsma-Wienk, L.D., van Hoek, P.H.W., de Kroon, H., 2005. Only seed size matters for germination in different populations of the dimorphic Tragopogon pratensis subsp. pratensis (Asteraceae). American Journal of Botany 92 (3), 432–437. https://doi.org/10.3732/ajb.92.3.432

Vasseur, F., Exposito-Alonso, M., Ayala-Garay, O.J., Wang, G., Enquist, B.J., Vile, D., Violle, C., Weigel, D., 2018. Adaptive diversification of growth allometry in the plant Arabidopsis thaliana. Proceedings of the National Academy of Sciences 115 (13), 3416–3421. https://doi.org/10.1073/pnas.1709141115

Vayssières, A., Mishra, P., Roggen, A., Neumann, U., Ljung, K., Albani, M.C., 2020. Vernalization shapes shoot architecture and ensures the maintenance of dormant buds in the perennial Arabis alpina. New Phytologist 227 (1), 99–115. https://doi.org/10.1111/nph.16470

Vega, A., O'Brien, J.A., Gutiérrez, R.A., 2019. Nitrate and hormonal signaling crosstalk for plant growth and development. Current Opinion in Plant Biology 52, 155–163. https://doi.org/10.1016/j.pbi.2019.10.001

Vidal, E.A., Moyano, T.C., Canales, J., Gutierrez, R.A., 2014. Nitrogen control of developmental phase transitions in Arabidopsis thaliana. Journal of Experimental Botany 65 (19), 5611–5618. https://doi.org/10.1093/jxb/eru326

Wahl, V., Brand, L.H., Guo, Y.-L., Schmid, M., 2010. The FANTASTIC FOUR proteins influence shoot meristem size in Arabidopsis thaliana. BMC Plant Biology 10, 285. https://doi.org/10.1186/1471-2229-10-285

Walker, C.H., Ware, A., Šimura, J., Ljung, K., Wilson, Z., Bennett, T., 2023. Cytokinin signaling regulates two-stage inflorescence arrest in Arabidopsis. Plant Physiology 191 (1), 479–495. https://doi.org/10.1093/plphys/kiac514

Wang, J., Luo, M.C., Chen, Z., You, F.M., Wei, Y., Zheng, Y., Dvorak, J., 2013. Aegilops tauschii single nucleotide polymorphisms shed light on the origins of wheat D-genome genetic diversity and pinpoint the geographic origin of hexaploidy wheat. New Phytologist, 198 (3), 925-937. https://doi.org/10.1111/nph.12164

Wang, J.-W., 2014. Regulation of flowering time by the miR156-mediated age pathway. Journal of Experimental Botany 65 (17), 4723–4730. https://doi.org/10.1093/jxb/eru246

Wang, L., Zhou, C.-M., Mai, Y.-X., Li, L.-Z., Gao, J., Shang, G.-D., Lian, H., Han, L., Zhang, T.-Q., Tang, H.-B., Ren, H., Wang, F.-X., Wu, L.-Y., Liu, X.-L., Wang, C.-S., Chen, E.-W., Zhang, X.-N., Liu, C., Wang, J.-W., 2019. A spatiotemporally regulated transcriptional complex underlies heteroblastic development of leaf hairs in Arabidopsis thaliana. The EMBO Journal 38 (8), e100063. https://doi.org/10.15252/embj.2018100063

Wang, R., Farrona, S., Vincent, C., Joecker, A., Schoof, H., Turck, F., Alonso-Blanco, C., Coupland, G., Albani, M.C., 2009. PEP1 regulates perennial flowering in Arabis alpina. Nature 459, 423–427. https://doi.org/10.1038/nature07988

Wang, Y., Kumaishi, K., Suzuki, T., Ichihashi, Y., Yamaguchi, N., Shirakawa, M., Ito, T., 2020. Morphological and Physiological Framework Underlying Plant Longevity in Arabidopsis thaliana. Frontiers in Plant Science 11, 1693. https://doi.org/10.3389/fpls.2020.600726

Wang, Y., Shirakawa, M., Ito, T., 2022. Dynamic Changes in Reactive Oxygen Species in the Shoot Apex Contribute to Stem Cell Death in Arabidopsis thaliana. International Journal of Molecular Sciences 23 (7), 3864. https://doi.org/10.3390/ijms23073864

Ware, A., Walker, C.H., Šimura, J., González-Suárez, P., Ljung, K., Bishopp, A., Wilson, Z.A., Bennett, T., 2020. Auxin export from proximal fruits drives arrest in temporally competent inflorescences. Nature Plants 6, 699–707. https://doi.org/10.1038/s41477-020-0661-z

Weberling, F., 1992. Morphology of Flowers and Inflorescences. Cambridge University Press Archive.

Weigel, D., 2012. Natural Variation in Arabidopsis: From Molecular Genetics to Ecological Genomics. Plant Physiology 158 (1), 2–22. https://doi.org/10.1104/pp.111.189845

Westoby, M., Leishman, M., Lord, J., 1997. Comparative ecology of seed size and dispersal. Philosophical Transactions of the Royal Society of London. Philosophical Transactions of the Royal Society B: Biological Sciences 351, 1309–1318. https://doi.org/10.1098/rstb.1996.0114

Whingwiri, E.E., Kemp, D.R., 1980. Spikelet development and grain yield of the wheat ear in response to applied nitrogen. Australian Journal of Agricultural Research 31 (4), 637–647. https://doi.org/10.1071/ar9800637

Wickland, D.P., Hanzawa, Y., 2015. The FLOWERING LOCUS T/TERMINAL FLOWER 1 Gene Family: Functional Evolution and Molecular Mechanisms. Molecular Plant 8 (7), 983–997. https://doi.org/10.1016/j.molp.2015.01.007

Wigge, P.A., Kim, M.C., Jaeger, K.E., Busch, W., Schmid, M., Lohmann, J.U., Weigel, D., 2005. Integration of Spatial and Temporal Information During Floral Induction in Arabidopsis. Science 309 (5737), 1056–1059. https://doi.org/10.1126/science.1114358

Wilcoxon, F., 1945. Individual Comparisons by Ranking Methods. Biometrics Bulletin 1 (6), 80–83. https://doi.org/10.2307/3001968

Wilczek, A.M., Roe, J.L., Knapp, M.C., Cooper, M.D., Lopez-Gallego, C., Martin, L.J., Muir, C.D., Sim, S., Walker, A., Anderson, J., Egan, J.F., Moyers, B.T., Petipas, R., Giakountis, A., Charbit, E., Coupland, G., Welch, S.M., Schmitt, J., 2009. Effects of Genetic Perturbation on Seasonal Life History Plasticity. Science 323 (5916), 930–934. https://doi.org/10.1126/science.1165826

Wilson, A.K., Pickett, F.B., Turner, J.C., Estelle, M., 1990. A dominant mutation in Arabidopsis confers resistance to auxin, ethylene and abscisic acid. Molecular and General Genetics MGG 222, 377–383. https://doi.org/10.1007/BF00633843

Wilson, R.N., Heckman, J.W., Somerville, C.R., 1992. Gibberellin Is Required for Flowering in Arabidopsis thaliana under Short Days. Plant Physiology 100 (1), 403–408.

Wimalasekera, R., 2019. Effect of Light Intensity on Photosynthesis, in: Ahmad, P., Abass Ahanger, M., Nasser Alyemeni, M., Alam, P. (Eds.), Photosynthesis, Productivity and Environmental Stress. Wiley, pp. 65–73. https://doi.org/10.1002/9781119501800.ch4

Wingler, A., Purdy, S.J., Edwards, S.-A., Chardon, F., Masclaux-Daubresse, C., 2010. QTL analysis for sugar-regulated leaf senescence supports flowering-dependent and -independent senescence pathways. New Phytologist 185 (2), 420–433. https://doi.org/10.1111/j.1469-8137.2009.03072.x

Wu, G., Park, M.Y., Conway, S.R., Wang, J.-W., Weigel, D., Poethig, R.S., 2009. The Sequential Action of miR156 and miR172 Regulates Developmental Timing in Arabidopsis. Cell 138 (4), 750–759. https://doi.org/10.1016/j.cell.2009.06.031

Wu, T., Hu, E., Xu, S., Chen, M., Guo, P., Dai, Z., Feng, T., Zhou, L., Tang, W., Zhan, L., Fu, X., Liu, S., Bo, X., Yu, G., 2021. clusterProfiler 4.0: A universal enrichment tool for interpreting omics data. The Innovation 2 (3), 100141. https://doi.org/10.1016/j.xinn.2021.100141

Wuest, S.E., Philipp, M.A., Guthörl, D., Schmid, B., Grossniklaus, U., 2016. Seed Production Affects Maternal Growth and Senescence in Arabidopsis. Plant Physiology 171 (1), 392–404. https://doi.org/10.1104/pp.15.01995

Würschum, T., Groß-Hardt, R., Laux, T., 2006. APETALA2 Regulates the Stem Cell Niche in the Arabidopsis Shoot Meristem. The Plant Cell 18 (2), 295–307. https://doi.org/10.1105/tpc.105.038398

Xu, Y., Zhu, Z., 2021. PIF4 and PIF4-Interacting Proteins: At the Nexus of Plant Light, Temperature and Hormone Signal Integrations. International Journal of Molecular Sciences 22 (19), 10304. https://doi.org/10.3390/ijms221910304

Yamada, H., Suzuki, T., Terada, K., Takei, K., Ishikawa, K., Miwa, K., Yamashino, T., Mizuno, T., 2001. The Arabidopsis AHK4 Histidine Kinase is a Cytokinin-Binding Receptor that Transduces Cytokinin Signals Across the Membrane. Plant and Cell Physiology 42 (9), 1017–1023. https://doi.org/10.1093/pcp/pce127

Yamaguchi, A., Kobayashi, Y., Goto, K., Abe, M., Araki, T., 2005. TWIN SISTER OF FT (TSF) Acts as a Floral Pathway Integrator Redundantly with FT. Plant and Cell Physiology 46 (8), 1175–1189. https://doi.org/10.1093/pcp/pci151

Yan, L., Loukoianov, A., Tranquilli, G., Helguera, M., Fahima, T., Dubcovsky, J., 2003. Positional cloning of the wheat vernalization gene VRN1. Proceedings of the national Academy of Sciences 100 (10): 6263-6268. https://doi.org/10.1073/pnas.0937399100

Yan, L., Loukoianov, A., Blechl, A., Tranquilli, G., Ramakrishna, W., Sanmiguel, P., Bennetzen, J.L., Echenique, V., Dubcovsky, J., 2004. The wheat VRN2 gene is a flowering repressor down-regulated by vernalization. Science 303 (5664): 1640-1644. 10.1126/science.1094305

Yan, L., Fu, D., Li, C., Blechl, A., Tranquilli, G., Bonafede, M., Sanchez, A., Valarik, M., Yasuda, S., Dubcovsky, J., 2006. The wheat and barley vernalization gene VRN3 is an orthologue of FT. Proceedings of the National Academy of Sciences 103 (51), 19581–19586. https://doi.org/10.1073/pnas.0607142103

Yang, W., Cortijo, S., Korsbo, N., Roszak, P., Schiessl, K., Gurzadyan, A., Wightman, R., Jönsson, H., Meyerowitz, E., 2021. Molecular mechanism of cytokinin-activated cell division in Arabidopsis. Science 371 (6536), 1350–1355. https://doi.org/10.1126/science.abe2305

Yu, B., He, X., Tang, Y., Chen, Z., Zhou, L., Li, X., Zhang, C., Huang, X., Yang, Y., Zhang, W., Kong, F., Miao, Y., Hou, X., Hu, Y., 2023. Photoperiod controls plant seed size in a CONSTANS-dependent manner. Nature Plants 9, 343–354. https://doi.org/10.1038/s41477-023-01350-y

Yu, J.-W., Rubio, V., Lee, N.-Y., Bai, S., Lee, S.-Y., Kim, S.-S., Liu, L., Zhang, Yiyue, Irigoyen, M.L., Sullivan, J.A., Zhang, Yu, Lee, I., Xie, Q., Paek, N.-C., Deng, X.W., 2008. COP1 and ELF3 control circadian function and photoperiodic flowering by regulating GI stability. Molecular Cell 32 (5), 617–630. https://doi.org/10.1016/j.molcel.2008.09.026

Zeng, J., Dong, Z., Wu, H., Tian, Z., Zhao, Z., 2017. Redox regulation of plant stem cell fate. The EMBO Journal 36, 2844–2855. https://doi.org/10.15252/embj.201695955

Zhang, B., Li, C., Li, Y., Yu, H., 2020. Mobile TERMINAL FLOWER1 determines seed size in Arabidopsis. Nature Plants 6, 1146–1157. https://doi.org/10.1038/s41477-020-0749-5

Zhang, W., To, J.P.C., Cheng, C.-Y., Eric Schaller, G., Kieber, J.J., 2011. Type-A response regulators are required for proper root apical meristem function through post-transcriptional regulation of PIN auxin efflux carriers. The Plant Journal 68 (1), 1–10. https://doi.org/10.1111/j.1365-313X.2011.04668.x

Zhao, H., Xu, D., Tian, T., Kong, F., Lin, K., Gan, S., Zhang, H., Li, G., 2021. Molecular and functional dissection of EARLY-FLOWERING 3 (ELF3) and ELF4 in Arabidopsis. Plant Science 303, 110786. https://doi.org/10.1016/j.plantsci.2020.110786

Zhu, Y., Klasfeld, S., Jeong, C.W., Jin, R., Goto, K., Yamaguchi, N., Wagner, D., 2020. TERMINAL FLOWER 1-FD complex target genes and competition with FLOWERING LOCUS T. Nature Communications 11, 5118. https://doi.org/10.1038/s41467-020-18782-1

Zubo, Y.O., Schaller, G.E., 2020. Role of the Cytokinin-Activated Type-B Response Regulators in Hormone Crosstalk. Plants 9 (2), 166. https://doi.org/10.3390/plants9020166

Zuo, Z., Liu, H., Liu, B., Liu, X., Lin, C., 2011. Blue Light-Dependent Interaction of CRY2 with SPA1 Regulates COP1 activity and Floral Initiation in Arabidopsis. Current Biology 21 (10), 841–847. https://doi.org/10.1016/j.cub.2011.03.048

Appendix

Supplementary Tables

Supplementary Table 1. Differentially expressed genes between *ft-10* and Col-0 annotated with the GO term 'meristem development' (GO:0048507)

Cluster	Gene ID	Symbol	Description
1	AT1G03840	*MGP*	Nuclear-localized transcription factor with three zinc finger domains, involved in root patterning
1	AT1G13710	*CYP78A5*	Cytochrome P450 monooxygenase, required for maternal control of seed size
1	AT1G14630		XRI1-like protein
1	AT1G23380	*KNAT6*	Homeodomain transcription factor, belongs to class I of KN transcription factor family
1	AT1G26310	*CAL*	K-box region and MADS-box transcription factor, homologous to AP1
1	AT1G27370	*SPL10*	Squamosa promoter binding protein-like
1	AT1G46480	*WOX4*	WUSCHEL-related homeobox gene, involved in maintenance of the vascular meristem
1	AT1G52150	*ATHB-15*	Homeobox-leucine zipper protein
1	AT1G54200	*BG3*	DNA mismatch repair Msh6-like protein
1	AT1G62360	*STM*	Class I knotted-like homeodomain protein, required for shoot apical meristem function
1	AT2G01830	*AHK4*	Histidine kinase protein, cytokinin-binding receptor that transduces cytokinin signals
1	AT2G05760	*NAT1*	Xanthine/uracil permease family protein
1	AT2G07680	*ABCC13*	Multidrug resistance-associated protein
1	AT2G22540	*SVP*	K-box region and MADS-box transcription factor, it acts as a floral repressor
1	AT2G28410		Transmembrane protein
1	AT3G06020	*FAF4*	FANTASTIC four-like protein, regulates shoot meristem size, can repress WUS
1	AT3G17840	*RLK902*	Receptor-like kinase
1	AT3G22410		Sec14p-like phosphatidylinositol transfer protein
1	AT3G24770	*CLE41*	CLAVATA3/ESR-related, involved in axillary bud formation
1	AT3G25560	*NIK2*	NSP-interacting kinase

Cluster	Gene ID	Symbol	Description
1	AT3G28100	*UMAMIT45*	Nodulin MtN21-like transporter
1	AT3G49180	*RID3*	Transducin/WD40 repeat-like protein
1	AT3G53190		Pectin lyase-like protein
1	AT4G00340	*RLK4*	Receptor-like protein kinase
1	AT4G00490	*BAM2*	Chloroplast beta-amylase
1	AT4G13195	*CLE44*	CLAVATA3/ESR-related, involved in axillary bud formation
1	AT4G24190	*HSD*	Chaperone protein htpG protein, involved in regulation of meristem size, required for correct formation of CLV proteins
1	AT4G24540	*AGL24*	MADS-box protein, involved in flowering, it regulates *SOC1* and is regulated by *SOC1*
1	AT4G24670	*TAR2*	Tryptophan aminotransferase related, involved in IAA biosynthesis
1	AT4G29720	*PAO5*	Polyamine oxidase
1	AT4G31140		O-glycosyl hydrolase
1	AT4G31890		ARM repeat protein
1	AT4G36360	*BGAL3*	Beta-galactosidase
1	AT4G37310	*CYP81H1*	Cytochrome P450 polypeptide
1	AT5G02030	*BLH9*	Homeodomain transcription factor, binds to the AGAMOUS cis-regulatory element.
1	AT5G11420		Transmembrane protein of unknown function
1	AT5G19440		NAD(P)-binding Rossmann-fold protein of unknown physiological function
1	AT5G22330	*RIN1*	Nucleoside triphosphate hydrolase, involved in telomerase assembly
1	AT5G37790		Protein kinase
1	AT5G46700	*TRN2*	Tetraspanin protein, required for the radial pattern of tissue differentiation in the root
1	AT5G47250		LRR and NB-ARC domains-containing protein
1	AT5G56530		tRNA-splicing ligase
1	AT5G59020		Hepatocyte growth factor activator
1	AT5G61480	*PXY*	Leucine-rich repeat kinase, essential for vascular-tissue development
1	AT5G64770	*RGF9*	Root meristem growth factor, required for maintenance of the root stem cell niche
1	AT5G65700	*BAM1*	Leucine-rich receptor-like kinase, required for shoot and flower meristem function

Cluster	Gene ID	Symbol	Description
2	AT1G03170	*FAF2*	FANTASTIC four-like protein, regulates shoot meristem size, can repress WUS
2	AT1G23010	*LPR1*	Cupredoxin protein, it adjusts root meristem activity to inorganic phosphate
2	AT1G50830		Aminotransferase-like protein
2	AT1G70280		NHL domain-containing protein
2	AT2G26170	*MAX1*	Cytochrome P450 polypeptide, involved in the synthesis of strigolactones
2	AT3G63500	*OBE4*	PHD finger protein, it is redundantly required for root meristem initiation
2	AT4G14740	*FL3*	Auxin canalization protein
2	AT4G14900		FRIGIDA-like protein
2	AT4G28703		RmlC-like cupin
2	AT5G12840	*NFY-A1*	Nuclear factor Y, subunit A1, binds to CCAAT box motifs present in promoter sequences
2	AT5G14010	*KNU*	C2H2-type zinc finger protein, transcriptionally represses *WUS* in floral meristems
2	AT5G62960		N-acetylglucosamine protein
3	AT1G50750		Aminotransferase-like protein, mobile
3	AT2G41510	*CKX1*	Cytokinin oxidase/dehydrogenase, catalyses the degradation of cytokinin
3	AT3G05980		Hypothetical protein
3	AT3G07780	*OBE1*	Nuclear PHD finger protein, it plays a role in maintenance of the root and shoot meristem
3	AT4G00180	*YAB3*	YABBY transcription factor, involved in patterning of the fruit
3	AT4G28190	*ULT1*	Cys-rich protein with B-box domain, negatively regulates meristem cell accumulation in inflorescence and floral meristems
3	AT4G32980	*ATH1*	Homeodomain transcription factor, involved in meristem maintenance, physically interacts with STM and KNAT6
3	AT4G36920	*AP2*	Floral homeotic transcription factor, involved in specification of floral organ identity, it acts on the WUS-CLV pathway
3	AT5G03840	*TFL1*	Phosphatidylethanolamine-binding protein, it controls inflorescence meristem identity
4	AT1G16640		AP2/B3-like transcription factor
4	AT1G65480	*FT*	Phosphatidylethanolamine-binding protein, floral promoter.

Cluster	Gene ID	Symbol	Description
4	AT1G50820		Aminotransferase-like protein
4	AT1G69180	*CRC*	YABBY transcription factor, involved in carpel development
4	AT2G25180	*ARR12*	Type-B Arabidopsis Response regulator (ARR), it acts in the cytokinin signaling pathway, directly activates *WUS*
4	AT2G33880	*HB-3*	Protein similar to WUS type homeodomain protein, required for meristem development, positive regulator of WUS
4	AT3G23930		Troponin T, skeletal protein
4	AT3G49670	*BAM2*	Leucine-rich receptor-like kinase, required for shoot and flower meristem function
4	AT4G40060	*HB16*	Homeodomain leucine zipper class I protein
4	AT5G03790	*HB51*	Homeodomain leucine zipper class I meristem identity regulator, acts together with LFY to induce *CAL*
4	AT5G09970	*CYP78A7*	Cytochrome P450 polypeptide, functions in shoot meristem maintenance
4	AT5G13570	*DCP2*	Decapping 2, it forms a mRNA decapping complex with DCP1
4	AT5G25130	*CYP71B12*	Cytochrome P450 polypeptide
4	AT5G47590		Heat shock protein HSP20/alpha crystallin
4	AT5G61850	*LFY*	Transcriptional regulator, floral promoter

Supplementary Table 2. Differentially expressed genes between Kondara and Col-0 annotated with the GO term 'meristem development' (GO:0048507)

Cluster	Gene ID	Symbol	Description
1	AT1G03170	*FAF2*	FANTASTIC four-like protein, regulates shoot meristem size, can repress WUS
1	AT1G26310	*CAL*	K-box region and MADS-box transcription factor, homologous to AP1
1	AT1G69180	*CRC*	YABBY transcription factor, involved in carpel development
1	AT1G71390	*RLP11*	Receptor like protein
1	AT2G26170	*MAX1*	Cytochrome P450 polypeptide, involved in the synthesis of strigolactones
1	AT3G23930		Troponin T, skeletal protein
1	AT3G63500	*OBE4*	PHD finger protein, it is redundantly required for root meristem initiation
1	AT4G00180	*YAB3*	YABBY transcription factor, involved in patterning of the fruit
1	AT4G14740	*FL3*	Auxin canalization protein
1	AT4G28703		RmlC-like cupin
1	AT4G32980	*ATH1*	Homeodomain transcription factor, involved in meristem maintenance, physically interacts with STM and KNAT6
1	AT5G47590		Heat shock protein HSP20/alpha crystallin
1	AT5G62960		N-acetylglucosamine protein
2	AT1G03840	*MGP*	Nuclear-localized transcription factor with three zinc finger domains, involved in root patterning
2	AT1G13710	*CYP78A5*	Cytochrome P450 monooxygenase, required for maternal control of seed size
2	AT1G20930	*CDKB2;2*	Cyclin-dependent kinase B2, required for the organization of the shoot apical meristem
2	AT1G23380	*KNAT6*	Homeodomain transcription factor, class I *KN*
2	AT1G27370	*SPL10*	Squamosa promoter binding protein-like

Cluster	Gene ID	Symbol	Description
2	AT1G69120	*AP1*	K-box region and MADS-box transcription factor, homologous to *CAL*, it specifies floral meristem and sepal identity
2	AT2G05760	*NAT1*	Xanthine/uracil permease family protein
2	AT2G07680	*ABCC13*	Multidrug resistance-associated protein
2	AT3G06020	*FAF4*	FANTASTIC four-like protein, regulates shoot meristem size, can repress WUS
2	AT3G49180	*RID3*	Transducin/WD40 repeat-like protein
2	AT3G53190		Pectin lyase-like protein
2	AT4G13195	*CLE44*	CLAVATA3/ESR-related, involved in axillary bud formation
2	AT4G24670	*TAR2*	Tryptophan aminotransferase related, involved in IAA biosynthesis
2	AT4G29720	*PAO5*	Polyamine oxidase
2	AT5G10140	*FLC*	MADS-box protein, it functions as a repressor of floral transition
2	AT5G19440		NAD(P)-binding Rossmann-fold protein of unknown physiological function
2	AT5G47250		LRR and NB-ARC domains-containing protein
2	AT5G56530		tRNA-splicing ligase
2	AT5G64770	*RGF9*	Root meristem growth factor, required for maintenance of the root stem cell niche
3	AT3G49670	*BAM2*	Leucine-rich receptor-like kinase, required for shoot and flower meristem function
3	AT4G20460		NAD(P)-binding Rossmann-fold protein
3	AT4G36920	*AP2*	Floral homeotic transcription factor, involved in specification of floral organ identity, it acts on the WUS-CLV pathway

Supplementary Table 3. Differentially expressed genes between Kondara and Col-0 with high impact SNPs in Kondara

Gene ID	Symbol	Description
AT1G02300	*CATHB1*	Capase, involved in stress-induced cell death
AT1G02670		P-loop containing nucleoside triphosphate hydrolase
AT1G11580	*PMEI-PME18*	Pectin methylesterase
AT1G15320	*INP2*	Seed dormancy control protein
AT1G20990		Cysteine/histidine-rich C1 domain protein
AT1G24220		Paired amphipathic helix repeat-containing protein
AT1G28695		Nucleotide-di-phospho-sugar transferase
AT1G51670	*HTT5*	Protein of unknown function
AT1G54030	*MVP1*	Vacuolar protein, involved in the secretory pathway
AT1G58280		Phosphoglycerate mutase
AT1G65150		TRAF-like protein
AT1G72830	*NF-YA3*	Subunit of CCAAT-binding complex
AT2G16900		Phospholipase-like protein
AT2G18700	*TPS11*	Enzyme involved in trehalose synthesis
AT2G22960	*FPT2*	Flavonol-phenylacyltransferase
AT2G32150	*XMPP*	Phosphatase, involved in purine nucleotide catabolism
AT2G35080		ATP-binding aminoacyl-tRNA ligase
AT3G01120	*MTO1*	Protein involved in methionine synthesis
AT3G05780	*LON3*	Protease-like, degrades damaged or unstable proteins

Gene ID	Symbol	Description
AT3G08690	*UBC11*	Ubiquitin-conjugating enzyme
AT3G10720	*PMEI-PME25*	Pectin methylesterase
AT3G11000		DCD (Development and Cell Death) domain protein
AT3G11930		Adenine nucleotide alpha hydrolase-like protein
AT3G12420		Polynucleotidyl transferase
AT3G18680	*PUMPKIN*	UMP kinase, located in the plastid
AT3G52720	*ACA1*	Alpha carbonic anhydrase, located in the chloroplast
AT3G58050		Protein of unknown function
AT3G62670	*ARR20*	B-type response regulator
AT4G12920	*UND*	Aspartyl protease
AT4G13430	*IIL1*	Isomerase involved in glucosinolate biosynthesis
AT4G15760	*MO1*	Monooxygenase, degrades salicylic acid
AT4G20430		Subtilase
AT4G23010	*UTR2*	UDP-galactose transporter
AT4G25170		Protein of unknown function
AT4G33860		Glycosyl hydrolase
AT4G39770	*TPPH*	Haloacid dehalogenase-like hydrolase
AT5G03260	*LAC11*	Laccase
AT5G17030	*UGT78D3*	UDP-glucosyl transferase
AT5G24780	*VSP1*	Acid phosphatase, induced by jasmonic acid
AT5G25230		Ribosomal protein elongation factor

Gene ID	Symbol	Description
AT5G53680		RNA-binding protein
AT5G54510	*DFL1*	IAA-amido synthase, conjugates amino acids to auxin
AT5G55180		O-glycosyl hydrolase
AT5G66053		Protein of unknown function
AT5G66790		Protein kinase